The University Of Sheffield.

Investigating Adenosine Deaminase and Purine Metabolism in C9orf72 Amyotrophic Lateral Sclerosis

Benjamin P. C. Hall

Thesis submitted for the degree of Doctor of Philosophy (PhD)

Sheffield Institute for Translational Neuroscience

Neuroscience

April 2023

SITraN
Sheffield Institute for Translational Neuroscience

Table of Contents

Acknowledgments

First and foremost, I would like to thank my supervisor, Dr Scott Allen for his support, guidance, and patience over the course of the project and, importantly, for giving me the chance to both carry out this PhD and at the outset of my career in research. Without him I would not be in the position I am today. Thanks also to my secondary supervisor Prof. Laura Ferraiuolo who has regularly offered sage advice throughout this study. Thank you to my advisors, Prof. Mimoun Azzouz and Prof. Kurt De Vos whose assistance has informed a substantial proportion of this study. Thank you also to the members of SITraN who have given me an inordinate amount of technical advice and guidance over the course of the project, in particular Dr Lydia Castelli, Dr Christopher P. Webster and Dr Adrian Higginbottom who have often felt close to pseudo-secondary supervisors due to how often I turned to them for counsel. Thank you to the members of the Allen lab past and present who have contributed to this project and have often provided welcome respite from my work over the past three years and beyond, Billie, Jess, Ryan, Lucy, Amelia, Tom, Amy, Sarah, Razan, Nikolas, Jonathan and Keaton thank you because, whether you know it or not, you have all contributed both directly and indirectly to this project. This extends to everyone who I've had the pleasure of interacting with in SITraN, this is a wonderful place to work. Thank you also to my friends outside of SITraN for taking my mind off work and providing an ear for my many, many complaints. And my family who have been a constant source of support.

Every single person here has contributed immeasurably to this project and it's hard to thank all of them enough.

Abstract

Background: ALS is a neurodegenerative disorder characterised by the death of motor neurons (MNs) in the brain stem and spinal cord. The most common genetic mutation associated with the development of ALS is a hexanucleotide repeat expansion (HRE) in the C9orf72 gene. Previous data from our laboratory has revealed that induced astrocytes (iAstrocytes) from C9orf72 ALS patients exhibit a significant downregulation in the purine metabolism enzyme adenosine deaminase (ADA), that deaminates adenosine to form inosine, leading to increased sensitivity to adenosine-mediated toxicity. Inosine supplementation to bypass the defect was beneficial bioenergetically in iAstrocytes and decreased iAstrocyte-mediated MN toxicity in co-cultures. Our data raised questions as to what other effects the C9orf72 HRE has on purine metabolism, why and how ADA is downregulated, and led us to hypothesise that restoring ADA levels would be beneficial for C9orf72 iAstrocytes.

Results: ADA activity and inosine levels were reduced in C9orf72 iAstrocytes. We also observed a downregulation of the purine enzymes ecto-5'-nucleotidase (CD73) and hypoxanthine-guanine phosphoribosyltransferase (HGPRT). ADA and CD73 downregulation were both recapitulated in C9orf72 HRE gain-of-function models. ADA gene therapy increased ADA activity and inosine output and restored ADA expression. p62 and NQO-1 were unaffected by ADA gene therapy. ADA gene therapy also did not alter CD73 or HGPRT levels and had no effect on adenosine-mediated toxicity or increase ATP levels.

Conclusions: These data demonstrate that the C9orf72 HRE induces several aberrations in purine metabolism, which may in part be caused by gain-of-function mechanisms. HGPRT upregulation may be induced via a separate mechanism currently under investigation. ADA gene therapy can restore ADA expression and function, but further study is required to more robustly characterise the effect of ADA gene therapy on ALS iAstrocytes.

Abbreviations

5-Phosphoribosyl-1-Pyrophosphate - **PRPP**

5-Phosphoribosyl-1-Pyrophosphate amidotransferase - **PPAT**

Amyotrophic Lateral Sclerosis - **ALS**

Adenosine Deaminase - **ADA**

Adenosine Deaminase Acting on RNA - **ADAR**

Adenosine Deaminase Activity Assay Buffer - **AB**

Adenosine Deaminase Lentivirus - **ADA-LV**

Adenosine Diphosphate - **ADP**

Adenosine Kinase - **ADK**

Adenosine Monophosphate - **AMP**

Adenosine Triphosphate - **ATP**

Bovine Serum Albumin - **BSA**

Central Nervous System - **CNS**

Chromosome 9, Open Reading Frame 72 - **C9orf72**

Coupled Respiration - **CR**

Cyclic Adenosine Monophosphate – **cAMP**

De novo purine biosynthesis - **DNPB**

Deoxyadenosine Triphosphate - **dATP**

Dipeptide Repeat Protein - **DPR**

DNA Damage Response - **DDR**

Dulbecco's Modified Eagle Medium - **DMEM**

Ecto-5'-nucleotidase - **CD73**

Empty Vector - **EV**

Empty Vector Lentivirus – **EV-LV**

Epidermal Growth Factor - **EGF**

Extracellular Acidification Rate - **ECAR**

Extracellular Signal-Regulated Kinases - **ERK**

Familial Amyotrophic Lateral Sclerosis - **fALS**

Fibroblast Growth Factor 2 - **FGF2**

Foetal Bovine Serum - **FBS**

Glycine-Alanine - **poly-GA**

Glycine-Proline - **poly-GP**

Glycine-Arginine - **poly-GR**

Glycolytic Reserve - **GR**

Glyoxalase - **Glo**

Guanosine Monophosphate - **GMP**

Hexanucleotide Repeat Expansion - **HRE**

Human Embryonic Kidney 293 T-Rex - **HEK293T**

Hypoxanthine Guanine Phosphoribosyltransferase - **HGPRT**

Induced Pluripotent Stem Cell - **iPSC**

Induced Neuronal Progenitor Cell - **iNPC**

Induced Neuronal Progenitor Cell Astrocyte - **iAstrocyte**

Induced Neuronal Progenitor Cell Neuron - **iNeuron**

Inosine Monophosphate - **IMP**

Jun Amino-Terminal Kinases - **JNK**

Lentiviral Vector - **LV**

Liquid-Liquid Phase Separation - **LLPS**

Maximal Glycolytic Capacity - **MGC**

Mitochondrial Respiration - **MR**

Mitochondrial Spare Respiratory Capacity - **SRC**

Mitogen Activated Protein Kinases - **MAPK**

Motor Neuron - **MN**

Multiplicity of Infection - **MOI**

N-Terminal Truncated p73 - **ΔNp73**

NAD(P)H quinone dehydrogenase 1 - **NQO1**

Neuro2a - **N2a**

Nuclear Factor Erythroid 2-Related Factor 2 **- Nrf2**

Oxygen Consumption Rate - **OCR**

Parkinson’s Disease - **PD**

Proline Alanine - **poly-PA**

Proline-Arginine - **poly-PR**

Purine Nucleoside Phosphorylase - **PNP**

Reactive Oxygen Species - **ROS**

S-Adenosylhomocysteine - **SAH**

S-Adenosylmethionine - **SAM**

Severe Combined Immunodeficiency - **SCID**

Single Nucleotide Variant - **SNV**

Sporadic Amyotrophic Lateral Sclerosis - **sALS**

Stress Activated Protein Kinases - **SAPK**

TAR DNA binding protein - **TDP-43**

Transactivating Domain p73 - **TAp73**

Tris-Buffered Saline with 0.01% Tween - **TBST**

Type 2 Diabetes Mellitus - **T2DM**

Xanthine Dehydrogenase - **XDH**

Xanthine Oxidoreductase - **XOR**

Xanthine Oxidase - **XO**

List of figures

List of tables

Attribution Statement

All work was my own except the following: iNPC lines were reprogrammed from fibroblasts by the Ferraiuolo lab (Meyer et al., 2014). ADA expressing plasmids were initially cloned by the Hautbergue lab, C9orf72 Knockout HELA were generated by the De Vos Lab, 36x repeat DPR plasmids were initially generated by the Isaacs lab (Hautbergue et al., 2017) and subcloned by the De Vos lab, 38x and 39x repeat G4C2 and C4G2 plasmids were initially cloned by the Hautbergue and Shaw labs (Hautbergue et al., 2017) and stably expressed in N2a lines by the Shaw lab. Several western blots were performed by placement students Jonathan George and Keaton Hamer under my supervision. Specifically blots investigating expression of HGPRT, ADK, PNP and XDH were partially performed by Jonathan George and the western blots investigating the expression of CD73 were partially performed by Keaton Hamer. Metabolic flux analysis on gene therapy treated iAstrocytes was performed by the MSc student Thomas Gough under my supervision. Several figures are taken from Hall et al (2022) with permission from co-authors and the Journal of Histology and Histochemistry. The figures in question are highlighted in the corresponding legends.

1. Introduction

1.1 Amyotrophic Lateral Sclerosis

Amyotrophic lateral sclerosis (ALS) is a neurodegenerative disorder characterised by the death of upper motor neurons (MNs) in the motor cortex and lower MNs in the brain stem and spinal cord (R. H. Brown & Al-Chalabi, 2017). Typically, onset occurs between the ages of 55 and 75, causing muscle weakening and wastage, eventual paralysis, and death within 5 years, generally caused by respiratory failure. Estimates of prevalence vary depending on region (C. A. Brown et al., 2021), but a recent study indicated that the global prevalence of ALS is 4.42 per 100,000 (L. Xu et al., 2020), whilst the cumulative lifetime risk is 1 in 436 for women and 1 in 347 for men in a European population (Ryan et al., 2019). The prevalence of ALS increased by 22% from 2005 to 2015 (Vos et al., 2017), and conservative estimates predict that the global incidence of ALS could have risen almost 70% by 2040, due to the increasing number of individuals in sub-populations most at risk of acquiring ALS in developing nations (Arthur et al., 2016). There are no cures for ALS and currently only two commercially available products exist for its treatment; riluzole, a glutamate antagonist that extends life expectancy by, on average, 3 months (Bensimon et al., 1994) and edaravone, an antioxidant that reduces the decline in ALSFRS-R score in a subset of patients (K. Abe et al., 2017). The rising prevalence of ALS, and its increasing burden on healthcare services has brought about a need to find efficacious therapies.

The difficulties in developing viable ALS therapies arise, at least partially, from the complexities in disease aetiology, with the only common hallmark being cytosolic TAR DNA binding protein (TDP-43) aggregation, that is present in 95% of cases (Neumann et al., 2006). Two classifications of ALS exist, familial ALS (fALS), which accounts for approximately 10% of cases and sporadic ALS (sALS), which accounts for the remaining 90%. fALS is defined by having at least one first- (or sometimes second-) degree family member previously diagnosed with ALS (Mulder et al., 1986). Over 50 genes have been linked with the development of ALS (Mejzini et al., 2019), with common genes including superoxide dismutase 1 (*SOD1*) (Rosen et al., 1993), fused in sarcoma (*FUS*) (Vance et al., 2009) and TAR DNA binding protein (*TARDBP43*) (Sreedharan et al., 2008). However, the most common genetic mutation associated with ALS is a G_4C_2 hexanucleotide repeat expansion (HRE) in the first intron of the chromosome 9, open reading frame 72 (*C9orf72*) gene, that codes for the C9orf72 protein and accounts for 33.7% of fALS and 5.1% of sALS cases in European populations (Majounie et al., 2012; Mejzini et al., 2019), though it is far rarer in Asian populations (2.3% fALS, 0.3% sALS) (Mejzini et al., 2019; Zou et al., 2017). Mechanistically, the C9orf72 HRE may contribute to MN degeneration via both a toxic gain-of-function and loss-of-function (Zhu et al., 2020).

1.2 C9orf72 mechanisms of toxicity

1.2.1 Loss-of-function

Reduction in the brain and cervical spinal cord expression of the C9orf72 protein has been observed in ALS patients (DeJesus-Hernandez et al., 2011; Gijselinck et al., 2012) and in induced pluripotent stem cell (iPSC) disease models (Donnelly et al., 2013; Y. Shi et al., 2018). This may contribute to a loss-of-function of the C9orf72 protein, that forms a complex with Smith-Magenis chromosome region 8 and tryptophan-aspartic acid repeat-containing protein (Amick et al., 2016; Sellier et al., 2016; Sullivan et al., 2016), coordinating Rab1a-dependent trafficking of ULK1 to the phagophore to initiate autophagy (Webster et al., 2016). C9orf72 has also been implicated in energetic output, as it was shown to translocate from the cytosol to the inner mitochondrial membrane to stabilise and prevent degradation of TIMMDC1, which is required for the assembly of complex I (T. Wang et al., 2021). Additionally, C9orf72 function has been linked to several cellular processes including vesicle trafficking, lysosome homeostasis, and mTORC1 signalling (Pang & Hu, 2021). Pathogenically, haploinsufficiency of C9orf72 *in vitro* has been shown to induce impairments in vesicle trafficking, complex I function and autophagy, along with reduced lysosomal expression, leading to the accumulation of TDP-43, p62 and glutamate receptor aggregates, inducing neurodegeneration via excitotoxicity (Sellier et al., 2016; Y. Shi et al., 2018; T. Wang et al., 2021). C9orf72 haploinsufficiency has also been shown to exacerbate motor dysfunction in a gain-of-function C9orf72 mouse model (Shao et al., 2019), whilst C9orf72 ablation alone induces motor deficit and neurodegeneration in *C. elegans* and zebrafish (Ciura et al., 2013; Therrien et al., 2013).

1.2.2 Gain-of-function

C9orf72's toxic gain-of-function arises from the bidirectional transcription and translation of the HRE, leading to the generation of sense and antisense RNA foci and dipeptide repeat (DPR) proteins, that have been shown to accumulate in the brains of patients (DeJesus-Hernandez et al., 2017; Gendron et al., 2013; Zu et al., 2013).

1.2.2.1 RNA foci

RNA foci arise from transcription of the C9orf72 HRE and have been reported in many cell models since the initial discoveries implicating the C9orf72 HRE in the pathogenesis of ALS (DeJesus-Hernandez et al., 2011). They are present throughout the central nervous system (CNS), though are less prevalent in glia (Mizielinska et al. 2013). RNA foci can be found in the nucleoplasm, lining the nuclear membrane or nucleolus, and less frequently in the cytoplasm

(Cooper-Knock et al., 2014; Donnelly et al., 2013; Mizielinska et al., 2013, 2017; Vatsavayai et al., 2016, 2018). RNA foci are thought to induce toxicity by impairing RNA binding, disrupting RNA splicing, transport and translation, and may also be linked to the mislocalisation of TDP-43 outside of the nucleus (Aladesuyi Arogundade et al., 2019; Cooper-Knock et al., 2015; Y. B. Lee et al., 2013; K. Mori et al., 2013; Reddy et al., 2013; Z. Xu et al., 2013). However, the exact pathological mechanisms of RNA foci are unknown (Vatsavayai et al., 2018). In other diseases in which RNA foci are a pathological feature, such as myotonic dystrophy, there is strong evidence that foci sequester RNA-binding proteins, preventing binding and inducing splicing irregularities (Fardaei et al., 2001; Jiang et al., 2004; Mankodi et al., 2001; Miller et al., 2000). This is likely the case for C9orf72 RNA foci as they have been shown to co-localise and sequester multiple RNA binding proteins (Cooper-Knock et al., 2014, 2015; Y. B. Lee et al., 2013; Sareen et al., 2013). *In vitro*, RNA foci can form secondary structures, such as hairpins and quadruplexes, that have been hypothesised to enhance sequestration and subsequent loss-of-function in RNA-binding proteins (Conlon et al., 2016; Fratta et al., 2012; Kovanda et al., 2015; Reddy et al., 2013; Vatsavayai et al., 2018; Zamiri et al., 2015). However, co-localisation is a relatively low-frequency event, and often does not induce abnormal protein distribution; the presence of repeat-containing secondary structures is as yet undocumented clinically, undermining protein sequestration as the mechanism underlying RNA-mediated toxicity (Vatsavayai et al., 2018). Furthermore, conflicting studies have observed positive and negative correlations with the frequency of RNA foci and age-of-onset (DeJesus-Hernandez et al., 2017; Mizielinska et al., 2013), and a recent study found no correlation between RNA foci aggregation and cognitive decline (Mehta et al., 2020) suggesting a weak relationship between RNA foci and the clinical pathology of C9orf72 ALS.

1.2.2.2 Dipeptide repeat proteins

Translation of the HRE via repeat-associated non-AUG translation, facilitated by translocation of the HRE from the nucleus to the cytoplasm by the nuclear exporter, SRSF1 (Cooper-Knock et al., 2014; Hautbergue et al., 2017), gives rise to five sense and antisense DPRs: Glycine-Arginine (poly-GR), Glycine-Alanine (poly-GA) Proline-Arginine (poly-PR), Proline-Alanine (poly-PA) and Glycine-Proline (poly-GP). These DPRs have been observed in p62 positive, TDP-43 negative inclusions in the brains and, to a lesser extent, spinal cords of those with C9orf72 ALS (Al-Sarraj et al., 2011; Cooper-Knock et al., 2012; Gomez-Deza et al., 2015; Hsiung et al., 2012; Mahoney et al., 2012; Schipper et al., 2016; Troakes et al., 2012) and have been shown to predate even TDP-43 aberrations in C9orf72 ALS pathology (Baborie et al., 2015; Vatsavayai et al., 2016). Each of these DPRs has a relatively unique profile.

Poly-PA and poly-GP are uncharged, have a flexible coil structure and they do not form aggregates and therefore interact with fewer proteins (Freibaum & Taylor, 2017; K. H. Lee et

al., 2016). This points towards these non-arginine containing DPRs as being less toxic, which is consistent with findings from *Drosophila* models (Freibaum et al., 2015; K. H. Lee et al., 2016; Mizielinska et al., 2014; Wen et al., 2014), though poly-GP was shown to be toxic in the presence of a proteasome inhibitor (Yamakawa et al., 2015) and may be useful as a biomarker distinguishing C9orf72 ALS from other neurodegenerative disorders, as it is stable in the CSF during disease course (Gendron et al., 2017; Lehmer et al., 2017).

Poly-GA is also uncharged but has a compact aggregate structure, forming cytoplasmic amyloidogenic fibrils, thought to share properties with the amyloid-beta plaques associated with Alzheimer's disease (Brasseur et al., 2020; Chang et al., 2016; Edbauer & Haass, 2016; May et al., 2014). It has been shown to induce apoptosis and endoplasmic reticulum stress, inhibit proteasomes and dendritic branching *in vivo*, and is thought to sequester proteins involved in protein trafficking and the proteasome (Božič et al., 2022; Khosravi et al., 2020; F. Liu et al., 2022; May et al., 2014; Schludi et al., 2015; Y. J. Zhang et al., 2014). This is mimicked in mice models expressing poly-GA, which exhibit motor and cognitive impairment (Chew et al., 2015; Khosravi et al., 2020). Despite this, poly-GA causes little toxicity when compared to the arginine-containing DPRs, poly-GR and poly-PR.

Poly-GR and poly-PR are highly charged and polar with a flexible coil structure (Freibaum & Taylor, 2017). They induce strong levels of toxicity both *in vivo* and *in vitro* when compared to all other DPRs (Freibaum et al., 2015; K. H. Lee et al., 2016; Mizielinska et al., 2014; Tao et al., 2015; Wen et al., 2014). The cause of this toxicity arises from the disruption of multiple cellular processes including nucleolar function, nucleocytoplasmic trafficking, stress granule formation and mitochondrial function amongst others (Boeynaems et al., 2017; Choi et al., 2019a; Kanekura et al., 2016; Kwon et al., 2014; K. H. Lee et al., 2016; Lin et al., 2016; Lopez-Gonzalez et al., 2016; K. Y. Shi et al., 2017; Tao et al., 2015; Wen et al., 2014; White et al., 2019; Y. J. Zhang et al., 2018). Interaction with low complexity sequence domains (LCDs) in RNA binding proteins has been hypothesised as the mechanism by which these DPRs induce widescale functional changes. Amongst multiple cellular processes, LCDs are key in the formation and function of membrane-less organelles including the nucleolus, nuclear pore complex and stress granules (Brangwynne et al., 2015) significantly disrupting their function and structural dynamics, in particular liquid-liquid phase separation (LLPS) (Boeynaems et al., 2017; K. H. Lee et al., 2016; Lin et al., 2016; Molliex et al., 2015; White et al., 2019; Y. J. Zhang et al., 2018). In possible confirmation of these interactions, both DPRs have been shown to localise to the nucleolus (Kwon et al., 2014; K. H. Lee et al., 2016; Wen et al., 2014), which can interfere with RNA synthesis, ribosome biogenesis, translation and nucleocytoplasmic trafficking (Kanekura et al., 2016; Kwon et al., 2014; K. H. Lee et al., 2016; Tao et al., 2015), with nucleocytoplasmic trafficking impairment most likely driven by direct

interactions with nuclear pore and trafficking components (K. H. Lee et al., 2016; Lin et al., 2016; K. Y. Shi et al., 2017). Both cytoplasmic poly-PR and poly-GR have been shown to induce spontaneous stress granule formation and also delay their disassembly to induce a chronic stress like state in cells (Boeynaems et al., 2017; Y. J. Zhang et al., 2018). In addition, their effect on LLPS has been hypothesised to contribute to the fibrillisation of TDP-43 stress granules (Freibaum & Taylor, 2017; Molliex et al., 2015). Cytoplasmic poly-GR has also been shown to interact with ribosomal subunits, inhibiting canonical and non-canonical translation (Y. J. Zhang et al., 2018), as well as localising to the mitochondria, binding mitochondrial ribosomes and inducing DNA damage and oxidative stress, leading to mitochondrial dysfunction in iPSC-derived MNs (Lopez-Gonzalez et al., 2016). Expression of poly-GR in a mouse model of ALS that demonstrated synaptic dysfunction, behavioural abnormalities, DNA damage, microgliosis and neurodegeneration similarly showed that poly-GR can induce mitochondrial dysfunction by binding directly to complex V component ATP5A1, provoking ubiquitination and degradation (Choi et al., 2019b).

There is significant evidence that the C9orf72 HRE causes widescale disruption in the CNS and its prevalence as a causative factor in ALS make it a strong target for therapeutic intervention. It's links to the disruption of energy generation in ALS provide a specific area to target in the search for these interventions.

1.3 Metabolism in ALS

Reviews highlight compromised metabolism as an untapped area of potential for the treatment of ALS (Dupuis et al., 2011; Vandoorne et al., 2018). To maintain energy homeostasis and therefore overall health, a balance between energy expenditure and uptake is required (Vandoorne et al., 2018). ALS patients lack this balance. Energy uptake is often lowered in ALS patients and malnutrition is a common feature, in part due to dysphagia (Onesti et al., 2017) or loss of appetite (Holm et al., 2013). The malnutrition phenotype is associated with hypermetabolism, in which the body's basal metabolic rate becomes abnormally increased (Bouteloup et al., 2009). This is observed in up to 41% of ALS patients and correlates with an increased rate of functional decline and shortened survival (Steyn et al., 2018) and investigation has shown that resting metabolic rate and nutritional status correlate with disease duration and survival (Desport et al., 1999, 2005). Conversely, hyperlipidaemia is observed in up to 52% of ALS patients and can increase survival by up to 12 months (Dupuis et al., 2008; Kostic Dedic et al., 2012). *In vitro*, ALS patient derived-cells show distinct metabolic profiles compared to controls (Allen et al., 2014, 2015, 2019a, 2019b; Gerou et al., 2021; Valbuena et al., 2016, 2017; Veyrat-Durebex et al., 2016) and C9orf72 ALS has been demonstrated to

induce significant dysfunction in both glycolytic and mitochondrial energy generation. Neurons have the highest energy requirements in the human brain (Howarth et al., 2012) and are highly susceptible to alterations in energy metabolism (Vandoorne et al., 2018). This means that aberrations in energy generating pathways could have a significant impact on disease course.

Mitochondrial dysfunction is a characteristic feature of ALS (Bowling et al., 1993) in which they undergo both morphological and functional changes. Dense clusters of mitochondria are found in patient's spinal cords and mitochondrial swelling has been observed in MNs (Sasaki & Iwata, 1996; Siklós et al., 1996). Levels of mitochondrial DNA, the activity of complexes I+II, I+III and IV and the activity of mitochondrial enzyme, citrate synthase are downregulated in patient spinal cords and the prefrontal cortex (Alvarez-Mora et al., 2022; Wiedemann et al., 2002). Functional and morphological changes have also been observed in several C9orf72 models. Membrane hyperpolarisation, increased adenosine triphosphate (ATP) production and impaired complex III activity, alongside both elongated and shortened mitochondria, have been observed in C9orf72 fibroblasts (Alvarez-Mora et al., 2022; Onesto et al., 2016). iPSC-derived C9orf72 MNs have compromised calcium buffering, reduced mitochondrial membrane potential, impaired mitochondrial bioenergetic output, reduced gene expression of electron transport chain machinery, and dysfunctional axonal transport of mitochondrial cargo that is strongly linked to axonal dysfunction (Dafinca et al., 2016, 2020; Mehta et al., 2021). Disrupted endoplasmic reticulum-mitochondrial tethering has also been observed in C9orf72 iPSC-derived MNs and in a transgenic mouse model of C9orf72, potentially induced by DPR expression (Gomez-Suaga et al., 2022). It has been hypothesised this mitochondrial dysfunction may be triggered by glutamate excitotoxicity (Dafinca et al., 2016, 2020; Epstein et al., 1994), which mediates mitochondrial Ca^{2+} overload (Grosskreutz et al., 2010), or via oxidative stress (Alvarez-Mora et al., 2022; Carrì et al., 2015; Onesto et al., 2016), potentially facilitated by expression of cytoplasmic poly-GR (Choi et al., 2019a; Lopez-Gonzalez et al., 2016).

Alongside mitochondrial dysfunction, abnormalities in glycolytic pathways have also been observed (Manzo et al., 2019; Valbuena et al., 2016). The brain itself utilises glucose metabolism as its main source of energy and upwards of 20% of the body's total glucose derived energy is consumed by the brain (Mergenthaler et al., 2013). Physiologically, glucose is converted to pyruvate via glycolysis, subsequently entering the TCA cycle and the electron transport chain. FDG-PET on ALS patient brains has shown that glucose uptake in the brain is reduced (Pagani et al., 2014) which has been linked to disease severity (Dalakas et al., 1987). In the spinal cords of individuals with ALS, glucose metabolism was increased, which was not coupled to spinal blood flow (Yamashita et al., 2017), despite this process typically being tightly coupled physiologically (Vandoorne et al., 2018). Glycogen metabolism

alterations have also been observed in ALS cell models (Allen et al., 2019a), likely caused by a reduction in glycogen phosphorylase, phosphoglucomutase and α-glucosidase (Allen et al., 2019b; Dodge et al., 2013), leading to reduced glycogen mobilisation and potentially contributing to reduced bioenergetic output in patients (Dodge et al., 2013). A reduction in fructose metabolism has also been observed in ALS patient derived induced neuronal progenitor cell (iNPC) astrocytes (iAstrocytes) (Allen et al., 2019a), though this is unlikely to be caused by the direct breakdown of fructose, and more likely from dysfunction downstream of fructose (Allen et al., 2019b). Fructose is a potent glycating agent, driving the production of advanced glycation end products through glycolysis, which interfere with multiple cellular functions including lipid metabolism, mitochondrial metabolism and antioxidant defence (Hamada et al., 1996) and has been linked to ALS previously (Juranek et al., 2015; Kaufmann et al., 2004; M. J. Kim et al., 2018). The glyoxalase (Glo) system, consisting of the enzymes Glo-1 and -2, is in place to prevent this, however, a significant downregulation in these enzymes has been observed in C9orf72 ALS iAstrocytes (Allen et al., 2019b). Therefore, the action of Glo-1 enzymes may be a key pathway in the induction of oxidative stress and mitochondrial dysfunction in ALS.

The above evidence demonstrates that metabolism in ALS warrants further investigation and presents itself as a compelling target for possible therapies. One of the major regulators of energy metabolism in the CNS are astrocytes, that can regulate energy generation for MNs.

1.4 Astrocytes

ALS, is a non-cell autonomous disease, affecting a wide range of cells in the body, including astrocytes. Astrocytes are one of the major glial cells, found in the brain and spinal cord that constitute 20-40% of all glial cells (Gaudet & Fonken, 2018). Astrocytes play crucial roles in supporting MNs in the CNS, controlling cerebral blood flow (Mulligan & MacVicar, 2004), shaping synaptic connectivity (Eroglu & Barres, 2010), regulating synaptic transmission (Araque et al., 1998), controlling composition of the extracellular space (Wiese, 2012) and maintaining the blood brain barrier (Abbott et al., 2006). Importantly, astrocytes play a key role in regulating energy metabolism in MNs (Bélanger et al., 2011). According to the lactate shuttle hypothesis, lactate is generated by anaerobic glucose metabolism, stimulated by glutamate, which is subsequently delivered to neurons and utilised as a fuel source (Pellerin & Magistretti, 1994). Because of their important role in neuronal regulation, astrocytes also play an important role in neurodegenerative disease, undergoing morphological and physiological changes, and often transitioning into a state of astrogliosis that can have both beneficial and detrimental effects on neuronal health (for a recent review see Brandebura et al., 2022). C9orf72 derived

iAstrocytes have been shown to be toxic to control MNs in co-culture (Meyer et al., 2014), which can be ameliorated by inhibition of SRSF1 (Hautbergue et al., 2017) and restoring depleted levels of the microRNA miR-494-3p (demonstrating the importance of extracellular vesicle dysfunction in C9orf72 astrocytes) (Varcianna et al., 2019). iPSC-derived C9orf72 iAstrocytes demonstrate aberrant glutamate content, enhanced oxidative stress and impaired antioxidant defence mechanisms, and their conditioned media is toxic to control MNs (Birger et al., 2019; Fomin et al., 2018) whilst MNs co-cultured with C9orf72 iPSC-derived astrocytes show electrophysiological dysfunction (C. Zhao et al., 2020). Mouse models expressing the C9orf72 HRE, and poly-GA also exhibit astrogliosis that actually precedes neurodegeneration (Chew et al., 2015, 2019; Y. J. Zhang et al., 2016).

There is emerging evidence of purine/pyrimidine dysfunction in ALS models (Lehmkuhl et al., 2021; Loganathan et al., 2022; Veyrat-Durebex et al., 2019). Recent work from our laboratory has demonstrated that purine metabolism is dysfunctional in C9orf72 iAstrocytes, whilst supplementing iAstrocytes with the purine nucleoside inosine reduced iAstrocyte mediated MN death, suggesting that astrocyte purine metabolism may play a key role in astrocyte cross-talk with MNs (Allen et al., 2019a).

1.5 Purine Metabolism

Cellular purine metabolism is comprised of *de novo* purine biosynthesis (DNPB), purine salvage and purine degradation (Figure 1.5A-B).

DNPB begins with the breakdown of glutamine 5-phosphoribosyl-1-pyrophosphate (PRPP) in to 5-phosphoribosyl-1-amine and ends at the production of inosine monophosphate (IMP), which can then be converted into guanosine monophosphate (GMP) or adenosine monophosphate (AMP) (Figure 1.5A) (Buchanan & Hartman, 1959; Greenberg & Jaenicke, 1957; Hartman & Buchanan, 1959). The flux of substrates generated by DNPB is facilitated largely by the purinosome, which involves the six purine biosynthetic enzymes clustering to form a dynamic multienzyme complex in conditions of high purine demand (An et al., 2008).

Purine salvage is the predominant source of purine nucleosides under normal conditions and involves the recycling of degraded bases via the reconversion of hypoxanthine and guanine (derived from inosine and guanosine via breakdown by purine nucleoside phosphorylase (PNP)) to IMP and GMP respectively, catalysed by the enzyme hypoxanthine-guanine phosphoribosyltransferase (HGPRT) (Figure 1.5B) (Henderson & Khoo, 1965; Murray, 1971; Yamaoka et al., 1997). Alternatively, hypoxanthine and guanine can be broken down to urate through the action of xanthine oxidoreductase (XOR), that exists as xanthine dehydrogenase

(XDH) in normal conditions, or as xanthine oxidase (XO) during cell stress. This process constitutes the purine degradation pathway (Figure 1.5B) (Corte & Stirpe, 1972). Metabolic flux through *DNPB* and salvage is strongly linked. Production of GMP and IMP can regulate DNPB, as both nucleotides are allosteric inhibitors of PRPP amidotransferase (PPAT) (Zhou et al., 1994), whilst PRPP is also an allosteric activator of PPAT (Boer & Sperling, 1995). Conversely, purine salvage is regulated by the availability of its substrates, chiefly PRPP, which is a co-substrate in both hypoxanthine and guanine salvage (Camici et al., 2018).

Purine metabolism is essential in the body as it is responsible for the production of key DNA and RNA nucleotides and is therefore required for DNA synthesis, particularly to meet the high nucleotide demand during cell development (Ansoleaga et al., 2015; Pedley & Benkovic, 2017). Moreover, purine metabolism produces important metabolites, including adenosine, that can be utilised for the generation of other metabolic intermediates. Adenosine plays a crucial role in cellular energy transfer as a key constituent of AMP, adenosine diphosphate (ADP) and ATP (Ansoleaga et al., 2015). Further, the breakdown of inosine, the direct downstream product of adenosine, into hypoxanthine also produces ribose-1-phosphate which enters glycolysis via the pentose phosphate pathway to generate energy (Balestri et al., 2007; Jurkowitz et al., 1998; Litsky et al., 1999; Módis et al., 2013). This is a particularly important pathway during times of cells stress and when energy generation is impaired in glial cells, as it has the advantage of bypassing the energy consuming glycolytic enzyme, hexokinase (Balestri et al., 2007; Jurkowitz et al., 1998; Litsky et al., 1999). Purine bases are also used to form cofactors for enzymatic reactions, for example adenosine is a component of S-adenosylmethionine (SAM), which is formed from the combination of ATP and methionine, and is crucial for SAM-facilitated methylation of nucleic acids and metabolic intermediates (Cantoni, 1953). The chief degradation product of purine metabolism, urate, is also hypothesised to be a potent antioxidant (Ames et al., 1981) stabilising antioxidant systems (Hink et al., 2002) and blocking iron-dependent oxidation reactions (Whiteman et al., 1996), which may be neuroprotective (Chen et al., 2012; Chen et al. 2013).

We have recently demonstrated that one of the key enzymes involved in purine metabolism, adenosine deaminase (ADA), might be linked to C9orf72 ALS pathology in iAstrocytes.

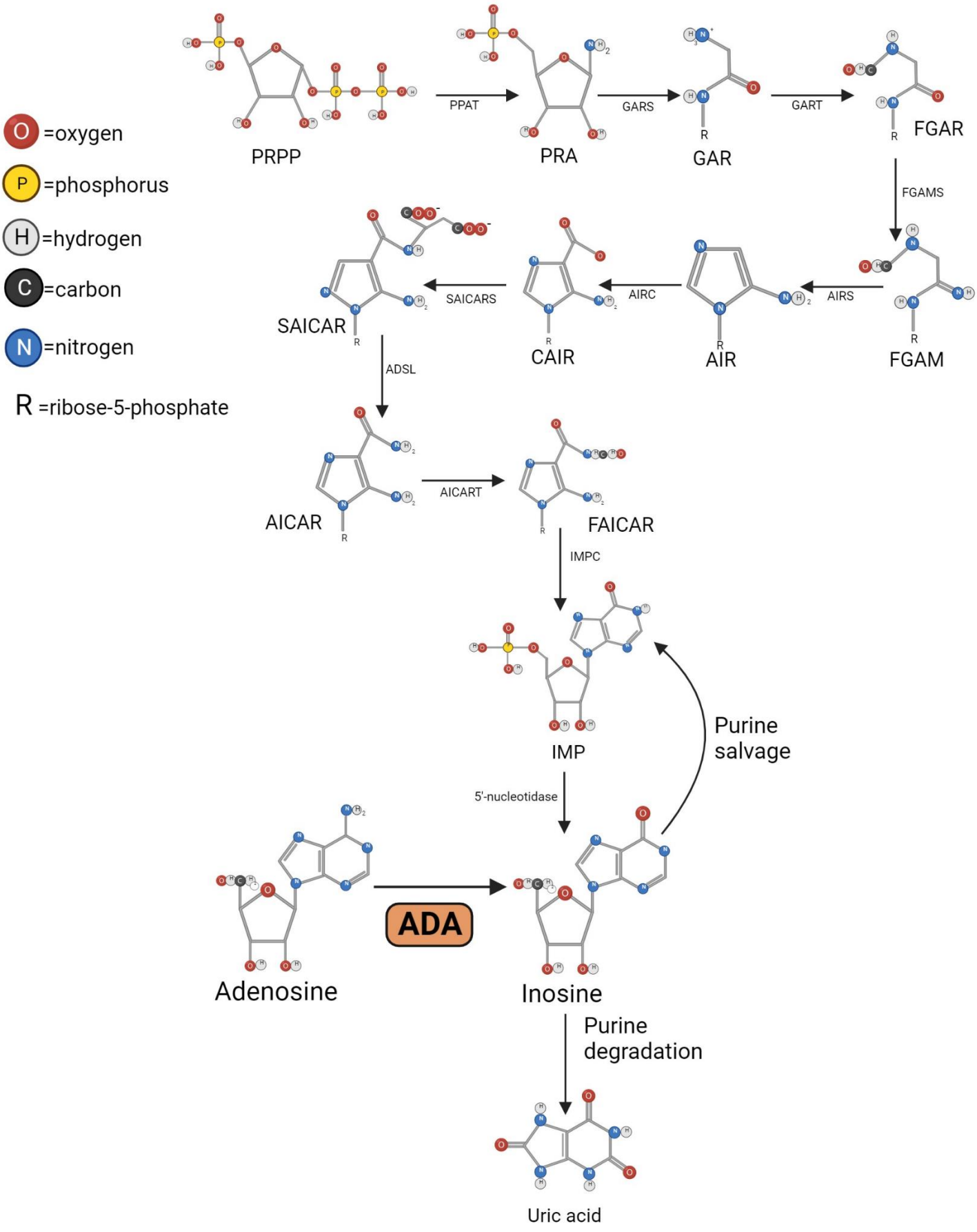
O =oxygen
P =phosphorus
H =hydrogen
C =carbon
N =nitrogen
R =ribose-5-phosphate
PRPP
PPAT
PRA
GARS
GAR
GART
FGAR
FGAMS
FGAM
AIRS
AIR
AIRC
CAIR
SAICARS
SAICAR
ADSL
AICAR
AICART
FAICAR
IMPC
IMP
Purine salvage
5'-nucleotidase
ADA
Adenosine
Inosine
Purine degradation
Uric acid

Figure 1.5A. *De novo* purine biosynthesis. DNPB, is composed of the following intermediates: 5-phosphoribosyl-1-pyrophosphate (PRPP); phosphoribosylamine (PRA); glycinamide ribonucleotide (GAR); N-formylGAR (FGAR); N-formylglycyamidine ribonucleotide (FGAM); aminoimidazole ribonucleotide (AIR); carboxyAIR (CAIR); succinylaminoimidazolecarboxamide ribotide (SAICAR); aminoimidazolecarboxamide ribotide (AICAR); *De novo* purine biosynthesis (DNPB); formAICAR (FAICAR); and inosine monophosphate (IMP); and the enzymes: phosphoribosyl pyrophosphate aminotransferase (PPAT); GAR synthase (GARS); GAR transformylase (GART); FGAM synthase (FGAMS); AIR synthetase (AIRS); AIR carboxylase (AIRC); SAIRCAR synthase (SAIRCARS); adenylosuccinate lyase (ADSL); AICAR transformylase (AICART); and IMP cyclohydrolase (IMPC). IMP produced by DNPB can then enter the purine salvage pathway or be broken down via the purine degradation pathway. Figure taken, with permission, from Hall et al., (2022).

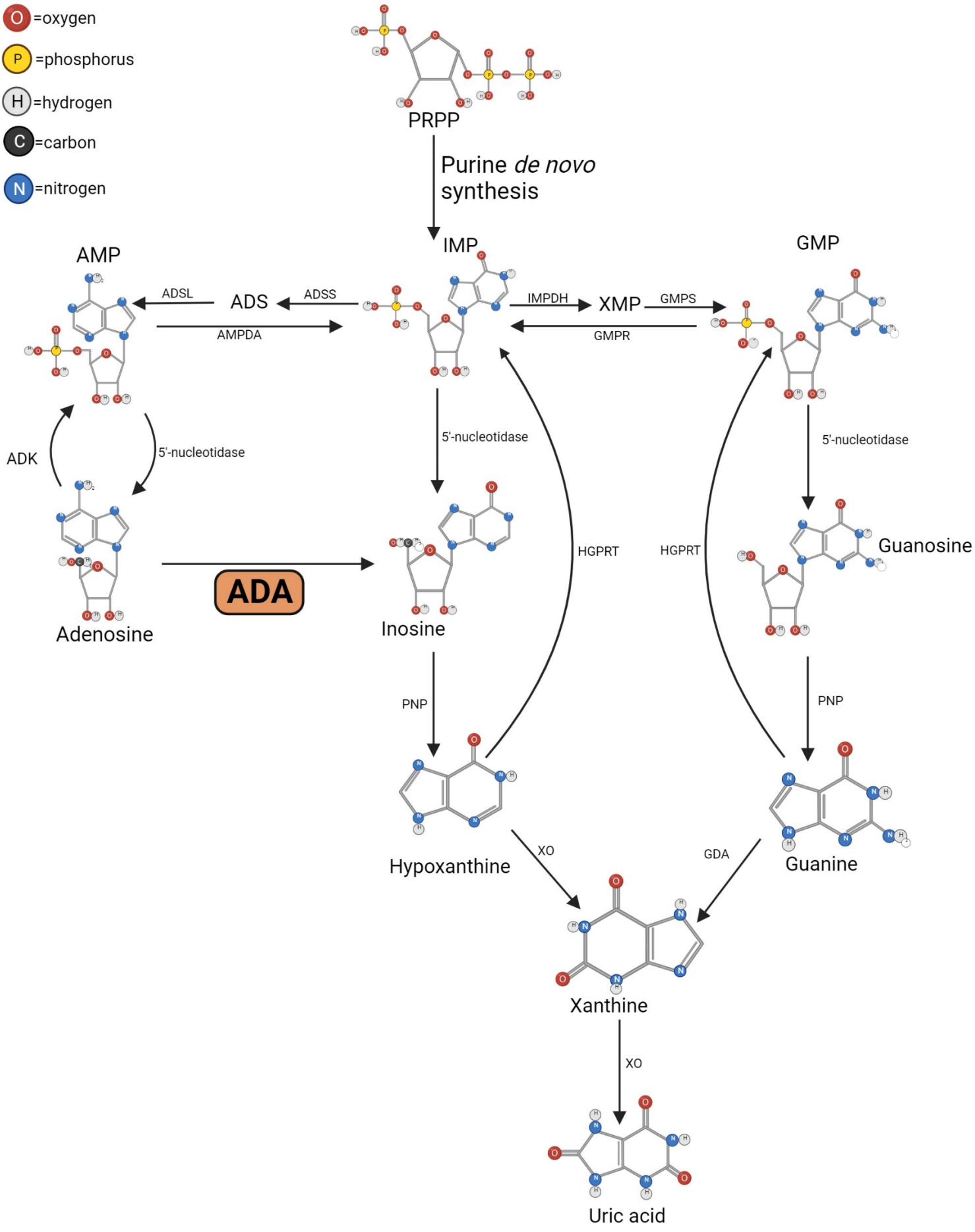
O =oxygen
P =phosphorus
H =hydrogen
C =carbon
N =nitrogen
PRPP
Purine *de novo* synthesis
IMP
AMP
GMP
ADSL
ADS
ADSS
AMPDA
IMPDH
XMP
GMPS
GMPR
ADK
5'-nucleotidase
5'-nucleotidase
5'-nucleotidase
Adenosine
ADA
Inosine
HGPRT
HGPRT
Guanosine
PNP
PNP
Hypoxanthine
Guanine
XO
GDA
Xanthine
XO
Uric acid

Figure 1.5B. Purine salvage and degradation. The purine salvage and degradation pathways involve the intermediates: adenosine monophosphate (AMP); adenylosuccinate (ADS); inosine monophosphate (IMP); xanthine monophosphate (XMP); guanosine monophosphate (GMP); adenosine; inosine; guanosine; hypoxanthine; guanine; xanthine and urate; and the enzymes: ADS lyase (ADSL); ADS synthase (ADSS); AMP deaminase (AMPDA); IMP dehydrogenase (IMPDH); GMP synthase (GMPS); GMP reductase (GMPR); adenosine kinase (ADK); 5'nucleotidase; adenosine deaminase (ADA); hypoxanthine-guanine phosphoribosyltransferase (HGPRT); purine nucleoside phosphorylase (PNP); xanthine oxidase (XO) and guanine deaminase (GDA). IMP generated via DNPB can be interconverted between AMP and GMP. AMP and IMP are both broken down to inosine and GMP is broken down into guanosine, which are further degraded to hypoxanthine and guanine respectively. Hypoxanthine and guanine can then either follow purine salvage and be reconverted to IMP or enter the purine degradation pathway and be broken down into urate. Figure taken, with permission, from Hall et al., (2022).

1.6 Adenosine deaminase

ADA is a vital enzyme in the body and emerging evidence of its involvement in numerous disorders that affect the CNS from our laboratory and others corroborate this theory (for a recent review see Hall et al., 2022).

ADA acts at a key junction in purine metabolism, as a precursor to purine salvage and degradation, by catalysing the irreversible hydrolytic deamination of adenosine and deoxyadenosine to inosine and deoxyinosine respectively, substituting a molecule of ammonia for a keto group, a reaction first described in 1936 (Conway and Cooke, 1938), (Figure 1.6A). The importance of ADA is highlighted by its substrates, as both adenosine and deoxyadenosine are crucial for maintaining homeostasis in the body. Adenosine has multiple important functions in the body, as outlined above and deoxyadenosine is a base (A) in double-stranded DNA. Both molecules and their breakdown products, inosine and deoxyinosine, are also key intermediaries in purine metabolism (Fox and Kelley, 1978).

There are two isoenzymes of ADA, ADA1 and ADA2, that are coded for by two different gene loci. The 363 amino acid ADA1 protein was initially purified from human erythrocytes and is a single polypeptide chain with a molecular weight of 41kDa (Daddona & Kelley, 1977; Venkatesh & Oommen, 1998). It is coded for by the 32-Kb *ADA* gene on chromosome 20q13.11 which is composed of 12 exons (Petersen et al., 1987). Monomeric ADA1 consists of a polypeptide chain folded in α/β barrels that surround the active site, in which substrates are stabilised by hydrogen bonds, using Zn^{2+} as a cofactor (Figure 1.6B) (Wilson and Rudolph, 1991). ADA1 can also exist as a heterooligomeric dimer which has an estimated molecular

weight of 213kDa, and consists of two ADA subunits bound to dipeptidyl peptidase IV (DPP4/CD26) on the cell surface, facilitating the extracellular breakdown of adenosine (Figure 1.6C) (Kameoka et al., 1993; Weihofen et al., 2004). ADA2, also known as ADA related growth factor in insects and first identified in the spleen (Schrader et al. 1978), is mechanistically similar to ADA1, also catalysing the breakdown of adenosine and deoxyadenosine. However, it is coded for by the *CECR1* (cat eye syndrome chromosome region, candidate 1) gene (Riazi et al., 2000), now referred to as the *ADA2* gene (Ombrello et al., 2019) that spans 10 exons on chromosome 22q11.1. The ADA2 protein exists as a comparatively complex homodimer, with a unique α helical domain located in the N-terminal region. This mediates the dimerisation of its two identical subunits (Anton V. Zavialov et al., 2010), giving it an estimated molecular weight of 100kDa (Ratech et al., 1981). Despite low sequence homology, ADA2 is structurally similar to ADA1, forming an eight stranded parallel β-sheet surrounded by an α/β, TIM barrel (Anton V. Zavialov et al., 2010). The active site is functionally similar to ADA1 but has a markedly different hydrophobic binding pattern, differing in both the structure of ligand binding segments and in distribution of the hydrophobic sidechains (amongst several other structural divergences), which lead to the specificity between certain inhibitors of ADA1 and ADA2 (Anton V. Zavialov et al., 2010). The contrasting active site structure means ADA2 has a 100-fold lower Km for adenosine, and an optimum pH of 6.8 (Zavialov and Engström, 2005) which is acidic compared to ADA1's optimum pH of 7-7.4 (Van Der Weyden and Kelley, 1976). The isomers also differ in their distribution, ADA1 is ubiquitous in humans whereas ADA2 is active only in monocytes-macrophages, coexisting with ADA1 (Ungerer et al., 1992).

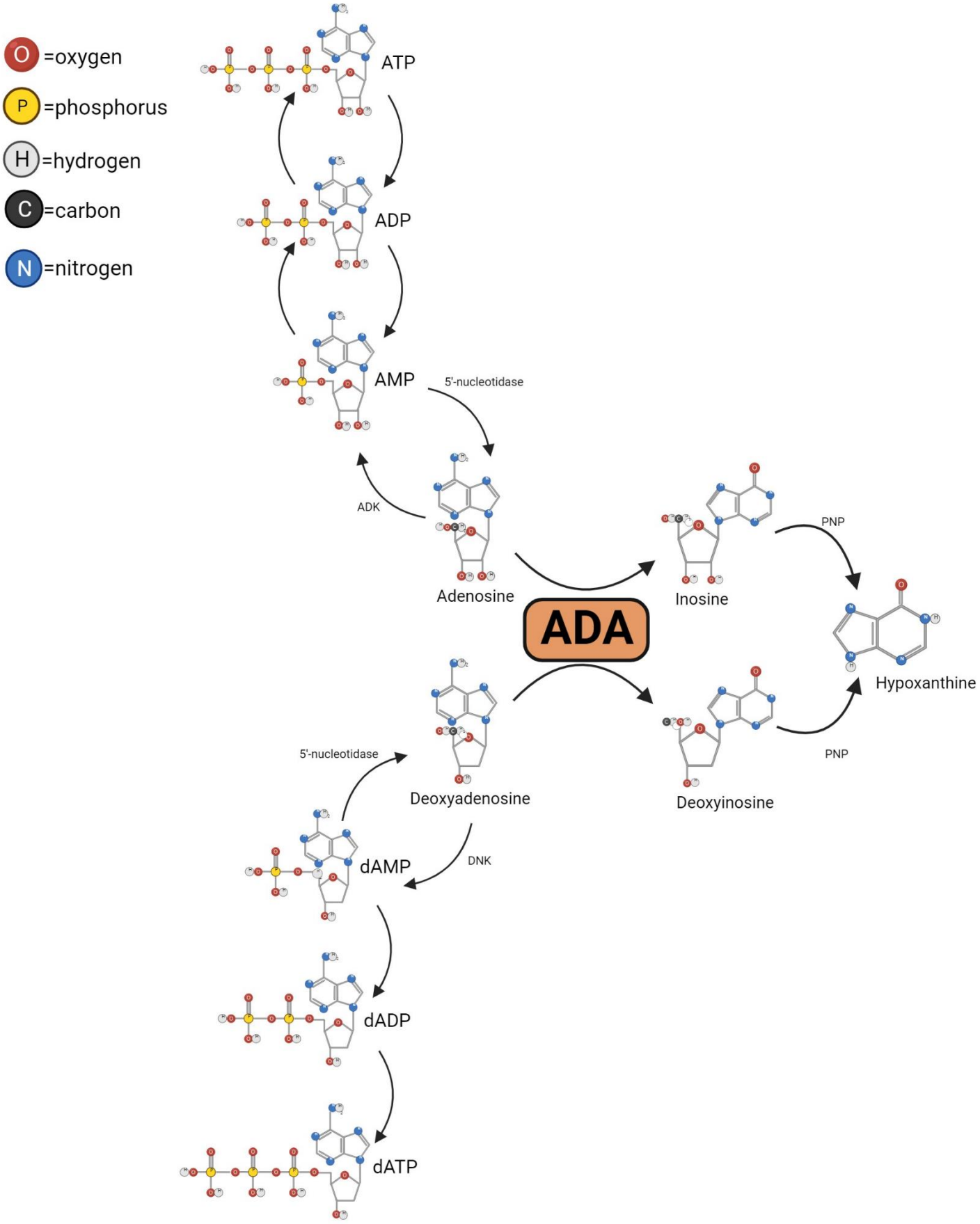
O =oxygen
P =phosphorus
H =hydrogen
C =carbon
N =nitrogen
ATP
ADP
AMP
5'-nucleotidase
ADK
Adenosine
ADA
Inosine
PNP
Hypoxanthine
Deoxyadenosine
Deoxyinosine
PNP
5'-nucleotidase
dAMP
DNK
dADP
dATP

Figure 1.6A. Adenosine metabolism. Adenosine trisphosphate (ATP) and deoxyATP (dATP) are dephosphorylated to form adenosine and deoxyadenosine respectively. They are then converted to inosine and deoxyinosine by adenosine deaminase (ADA) and are both broken down to hypoxanthine by purine nucleoside phosphorylase (PNP). Abbreviations: ADP, adenosine diphosphate; AMP, adenosine monophosphate; ADK, adenosine kinase; DNK, deoxynucleoside kinase. Figure taken, with permission, from Hall et al., (2022).

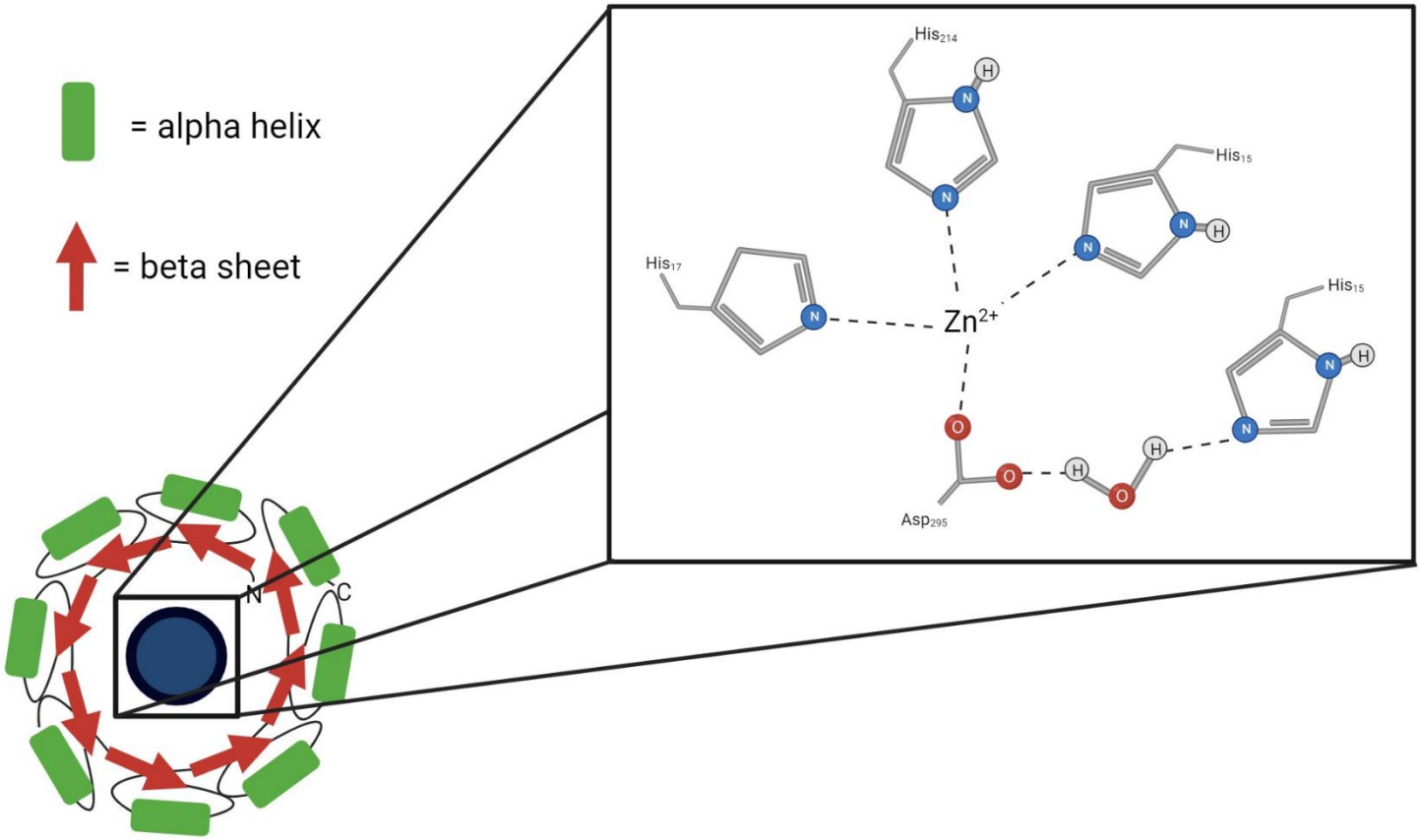

Figure 1.6B. ADA structure and active site. Adenosine structure consisting of a single polypeptide chain folded in α/β barrels that surround the active site, using Zn^{2+} as a cofactor, coordinated by binding to His15, His17, His 214 and Asp295. Figure taken, with permission, from Hall et al., (2022).

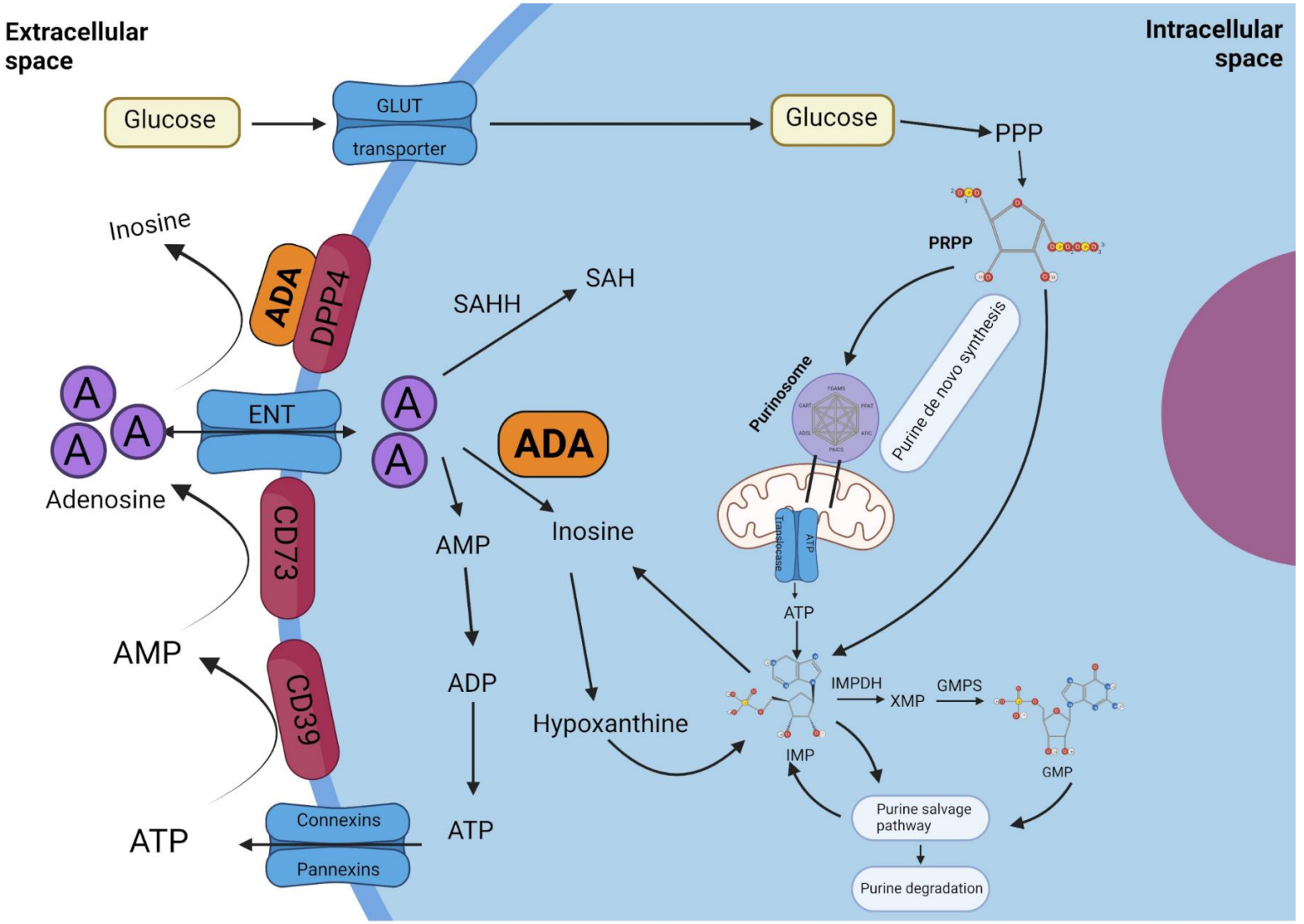

Figure 1.6C. Adenosine and purine metabolism in the cell. A representation of extra- and intercellular regulation of adenosine and purine metabolism. Ribose-5-phosphate, derived from glucose enters the *de novo* purine biosynthesis (DNPB) pathway via the purinosome which is co-localised to the mitochondria or via traditional purine synthesis to generate inosine monophosphate (IMP). IMP transitions between adenosine monophosphate (AMP) and guanosine monophosphate (GMP) and can also enter purine salvage and purine degradation pathways. Adenosine breakdown into inosine, catalysed by adenosine deaminase (ADA) is also represented. Extracellular ATP can be broken down by the cell surface enzymes CD39 and CD73 into adenosine, which can then be converted into inosine by ADA anchored to dipeptidyl peptidase 4 (DPP4), re-enter the cell via equilibrative nucleoside transporters (ENT; pictured) or can bind to adenosine receptors (not depicted). Adenosine can then be converted to inosine by ADA or combine with homocysteine to form S-Adenosylhomocysteine (SAH), catalysed by SAH hydrolase (SAHH). Abbreviations: GLUT, glucose transporter; PPP, pentose phosphate; PRPP, 5-phosphoribosyl-1-pyrophosphate;

IMPDH, inosine monophosphate dehydrogenase; XMP, xanthine monophosphate; GMPS, guanosine monophosphate synthetase. Figure taken, with permission, from Hall et al., (2022).

1.7 Conservation

ADA1 is an ancient enzyme, expressed by both prokaryotes and eukaryotes (Kathiresan et al., 2013). Recent phylogenetic analysis of over 240 genomes has indicated that whilst ADA1 is widespread, it may not be universal as it was not detected in plants, low fungi, some insect species, and some pathogenic eukaryotes (Skaldin et al., 2018). ADA2 was found in higher fungi and most animals, but with a non-uniform phylogenetic distribution, suggesting that ADA1 may compensate for the loss of ADA2 cell signalling function as ADA1 can be found extracellularly (Franco et al., 1997). Data also indicates that ADA2 is an ancient protein, originating in prokaryotes and may have been transferred between bacteria by horizontal gene transfer. Bioinformatic analysis suggested that bacterial ADA2 is a close homologue of eukaryotic ADA2 predicting homodimer formation, secretion into the extracellular space, and similar catalytic activities of both proteins (Dolezal et al., 2005).

As ADA1 is the most common and widely researched isoenzyme and the target of this project, further reference to 'ADA' will therefore refer to ADA1 and any mention of ADA2 will be specified.

1.8 Regulation

The regulation of ADA is complex, as it is facilitated by several factors. This is due to the ubiquitous nature of the enzyme and its involvement in wide-ranging cellular processes.

1.8.1. Transcriptional regulation

The *ADA* gene is a direct target of the transcription factors p63 and p73, homologs of the p53 tumour suppressor gene, which is involved in regulating apoptosis and the cell cycle (Jost et al., 1997; Kaghad et al., 1997; Yang et al., 1998). The *p63* and *p73* genes code for several isoforms. Depending on the promoter p63 and p73 are transcribed from, they can have either an N-terminal transactivating domain (TA) (Kaghad et al., 1997; Yang et al., 1998) or a truncated N-terminal region (ΔN) that does not contain the TA-domain (Yang et al., 1998, 2000). p63 and p73 can also be spliced at the C-terminal region giving rise to several further isoforms (typified as α, β, γ etc.) (Murray-Zmijewski et al., 2006; Marshall et al. 2021). The TA and ΔN isoforms of p63 and p73 have been purported to have some conflicting functions, but both are associated with ADA induction (Sbisà et al., 2006; Tullo et al., 2003). Reductions in ADA activity lead to an accumulation of deoxyadenosine, that in turn leads to a build-up of

deoxyadenosine triphosphate (dATP), inhibiting ribonucleotide reductase and causing an imbalance in other dNTP molecules (Cohen et al., 1978). This causes disruption of both DNA repair and DNA synthesis which has been shown to lead to activation of p73α and β, increasing ADA mRNA activation by binding to intron 1 of the *ADA* gene through p53 responsive elements (Tullo et al., 2003). Inducible p73α expression in a human osteosarcoma SAOS-2 cell line led to an increase in ADA levels and concomitant purine metabolism changes including upregulation of adenosine and inosine (Tullo et al., 2003). Similarly, p53 responsive elements that interact with TA-p63α and ΔN-p63α have been reported in the *ADA* gene promoter region - overexpression of these isoforms confers transcriptional activation in MCF and 293T-Rex lines, whilst in epidermal keratinocytes, p63 knockdown correlated with a decrease in mRNA and protein levels of ADA (Sbisà et al., 2006). These data imply that modulating p73 and p63 levels may directly affect ADA activity, though the process may involve feedback mechanisms via the purine salvage pathway, as it is unclear how an increase in ADA levels causes adenosine levels to rise, as presented in Tullo et al., (2003).

ADA regulation has also been linked with the transcription factor Sp1 through binding of Sp1 to the *ADA* gene promoter (Xie et al., 1999). Sp1 regulates cell differentiation, immune signalling, DNA repair, apoptosis, and chromatin remodelling. Dusing and Wiginton (1994) demonstrated that the ADA promoter region contains six Sp1 binding sites. Knockout of these sites also showed that Sp1 was necessary but not sufficient by itself for high levels of ADA expression (Dusing and Wiginton, 1994).

1.8.2. Cell signalling regulation

Activity of ADA has been linked to the mitogen activated protein kinases (MAPK) pathway (Eguchi, 2020). The MAPK signalling pathway is activated in protein kinase cascades which consist of extracellular signal-regulated kinases (ERKs), Jun amino-terminal kinases (JNKs), and stress activated protein kinases pathways (SAPKs) (Boulton et al., 1990; Dérijard et al., 1994; Han et al., 1994). MAPK signalling is an important regulator of cell proliferation, differentiation, and death (for a review see Morrison, 2012). Eguchi et al., (2020) demonstrated that fibroblast growth factor 2 (FGF2) binding to FGF receptors, activated tyrosine kinase signalling, leading to downstream activation of ERK, JNK and SAPK. This induced an increase in ADA expression and activity (along with ecto-5'-nucleotidase (CD73)) in rat spinal cord astrocytes, whilst inhibition of both the FGF2 receptor and MAPKs downregulate ADA expression (Eguchi, 2020). These data demonstrate that the FGF2/MAPK pathway is an important regulator of ADA amongst other purine metabolism enzymes.

Evidence has also shown that ADA expression levels can be regulated by 17β-oestradiol (E2), a member of the oestrogen family and a hormone that also modulates the expression of

enzymes in the purine and pyrimidine biosynthesis pathways. Treating MCF-7 human breast cancer cells with E2 induces ADA mRNA activation, a finding that can be recapitulated with the use of tamoxifen - a breast cancer treatment drug (Xie et al., 1999).

1.9 Function

ADA's primary function is within the purine salvage pathway, but it also plays a role in regulation of the immune response through its control of adenosine levels. Pharmacological estimates of basal extracellular adenosine concentrations typically lie between 25-250nM (Dunwiddie and Masino, 2001), but in instances of cell stress such as hypoxia or tissue damage, adenosine levels spike rapidly (Winn et al., 1981). This spike in adenosine leads to immunosuppression via activation of the A_{2A} receptor, leading to an accumulation of intracellular cyclic AMP (cAMP) and inhibition of the immune response (Henney and Lichtenstein, 1971), thus preventing edema and excessive inflammation (Sitkovsky and Ohta, 2005; Fredholm, 2007). However, the immunosuppressant-role of A_{2A} activation is context dependent (Ingwersen et al., 2016), and can become pro-inflammatory in the presence of high glutamate levels (Dai et al., 2010). Furthermore, persistently high levels of adenosine can lead to tissue damage (Van Linden and Eltzschig, 2007) and ADA tethered to DPP4 therefore functions to reduce potentially harmful extracellular adenosine levels and prevent chronic activation of adenosine receptors.

ADA also plays a key role in the differentiation and function of immune cells. Monocytes are white blood cells that can differentiate into macrophages and dendritic cells. During the early stages of monocyte maturation and differentiation into macrophages, ADA activity is significantly increased (Fischer et al., 1976) with $ADA^{-/-}$ mice developing aberrant dendritic cells that have proangiogenic and proinflammatory properties (Novitskiy et al., 2008). ADA2 has also been shown to induce monocyte to macrophage differentiation (Andrey V. Zavialov et al., 2010) suggesting both ADA and ADA2 play an important role in immune cell differentiation. ADA is also required for macrophage activation by regulating superoxide generation, a process that is key for killing phagocytosed bacteria (Johnston Jr. et al., 1975), as ADA activity correlates with superoxide generation (Tritsch & Niswander, 1981; Yagawa & Okamura, 1981).

In T-lymphocytes an accumulation of deoxyadenosine due to loss of ADA leads to increased levels of dATP, which concomitantly inhibits DNA synthesis, preventing T-lymphocyte differentiation (Carson et al., 1979). ADA also facilitates the immune response of T-lymphocytes. Extracellular ADA breaks down adenosine, preventing T-lymphocyte adenosine receptor activation and therefore inhibiting immunosuppression (Dong et al., 1996). Moreover, ADA can activate the immune response by sending costimulatory signals to T-cells via DPP4

binding (Martín et al., 1995). ADA also 'bridges' between adenosine receptors on dendritic cells and DPP4 on T-cells (Pacheco et al., 2005; Moreno et al., 2018), which can induce T-lymphocyte proliferation and increase the production of proinflammatory cytokines (Pacheco et al., 2005), this also leads to the increased generation of T-effector cells, T-memory cells and regulatory T-cells (Martinez-Navio et al., 2011). ADA is also key for B lymphocyte differentiation as $ADA^{-/-}$ mice develop B lymphocytes with proliferative, activational and structural defects and an increasing propensity to undergo apoptosis, likely caused by dATP and S-adenosylhomocysteine (SAH) accumulation as observed in T-lymphocytes (Aldrich et al., 2003). This demonstrates the vital function of ADA in not only immune cell generation but also in overall function and makes ADA an important choreographer of the body's immune response.

1.10 ADA in the CNS

ADA can function as a neuromodulator via the regulation of adenosine. Adenosine modulates activity in the brain via the G-protein-coupled receptors, A_1, A_{2A}, A_{2B} and A_3 with the A_1 and A_3 receptors coupling $G_{i/o}$ receptors and A_{2A} and A_{2B} receptors coupling G_s receptors (Dunwiddie and Masino, 2001). This coupling means activation of A_1 and A_3 receptors inhibits adenylyl cyclase activation, preventing the conversion of ATP to cAMP; conversely, activation of A_{2A} and A_{2B} receptors stimulates adenylyl cyclase activation, promoting cAMP production. The A_1 receptor has the highest affinity for adenosine and is widely expressed in tissues of the brain (Dixon et al., 1996); its activation is coupled with the inhibition of Ca^{2+} influx (Dolphin et al., 1986) and the activation of K^+ influx (Trussell and Jackson, 1985). This mechanism prevents the release of neurotransmitters such as dopamine, glutamate, and acetylcholine amongst others, effectively reducing excitability (Dunwiddie and Masino, 2001). A_{2A} receptor expression can also be found in all brain regions (Dixon et al., 1996) and is coupled with Ca^{2+} inhibition. The A_{2B} and A_3 receptors are similarly widely expressed in the brain but at very low levels (undetectable by *in situ* hybridisation in the rat brain (Dixon et al., 1996)) and have very low affinities for adenosine in comparison to the A_1 and A_{2A} receptors and are thus less well characterised. However, activation of A_{2B} in the CNS has recently been shown to improve intestinal barrier function via the vagus nerve (Ishioh et al., 2021) and protect against ischemic damage (Dettori et al., 2021); and A_3 receptor activation can induce a PKC-dependent inhibition of group 3 metabotropic glutamate receptor (mGluR) function at the Schaffer collateral-CA1 synapse, inhibiting neurotransmission (Macek et al., 1998). The physiological roles of adenosine in the brain include the regulation of the sleep-wake cycle (Z. Huang et al., 2014), coupling cerebral blood flow with energy demands (Winn et al., 1981), modulating synaptic plasticity (Sebastião et al., 2001), the prevention/repair of ischemic damage

(Rudolphi et al., 1992), motor function (El Yacoubi et al., 2000), astrocyte function (Florian et al., 2011), aging (Castillo et al., 2009; Costenla et al., 2011) and feeding (K. Lee et al., 2005).

Any disturbance therefore in the regulation of adenosine can have catastrophic effects on homeostasis in the brain, hence the prominent role ADA aberration plays in various disease pathologies.

1.11 Mutations and Splicing

Mechanisms leading to ADA dysregulation are caused by alterations at the level of transcription, translation, or alterations in the protein itself. A reduction in the levels (or complete loss) of ADA protein can arise through mutations that repress transcription of the *ADA* gene or decrease the stability of the encoded mRNA or protein. Whilst mutations that reduce substrate or cofactor (Zn^{2+}) binding in the active site, or change key catalytic residues, have also been reported, that give rise to ADA with reduced enzymatic activity. Alternatively, in the absence of changes to the nucleotide sequence, altered epigenetic regulation of the *ADA* gene may be responsible for increases or decreases in ADA levels.

A high number of ADA mutations lead to severe combined immunodeficiency (SCID) (Atasoy et al., 1993; Santisteban et al., 1993; Hershfield, 2003; Kalman et al., 2004). These mutations arise from premature stop codons, DNA deletions or insertions, amino acid substitutions, RNA splicing defects and post-translational modification defects. In terms of splicing, it has been historically hypothesised that, despite mutations being present in people, low levels of "normal" pre-mRNA splicing may still occur. Moreover, the level of splicing efficiency may be linked to ADA activity levels and therefore clinical severity (Santisteban et al., 1993; Arredondo-Vega et al., 1994). Mutation in the last acceptor splice site in the *ADA* gene led to aberrant splicing, which altered the structure of the ADA protein, adding a short tail residue section leading to protein instability, loss of ADA activity and disease (Arredondo-Vega et al., 2002). Interestingly, an 11 base pair deletion adjacent to the g.31701T>A mutation in one sibling pair suppressed aberrant splicing, increasing ADA activity and protein stability (Arredondo-Vega et al., 2002). Enhanced splicing in ADA has also been observed. Several genes contain purine-rich exonic regions which interact with splicing factors and cis-acting intronic elements defining exons (Lavigueur et al., 1993; Mayeda et al., 1993; Staknis & Reed, 1994; K. Tanaka et al., 1994; Tian & Maniatis, 1993, 1994; Watakabe et al., 1993). It has been reported that an ADA R142X mutation located within a purine-rich region of exon 5, caused exon skipping, possibly by splicing enhancer disruption (Santisteban et al., 1995). G to A transition at nucleotide 22 of exon 1 of the *ADA* gene gives rise to an Asp to Asn amino acid substitution in position 8 of the mature protein. Although rare (allelic frequency of 0.03–0.11 in Caucasian

populations), this reduces ADA activity by 35% compared to the Asp allozyme (Hirschhorn et al., 1994).

1.12 ADA in neurological disorders

1.12.1 ADA-deficient severe combined immunodeficiency

ADA deficiency is the second most common cause of SCID, accounting for 15% of all cases (for a review see Hershfield, 2017). ADA-deficient SCID is an inherited autosomal recessive disease caused by complete or partial loss of ADA activity (Giblett et al., 1972). ADA-deficient SCID has two major pathogenic mechanisms. Firstly, as previously mentioned, via an accumulation of dATP, inhibiting T-lymphocyte proliferation (Carson et al., 1979). Secondly, adenosine can combine with homocysteine to form SAH (Figure 1.6C). Accumulation of adenosine causes a subsequent accumulation of SAH that inhibits SAM generation and therefore SAM-mediated DNA methylation, a process which is required for normal thymocyte differentiation (Benveniste et al., 1995). SCID results in the almost total depletion of the body's immune response and can have devastating effects on the host (Giblett et al., 1972). However, all forms of SCID can be treated with allogeneic hematopoietic stem cell transplantation, bone marrow transplant, enzyme replacement therapy using ADA conjugated to polyethylene-glycol (Hershfield, 2017), and through lentivirus (LV) mediated autologous hematopoietic stem cell gene therapy (Aiuti et al., 2009).

Along with the devastating immunological implications of SCID, patients can also experience severe neurological manifestations, a phenomenon that is particularly relevant for ADA-deficient SCID patients and which can persist even after treatment. ADA-deficient SCID patients have lower IQ scores than patients with other forms of SCID and the general population (Rogers et al., 2001; Titman et al., 2008; Sauer et al., 2017); exhibit behavioural abnormalities including hyperactivity disorder like symptoms, aggressive behaviour and social problems, not reported in other forms of SCID (Rogers et al., 2001; Hönig et al., 2007; Scott et al., 2017); display motor dysfunction with symptoms including hypotonia and nystagmus (Hirschhorn et al., 1980; Hönig et al., 2007; Nofech-Mozes et al., 2007) and also auditory dysfunction (C. Tanaka et al., 1996). The neurological defects observed in SCID are overshadowed by the profound immunological changes that occur in early childhood meaning little research has been conducted into the changes that occur neurologically. Therefore, the exact mechanisms of the neurological manifestations of ADA-deficient SCID are unknown. It has been noted that patients' IQ scores were inversely correlated with dATP levels at the time of diagnosis (Rogers et al., 2001), implying that the neurological manifestations of ADA-

deficient SCID are caused by or at least correlated with levels of toxic metabolite accumulation caused by the loss of ADA activity. In evidence of this, the neurological effects of ADA deficiency in $ADA^{-/-}$ mice became more prominent during the postnatal period, when ADA substrates begin to accumulate, and may be linked with A_{2A} receptor activation (Sauer et al., 2017). MRI and tomographic scans also reveal volume loss of the basal ganglia and thalamus, possibly linked to atypical adenosine receptor activation in patients (Nofech-Mozes et al., 2007). Due to the influence ADA exerts in control of the CNS, specifically in its control of adenosine and adenosine's interaction with adenosine receptors in the brain (Haas & Selbach, 2000; Nagy et al., 1984), it is no surprise that ADA-deficient SCID patients exhibit these neurological defects, as any disturbance in the delicate balance of this system is likely to have significant, lasting effects.

1.12.2 Autism

Historic evidence has correlated lower ADA levels and autism (Stubbs et al., 1982). Moreover, an increase in the frequency of the previously discussed Asp8Asn polymorphism which reduces ADA activity was observed in Italian children diagnosed with autism, suggesting that this genotype-dependent reduction in ADA activity may be a risk factor for development of the disease (Bottini et al., 2001). These findings may be population dependent as a similar study on a North African cohort did not produce a clear link between the polymorphism and autism (Hettinger et al., 2008), whereas a study in Saudi Arabia found decreased ADA levels in the plasma of autistic boys (Abu Shmais et al., 2012). More recently a zebrafish model of autism linked a dysfunction in ADA with disease pathogenic mechanisms including altered intracellular and extracellular purine metabolism (Zimmermann et al., 2016).

1.12.3 Parkinson's Disease

Evidence has shown that ADA levels are also dysregulated in Parkinson's disease (PD), as serum isolated from idiopathic PD patients was shown to have significantly higher total ADA and ADA2 activity levels compared to controls (Chiba et al., 1995). Moreover, expression correlated with activated T-lymphocyte populations, suggesting peripheral T-lymphocyte activation was the cause. Similar results were observed more recently in a metabolomics study performed in mice treated with lipopolysaccharide plus 1-methyl-4-phenyl-1,2,3,6-tetrahydropyridine (MPTP), which evokes a PD-like response in rodent models (W. Huang et al., 2019). Widespread metabolic alterations were observed, including in purine metabolism where adenosine levels were decreased, and inosine levels increased. ADA inhibition by

deoxycoformycin and/or A_{2A} antagonism with KW6002 reduced dopamine loss and dopaminergic cell death and improved motor function. These data demonstrate that targeting dysregulated purine metabolism by ADA regulation is a potential therapeutic approach in PD by reducing inflammatory pathways. These mechanisms may be similar to the action of caffeine which is known to be neuroprotective in PD via A_{2A} (for a review see Ren & Chen, 2020).

1.12.4 ADA dysregulation in ALS

As mentioned, research published from our laboratory has shown a dysregulation in adenosine metabolism in ALS iAstrocytes, ostensibly caused by a downregulation in ADA (Allen et al., 2019a). Using a metabolic profiling assay (Bochner et al., 2011), we screened C9orf72 cells for their ability to metabolise 91 different substrates, demonstrating adenosine hypometabolism in these models. Further investigation, to elucidate a mechanism, revealed that ADA was downregulated in C9orf72 iAstrocytes, fibroblasts, and iNPC neurons (iNeurons) at both a protein and mRNA level. We subsequently established that C9orf72 iAstrocytes had an increased susceptibility to adenosine-mediated toxicity, which negatively correlated with ADA expression (Allen et al., 2019a). Moreover, control iAstrocytes, treated with the ADA inhibitor pentostatin, exhibited a level of adenosine-mediated toxicity equivocal to the C9orf72 lines. This indicated that ALS iAstrocytes' increased sensitivity to adenosine was, at least partially, ADA dependent. Bypassing the ADA defect with inosine supplementation was found to be bioenergetically beneficial in iAstrocytes, increasing ATP output, predominantly via glycolysis, which was confirmed by measuring metabolic flux. Furthermore, inosine increased both respiratory and glycolytic capacity in the cells and induced a significant increase in urate. Inosine supplementation was also able to ameliorate iAstrocyte-mediated MN toxicity in co-culture, possibly due to bypassing the ADA defect, as pentostatin treatment in controls increased their toxicity to MNs. With these data in mind, we also recently showed that inosine metabolism positively correlates with disease duration in ALS fibroblasts (Gerou et al., 2021). This suggests that higher ADA activity, in addition to reducing toxic adenosine levels, would produce more inosine and may be protective in ALS.

Prior to this, no literature existed for the behaviour of ADA in ALS patients and models. However, compelling historic and recently published studies have suggested a link between ALS disease mechanisms and ADA. Dysfunction in an analogue of ADA called ADA acting on RNA (ADAR) has been widely linked to ALS (Suzuki & Matsuoka, 2021). ADAR is an enzyme that partakes in RNA editing via post-transcriptional modification, converting adenosine bases to inosine (Melcher et al., 1996), suggesting a precedent for incorrect ADA function in ALS.

There have also recently been links made with sALS and a mutation in p73 (Russell et al., 2021), a key regulator of ADA expression in the cell (Tullo et al., 2003). Further, three of the major mechanisms associated with ADA deficiency, abnormal inflammation patterns (Béland et al., 2020), dysregulated DNA damage response (DDR) (Kok et al., 2021), and atypical DNA methylation (Martin & Wong, 2013) have all been presented as pathogenic mechanisms that could contribute to MN degeneration. Moreover, inosine and urate, the downstream products of ADA's hydrolytic deamination of adenosine, have been investigated as therapeutics in ALS. Urate has been consistently correlated with disease progression (Ikeda et al., 2012; Keizman et al., 2009; Nicholson et al., 2015; Oh et al., 2015; Paganoni et al., 2018; F. Zhang et al., 2018), whilst inosine has been trialled as a therapeutic to increase urate output (Nicholson et al., 2018).

All these data combined implicate ADA dysfunction as a key factor in C9orf72 ALS, highlighting ADA as a target for ALS treatments. My project therefore focuses on the causes, effects, and treatment of ADA dysfunction in C9orf72 ALS iAstrocytes.

1.13 Hypotheses

Based on the evidence outlined above, I have drawn several hypotheses. Firstly, that loss of ADA may drive, or be concomitant with, further dysregulation in purine metabolism; secondly, that loss of ADA in C9orf72 iAstrocytes is driven by one of the mechanisms associated with the C9orf72 HRE or caused by aberrations in transcriptional activation; and finally, that increasing ADA levels would protect against pathogenic mechanisms of ALS and increase astrocytic support for MNs.

1.13.1 Aims

The aims of the study are therefore:

- To investigate the wider effect of the C9orf72 HRE on purine metabolism, including the biochemical implications of ADA downregulation and the expression of other key enzymes involved in this pathway;
- To investigate the potential mechanisms that lead to loss of ADA by investigating the transcriptional regulation of ADA and ADA expression directly in cellular models mimicking C9orf72 ALS;
- To upregulate ADA expression and activity in iAstrocytes using a targeted gene therapy approach and subsequently investigate the effect on other purine metabolism enzymes, markers of antioxidant defence and autophagy, adenosine-mediated toxicity and astrocyte bioenergetic profile.

2. Materials and methods

2.1 Materials

2.1.1 Human Biosamples

Experiments were carried out using skin samples from four C9orf72 ALS cases (cell lines C9-52, C9-78, C9-183 and C9-201) and four age- and sex-matched (where possible) controls (cell lines Con-14, Con-155, Con-209 and Con-3050) (Table 2.1.1). The average age at time of skin biopsy was 57.5 (± 8.5) years in C9orf72 ALS and 56.5 (± 11.4) years in controls. The average disease duration in C9orf72 ALS cases was 26 (± 5.1) months (at the time of writing ALS donor 52 was still alive and therefore not included in the disease duration calculation).

Cell line	**Sex (M/F)**	**Age at biopsy (years)**	**Disease duration (months)**
Con-14	F	52	N/A
Con-155	M	40	N/A
Con-209	F	69	N/A
Con-3050	M	65	N/A
C9-52	M	48	N/A
C9-78	M	66	31.7
C9-183	M	50	27
C9-201	F	66	19.4

Table 2.1.1. Details of control and C9orf72 ALS sample donors.

2.1.2 Primary antibodies

Antibody	Species	Western blot dilution	Immunofluorescence dilution	Source	Cat. No.
ADA	Mouse	1:250-1,000	N/A	Santa Cruz	sc28346
ADA	Rabbit	1:1000	1:25-50	Proteintech	13328-1-AP
ADK	Rabbit	1:1000	N/A	Proteintech	66929-1-IG
Actin	Rabbit	1:3000	N/A	Proteintech	20536-1-AP
CD73	Rabbit	1:2000	N/A	Proteintech	12231-1-AP
HGPRT	Rabbit	1:2000	N/A	Proteintech	15059-1-AP
NQO-1	Rabbit	1:1000	N/A	Proteintech	11451-1-AP
P62	Mouse	1:1000	N/A	BD Biosciences	610833
P73	Mouse	1:2000	N/A	ThermoFisher	38C674.2
PNP	Mouse	1:1000	N/A	R&D Systems	MAB6486
V5-Tag	Mouse	N/A	1:1000	ThermoFisher	MA5-15253
XDH	Rabbit	1:2000	N/A	Proteintech	55156-1-AP

Table 2.1.2. Details of the primary antibodies used in this study, including species, western blot dilution, immunofluorescence dilution, supplier, and catalogue number.

2.1.3 Secondary antibodies

Species	Western blot dilution	Immunofluorescence dilution	Excitation/ Emission (nm)	Source	Cat. No.
Hoescht	N/A	1:2,000-10,000	350/461	ThermoFisher	H3570
Anti-Mouse	1:5,000	N/A	N/A	Abcam	ab97040
Anti-Rabbit	1:5,000	N/A	N/A	Sigma-Aldrich	A0545
Fluorescent Anti-Mouse	N/A	1:1,000	499/520	ThermoFisher	A11001
Fluorescent Anti-Rabbit	N/A	1:1,000	579/603	ThermoFisher	A11011

Table 2.1.3. Details of the secondary antibodies used in this study, including species, western blot concentration, immunofluorescence concentration, supplier, and catalogue number**.**

2.1.4 Primers

Primer	Fwd/Rev (F/R)	Sequence (5'-3')
18s	F	ATGGCCGTTCTTAGTTGGTG
18s	R	CGCTGAGCCAGTCAGTGTAG
ADA	F	CTGCTGAACGTCATTGGCATGG
ADA	R	GGCGATCCTTTTGATAGCCTCC
CD73	F	CTCCTCTCAATCATGCCGCT
CD73	R	TGGATTCCATTGTTGCGTTCA
GAPDH	F	CAACTTTGGTATCGTGGAAGGAC
GAPDH	R	ACAGTCTTCTGGGTGGCAGTG
HGPRT	F	CATTATGCTGAGGATTTGGAAAGG
HGPRT	R	CTTGAGCACACAGAGGGCTACA
P73	F	CATGGAGACGGAGGACACGTACT
P73	R	TGCCGATAGGAGTCCACCAGTG
U1	F	CCATGATCACGAAGGTGGTT
U1	R	ATGCAGTCGAGTTTCCCACA
WPRE	F	CCCGTACGGCTTTCGTTTTC
WPRE	R	CAAACACAGAGAGCACACCACG

Table 2.1.4. Details of the primer pairs used in this study including 5'-3' sequence.

2.1.5 Ethical Approval

Informed consent was obtained from all human subjects before skin sample collection (Study number STH16573, Research Ethics Committee reference 12/YH/0330).

2.2 Plasmid and viral preparations

2.2.1 ADA

The ADA plasmid was cloned by the Hautbergue group into a SIN-PGK-cPPT-GDNF-WHV vector. For plasmid map see section 5.1.

2.2.2 Poly-GA, Poly-GR, and Poly-PR (36x) DPRs

36x repeat DPR plasmids were originally provided by the Isaacs group in a pcDNA5.1 vector and DPR sequences subsequently cloned into a pCI-neo-V5 plasmid by the De Vos group (Hautbergue et al., 2017).

2.2.3 Sense and Antisense HREs

C9orf72 G_4C_2 (sense) and C_4G_2 (antisense) repeats in a pcDNA3.1 plasmid were generated as described previously (Hautbergue et al., 2017) by the Hautbergue lab and subcloned into a lentiviral backbone by the Hautbergue and Shaw labs.

2.2.4 Plasmid propagation

Plasmids were transformed into *E. coli* by incubating 100ng of plasmid DNA with *E. coli* on ice for 10 minutes prior to inducing heat shock by heating at 42°C for 45 seconds and then returning to ice for a further 2 minutes. The transformed *E. coli* were incubated at 37°C in LB media for 1 hour before streaking a petri dish of LB agar containing 50µg/ml ampicillin and grown overnight at 37°C. A colony from this plate was selected and used to inoculate a starter culture of LB medium containing 0.1µg/ml ampicillin and incubated overnight at 37°C. A QIAGEN Plasmid Purification kit was then used to propagate the plasmid. Briefly, the bacterial cells were harvested by spinning at 6000 x *g* for 15 minutes at 4°C. The pellet was resuspended in 4-10ml of Buffer P1 (according to manufacturer's instruction - QIAGEN)

containing RNase A. Equal volumes of Buffer P2 (QIAGEN) and P3 (QIAGEN) were mixed before incubating on ice for 15 or 20 minutes. Lysate was then centrifuged at 20,000 x *g* for 30 minutes at 4°C. The supernatant was collected and centrifuged again in the same conditions for a further 15 minutes. A QIAGEN-tip was equilibrated with Buffer QBT (QIAGEN) before the supernatant was added. The tip was then washed twice with Buffer QC (QIAGEN). Plasmid DNA was eluted with Buffer QF (QIAGEN) and the DNA precipitated by adding 0.7 volumes isopropanol and then centrifuging at 15,000 x *g* for 30 minutes at 4°C. Pelleted DNA was then washed with 70% ethanol, air-dried and resuspended in TE buffer (QIAGEN). Plasmid concentration was quantified using a NanoDrop 1000 (LabTech).

2.2.5 Lentiviral production

Lentivirus was produced by transfecting Human Embryonic Kidney 293 T-Rex (HEK293T)/17 cells with 13µg of SIN-PGK-cPPT-GDNF-WHV plasmid containing target gene, 13µg pCMVDR8.92, 3µg pRSV-Rev and 3.75µg M2G plasmids per 10cm dish (10-20x dishes depending on required amount of LV) using calcium phosphate and incubated for 3 days, at which point media was harvested and filtered through a 45µm filter to isolate the virus. Filtered media was centrifuged at 19,000rpm for 90 minutes at 4°C. The pelleted LV DNA was resuspended in 1% bovine serum albumin (BSA). To titre, the LV was transduced into HeLa cells. Genomic DNA was then isolated from HeLa cells and WPRE DNA concentration was determined using RT-qPCR (see section 2.4.3) and compared to a known viral titre.

2.3 Cell Culture

2.3.1 Cell storage

All cells were maintained at 37°C, 5% CO_2 and 95% humidity.

2.3.2 HEK293T and HeLa cell culture

HeLa cells and HEK293T cells were cultured in high glucose (25mM) Dulbecco's Modified Eagle Medium (DMEM) (Sigma-Aldrich) supplemented with 10% Foetal Bovine Serum (FBS) (Gibco). Cells were harvested by initially removing media, then incubating at 37°C in trypsin (Lonza) for 2-3 minutes. Trypsin was quenched in 25mM DMEM, and the cell suspensions collected in a falcon tube, pelleted by centrifugation at 400 x *g* and then either resuspended for plating, stored at -80°C or immediately lysed prior to storage.

2.3.3 N2a cell culture

Neuro-2a (N2a) cells were cultured in 25mM DMEM supplemented with 10% FBS and 5mM sodium pyruvate. N2a cells were harvested as described in section 2.3.2. N2a cells transduced with either the G_4C_2 or C_4G_2 repeat expansion were propagated from a single colony to develop sense and antisense N2a lines. Confirmation of the expression of RNA foci and DPRs has been previously established in lines transfected with these plasmids (Hautbergue et al., 2017) and DPR expression has also been confirmed using a Mesoscale Discovery assay (unpublished, personal communication, Dr Adrian Higginbottom).

2.3.4 iAstrocyte culture

iNPC lines (for details see table 2.1.1) were initially reprogrammed as described in Meyer et al. (2014) by the Ferraiuolo lab. Briefly, skin biopsies were treated with a mixture of retroviral vectors: Kruppel-like factor 4, POU transcription factor *Oct-3/4*, SRY-related HMG-Box Gene 2 and c-*Myc.* 72 hours post-infection standard culture medium was exchanged for medium containing the growth factors FGF2, epidermal growth factor (EGF) and heparin to provoke NPC conversion. This was maintained for 18 days at which point EGF and heparin were removed from the culture medium. NPC reprogramming was confirmed using immunohistochemistry and RNA expression of the NPC markers Pax6, Nestin, NCAN and NKX2-2. Post-reprogramming iNPCs were cultured in DMEM Glutamax containing 1% N-2 supplement (Life Technologies), 1% B27 and 20ng/ml FGF2 (Preprotech).

iNPCs were subsequently differentiated into iAstrocytes through the addition of 25mM DMEM with 10% FBS and 0.2% N-2 supplement and differentiated for 6-8 days before any assay. As published previously (Meyer et al., 2014, Allen et al., 2019b), this procedure produces iAstrocytes that are 100% positive for vimentin, CD44 and glial fibrillary acidic protein. iAstrocytes were lifted by washing away media then incubating cells at 37°C in Accutase (Sigma-Aldrich) for 5-7 minutes, Accutase was quenched in PBS. Cells were pelleted by centrifuging at 200 x *g* and then either resuspended for plating, stored at -80°C or immediately lysed prior to storage.

2.3.5 Transfection

Cells were transfected using a jetPRIME transfection kit (Polyplus). Xµg of plasmid DNA was mixed with Wµl jetPRIME buffer and vortexed. Yµl of jetPRIME reagent was then added and

again briefly vortexed. The mixture was incubated at room temperature for 10 minutes prior to addition to wells. For specific volumes used see Table 2.3.5.

Plate size	W = jetPRIME buffer (µl)	X = DNA (µg)	Y = jetPRIME reagent (µl)
24-well	50	0.5	1
6-well	200	2	4

Table 2.3.5. Details of the mix of jetPRIME buffer, plasmid DNA and jetPRIME reagent used for transfections depending on plate size.

2.3.6 Transfection confirmation

Transfection in HEK293T and HeLa cells was confirmed by initially plating cells in a 24-well plate on top of cover slips. Cells were then transfected and incubated for 24 hours prior to fixing with 3.7% paraformaldehyde solution for 20 minutes and then permeabilised with 0.2% Triton 100X for 3 minutes. Cells were then either stored at 4°C in PBS or immediately blocked in 4% goat serum for 30 minutes, then stained with primary antibody and subsequently secondary antibody for 1 hour (for dilutions see Tables 2.1.2-3). Cells were then stained with Hoescht for 20 minutes and cover slips were mounted on a slide with Immunomount and imaged on the BX53 fluorescent microscope (Olympus). All incubations were performed at room temperature.

2.3.7 Transduction

iAstrocytes and N2a were transduced by initially cell counting using a haemocytometer and then calculating the volume of LV to add with the formula:

Vol. of virus (µl) = ((Multiplicity of Infection (MOI) x cell number per well)/viral titre)) x (number of wells virally treated x 1000)

2.4 Experimental methods

2.4.1 Western blot analysis

2.4.1.1 Cell lysis and protein concentration determination

Cells were harvested and pelleted as described in section 2.3.4. Pelleted cells were re-suspended post-storage at -80°C in an appropriate volume of lysis buffer (89% Radio-

Immunoprecipitation Assay buffer, 10% protease inhibitor cocktail and 1% phosphatase inhibitor, all Sigma-Aldrich) and lysed on ice for 30 minutes. Lysed cells were centrifuged at 13,000rpm and 4°C for a further 30 minutes. The supernatant was collected and stored on ice. Protein concentration was quantified by Bradford analysis as per the manufacturer's instructions. Briefly, 5µl lysed sample at dilutions of 1/15, 1/30 and 1/45 in triplicate was mixed with 195µl Coomassie reagent. 5µl of BSA, with concentrations of 1000µg/ml, 500µg/ml, 250µg/ml, 125µg/ml, 62.5µg/ml, 31.25µg/ml and 15.125µg/ml, in triplicate were also mixed with 195µl Coomassie to generate a standard curve. Absorbance was measured at 595nm on a PHERAstar plate reader (BMG LABTECH), and protein concentration was calculated by plotting sample absorbance against the standard curve based on rearrangement of the linear equation (y=mx+C) to the following formula:

$$x = (y-c)/m$$

Where:
X = Protein concentration (µg/µl)
Y = Absorbance 595nm
C = y-intercept
M = gradient of the line

Protein concentration values were adjusted to represent the concentration of the whole sample by multiplying by the corresponding dilution (15, 30 or 45) and samples were denatured at 95°C in 1x Laemmli buffer for 5 minutes prior to storage at -20°C.

2.4.1.2 Electrophoresis, Transfer, and Imaging

A 10-20µg of protein was loaded onto 8-12% SDS polyacrylamide gels and electrophoresis was performed using Mini-PROTEAN Tetra Handcast systems (Bio-Rad). Protein was transferred to methanol treated polyvinylidene difluoride (PVDF) (Millipore) membranes at 250mA for 1 hour at room temperature. PVDF membranes were then incubated with blocking solution (Tris-buffered saline with 0.01% Tween (TBST) plus 5% BSA). Membranes were incubated at 4°C overnight in blocking solution with primary antibody (for dilutions see Table 2.1.2). Excess antibody was then removed using six 10-minute TBST washes and the membrane incubated with secondary HRP-conjugated antibody (for dilutions see Table 2.1.3) in blocking solution for an hour at room temperature. Excess secondary antibody was then removed in three 10-minute TBST washes and protein bands were detected with an EZ-ECL HRP chemiluminescence kit (Biological Industries) using an Odyssey XF imaging system (LI-COR). Protein signal levels were quantified using Image Studio Lite v5.2 (LI-COR).

2.4.2 ADA activity assay

ADA activity assays were performed using an ADA activity assay kit (Abcam). Briefly, cells were harvested as described in section 2.3.4 and lysed immediately in manufacturer's ADA activity assay buffer (AB) before being stored at -80°C. Protein content in lysed samples was assessed using a Bradford assay as described in section 2.4.1.1 Inosine standards were prepared in AB at 0, 20, 40, 80, 160, 240 and 320nmol/well and added to the wells of a 96-well white-walled plate in 50µl AB. Between 0.1 and 4µg of protein per sample (depending on cell line and viral treatment) was also added to wells. A reaction mix containing 40µl AB, 2µl ADA converter, 2µl ADA developer, 1µl ADA probe and 5µl ADA substrate was then added to a portion of the wells containing samples. A background control mix with the 5µl of ADA substrate replaced with AB was added to the remaining sample wells and the wells containing the standard solutions. Fluorescence was then measured at Ex/Em = 535nm/587nm on a PHERAstar plate reader every 2 minutes for 90 minutes. Inosine output was calculated by normalising RFU at an individual time point to protein content in each well. ADA activity was calculated by taking the RFU from two timepoints over the course of the kinetic read and entering those values into the following formulae:

$$\Delta T = T_2 - T_1$$

$$\Delta RFU = (RFU_2 - RFU_{2BG}) - (RFU_1 - RFU_{1BG})$$

$$ADA\ activity = (\Delta RFU/\Delta T * \mu g\ protein) * Dilution\ factor = pmol/min/\mu g$$

Where:
T_1 = *Timepoint 1*
T_2 = *Timepoint 2*
RFU_1 = *RFU at timepoint 1*
RFU_2 = *RFU at timepoint 2*
RFU_{1BG} = *Background RFU at timepoint 1*
RFU_{2BG} = *Background RFU at timepoint 2*

2.4.3 RT – qPCR

RNA was extracted from iAstrocytes 7 days post-differentiation using the EZ Total RNA Isolation Kit (Geneflow). Pelleted cells were lysed using the denaturing solution. An equal volume of extraction solution was then added, and the mixture shaken vigorously for 15

seconds before being incubated at room temperature for 10 minutes. The mixture was then centrifuged for 15 minutes at 12,000 x *g* and 4°C. The upper phase was collected, and RNA precipitated by adding an equal volume of isopropanol prior to storage overnight at -20°C. The RNA was then pelleted by centrifuging at 12,000 x *g* and 4°C for 15 minutes. The supernatant was discarded, and the pellet washed in 70% ethanol before being resuspended in 22µl DEPC H_2O. Samples were treated with DNaseI (Roche), by adding 2.5µl 10X DNase and 0.5µl DNaseI to each sample and incubating at 37°C for 30 minutes. The enzyme was then denatured by incubating at 75°C for 10 minutes and the samples quantified on a NanoDrop 1000. 2µg RNA was converted to cDNA by mixing with 1µl random hexamers, 1µl 10mM dNTPs and making up to 13.5µl with DEPC H_2O. The solution was then incubated at 50°C for 5 minutes before cooling on ice water for 1 minute. The solution was mixed with 4µl 5x first strand buffer, 2µl 0.1M DTT and 1µl M-MLV reverse transcriptase (all reagents acquired from Bioline) and incubated at 25°C for 10 minutes, 42°C for 60 minutes and 85°C for 5 minutes in a PCR machine (G-Storm) and cDNA was then mixed with 1µl of 5µM of the relevant forward and reverse primer pairs (for primer sequences see Table 2.1.4), 3µl of DEPC water and 5µl Brilliant III Ultra-Fast SYBR Green qPCR (Agilent Technologies). RT-qPCR was performed on a CFX96 RealTime System C1000 Touch Thermal Cycler (Bio-Rad) and was analysed using CFX Maestro v2.2 (Bio-Rad). Thermocycler conditions for RT-qPCR are described in Table 2.4.3.

Step	**Temperature (^{O}C)**	**Time**	**Cycles**
PCR activation	95	5m	N/A
Denaturation	95	10s	40
Annealing	60	30s	
Melt Curve analysis	65	5s	
Melt Curve analysis	Ramp	0.5°C/5s	N/A
Melt Curve analysis	95	-	N/A
Storage	10	Hold	N/A

Table 2.4.3. Details of the stages of RT-qPCR reaction including temperature, time and the number of cycles.

2.4.4 Adenosine cell survival analysis

At 6 days post-differentiation iAstrocytes were lifted and plated, as described in section 2.3.4, in 96-well clear-bottom plates (Greiner) coated in 0.25µg/ml fibronectin (Millipore) at 7,500-

10,000 cells/well in 100µl of 25mM DMEM. Plates were then incubated at 37°C/5% CO_2 for 24 hours. Media was then changed for 200µl low glucose (5mM) DMEM plus 10% FBS and 0.3mM glutamine (Lonza) with adenosine at concentrations of 4.0mM and 10mM plus untreated controls at both 5mM glucose DMEM (as this is more representative of physiological glucose levels) and 25mM glucose DMEM (higher glucose level that is standard for iAstrocyte cell culture. After 24 hours incubation, plates were washed three times with 100µl PBS before being incubated for at least 24 hours at -80°C. Cell number was quantified using a CyQUANT Cell Proliferation kit (Invitrogen – C7026) by adding 400X CyQUANT dye at 1/400 and 20X HBSS buffer at 1/20, diluted in dH_2O to wells following manufacturer's instructions. Fluorescence was measured on a PHERAstar plate reader at Ex/Em = 485nm/520nm.

2.4.5 ATP assay

At 6 days post-differentiation iAstrocytes were lifted and plated, as described in section 2.3.4, in a 96-well white-walled clear-bottom plate (Greiner) and incubated for 24 hours at 37°C/5% CO_2. Media was then changed for 100µl 5mM DMEM with an inosine positive control at 7.5mM plus a 25mM DMEM control and incubated for 24 hours. After incubation, media was removed, the plate washed with 200µl PBS and ATP levels quantified using a cellular ATPlite assay kit (PerkinElmer). Briefly, each well had 50µl lysis buffer, 50µl ATP substrate and 100µl PBS, and a portion of wells also had 10µl ATP standard solution at 50µM, 25µM, 12.5µM, 6.125µM, 3.063µM, 1.531µM and 0.766µM. Between the addition of each reagent, plates were shaken on a plate shaker for 5 minutes. After this process, plates were stored in the dark at room temperature for 10 minutes, and luminescence was subsequently measured on a PHERAstar plate reader. Cell number was quantified using a CyQUANT Cell Proliferation kit (Invitrogen – C35006), 100µl of 500X CyQUANT at 1/500 and 5X HBSS buffer at 1/5, diluted in dH_2O was added to wells and plates incubated for 1 hour. Fluorescence was measured on a PHERAstar plate reader at Ex:485/Em:520nm.

2.4.6 Metabolic flux assay

Six days post-differentiation, iAstrocytes were lifted and plated, as described in section 2.3.4, in 96-well cell culture plates (Agilent) in 25mM DMEM and incubated overnight. Media was then replaced with phenol-red free DMEM containing 5mM glucose, 1mM glutamine and 1mM sodium pyruvate (Gibco) plus an inosine positive control at 7.5mM and incubated for 24 hours. On the same day an XF96e probe (Agilent) plate was primed with XF calibrant (Agilent). The next day, cell media was replaced with XF assay media containing 5mM glucose, 1mM

glutamine and 1mM sodium pyruvate at pH 7.4 (Agilent) and incubated at 37°C in a non-CO_2 incubator for 1 hour. XF probe plates were loaded with 20µl 13µM oligomycin, 22µl 17.5µM carbonyl cyanide-p-trifluoromethoxyphenylhydrazone (FCCP) and 24µl of 13µM antimycin A and 13µM rotenone in ports A-C respectively. Oxygen consumption rate (OCR) and extracellular acidification rate (ECAR) was then measured on an XF96e bioanalyser (Agilent) in the presence and absence of 1.3µM oligomycin, 1.75µM FCCP and the 1.3µM antimycin A/rotenone mix. Cell number was determined using a CyQUANT Cell Proliferation kit as described in section 2.4.4.

2.4.7 Urate assay

Urate assays were carried out using a urate assay kit (Sigma-Aldrich). Samples were collected as described in section 2.3.4 and subsequently lysed in manufacturers urate assay buffer. Samples were then centrifuged at 13,000 x *g* and 4°C for 10 minutes to remove insoluble material. Protein content was assessed using a Bradford assay as described in section 2.4.1.1. Urate standards at 0, 2, 4, 8, 16, 32 and 64nmol/well were prepared in 50µl urate buffer. These, along with 50µl of the lysed iAstrocyte samples (at appropriate concentrations based on protein content), were added to a 96-well white walled plate before being mixed with a master mix containing 46µl urate assay buffer, 2µl urate probe and 2µl urate enzyme mix. The plate was then incubated in the dark at 37°C for 30 minutes before measuring fluorescence at Ex/Em = 535nm/590nm on a PHERAstar plate reader.

2.5 Statistical Methodology

Statistical analysis was carried out in Graphpad Prism Software (v10.0.3). Where possible raw data was analysed, however, this was not always the case as inter-assay variability sometimes biased data. Where this occurred, we used two methods to avoid this. Firstly, assays where all controls and patients were run alongside each other in the same assay a control average was taken, and all individual data points were taken as a ratio of this. Secondly, if all cell lines were not analysed within the same assay, a fold change against the matched control was used. These methods prevented variability from biasing data and allowed for more accurate statistical analysis. All data underwent normality distribution analysis by D'Agostino-Pearson omnibus normality test, Anderson-Darling test, Shapiro-Wilk normality test and Kolmogorov-Smirnov normality test with Dallal-Wilkinson-Lilliefor P value to test for Gaussian distribution prior to parametric or non-parametric analysis. Subsequently, statistical tests were performed using t-tests or one-way ANOVAs for single or group (more than 2) analysis respectively. All single analysis data was unmatched and therefore a Welch's t test or Mann-Whitney t test depending on parametric or non-parametric

distribution was performed. All grouped data was also matched and therefore an RM one-way ANOVA or Friedman test was performed, again depending on distribution.

For the iAstrocyte data sets (aside from a few highlighted exceptions – see COVID statement), at least three biological repeats of each control or C9orf72 line were compared with each another. In many of the assays these individual biological repeats were the average of at three technical repeats. This approach was used in the publications leading to this Thesis involving the similar analysis of the same cell lines (Allen et al., 2019a and 2019b). Therefore, to aid continuity, we continued with this approach.

3. Investigating purine metabolism dysfunction in C9orf72 iAstrocytes

Allen et al., (2019a) demonstrated that compromised adenosine metabolism in C9orf72 iAstrocytes is an area that can be targeted for therapeutic intervention. These investigations, however, did not investigate the direct functional ramifications of reduced ADA expression, nor the potential effect of C9orf72 ALS on the pathway that ADA is involved in, purine metabolism. In this chapter, I therefore investigated the extent to which a loss of ADA at the protein level translates to loss in global cellular ADA activity, inosine output and urate levels. We also examine the effect of C9orf72 ALS on other enzymes involved in purine metabolism, alongside the reconfirmation of data initially presented by Allen et al. (2019a), such as loss of ADA expression and elevated p62 expression in these models.

3.1 ADA activity and inosine output are reduced in C9orf72 iAstrocytes

We initially wanted to re-confirm and further validate adenosine metabolism dysfunction in C9orf72 iAstrocytes. To do this, we investigated ADA expression, ADA activity, inosine output and urate output. When directly comparing C9orf72 iAstrocyte ADA expression to age- and sex-matched controls, two of three C9orf72 cell lines (C9-78 and C9-183) exhibited a significant decrease in ADA levels. Interestingly, C9-201 did not exhibit this reduction in ADA expression compared to its matched control. C9-201, in our previously published work, tended to exhibit the highest ADA level of the three C9orf72 lines, but still showed an overall reduction in ADA expression compared to controls. Conversely, it's matched control, Con-209, often had lower ADA expression compared to other control iAstrocytes. As we were directly comparing matched control/patient pairs as opposed to collectively comparing control and patient groups on a single gel, this skewed the data, meaning that, when combined, we observed no overall significant downregulation in ADA expression (Figure 3.1A-B).

Although we have previously observed a downregulation in C9orf72 lines at the protein and the RNA level (Allen et al., 2019a), it was unknown whether this translated to a reduction in ADA activity and therefore inosine output. To test this, we established the first ADA activity assay in ALS cell lines. Our data showed that, as expected, loss of ADA at the protein level reduces ADA activity in C9orf72 iAstrocytes compared to controls (Figure 3.1C). This induces a reduction in iAstrocyte inosine output, which is the first time this has been shown in the context of C9orf72 ALS. Predictably, ADA activity and inosine output levels corresponded with ADA expression, as C9-201 experienced the lowest reduction in both ADA activity and inosine output compared to controls, whilst both C9-78 and C9-183 both experienced more severe

reductions in both parameters. Alongside inosine output, we assessed the level of urate production in our iAstrocytes, allowing a proxy measure of purine metabolism beyond adenosine to inosine conversion. Overall, urate output was reduced in C9orf72 iAstrocytes compared to controls, but this did not reach significance due to C9-78 displaying high levels of urate output (Figure 3.1E, top three data points), compared to C9-183 and C9-201 (Figure 3.1E, bottom six data points). These data indicate that urate levels may not be directly linked to inosine levels and may be dependent on enzyme activity downstream of adenosine-inosine metabolism.

These data, taken together with the data presented by Allen et al. (2019a), demonstrated that the C9orf72 HRE reduces ADA levels, which decreases ADA activity and inosine levels but may have less effect further downstream.

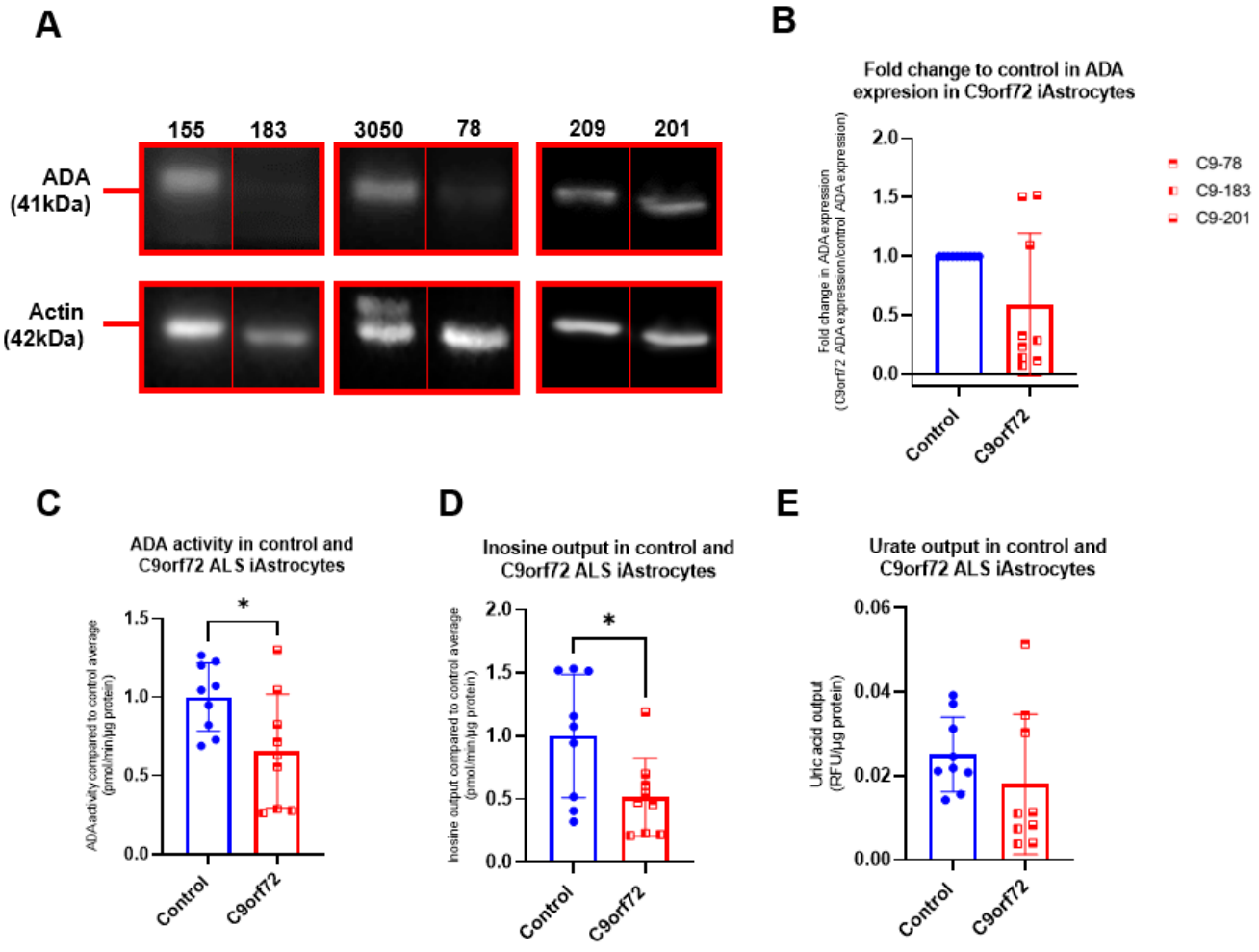

Figure 3.1. ADA activity and inosine output are reduced in C9orf72 iAstrocytes. (A) Representative images of ADA expression in control and C9orf72 iAstrocytes. (B) ADA expression in control and C9orf72 iAstrocytes. (C) ADA activity in control and C9orf72 iAstrocytes. (D) Inosine output in control and C9orf72 iAstrocytes. (E) Urate output in control and C9orf72 iAstrocytes. Data presented as mean and standard deviation of three biological replicates from three control and three C9orf72 iAstrocytes. Statistical analysis performed by setting control values to 1 (B), normalising values to a control average in each assay (C and D) or analysing raw data (E) and performing a Welch's t test (C and D) or Mann-Whitney test (B and E). *$P \leq 0.05$. Where P value is not indicated results were non-significant.

3.2 A pathogenic marker of C9orf72 ALS is significantly upregulated, but antioxidant defence mechanisms remain unaffected in C9orf72 iAstrocytes

3.2.1 p62 expression is significantly upregulated in C9orf72 iAstrocytes

p62 positive cytoplasmic inclusions are a clinical hallmark of C9orf72 ALS, observed in the hippocampus, cerebral cortex and cerebellum (Al-Sarraj et al., 2011; Troakes et al., 2012). p62 accumulation has also been observed in C9orf72$^{+/-}$ HeLa and rat cortical neurons (Webster et al., 2016) and we have demonstrated that p62 expression is significantly higher in C9orf72 iAstrocytes (Allen et al., 2019a). The exact mechanism that leads to the accumulation of p62 is unknown, but is likely related to the C9orf72 protein, as C9orf72 and p62 form a complex to eliminate stress granules (Chitiprolu et al., 2018). Here we sought to recapitulate the finding that p62 expression is elevated in C9orf72 iAstrocytes (Allen et al., 2019a). Using western blots to assess protein expression, we demonstrated here that p62 is indeed elevated in our cell models (Figure 3.2A-B). These data validate our current iAstrocyte cell lines as effective tools to investigate purine metabolism in C9orf72 ALS astrocytes and will be one of the key biomarkers investigated to assess the effect of gene therapy on iAstrocytes, which will be explored in Section 5.

3.2.2 NQO1 expression is unaffected in C9orf72 iAstrocytes

Reduced expression of nuclear factor erythroid 2-related factor 2 (Nrf2), a coordinator of the oxidative stress response, has been observed in ALS cell models (Petri et al., 2012). One of the targets of Nrf2, the antioxidant enzyme NAD(P)H quinone dehydrogenase 1 (NQO1), was

shown to be downregulated in C9orf72 iAstrocytes, suggesting impaired antioxidant defence, likely triggered by loss of Nrf2 (Allen et al., 2019a). As with p62, we sought to reconfirm the loss of NQO1 expression observed in C9orf72 iAstrocytes previously. To do this, we again utilised western blots to assess NQO1 protein expression. As with several other data sets that we present in this chapter, we observed a significant downregulation in two of three C9orf72 cell lines, when analysed independently. In this instance, C9-78 and C9-201, when analysed separately, exhibited a downregulation in NQO1 that reached significance. C9-183, conversely, displayed consistent upregulation in NQO1, though this upregulation did not reach significance. Therefore, when combined, there was no overall significant difference in NQO1 expression between control and C9orf72 iAstrocytes (Figure 3.2C-D). Again, this is possibly attributable to the fact that control/C9orf72 matched pairs were run on the same gel, instead of all three control and C9orf72 iAstrocytes samples being collected onto a single gel, as was performed previously (Allen et al., 2019a).

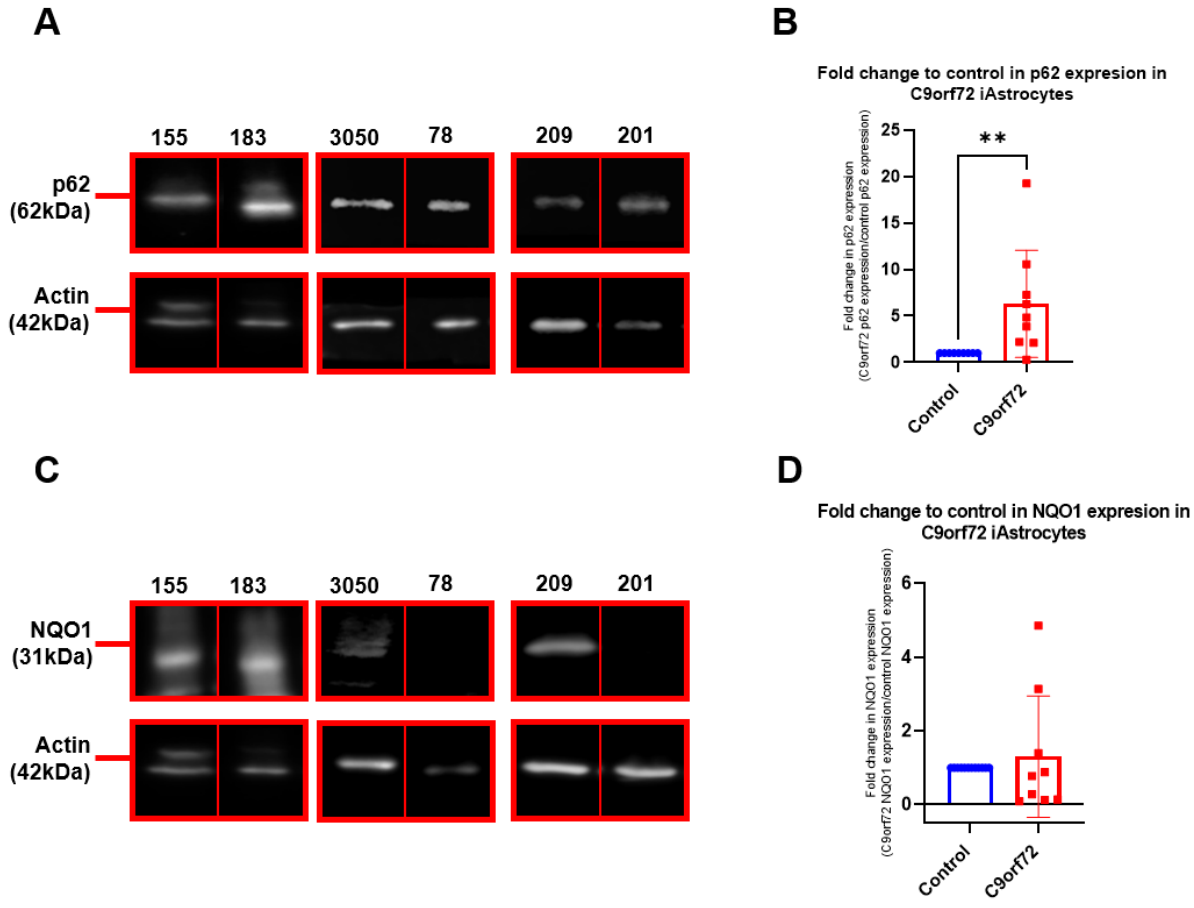

Figure 3.2. p62 and NQO1 expression are significantly altered in C9orf72 iAstrocytes. (A) Representative images of p62 expression in control and C9orf72 iAstrocytes. (B) Densitometry analysis of p62 expression in control and C9orf72 iAstrocytes. (C) Representative images of NQO1

expression in control and C9orf72 iAstrocytes. (D) Densitometry analysis of NQO1 expression in control and C9orf72 iAstrocytes. Data presented as mean and standard deviation of three biological replicates from three control and three C9orf72 cell lines. Densitometry analysis performed by normalizing the specified protein level to actin loading control and then setting control values to 1, before statistical analysis by Mann-Whitney test (B and D). $^{**}P \leq 0.01$. Where *P* value is not indicated results were non-significant.

3.3 The upstream enzyme of ADA, CD73, is downregulated in C9orf72 iAstrocytes

To further elucidate the effect of C9orf72 on purine metabolism in iAstrocytes, we examined the two enzymes that act directly upstream of ADA, adenosine kinase (ADK) and CD73. ADK phosphorylates adenosine to form AMP. CD73, conversely, dephosphorylates AMP to form adenosine (Figure 1.5B). Both enzymes, like ADA, are key regulators of adenosine metabolism. CD73 has not been previously linked directly to ALS of any form, but CD73 inhibition was shown to ameliorate inflammation, neurodegeneration and motor dysfunction in a PD mouse model (Meng et al., 2019) and both have been discussed as potential coordinators of adenosine and adenosinergic receptor activation during neurodegeneration in ALS (A. Mori et al., 2021). Interestingly, cervical spinal cord astrocytes undergoing astrogliosis from ALS patients show higher expression of ADK (Boison & Aronica, 2015). We therefore hypothesised that C9orf72 ALS might induce variations in the expression of these two enzymes, as we had observed with ADA. The fact that these enzymes act upstream of ADA was also key, as aberration here could provide a mechanistic basis for loss of ADA. To investigate this stage of the pathway, we again utilised western blots to assess the protein expression of CD73 and ADK in control and C9orf72 iAstrocytes. Here we demonstrate that ADK expression is unaffected, whilst CD73 is significantly downregulated in C9orf72 iAstrocytes compared to controls (Figure 3.3A-D). Both findings are crucial to our understanding of how purine metabolism becomes dysregulated in C9orf72 iAstrocytes.

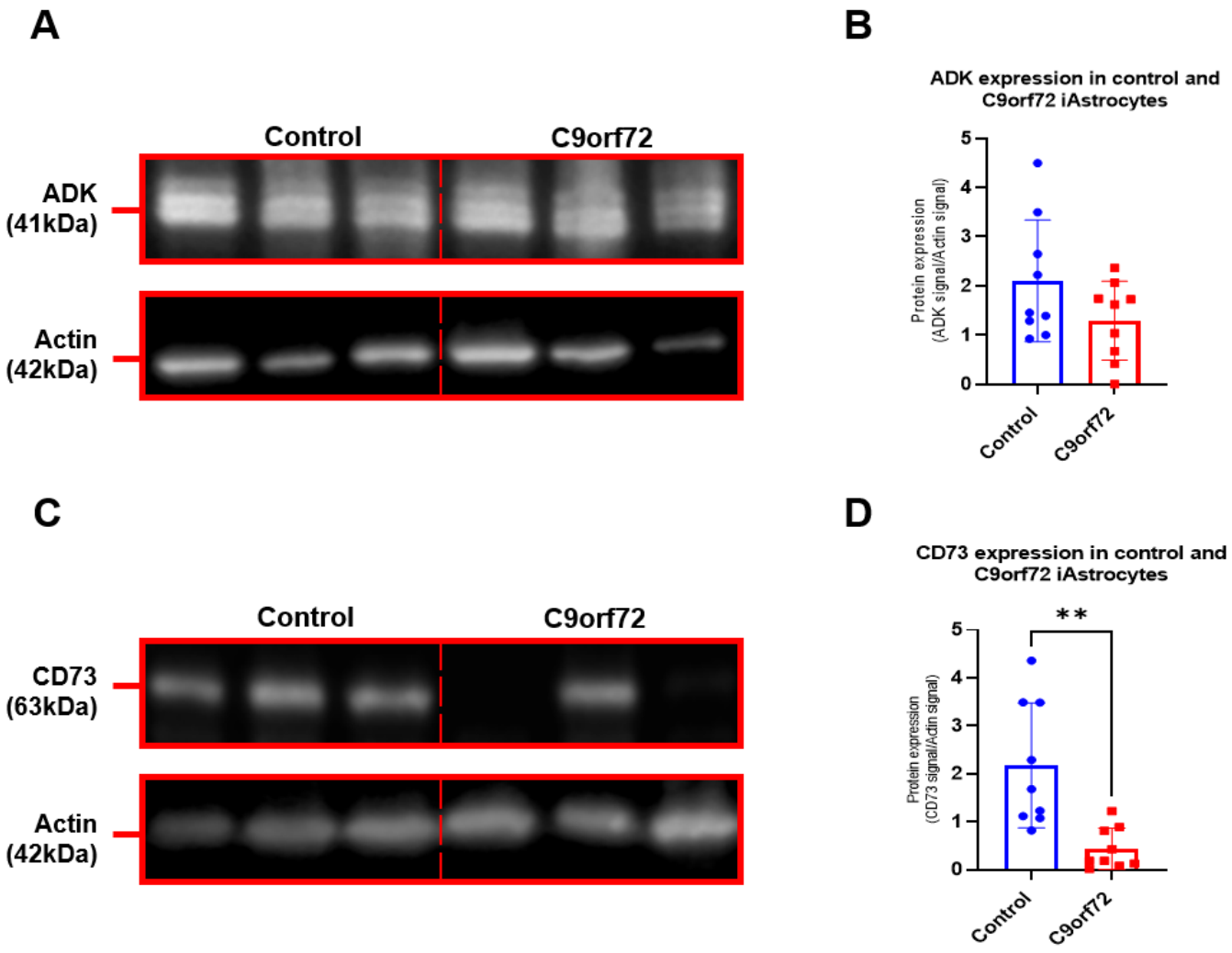

Figure 3.3. CD73 expression is downregulated in C9orf72 iAstrocytes. (A) Representative image of ADK western blot. (B) Densitometry analysis of ADK western blot. (C) Representative image of CD73 western blot. (D) Densitometry analysis of CD73 western blot. Data presented as mean and standard deviation of three biological replicates from three control and three C9orf72 iAstrocytes. Densitometry analysis performed by normalizing the specified protein level to actin loading control before statistical analysis by Welch's t-test (B and D). $^{**}P \leq 0.01$. Where *P* value is not indicated results were non-significant.

3.4 The purine salvage enzyme, HGPRT, is upregulated in C9orf72 iAstrocytes

We next wanted to investigate the effect of C9orf72 ALS on the enzymes that regulate other key stages of purine salvage and purine degradation. These enzymes were PNP, XDH and HGPRT. PNP catalyses the conversion of inosine and guanosine to hypoxanthine and

guanine, producing ribose-1-phosphate, a key source of energy production in the CNS during cell stress (Balestri et al., 2007; Jurkowitz et al., 1998; Litsky et al., 1999); XDH converts hypoxanthine into xanthine and subsequently xanthine into the antioxidant, urate (Ames et al., 1981; Corte & Stirpe, 1972); and HGPRT is the key enzyme in purine salvage (Henderson & Khoo, 1965; Murray, 1971). None of these enzymes have been directly linked to the pathology of any form of ALS, however all are involved in mediating the response of cells to pathogenic insults commonly observed in ALS. PNP to energy generation, XDH to oxidative stress and HGPRT to DNA damage. In addition, as described previously, we have observed reduced urate production in a cell-line specific manner, that was independent of variations in inosine output in C9orf72 iAstrocytes. These data, taken together, strongly suggested that expression of one or more of these enzymes might be altered in C9orf72 iAstrocytes. To explore this hypothesis, we examined the protein expression of these enzymes using western blots. These investigations demonstrated that, as with ADK, the expression of PNP and XDH were unaffected in C9orf72 iAstrocytes (Figures 3.4A-D). HGPRT, however, was significantly upregulated (Figures 3.4E-F). Interestingly, this increase in expression was largely driven by cell lines C9-183 and C9-201, which corresponds to the two lines that exhibited a significant downregulation in urate output (Figure 3.1E). This indicated that, as had been hypothesised, the level of urate production is ultimately controlled independently of ADA action and is likely regulated by HGPRT activity.

Regardless of the specific mechanistic implications of increased HGPRT, these data demonstrate a further irregularity in purine metabolism in C9orf72 iAstrocytes that has not been previously reported and broadens our knowledge of the full extent of purinergic aberration in C9orf72 ALS.

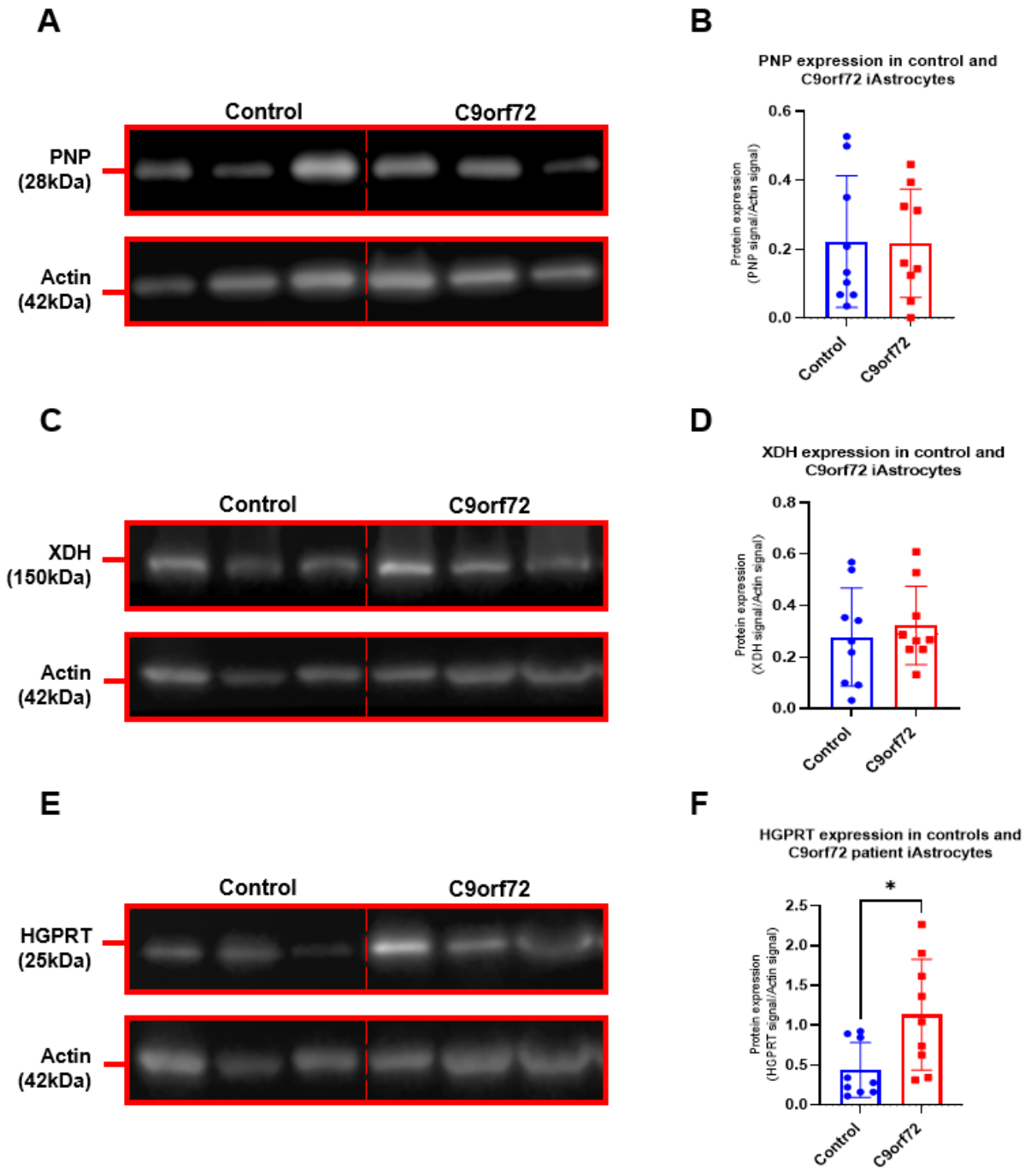

Figure 3.4. HGPRT expression is upregulated in C9orf72 iAstrocytes. (A) Representative image of PNP western blot. (B) Densitometry analysis of PNP western blot. (C) Representative image of XDH western blot. (D) Densitometry analysis of XDH western blot. (E) Representative image of HGPRT western blot. (F) Densitometry analysis of HGPRT western blot. Data presented as mean and standard deviation of three biological replicates from three control and three C9orf72 iAstrocytes. Densitometry analysis performed by normalizing the specified protein level to actin loading control before statistical analysis by Welch's t-test (B and D) or Mann-Whitney test (F). *$P \leq 0.05$. Where P value is not indicated results were non-significant.

3.5 CD73 is downregulated but HGPRT unaffected at the RNA level in C9orf72 iAstrocytes

We previously established that, alongside a reduction at the protein level, relative RNA expression of ADA was also significantly reduced in C9orf72 iAstrocytes. This indicated that a reduction in transcription was responsible for the downregulation of ADA observed at a protein level. Therefore, we next wanted to investigate whether the changes we observed at the protein level in HGPRT and CD73 shared the same transcriptional origin. To do this, we utilised RT-qPCR to survey the relative RNA expression of the two enzymes in C9orf72 iAstrocytes. CD73 RNA expression was significantly downregulated, as was observed at the protein level (Figure 3.5A). HGPRT showed an overall upregulation at the RNA level, but this upregulation did not reach significance (Figure 3.5B). This suggested that CD73 downregulation occurs at a transcriptional level. This may also be the case for HGPRT, but post-transcriptional regulation may also be a factor in enhanced HGPRT expression which is why we observe no significant alterations at the RNA level (though this could also be attributable to variations in the data).

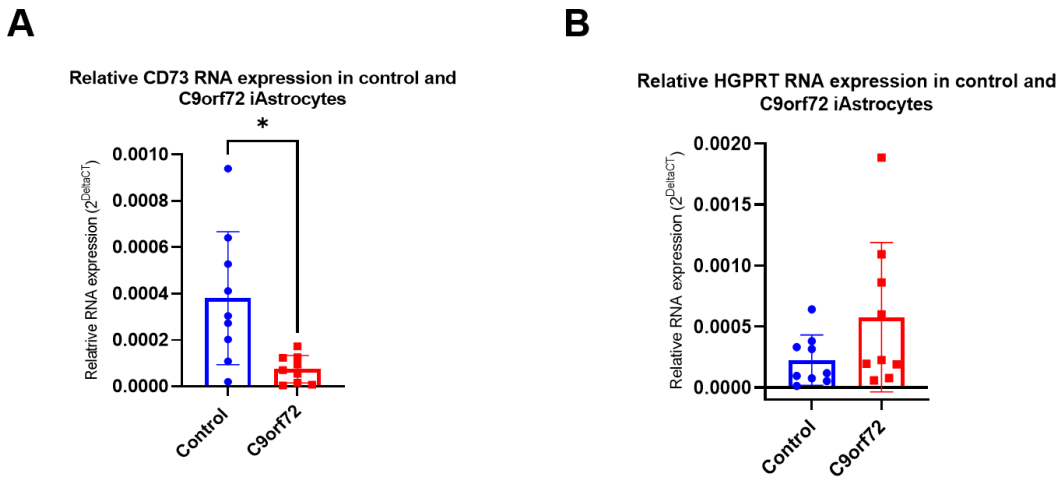

Figure 3.5. Relative CD73 RNA expression is downregulated in C9orf72 iAstrocytes. (A) Relative RNA expression of CD73 in iAstrocytes. (B) Relative RNA expression of HGPRT in iAstrocytes. Data presented as mean and standard deviation of three biological replicates from three control and three C9orf72 iAstrocytes. Statistical analysis by Welch's t-test. *$P \leq 0.05$. Where *P* value is not indicated results were non-significant.

3.6 Discussion

This chapter's focus was on investigating purine metabolism dysfunction in C9orf72 iAstrocytes, to re-confirm and further validate the data presented by Allen et al. (2019a). We also aimed to investigate additional defects that may be present in purine metabolism, that could be caused by (or be the cause of) dysfunction in ADA metabolism.

3.6.1 ADA metabolism dysfunction

Despite divergences in ADA expression in C9-201 compared to the two other C9orf72 cell lines, we did observe a reduction (albeit non-significant) in ADA levels in C9orf72 iAstrocytes, as previously published. For these investigations, age- and sex-matched control/C9orf72 pairs were compared directly to each other and were run side-by-side on the same gel to accommodate for gene therapy-treated samples. This meant that fold-change to the relevant control was used to account for inter-assay variability. C9-201 has the least severe ADA phenotype, whereas Con-209, its control pair, is often closer in phenotype to the C9orf72 lines. This introduced data that contradicted our two other control/C9orf72 pairs. This therefore led to an overall lack of significance in the reduction in ADA expression we observed. Despite the inter-cell line heterogeneity in C9orf72 and control ADA expression, we still observed a significant loss of both ADA activity and inosine output in C9orf72 iAstrocytes. This suggests that loss of ADA at the protein level leads to loss of adenosine activity that may reduce endogenous inosine production. These results also emphasise the disparity in phenotypes in ALS, even within the same genetic cohort, indicating that distinct pathological profiles still lead to the same or similar outcomes and highlighting the need for patient stratification for efficacious treatment, which has been discussed extensively within the field previously (Beghi et al., 2007; Goyal et al., 2020; Sabatelli et al., 2013).

3.6.2 Reduced ADA expression leads to a reduction in ADA activity and inosine output, but not reduced urate output

3.6.2.1 ADA activity and inosine output

Here we showed, for the first time in C9orf72 ALS, that a reduction in ADA expression leads to an accompanying reduction in ADA activity and inosine output (Figure 2C-D), confirming a precedent for dysfunctional adenosine metabolism. As with ADA expression, this downregulation was driven by two cell lines, with expression correlating closely with activity and inosine output. This data confirms that loss of ADA expression leads to a tangible functional dysregulation in enzyme activity, which we had not previously shown. This also

adds to the wealth of evidence already available that adenosine metabolism is dysfunctional in ALS. Breakdown in this essential stage of purine metabolism has two major potential repercussions.

Firstly, reduced ADA activity and ADA expression could lead to a build-up of adenosine, inducing adenosine-mediated toxicity. We have previously shown that C9orf72 iAstrocytes are more susceptible to adenosine-mediated toxicity (Allen et al., 2019a) a finding that has also been observed in iPSC-derived ALS MNs (Ng et al., 2015). ADA inhibition in several *in vitro* models, including control iAstrocytes also leads to adenosine-induced toxicity (Allen et al., 2019a; Archer et al., 1985; Kredich & Martin, 1977). A_{2A} receptor activation is also known to be involved in the transition of astrocytes to a reactive state (Brambilla et al., 2003; Hindley et al., 1994), suggesting that adenosine accumulation is involved in the induction of astrogliosis, which is likely detrimental to neuronal health (Vargas & Johnson, 2010). These data demonstrate the potential for ADA loss to contribute to neurodegeneration. In apparent evidence of ADA loss in a clinical setting, the CSF of individuals with ALS exhibits a significant increase in adenosine levels, despite no concomitant increase in inosine output (Yoshida et al., 1999). Yoshida et al. (1999) attributed spikes in adenosine levels to hypoxic conditions, as adenosine acts as an immunosuppressor via activation of the A_{2A} receptor (Fredholm, 2007; Henney & Lichtenstein, 1971; Sitkovsky & Ohta, 2005; Winn et al., 1981). However, this may inadvertently exacerbate adenosine-mediated toxicity and propagate neurodegeneration, instead of preventing it, particularly as the spike in adenosine levels did not induce a concomitant increase in inosine output, indicating ADA-mediated adenosine metabolism dysfunction in those individuals.

The other possible consequence of reduced ADA activity is reduced ATP output, as inosine is important for energy production (Balestri et al., 2007; Jurkowitz et al., 1998; Litsky et al., 1999; Módis et al., 2013). We know that C9orf72 iAstrocytes are less able to efficiently metabolise adenosine for energy production (Allen et al., 2019a) and demonstrate here that they also have reduced inosine output (Figure 1D). Supplementing cells with inosine improves bioenergetic output and MN survival in iAstrocyte/MN co-cultures (Allen et al., 2019a) and inosine metabolism also positively correlates with disease duration in ALS fibroblasts (Gerou et al., 2021). These data suggest that reduced inosine output, caused by a loss of astrocyte ADA, is detrimental to MN survival in C9orf72 ALS, highlighting an area for therapeutic intervention. Both outcomes would significantly disrupt astrocyte homeostasis and potentially induce cytotoxicity and could therefore be contributory factors in MN degeneration.

3.6.2.2 Possible effects of a reduction in urate output

Along with higher susceptibility to adenosine-mediated toxicity from diminished ADA activity, and dysfunctional bioenergetics caused by reduced inosine output, you might also expect an effect further downstream in purine metabolism. Hence our investigation into urate output, the end-product of purine degradation. Here we observed a significant downregulation in two of three C9orf72 cells lines. These cell lines were C9-183 and C9-201, suggesting that loss of urate may not be directly related to loss of ADA. Loss of urate output may instead be dependent on HGPRT expression, as the two cell lines with the highest HGPRT expression were the two cell lines with the lowest urate output. Urate levels are widely reported as lower in ALS patients (Bjornevik et al., 2019; Ikeda et al., 2012; Keizman et al., 2009; O'Reilly et al., 2017; Oh et al., 2015; Paganoni et al., 2018; Zoccolella et al., 2011) which correlates with a faster disease progression (Ikeda et al., 2012; Keizman et al., 2009; Nicholson et al., 2015; Oh et al., 2015; Paganoni et al., 2012, 2018; F. Zhang et al., 2018), whilst elevated baseline urate levels and stable urate levels throughout treatment were associated with prolonged survival in those treated with edaravone (Takahashi et al., 2022). The level of urate in individuals with ALS therefore plays an important role in ALS disease progression. We have shown that inosine supplementation can significantly increase urate output in C9orf72 iAstrocytes (Allen et al., 2019a) and inosine supplementation has also been shown to boost CSF urate levels in PD patients (Iwaki et al., 2017) and ALS patients (Nicholson et al., 2018). Reactive astrocytes are one of the main contributors to oxidative stress in ALS (Park & Yang, 2021), therefore, astrocyte-targeted treatments that can improve urate output are another area for therapeutic intervention.

3.6.2.3 Conclusions

Due to the importance of astrocytes for the maintenance of neuronal homeostasis and their hypothesised significance in the pathogenesis of ALS, repairing dysfunctional adenosine metabolism and therefore restoring ADA activity, inosine output and potentially urate output to C9orf72 iAstrocytes, therefore has potential three-fold benefit to the cell, of alleviating adenosine- and deoxyadenosine-mediated toxicity, improving bioenergetic output via inosine production and improving antioxidant defence via urate production.

3.6.3 ADK is unaltered and CD73 is downregulated in C9orf72 iAstrocytes

We next wanted to investigate the enzymes that directly regulate adenosine metabolism alongside ADA. To do this we used western blots to examine levels of the enzymes CD73 and ADK. The nucleoside kinase ADK is an incredibly important enzyme that is found ubiquitously throughout the body (Krenitsky et al., 1974). ADK has been referred to as the key upstream regulator of adenosinergic neuromodulation (Boison, 2011) and is an important regulator of

adenosine alongside ADA. Understanding the expression of ADK was therefore important in further elucidating dysfunction in adenosine metabolism. We have shown here that ADK is not significantly altered in C9orf72 iAstrocytes. This further strengthens our observations that reduction in the ability of iAstrocytes to metabolise adenosine, leading to reduced adenosine-derived energy output and increased adenosine-mediated toxicity (Allen et al., 2019a), is triggered solely by a loss of ADA. This data does, however, provide an interesting contrast to the data presented by Boison and Aronica (2015), who demonstrated that ADK was upregulated in reactive astrocytes from the cervical spinal cord of ALS patients. This is most likely because the C9orf72 iAstrocytes were not currently undergoing astrogliosis, but an investigation into the expression of astrogliosis and inflammatory markers in our model would confirm this. It would therefore also be interesting to induce inflammation in C9orf72 iAstrocytes and subsequently investigate the effect on purine metabolism enzymes and the subsequent effect on MN survival in co-cultures.

CD73 is an ecto-enzyme found on the cell surface that dephosphorylates extracellular AMP to form adenosine (Zimmerman, 1992). CD73 is also a powerful regulator of adenosine and adenosinergic activation of the A_{2A} receptor, and therefore the immune response (Meng et al., 2019; Orr et al., 2009). Generally, adenosine acts as an immunosuppressant via agonism of A_{2A} and consequent activation of the cAMP-PKA pathway (Fredholm, 2007; Henney & Lichtenstein, 1971; Sitkovsky & Ohta, 2005; Winn et al., 1981). However, this is context dependent and can be altered by factors such as disease stage (Dai et al., 2010). For example, in a mouse model of MS, A_{2A} activation shifted from anti-inflammatory in early disease-states, to pro-inflammatory in the late stages of disease (Ingwersen et al., 2016). The potential cause for this comes from glutamate levels (Dai et al., 2010). Dai et al. (2010) observed that in the presence of high glutamate levels, the effect of A_{2A} receptor activation switches from the PKA pathway to the PKC pathway, therefore becoming proinflammatory. This is pertinent in times of brain injury, as, in addition to the release of adenosine, a rapid increase in glutamate is observed (Dai et al., 2010). This would explain the conflicting literature surrounding A_{2A} activation in ALS. In ALS, increased expression of A_{2A} has been observed in the lymphocytes and post-mortem spinal tissues of ALS patients and in the spinal cords of SOD1G93A mouse models in early disease stages (Ng et al., 2015; Vincenzi et al., 2013). A_{2A} antagonism was shown to protect MNs from SOD1G93A astrocyte-induced toxicity by inhibiting downstream signalling and preventing mutant protein expression (Ng et al., 2015). Conversely, the A_{2A} agonist CGS21680 has been shown to improve MN survival in culture (Komaki et al., 2012) and prolong the survival of SOD1G93A mice (Yanpallewar et al., 2012). CD73 has not previously been linked to ALS, however, it is an enzyme of interest because of its links to adenosine mediated A_{2A} activation (Meng et al., 2019; Orr et al., 2009). With this information

in mind, we show here, for the first time in C9orf72 iAstrocytes, that CD73 is significantly downregulated at the protein level (Figure 3.3C-D), which is likely driven by transcriptional aberration, as we also observe downregulation in relative RNA levels (Figure 3.5A).

The exact repercussions of this for C9orf72 iAstrocytes are unclear. As mentioned, adenosine is a strong immunosuppressant, and its release is thought of as a protective mechanism to prevent excessive inflammation (Fredholm, 2007; Henney & Lichtenstein, 1971; Sitkovsky & Ohta, 2005; Winn et al., 1981). This would explain why several studies have demonstrated that A_{2A} agonism is beneficial. Therefore, CD73 downregulation could be considered a pathogenic mechanism, causing reduced adenosine output and exacerbating neuroinflammation. Conversely, A_{2A} antagonism has also been shown to be beneficial in ALS cell models, which is presumably because of the situation-dependent pro-inflammatory effect of A_{2A} activation. It would make sense, then, that CD73 downregulation can also act as a protective mechanism in ALS – an attempt to reduce adenosine output in the extracellular space. CD73 loss in C9orf72 could therefore have dual outcomes, both protective and toxic which could be determined by a number of factors, from disease stage to the extent of brain injury (Blum et al., 2003; Jones et al., 1998; Li et al., 2006).

CD73 downregulation could point towards reduced adenosine production, possibly suggesting that lower ADA expression might therefore be a direct response to an initial reduction in adenosine output caused by a loss of CD73. However, whether this is the case or not, several factors also regulate adenosine levels in the extracellular space. Adenosine release in $CD73^{-/-}$ mice was mediated by glutamate receptor dependent release of ATP (Klyuch et al., 2012) and nerve stimulation also mediates adenosine release (Pajski & Venton, 2010). Higher adenosine levels have also been observed in ALS patients (Yoshida et al., 1999) and neuroinflammation is widely reported (Hooten et al., 2015; J. Liu & Wang, 2017). Further, CD73 functions extracellularly and would not account for intracellular adenosine production via 5'-nucleotidases. Adenosine produced in this fashion could induce toxicity intracellularly and be released into the extracellular space via equilibrative nucleoside transporters (Figure 1.6C). Thus, CD73 may be a response to adenosine accumulation caused by ADA downregulation but may not be sufficient to reduce adenosine output, and adenosine-mediated cytotoxicity would, in this instance, still pose a threat to MN health. Alternatively, the trigger for loss of both ADA and CD73 could arise from the C9orf72 HRE itself, whether that be directly, potentially via interactions with DPRs or RNA foci, or indirectly, through an intermediate stimulus, meaning that atypical ADA and CD73 expression may be independent of each other.

Understanding the enigmatic interplay between expression of CD73 and ADA, and adenosine levels in C9orf72 iAstrocytes is crucial in interpreting the true effect of abnormal adenosine metabolism. There are several potential triggers for adenosine metabolism dysfunction, along with several potential outcomes. It is even possible that several causes and effects are true, depending on a number of physiological factors. Investigation in this area should establish the levels of intermediates in this pathway, possibly via carbon labelling, to ascertain how loss of CD73 and ADA alter carbon flow through the pathway. Establishing a timeline to determine which enzyme becomes downregulated first is also key and so investigating whether inhibition of either CD73 or ADA leads to loss of the other enzyme in a control iAstrocyte model is an important experiment. Elevation of either enzyme through targeted gene therapy to observe the effect on the other is another experiment that would shed light on the area and is something that we explore in section 5. Assessing the expression of intracellular nucleotidases could also explain why there is a reduction in CD73 expression. *In vivo* investigation of these purine metabolism enzymes both pre- and post-symptomatically would also shed light on this interplay. These experiments would allow us to conclude whether loss of either enzyme is the stimulus that instigates reduction in the other and potentially answer the question of why each enzyme becomes downregulated at all.

3.6.3.2 HGPRT upregulation

We also investigated how enzymes downstream of ADA were affected in C9orf72 iAstrocytes, investigating the expression levels of PNP, XDH, and HGPRT.

As PNP regulates the production of hypoxanthine and guanine, it is the immediate precursor to both purine degradation and purine salvage and is key for purine-driven energy production. PNP deficiency, causing the body to be unable to process inosine, deoxyinosine, guanosine and deoxyguanosine, leads to SCID, as with ADA deficiency (P. L. C. Walker et al., 2011). This leads to developmental dysfunction in T cells, and more rarely, B cells. Comparatively, PNP-deficient SCID is incredibly rare, but markedly more fatal. A significant proportion of patients suffer from profound neurological disorders, including spasticity, developmental delay and intellectual disability (Markert, 1991). A polymorphism in PNP has also been found to correlate with elevated cognitive decline in AD patients (Tumini et al., 2007). PNP, like most purine enzymes, is an important regulator of neuronal function, and aberration in its expression can therefore have striking neurological effects. No prior links to ALS have been observed with PNP, and we demonstrate here that C9orf72 iAstrocytes also have no dysfunction in PNP expression (Figure 3.4A-B). We have previously demonstrated that C9orf72 iAstrocytes are able to metabolise inosine on a par with controls and inosine supplementation is able to

significantly induce increases in ATP output and glycolytic flux (Allen et al., 2019a). Had there been dysfunction in PNP expression, metabolic profiling of C9orf72 iAstrocytes would have likely revealed either hypo- or hypermetabolism in inosine, and inosine supplementation would have had a response distinct from control iAstrocytes. It was therefore not unexpected to observe no alteration in the expression of PNP.

XDH is a flavoprotein enzyme that exists as a homodimer and is the predominant form of XOR under normal conditions. XORs catalyse the final two stages of purine metabolism, known as purine degradation. This involves dehydrogenating hypoxanthine to form xanthine and xanthine to form urate, utilising NAD+ as an electron acceptor. During ischemia, XDH is irreversibly converted to XO by sulfhydryl oxidation or Ca^{2+}-activated proteases (Granger., 1986). This alters the mechanism of action, producing reactive oxygen species (ROS) as by-products of both reactions, exacerbating oxidative stress (Abramov et al., 2007; Granger et al., 1986). Because C9orf72 ALS can induce oxidative stress, it could be hypothesised that XDH levels are downregulated whilst XO levels are upregulated. We show here however that XDH expression is unaffected in C9orf72 iAstrocytes. Neurologically, elevated expression of XO has been reported in people diagnosed with major depression (Herken et al., 2007; Michel et al., 2010) which is ameliorated by antidepressant treatment (Herken et al., 2007). Elevated XO has also been reported in a mouse model of AD, whilst inhibition via oxypurinol was able to attenuate ROS production and protect from neuronal toxicity (Y. Abe et al., 2004). Similar findings were also reported in the rat striatum of a PD model (Obata et al., 2001). The balance between XDH and XO expression is therefore an important predictor of, and contributor to, oxidative stress and might therefore influence the pathology of C9orf72 ALS. Efforts should therefore be undertaken to investigate levels of XO in this cell model.

Purine metabolism is essential in the body as it is responsible for the production of key DNA and RNA nucleotides and is therefore required for DNA synthesis and repair (Ansoleaga et al., 2015). HGPRT initiates purine salvage, the predominant source of nucleotides physiologically, making it key for DNA synthesis and repair. DNA damage has been widely implicated in multiple forms of ALS (for a review see Kok et al 2021), and for C9orf72 ALS specifically, poly-GR expression has been shown to induce DNA damage in *in vivo* and *in vitro* models (Lopez-Gonzalez et al 2016; Choi et al 2019). This suggests that elevated HGPRT expression is the cell's response to enhanced DNA damage and insufficient purine production. To confirm this, future work should examine the expression of DNA damage markers in individual cell lines and correlate that with the expression of HGPRT. This was planned at the start of the PhD, but due to the effect of COVID on lab access we were unable to measure DNA damage markers before the end of the funding period.

Alternatively, enhanced purine salvage could point towards the induction of astrogliosis. Astrogliosis has been reported in the brain and spinal cord of ALS patients (Kushner et al., 1991; Schiffer et al., 1996), and is hypothesised to be a contributory factor to MN degeneration (Vargas & Johnson, 2010). The C9orf72 HRE has been shown to induce astrogliosis *in vivo* (Chew et al., 2015; Y. Liu et al., 2016; Y. J. Zhang et al., 2016). A feature of astrogliosis is the enhanced proliferation of astrocytes, which would require higher DNA synthesis. Thus, enhanced HGPRT expression could facilitate the transition of astrocytes to a reactive state. Though elevation of HGPRT has not been directly linked to astrogliosis previously, and we have hypothesised that the C9orf72 iAstrocytes would not be currently undergoing astrogliosis as ADK expression was unaltered.

The two cell lines that exhibited the strongest upregulation in HGPRT were C9-183 and C9-201. These are also the two cell lines with significantly low urate output, whilst C9-78, that exhibits lower ADA expression, activity and inosine output has a urate output comparable to control level. The opposite is true in C9-201. This implies that urate production is dependent on HPGRT expression as opposed to ADA activity or inosine output. HGPRT elevation may therefore be counterproductive for C9orf72 iAstrocytes, as this likely reduces urate output which is consistently associated with a worse prognosis in patients (Ikeda et al., 2012; Keizman et al., 2009; Nicholson et al., 2015; Oh et al., 2015; Paganoni et al., 2018; F. Zhang et al., 2018) and may facilitate enhanced astrocyte proliferation and therefore astrogliosis. Inhibition of HGPRT expression could therefore be a method of increasing urate output, obstructing astrogliosis and improving neuronal health. This would, however, come with the unwanted effect of reducing purine salvage, potentially impairing DNA synthesis and repair.

One plausible explanation for urate levels correlating with survival in ALS patients is that patients that have lower levels of urate experience higher levels of DNA damage and therefore a higher requirement for purine salvage, causing an elevation in HGPRT. This means that urate output may correlate with better survival, but not in fact be causative, despite the current consensus. With a larger cohort we could investigate whether urate output in C9orf72 iAstrocytes matches clinical prognosis and definitively determine whether urate output inversely correlates with HGPRT expression.

3.6.3.3 Conclusions

Identifying aberrations in HGPRT and CD73 has given us a clearer picture of purine metabolism, but further work is required. As stated, establishing a timeline of events linking the occurrence of loss of ADA and CD73 and upregulation in HGPRT is key in understanding how and why these changes occur.

3.6.4 Future work

The results presented here prove that further investigation is warranted in this pathway. This section will discuss potential future work not already considered.

Firstly, investigation is required into the exact causes of changes in ADA, CD73 and HGPRT expression. One key question is how alterations in the expression of each enzyme effects expression of the other two. We have possibly already answered the question of whether HGPRT expression and CD73 and ADA expression are intrinsically linked as CD73 and ADA reduction in cell line C9-78 does not lead to a subsequent increase in HGPRT.

It should also be reiterated that, though we have hypothesised here that alterations in this pathway cause a ripple effect that initiate downstream or upstream effects, the trigger could instead be the C9orf72 HRE itself, whether that be directly, potentially via interactions with DPRs or RNA foci, or caused by another stimuli, such as transcriptional regulation or a response to DNA damage, itself triggered by the presence of the C9orf72 HRE. There is the possibility therefore, that the changes observed at each stage of this pathway are independent of each other. Investigation into this area will be partly covered in Section 4.

Additional investigation is also required of DNPB and the purinosome, which become more important in times of high purine demand (An et al., 2008; Buchanan & Hartman, 1959; Greenberg & Jaenicke, 1957; Hartman & Buchanan, 1959), and it could be theorised that aberration in this pathway may be the driver of the dysfunction we have observed in purine salvage and degradation. Investigating how the expression of enzymes involved in this pathway are affected by C9orf72 ALS is therefore key. Further, as previously mentioned, exploring the exact levels of intermediaries in this pathway, using time-of-flight mass spectrometry and carbon-labelling to examine all three combined pathways would give a far clearer picture of why these abnormalities might occur initially and how they influence carbon flow through the pathway, elucidating the potential ramifications for the cell caused by these aberrations (such as adenosine accumulation leading to toxicity).

These experiments would allow the establishment of cause and effect for the abnormalities we have demonstrated in purine metabolism in C9orf72 iAstrocytes, making it more straightforward to develop targeted therapies. Therapeutic intervention in this pathway, by restoring ADA expression to cells, has the potential to benefit C9orf72 iAstrocytes in numerous ways. Further work into this area will be covered in section 5.

4. Mechanisms leading to purine metabolism dysfunction in C9orf72 ALS iAstrocytes

Understanding why the aberrations in C9orf72 iAstrocyte purine metabolism occur is vital in understanding C9orf72 pathology and in the development of targeted treatments. Therefore, in this chapter, we investigated whether the transcription of ADA was altered in our C9orf72 iAstrocytes and which (if any) C9orf72 HRE specific pathogenic mechanisms are the cause of the purine metabolism alterations.

4.1 Transcriptional regulation by p73 is not responsible for loss of ADA in C9orf72 iAstrocytes

p73 is important in the maintenance of neuronal homeostasis, as abrogation of p73 *in vivo* and *in vitro* induces neuronal dysfunction (Yang et al., 2000) and several mutations in ΔN-p73 (the isoform found predominantly in the CNS), have been recently implicated in sALS patients (Russell et al., 2021). As p73 is involved in the transcriptional regulation of ADA (see introduction) (Tullo et al., 2003), we decided to examine ΔN-p73 expression in C9orf72 iAstrocytes, with the hypothesis that a loss of p73 might correlate with the downregulation we see in ADA expression. To do this, we initially measured ΔN-p73 protein expression via western blot. Several bands were visible on the blot, possibly due to the various isoforms of ΔN-p73 (Murray-Zmijewski et al., 2006; Marshall et al. 2021). The most prominent and consistent band was between 37-50kDa, whilst ΔN-p73's predicted size is 66kDa. There was some evidence of banding at other heights, but none were consistently detected by western blot in all biological replicates. Densitometry analysis of the band appearing between 37-50kDa suggested that protein expression of ΔN-p73 was unaffected in C9orf72 iAstrocytes compared to controls (Figure 4.1A-B), but it may be unlikely that this band is a true representation of ΔN-p73 expression. To further investigate this, we examined the relative RNA expression of ΔN-p73 using RT-qPCR. This demonstrated that ΔN-p73 was unaffected at the RNA level (Figure 4.1C). We also investigated the relative RNA expression of ΔN-p73 in sALS iAstrocytes demonstrating that, interestingly, the RNA expression of ΔN-p73 was significantly downregulated in sALS cell lines (Figure 4.1D). These data suggest that transcriptional regulation via p73 is not the trigger for abnormal ADA expression in C9orf72 iAstrocytes but may provide the mechanistic basis for the downregulation of ADA observed in sALS iAstrocytes (Allen et al., 2019a). We next investigated how the pathogenic mechanisms of the C9orf72 HRE affect ADA expression.

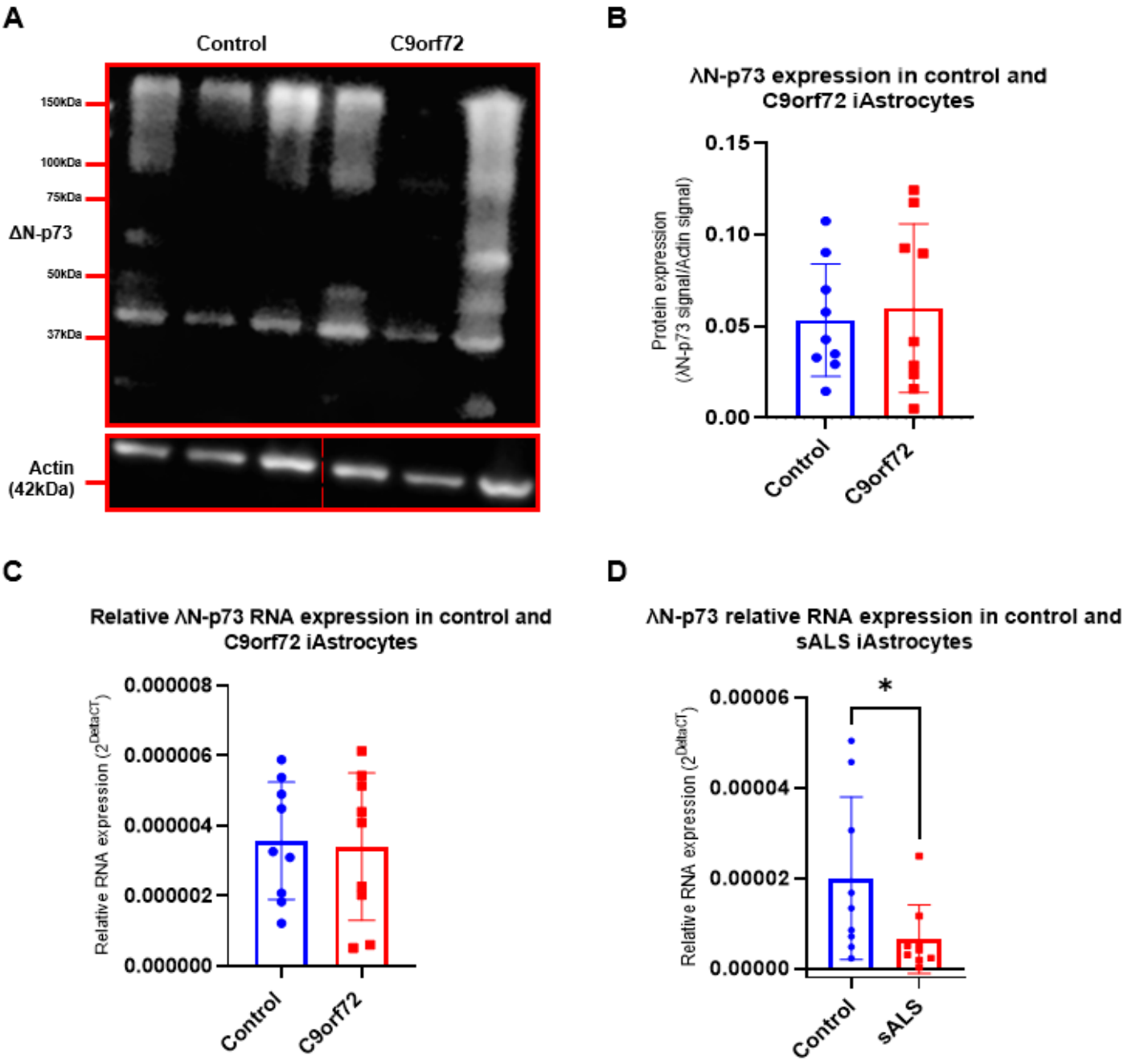

Figure 4.1. ADA activity loss in C9orf72 iAstrocytes is not due to a reduction in p73. (A) Representative image of ΔN-p73 western blot. (B) Densitometry analysis of ΔN-p73 western blot. (C) Relative RNA expression of ΔN-p73 in C9orf72 iAstrocytes. (D) Relative RNA expression of ΔN-p73 in sALS iAstrocytes. Data presented as mean and standard deviation of three biological replicates from three control and three C9orf72 or sALS iAstrocytes. Densitometry analysis performed by normalizing the specified protein level to actin loading control before statistical analysis by Welch's t-test (B and C) or Mann-Whitney test (D).

4.2 C9orf72 knockout in HeLa cells does not affect ADA, CD73 or HGPRT expression

Having potentially ruled out reduction in ΔN-p73 expression as a cause for loss of ADA in C9orf72 iAstrocytes, we next chose to examine whether the toxic mechanisms that are hypothesised to contribute to the pathology of the C9orf72 HRE would affect ADA expression. We also used this as an opportunity to understand whether they result in aberration in the wider purine metabolism. Dysfunction in the C9orf72 protein is widely reported to exacerbate inflammation and interfere with immune cell function (for a review see Pang & Hu, 2021). As adenosine metabolism is known to regulate inflammation (Sitkovsky and Ohta, 2005; Fredholm, 2007) and ADA is key in the functioning of several immune cells (Aldrich et al., 2003; Carson et al., 1979; Fischer et al., 1976; Martín et al., 1995; Yagawa & Okamura, 1981), we hypothesised that C9orf72 protein loss could influence purine metabolism. To investigate this, we used a C9orf72$^{-/-}$ HeLa line, provided by Prof. Kurt De Vos, to mimic loss-of-function of the C9orf72 protein. As with our C9orf72 iAstrocytes, we utilised western blots to examine the protein expression of purine metabolism enzymes for the first time in a model of this type. Along with ADA, we examined HGPRT and CD73 expression as these were the enzymes differentially expressed at a protein level in C9orf72 iAstrocytes (Figure 3.3-3.5). Our data showed that ADA, CD73 and HGPRT protein expression were not significantly altered in the C9orf72$^{-/-}$ line (Figure 4.2A-F).

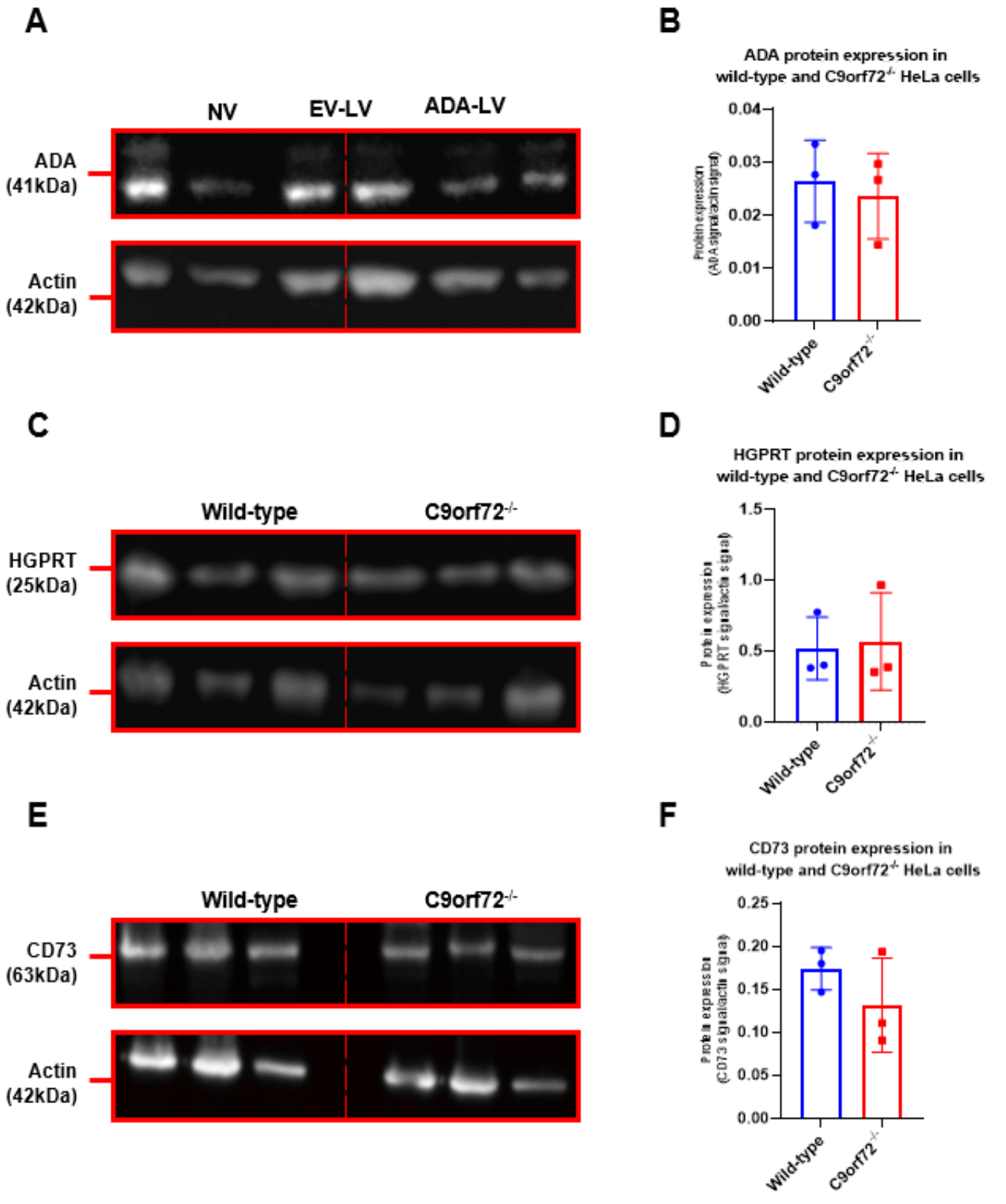
A
NV
EV-LV
ADA-LV
ADA
(41kDa)
Actin
(42kDa)
B
ADA protein expression in
wild-type and C9orf72-/- HeLa cells
Protein expression
(ADA signal/actin signal)
0.04
0.03
0.02
0.01
0.00
Wild-type
C9orf72-/-
C
Wild-type
C9orf72-/-
HGPRT
(25kDa)
Actin
(42kDa)
D
HGPRT protein expression in
wild-type and C9orf72-/- HeLa cells
Protein expression
(HGPRT signal/actin signal)
1.5
1.0
0.5
0.0
Wild-type
C9orf72-/-
E
Wild-type
C9orf72-/-
CD73
(63kDa)
Actin
(42kDa)
F
CD73 protein expression in
wild-type and C9orf72-/- HeLa cells
Protein expression
(CD73 signal/actin signal)
0.25
0.20
0.15
0.10
0.05
0.00
Wild-type
C9orf72-/-

Figure 4.2. C9orf72 knockout in HeLa cells does not affect ADA, CD73 or HGPRT expression. (A) Representative image of ADA western blot in C9orf72$^{-/-}$ HeLa. (B) Densitometry analysis of ADA western blot in C9orf72$^{-/-}$ HeLa. (C) Representative image of HGPRT western blot in C9orf72$^{-/-}$ HeLa. (D) Densitometry analysis of HGPRT western blot in C9orf72$^{-/-}$ HeLa. (E) Representative image of CD73 western blot in C9orf72$^{-/-}$ HeLa. (F) Densitometry analysis of CD73 western blot in C9orf72$^{-/-}$ HeLa. Data presented as mean and standard deviation of three biological replicates from wild-type and C9orf72$^{-/-}$ HeLa. Densitometry analysis performed by normalizing the specified protein level to actin loading control, before statistical analysis by Welch's t-test (B, D and F).

4.3 Gain-of-function mechanisms of the C9orf72 HRE led to a significant reduction in ADA expression in an N2a model

We next investigated gain-of-function mechanisms as a trigger of purine metabolism dysfunction. For this we utilised an N2a line, transduced with a 38x G_4C_2 or 39x C_4G_2 HRE LV, provided by the Shaw lab. The expression of RNA foci and poly-GP from both sense and antisense transcripts, along with the expression of poly-GA from the sense transcript in transfected N2a cells has been confirmed (Hautbergue et al. 2017), making them a suitable gain-of-function model. The expression of DPRs and RNA foci has been associated with several pathways linked to purine metabolism, such as the induction of DNA damage (Maor-Nof et al., 2021). Poly-PR has also been shown to bind directly to ADAR1 and ADAR2, analogues of ADA, impairing function (Suzuki & Matsuoka, 2021). We therefore hypothesised that these gain-of-function mechanisms could induce purine metabolism dysfunction. We used western blots to examine the expression of ADA, CD73 and HGPRT. We demonstrated here that gain-of-function mechanisms from an antisense origin led to a significant downregulation in ADA expression, whilst in the sense model no overall downregulation was observed (Figure 4.3.1A-B). For both CD73 and HGPRT, the findings are unclear and were most likely influenced by loading control protein expression. Qualitatively, CD73 expression did not appear to be altered in G_4C_2 or C_4G_2 N2a, however, when normalising to actin, a small, non-significant decrease in expression was observed, which could reach significance, given further replicates (Figure 4.3.1E-F). Similarly, HGPRT expression appeared moderately raised in the G_4C_2 model, but moderately decreased in the C_4G_2 model. However, when normalised to actin, no upregulation of HGPRT in G_4C_2 N2a was observed, whilst a significant downregulation in HGPRT was observed in C_4G_2 N2a cells (Figure 4.3.1C-D). These findings, unlike with ADA, did not seem to reflect what appeared in the western blot image. Interestingly, what we did observe was an increase in actin levels in both the G_4C_2 and C_4G_2 expressing N2a lines. This trend was consistent across multiple biological replicates and therefore unlikely

to be related to erroneous protein quantification. To assess whether this was actin related, we tested two other loading control proteins regularly used as western blot loading controls, namely tubulin and GAPDH, and saw even larger differences, which reached significance (Figure 4.3.2A-F). Therefore, we could not rule out a loading control protein normalisation effect on our analysed data, which would potentially mask the true effects of sense and antisense HRE expression. For example, in G_4C_2 N2a, an increase in HGPRT expression would be masked by normalising to an artificially higher loading control signal. Conversely, a moderate decrease in HGPRT expression in the C_4G_2 N2a would be artificially inflated by enhanced loading control signal. There was evident loss of ADA in the C_4G_2 model, and we were therefore confident that this effect was induced by HRE expression. These data therefore provides a potential mechanism for the adenosine metabolism dysfunction observed by Allen et al. (2019a), that leads to a subsequent loss of ADA activity and inosine output (Figure 3.1C-D). However, the extent of the loss must be caveated with the loading control signal increase. Partially because of this caveat, and to explore the mechanisms of ADA loss further, we next investigated the expression of individual DPRs to measure the effect on purine metabolism enzyme expression.

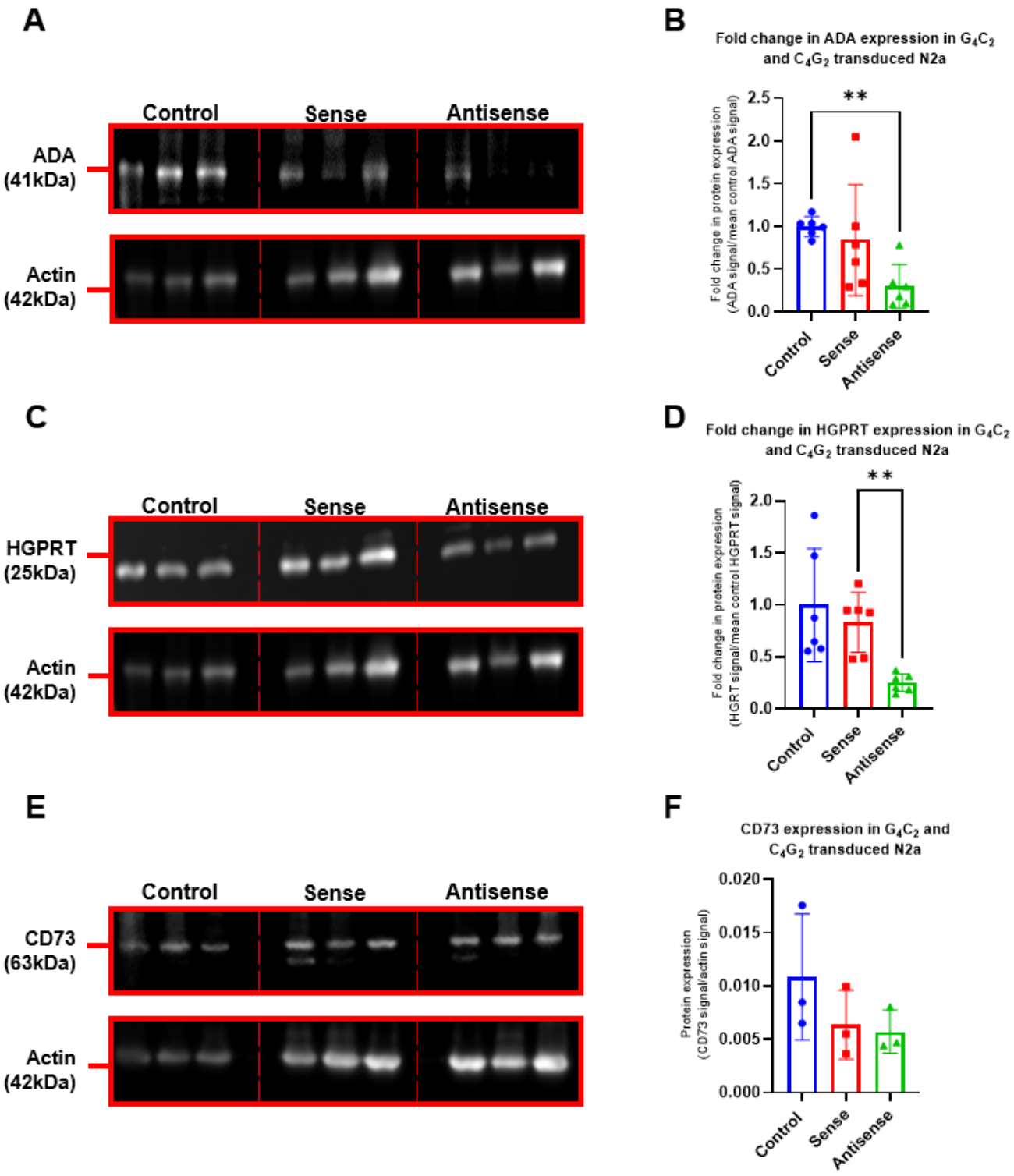
A
Control
Sense
Antisense
ADA
(41kDa)
Actin
(42kDa)
B
Fold change in ADA expression in G_4C_2 and C_4G_2 transduced N2a
Fold change in protein expression (ADA signal/mean control ADA signal)
2.5
2.0
1.5
1.0
0.5
0.0
**
Control
Sense
Antisense
C
Control
Sense
Antisense
HGPRT
(25kDa)
Actin
(42kDa)
D
Fold change in HGPRT expression in G_4C_2 and C_4G_2 transduced N2a
Fold change in protein expression (HGRT signal/mean control HGPRT signal)
2.0
1.5
1.0
0.5
0.0
**
Control
Sense
Antisense
E
Control
Sense
Antisense
CD73
(63kDa)
Actin
(42kDa)
F
CD73 expression in G_4C_2 and C_4G_2 transduced N2a
Protein expression (CD73 signal/actin signal)
0.020
0.015
0.010
0.005
0.000
Control
Sense
Antisense

Figure 4.3.1. Transduction of the sense and antisense HRE leads to loss of ADA and HGPRT in N2a cells. (A) Representative image of ADA western blot in sense and antisense C9orf72 HRE transduced N2a cells. (B) Densitometry analysis of ADA western blot in sense and antisense C9orf72 HRE transduced N2a cells. (C) Representative image of HGPRT western blot in sense and antisense C9orf72 HRE transduced N2a cells. (D) Densitometry analysis of HGPRT western blot in sense and antisense C9orf72 HRE transduced N2a cells. (E) Representative image of CD73 western blot in sense and antisense C9orf72 HRE transduced N2a cells. (F) Densitometry analysis of CD73 western blot in sense and antisense C9orf72 HRE transduced N2a. Data presented as mean and standard deviation of six (B and D) or three (F) biological replicates from control, sense and antisense transduced N2a cells. Densitometry analysis performed by normalising the specified protein level to actin loading control, and then normalising values to a control average (B and D), or using raw data (F) and performing statistical analysis by Brown-Forsythe and Welch ANOVA (B, D, and F). *$P \leq 0.05$, **$P \leq 0.01$. Where P value is not indicated results were non-significant.

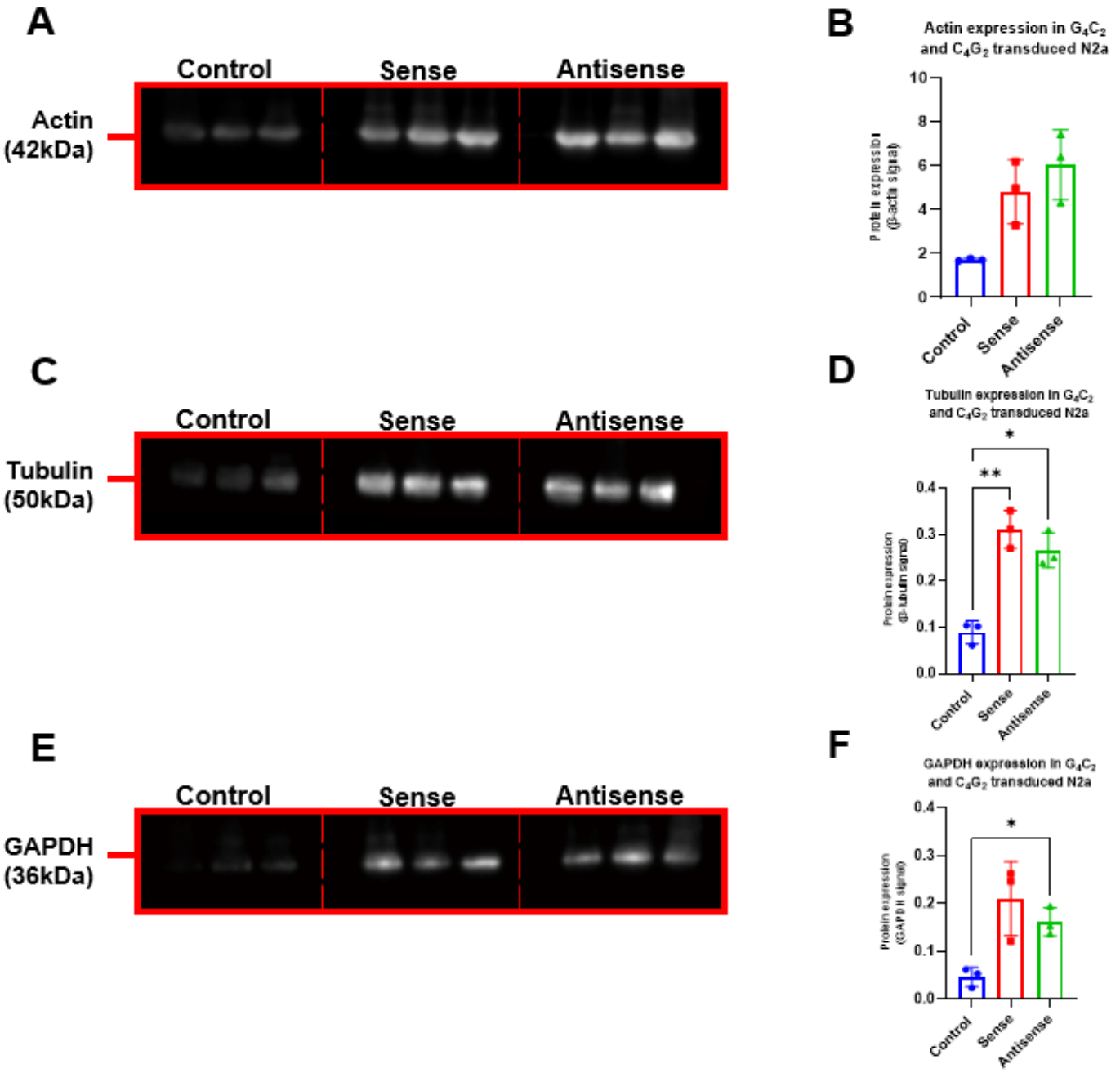
A
Control
Sense
Antisense
Actin
(42kDa)
B
Actin expression in G_4C_2 and C_4G_2 transduced N2a
Protein expression (β-actin signal)
10
8
6
4
2
0
Control
Sense
Antisense
C
Control
Sense
Antisense
Tubulin
(50kDa)
D
Tubulin expression in G_4C_2 and C_4G_2 transduced N2a
*
**
Protein expression (β-tubulin signal)
0.4
0.3
0.2
0.1
0.0
Control
Sense
Antisense
E
Control
Sense
Antisense
GAPDH
(36kDa)
F
GAPDH expression in G_4C_2 and C_4G_2 transduced N2a
*
Protein expression (GAPDH signal)
0.4
0.3
0.2
0.1
0.0
Control
Sense
Antisense

Figure 4.3.2. Transduction of the sense and antisense HRE leads to increases in loading control protein expression in N2a cells. (A) Representative image of actin western blot in sense and antisense C9orf72 HRE transduced N2a cells. (B) Densitometry analysis of actin western blot in sense and antisense C9orf72 HRE transduced N2a cells. (C) Representative image of Tubulin western blot in sense and antisense C9orf72 HRE transduced N2a cells. (D) Densitometry analysis of Tubulin western blot in sense and antisense C9orf72 HRE transduced N2a cells. (E) Representative image of GAPDH western blot in sense and antisense C9orf72 HRE transduced N2a cells. (F) Densitometry analysis of GAPDH western blot in sense and antisense C9orf72 HRE transduced N2a cells. Data presented as mean and standard deviation of three biological replicates from control, sense and antisense transduced N2a, with statistical analysis by Brown-Forsythe and Welch ANOVA (B, D, and F). *$P \leq 0.05$, **$P \leq 0.01$. Where P value is not indicated results were non-significant.

4.5 DPR transfection in HEK293T cells

As we had observed that C9orf72 gain-of-function mechanisms cause a significant reduction in ADA expression, we chose next to determine whether DPR expression in isolation would recapitulate these results and, if so, which DPR was responsible. To do this we initially transfected HEK293T cells with V5-tagged 36x repeat poly-GA, poly-GR, and poly-PR DPRs, provided by Prof. Kurt De Vos. These lengths were chosen as expression of 36x poly-GR and poly-PR is sufficient to induce neurodegeneration in a *Drosophila* model (Hautbergue et al., 2017; Mizielinska et al., 2014) whilst, clinically, more than 30 copies of the HRE are considered pathogenic (Renton et al., 2011). Poly-GA, poly-GR and poly-PR were investigated as they have been proven to induce neuronal impairment and toxicity *in vivo* and *in vitro* previously (Chew et al., 2015; Freibaum et al., 2015; Khosravi et al., 2020; K. H. Lee et al., 2016; Mizielinska et al., 2014; Tao et al., 2015; Wen et al., 2014). Initially, plasmids containing the 36x DPR sequence were transfected using a jetPRIME transfection kit. We also assayed untransfected cells and cells that had undergone a mock transfection to distinguish between the effect of the DPR transfection and the transfection process itself. Further, we initially transfected cells with a GFP-tagged plasmid to confirm the efficacy of transfection. Cells were then stained with DAPI and V5 antibody and imaged on an IN-cell analyser 2000. We observed background expression of V5 antibody in UT and mock cells, as expected (Figure 4.5A-B). The same was observed in GFP transfected HEK293T cells, though clear GFP expression was present in the cells, demonstrating that transfection was successful (Figure 4.5F). However, background expression levels of V5 were also observed in cells that had been transfected with V5-tagged DPR plasmids (Figure 4.5C-E) indicating that DPR transfection was unsuccessful. The expression of GFP in GFP-transfected cells demonstrated that the

issue did not lie with the process of transfection, instead pointing towards the functioning of the DPR-plasmids as the reason for a lack of expression. We therefore prepped fresh plasmid stocks for transfection. We were also unable to observe consistently high-quality images in HEK293T cells to produce robust, reliable data and therefore began to use HeLa cells.

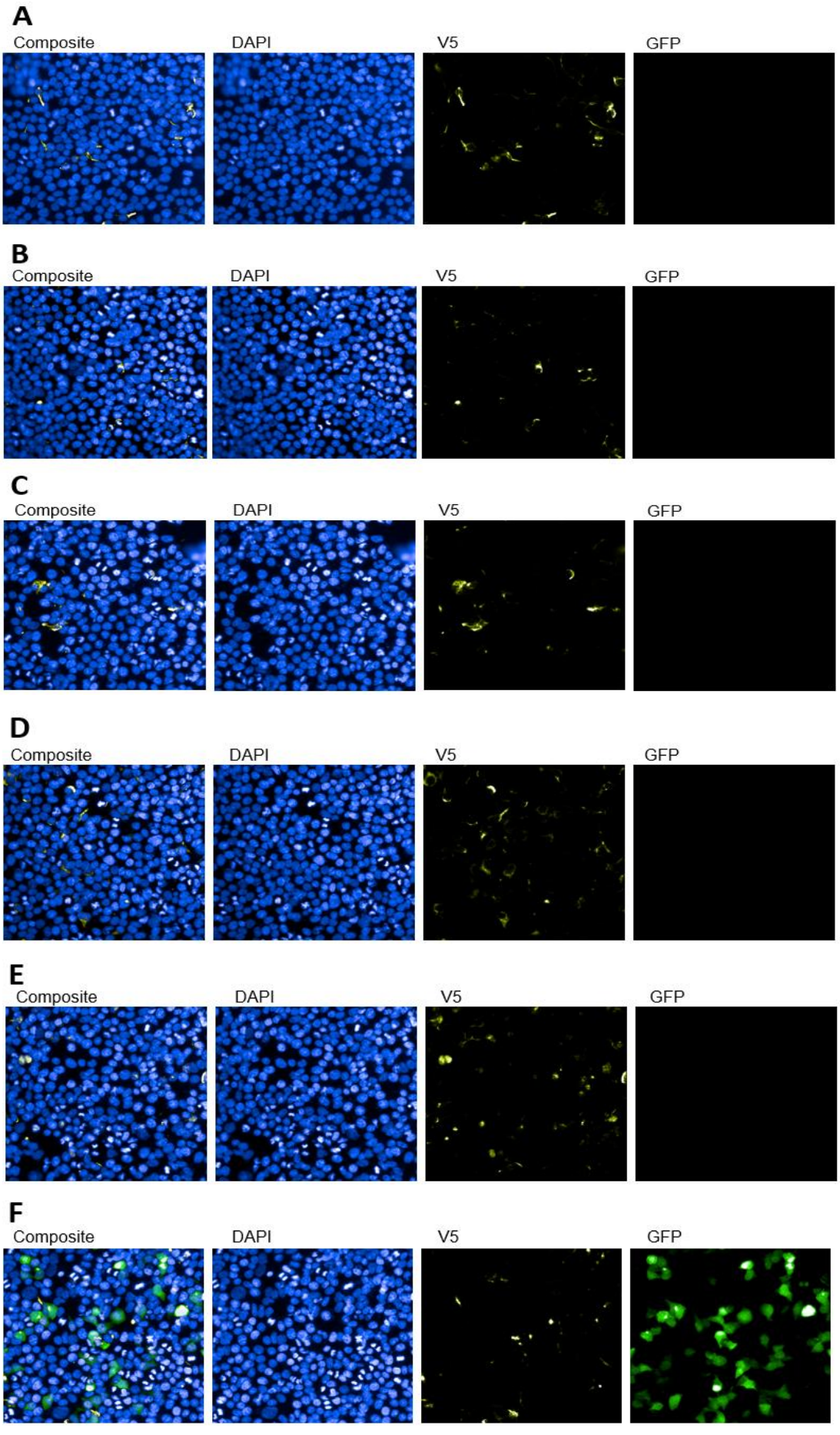
A
Composite
DAPI
V5
GFP
B
Composite
DAPI
V5
GFP
C
Composite
DAPI
V5
GFP
D
Composite
DAPI
V5
GFP
E
Composite
DAPI
V5
GFP
F
Composite
DAPI
V5
GFP

Figure 4.5. Immunofluorescence images of HEK293T cells transfected with DPRs and GFP. (A-F) Representative images of untransfected HEK293T cells (A), HEK293T cells that underwent a mock transfection (B) and HEK293T cells transfected with V5-tagged poly-GA (C), poly-GR (D), and poly-PR (E) or GFP (F) encoding vectors. 24hr post-transfection cells were fixed and stained with V5 (yellow) antibody. Nuclei were stained with DAPI (blue).

4.6 Confirmation of DPR transfection in HeLa cells

After generating fresh DPR plasmids as described in sections 2.2.2 and 2.2.4, we transfected and stained HeLa cells as described above, though without this time confirming transfection using GFP. Instead, we stained Hela cells with an ADA antibody to examine the expression and distribution pattern of ADA in HeLa cells expressing DPRs. This was intended to enable us to directly examine ADA expression in DPR positive cells and to understand whether DPR expression would induce abnormal distribution patterns in ADA. Imaging was also performed on a BX53 light microscope as opposed to the IN-cell analyser. Initially, we were able to confirm transfection by immunofluorescence, staining cells with DAPI and a V5 antibody. Here we showed no presence of V5 staining (beyond background) in the untransfected and mock cell lines (Figure 4.6A-B). However, there was evidence of strong expression of V5 in all three DPR transfected lines with unique distribution patterns (Figure 4.6C-E). This imaging demonstrated that poly-GA was present in both the nucleus and cytoplasm of cells (Figure 4.6C), poly-GR in the cytoplasm (Figure 4.6D) and poly-PR formed aggregates in the nucleus (Figure 4.6E). This confirmed published work showing that poly-GA is cytosolic and perinuclear in distribution (Wen et al., 2014), whilst poly-GR has been shown to concentrate in the cytoplasm and poly-PR localises preferentially to the nucleus (K. H. Lee et al., 2016; Schmitz et al., 2021; Suzuki et al., 2019; Wen et al., 2014) (although both arginine-containing DPRs can enter the nucleus due to their similarity to nuclear localisation signal domains (Kwon et al., 2014)). Importantly, this confirmed that we were able to successfully transfect HeLa cells with DPR-expressing plasmids. No evidence of abnormal distribution of ADA was observed compared to untransfected or mock transfections in DPR transfected HeLa cells (Figure 4.6A-E). We next utilised western blots to examine ADA expression directly in DPR-expressing HeLa cells, which also allowed us to investigate CD73 and HGPRT expression in these models.

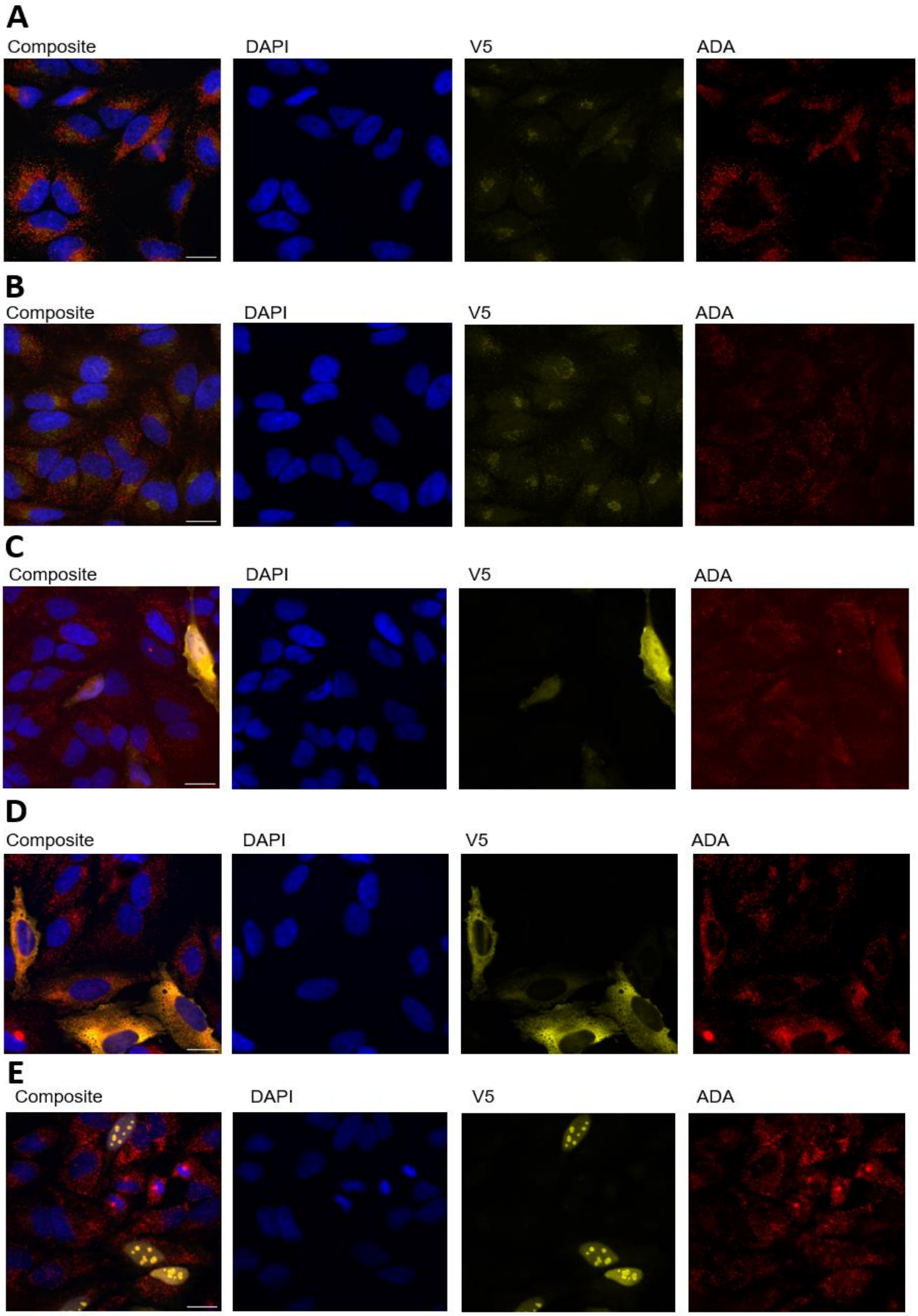
A
Composite
DAPI
V5
ADA
B
Composite
DAPI
V5
ADA
C
Composite
DAPI
V5
ADA
D
Composite
DAPI
V5
ADA
E
Composite
DAPI
V5
ADA

Figure 4.6. Confirmation of DPR transfection in HeLa cells. (A-E) Representative images of untransfected HeLa cells (A), HeLa cells that underwent a mock transfection (B) and HeLa cells transfected with V5-tagged poly-GA (C), poly-GR (D), or poly-PR (E) encoding vectors. 24hrs post-transfection cells were fixed and stained with V5 (yellow) and ADA (red) antibody. Nuclei were stained with DAPI (blue). Scale bar = 300μm.

4.7 Expression of poly-PR induces a significant downregulation in ADA and CD73

We next investigated the protein expression of ADA, HGPRT and CD73. We demonstrated here that poly-PR expression in these Hela cells led to a significant downregulation in the expression of ADA and CD73 (Figure 4.7A-D), a finding that recapitulated what we had observed in C9orf72 iAstrocytes. Downregulation in the expression of both CD73 and ADA was also observed in HeLa transfected with poly-GA and poly-GR without reaching significance. This suggests that there is also a role for sense DPRs in the purine metabolism dysfunction observed in C9orf72 iAstrocytes, though possibly not as pronounced as the role that poly-PR expression plays. HGPRT, conversely, was unaffected by DPR transfection (Figure 4.7E-F). These data point towards a key role for the antisense DPR, poly-PR, as a driver of the purine metabolism dysfunction observed in C9orf72 ALS iAstrocytes.

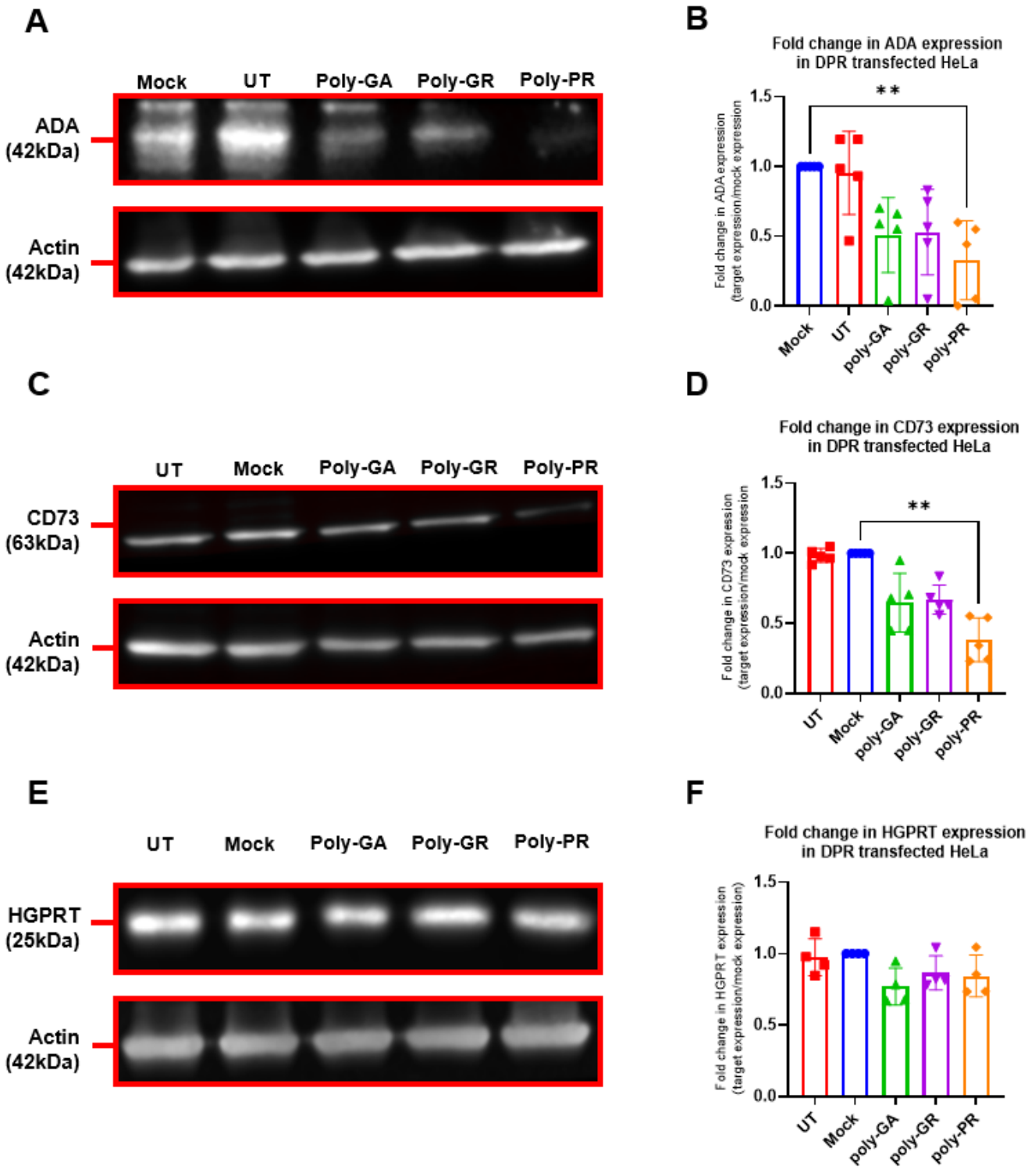
A
Mock
UT
Poly-GA
Poly-GR
Poly-PR
ADA
(42kDa)
Actin
(42kDa)
B
Fold change in ADA expression
in DPR transfected HeLa
**
Fold change in ADA expression
(target expression/mock expression
1.5
1.0
0.5
0.0
Mock
UT
poly-GA
poly-GR
poly-PR
C
UT
Mock
Poly-GA
Poly-GR
Poly-PR
CD73
(63kDa)
Actin
(42kDa)
D
Fold change in CD73 expression
in DPR transfected HeLa
**
Fold change in CD73 expression
(target expression/mock expression
1.5
1.0
0.5
0.0
UT
Mock
poly-GA
poly-GR
poly-PR
E
UT
Mock
Poly-GA
Poly-GR
Poly-PR
HGPRT
(25kDa)
Actin
(42kDa)
F
Fold change in HGPRT expression
in DPR transfected HeLa
Fold change in HGPRT expression
(target expression/mock expression)
1.5
1.0
0.5
0.0
UT
Mock
poly-GA
poly-GR
poly-PR

Figure 4.7. Expression of poly-PR induces a significant downregulation in ADA and CD73. (A) Representative image of ADA western blot. (B) Densitometry analysis of ADA western blot. (H) Representative image of CD73 western blot. (C) Densitometry analysis of CD73 western blot. (J) Representative image of HGPRT western blot. (K) Densitometry analysis of HGPRT western blot. Data presented as mean and standard deviation of four or five biological replicates from untransfected HeLa cells, Hela cells that underwent a mock transfection and HeLa cells transfected with V5-tagged poly-GA, poly-GR, and poly-PR encoding vectors. Densitometry analysis performed by normalizing the specified protein level to actin loading control and then setting mock values to 1, before statistical analysis by Friedman test (G, I and K). $^{**}P \leq 0.01$, Where *P* value is not indicated results were non-significant.

4.8 Discussion

In this chapter we assessed expression levels of a transcriptional regulator of ADA in C9orf72 iAstrocytes and the effect of C9orf72 HRE mechanisms of toxicity models on purine metabolism regulation. This allowed us to determine the mechanistic origins of purine metabolism dysfunction in C9orf72 ALS.

4.8.1 p73 expression is unaltered in C9orf72 iAstrocytes, but downregulated in sALS iAstrocytes

We initially investigated transcriptional regulation of ADA by p73. $p73^{-/-}$ mice show signs of severe neurological defects along with immune and inflammatory dysfunction (Yang et al., 2000; Wilhelm et al., 2010) and p73 was proven to be important for neuronal survival (Tissir et al., 2009), likely because of its anti-apoptotic effects that counteract the effect of p53 (Pozniak et al., 2000). In addition, $p73^{+/-}$ Alzheimer's models have shown that p73 may be required to protect against neurodegeneration (Wetzel et al. 2008; Cancino et al., 2013) and induction of p73 may be neuroprotective (Shekhar and Dey, 2019). As p73 is a transcriptional regulator of ADA, it could be hypothesised that, at least partially, the neuronal dysfunction observed in p73 knockdown/knockout models is facilitated by subsequent irregularity in ADA expression caused by the loss of p73. In the context of ALS, Russell et al., (2021) utilising exome sequencing on a cohort of 87 sALS patients against 324 control cases identified 5 missense single nucleotide variants (SNVs) that were potentially ALS causing pathogenic variants in the p73 gene. The finding was subsequently confirmed in a cohort of 53 and 2,800 further ALS patients on which exome sequencing identified 19 further rare, nonsynonymous variants. In total, 22 missense SNVs and 2 in-frame indels were found in the three cohorts (Russell et al., 2021). Four variants were then modelled *in vitro*. They were initially cloned into

ΔN-p73α and expressed in a C212 myoblast line, in which two of the four mutants inhibited differentiation, indicating functional aberration. p73 knockout in a zebrafish model induced apoptosis which led to a reduction in spinal MN levels and in spinal motor neuronal axon branching (Russell et al., 2021). Because of this data, we investigated the expression of p73 in our C9orf72 iAstrocyte models. We demonstrate here, for the first time in a C9orf72 ALS model, that no aberration in p73 expression exists at the RNA level and possibly at the protein level (Figure 4.1A-C). Regulation of ADA via p73 can likely be ruled out as the causative factor leading to a loss of ADA in C9orf72 iAstrocytes, though investigation of epigenetic regulation of p73 would be interesting as well as localisation patterns that may affect function and whether differential splicing. Possibly corroborating our observations, Maor-Nof et al. (2021) recently showed that p53, but not p63 or p73, can facilitate arginine-containing DPR driven neurodegeneration. Mouse primary cortical neurons expressing a 50x repeat poly-PR and poly-GR LV displayed activation of p53, possibly caused by DNA damage present in the neurons. Ablation or reduction of p53 expression in these neurons prevented axonal degeneration and cell death. It also prevented neurodegeneration and improved survival in a poly-PR expressing mouse model and prevented neurodegeneration in a C9orf72-HRE *Drosophila* model. Deletion of p53 from C9orf72 iPSC-derived MNs was also shown to protect against axonal degeneration and reduce DNA damage (Maor-Nof et al., 2021). Abrogation of neither p63 nor p73 was able to produce the same results. These data show that p53, but most likely not p63 or p73, play an important role in the pathology of C9orf72 ALS. This validates the data we have presented here that p73 expression is unaltered in C9orf72 iAstrocytes.

Despite our data indicating that no relationship exists between ADA downregulation and p73 expression in C9orf72 iAstrocytes, we demonstrate that there is a possibility that p73 downregulation could be related to ADA loss in sALS iAstrocytes. Allen et al. (2019a) showed that, along with C9orf72 iAstrocytes and iNeurons, a significant downregulation in the expression of ADA was also present in sALS iAstrocytes, which we demonstrate also exhibit a significant downregulation in relative p73 RNA expression (Figure 4.1D). This suggests that ADA dysregulation in sALS iAstrocytes is linked to aberrant p73 expression. Future work should therefore focus on investigating the protein expression levels of p73 in sALS iAstrocytes. Upregulation of p73 could also be a viable method for upregulating ADA in sALS iAstrocytes as a potential therapy (as we investigate in C9orf72 iAstrocytes with the use of LV gene therapy in section 5). Such work would also further confirm the importance of ADA in the pathology of ALS, as the same phenotype may be reached via two separate mechanisms in two different forms of the disease.

4.8.1.1 Potential role of p63 expression

Along with p73, ADA expression is also regulated by p63 (Sbisà et al., 2006) and in ALS p63 was found to be downregulated in a genetic profile of SOD1 cells (Kirby et al., 2011), though SOD1 ALS cells models have not been associated with a downregulation in ADA. It would therefore be interesting to investigate whether there are any aberrations in p63 expression in C9orf72 or sALS cells.

4.8.1.2 Conclusions

Despite our data demonstrating that p73 expression is unaffected in C9orf72 cells, this entire family clearly plays a key role in ALS. p53 in the facilitation of DPR and RNA foci-induced neurodegeneration (Maor-Nof et al., 2021), and p73 in sALS patients (Russell et al., 2021). This pathway therefore warrants further investigation in the context of multiple forms of ALS.

4.8.2 C9orf72 protein loss-of-function is unrelated to loss of ADA

We next examined the potential effect on purine metabolism of the C9orf72 HRE pathogenic mechanisms. Initially, we investigated C9orf72 knockout as a model of the loss-of-function mechanism. Functionally, the C9orf72 protein regulates autophagy by complexing with SMCR8 (Amick et al., 2016; Sellier et al., 2016; Sullivan et al., 2016) and directly interacting with Rab1a and ULK1 (Webster et al., 2016). Reduction in C9orf72 expression in patient tissue and iPSC-derived models is widely reported (DeJesus-Hernandez et al., 2011; Donnelly et al., 2013; Gijselinck et al., 2012; Rizzu et al., 2016; Y. Shi et al., 2018; van Blitterswijk et al., 2015) which is hypothesised to contribute to C9orf72 HRE pathology. We therefore investigated whether knockout of the C9orf72 protein in a HeLa line would affect ADA, CD73 or HGPRT protein expression using western blots. With this we demonstrated that there was no significant alteration in any of ADA, CD73 or HGPRT in the C9orf72$^{-/-}$ HeLa (Figure 4.2A-F). The C9orf72 protein is not known to have any direct interaction with purine metabolism regulation, but there is a potential link between the two through regulation of the immune response and inflammation. C9orf72 haploinsufficiency has been linked to alterations in lysosomal function, including in lysosomal acidification, size, exocytosis, fusion/fission and lysosomal protein level (Amick et al., 2016; Corrionero & Horvitz, 2018; McAlpine et al., 2018; O'Rourke et al., 2016; Shao et al., 2020; Sullivan et al., 2016; Ugolino et al., 2016; M. Wang et al., 2020; Y. Zhang et al., 2018). Lysosomal dysfunction can lead to the accumulation of intracellular materials, eventually leading to toxicity (Malik et al., 2019). Importantly, lysosomes are tightly linked to the immune response, acting as the site for pathogen degradation and also acting as a platform for Toll-like receptors 3, 7 and 9, mTORC1 and TBK1 (Amick et al.,

2016; McAlpine et al., 2018; Shao et al., 2020; Ugolino et al., 2016; M. Wang et al., 2020). C9orf72 function was also shown to be key for correct macrophage function in a C9orf72$^{-/-}$ model (O'Rourke et al., 2016) and has been hypothesised to be required for correct T cell function (Lai & Ichida, 2019). Lysosomal dysfunction also exacerbates inflammation, as demonstrated in multiple cell models (Atanasio et al., 2016; Burberry et al., 2016; Lan et al., 2014; Martínez-Fábregas et al., 2018; McAlpine et al., 2018; McCauley et al., 2020; O'Rourke et al., 2016; Shao et al., 2020). ADA plays a key role in the differentiation and activation of macrophages and T cells (Aldrich et al., 2003; Carson et al., 1979; Fischer et al., 1976; Martín et al., 1995; Yagawa & Okamura, 1981). Further, adenosine, and therefore CD73 and ADA, are important coordinators of inflammation in the body (Fredholm, 2007; Henney & Lichtenstein, 1971; Sitkovsky & Ohta, 2005; Winn et al., 1981). Adenosine has also been shown to regulate autophagy in rat hepatocytes (Samari & Seglen, 1998). Because of these overlapping functions, we hypothesised that there might be some aberration in purine metabolism homeostasis in the C9orf72$^{-/-}$ line, particularly as C9orf72 haploinsufficiency has been demonstrated to alter lysosomal function specifically in a HeLa line previously (Amick et al., 2016). The fact that we observe no changes in expression of purine metabolism enzymes in our C9orf72$^{-/-}$ HeLa cells (Figure 4.2A-F) suggests that this model may not exhibit the expected activation of inflammatory pathways which could be expected to induce a concomitant alteration in ADA or CD73 expression or activity. Alternatively, any alterations to the immune response in the model may simply not be sufficient to also induce alterations in either ADA or CD73. Future work should investigate inflammation or lysosomal dysfunction in this C9orf72$^{-/-}$ HeLa line and correlate them with levels of CD73 and ADA. Other work could look at how ADA and CD73 expression is regulated in *in vivo* models that have demonstrated immune cell dysfunction, such as the mouse C9orf72$^{-/-}$ investigated by O'Rourke et al. (2016). It has also been shown recently that C9orf72 loss in combination with the expression of DPR and RNA foci was able to exacerbate cognitive deficit, neuronal death, glial activation and expression level of both DPRs and RNA foci (Zhu et al., 2020). These data therefore do not rule out the possibility that the true effect C9orf72 loss on purine metabolism only becomes apparent when scrutinised in combination with toxic gain-of-function mechanisms. Thus, future work could investigate purine metabolism in C9orf72$^{-/-}$ HeLa cells expressing DPRs.

4.8.2.1 Conclusions

The data presented here suggest that C9orf72 knockout alone is not sufficient to induce dysfunction in purine metabolism. However, future work could investigate the immune response in these cells and how the interplay between C9orf72 knockout and DPR expression might affect purine metabolism.

4.8.3 Toxic gain-of-function mechanisms and purine metabolism

4.8.3.1 Antisense gain-of-function C9orf72 HRE mechanisms lead to significant downregulation of ADA in N2a cells

We next investigated whether the expression of gain-of-function mechanisms could affect purine metabolism enzyme expression. To do this we used an N2a model transduced with 38x G_4C_2 or 39x C_4G_2 LV repeats. N2a that were transfected with the same sense or antisense plasmids used to generate the LV were shown to express the corresponding DPRs and RNA foci (Hautbergue et al., 2017). Here we utilised LV expressing the sense or antisense repeats to transduce N2a. We used western blots to measure protein expression levels of the enzymes ADA, CD73 and HGPRT in these models. Here we show for the first time that expression of the antisense C9orf72 HRE leads to a significant downregulation in ADA, providing the potential mechanistic basis behind the loss of ADA observed by Allen et al. (2019a). This strongly suggests that the cause of ADA downregulation is linked to the expression of antisense RNA-foci or DPR accumulation. However, there is a major caveat to our observations in this model. Alongside a downregulation in ADA, we also observe a significant downregulation of HGPRT in C_4G_2 HRE expressing N2a compared to G_4C_2 HRE expressing N2a cells (Figure 4.2C-D). This contradicts the observations we have made in C9orf72 iAstrocytes, in which we saw a significant upregulation of HGPRT (Figure 3.3E-F). We also did not observe any significant aberration in CD73 expression (Figure 4.2E-F), whereas in C9orf72 iAstrocytes there was a significant downregulation in CD73 expression (Figure 3.2C-D). We also observed significant upregulation in several of the loading controls we used (Figure 4.3.2). Initially we reasoned that this may be limited to cytoskeletal proteins, as we observed similar upregulations in both actin and tubulin expression (Figure 4.3.2A-D), however, we also observe this upregulation in GAPDH, a glycolytic enzyme (Figure 4.3.2E-F). This would suggest that the initial calculation of protein concentration was incorrect. However, this was a phenomenon we observed consistently in both G_4C_2 and C_4G_2 expressing N2a cells over multiple biological replicates, making this explanation unlikely. The exact cause of this is unknown but could be related to the potential off-target effects induced by LV transduction (discussed further in sections 5.11.1 and 5.11.4) (Ciuffi, 2008; Sinn et al., 2005, Annoni et al., 2019), though we do not observe alterations in loading control proteins arising from the LV expression of ADA (section 5). However, these N2a lines express the G_4C_2 and C_4G_2 transgene over several generations, whilst LV in iAstrocytes was only expressed for no longer that 86 hours and within a single passage, which might be the reason for the differences in loading control expression between the two models. Regardless of the exact cause of loading control irregularities, this could mean that the significant downregulation that we have observed in purine metabolism enzymes is caused by upregulation in loading controls in those

lines as opposed to being induced by C9orf72 HRE expression. Despite this, and although it is subjective, loss of ADA appears to be almost total in the C_4G_2 N2a lines (Figure 4.3.1A-B), whilst downregulation is not as apparent in the same line for HGPRT (Figure 4.3.1C-D). This could indicate that the downregulation we observe in HGPRT is driven by aberrant loading control expression, whilst ADA downregulation is induced directly by the C_4G_2 HRE. Either way, these caveats meant that we were unable to draw distinct conclusions from this model and we proceeded to further investigate the effect of DPR expression on purine metabolism in HeLa lines.

4.8.3.2 DPR expression in a HeLa line leads to downregulation in ADA and CD73

We initially transfected individual DPRs into HEK293T cells (which was unsuccessful) and subsequently a HeLa model and observed the effect on purine metabolism. This also allowed us to determine which individual, or combination of DPRs was responsible for purine metabolism dysfunction. We first transfected cells with V5-tagged poly-GA, poly-GR and poly-PR plasmids and confirmed their expression using immunofluorescence with a V5 antibody, also co-staining with ADA (Figure 4.6A-E). Using this method, we aimed to pinpoint ADA expression in cells transfected with DPRs and compare them to the expression level of purine metabolism enzymes in surrounding, untransfected cells. Co-staining for ADA and V5 expression also allowed us to detect whether ADA co-localises with DPRs and would therefore tell us whether direct binding was involved as a mechanism for loss of ADA expression or activity. In ALS, glutamate excitotoxicity can be caused by a genetic variant in the AMPA receptor; it has been hypothesised that incorrect adenosine to inosine conversion at the pore-lining domain GluA2 of AMPA may underlie this toxicity (Aizawa et al., 2010) caused by significant disturbances in both ADAR2 expression (Hideyama et al., 2012) and localisation (Moore et al., 2019). A recent paper has indicated that, in C9orf72 ALS, this dysfunction is likely caused by poly-PR binding to ADARs, inhibiting the RNA editing capability of both ADAR1 and 2 *in vitro* (Suzuki and Matsuoka, 2021). This therefore suggests a precedent for direct poly-PR binding inducing dysfunction in C9orf72 ALS. However, our data suggests that direct binding of DPRs to ADA is not a mechanism for reduced ADA expression or activity, as we did not observe co-localisation (Figure 4.6C-E). This is logical in regard to poly-PR, as poly-PR is generally localised to the nucleus (Figure 4.6E) whilst ADA is principally a cytoplasmic enzyme, though this mechanism could be further explored with immunoprecipitation assays.

We then, as before, surveyed ADA, CD73 and HGPRT expression using western blots (Figure 4.7A-F). Here we showed that poly-PR DPR expression leads to a significant loss of both ADA and CD73 (Figure 4.7A-D), as observed in C9orf72 iAstrocytes. A comparable downregulation

of both enzymes was observed in HeLa cells expressing poly-GA and poly-GR that does not reach significance when compared to mock and untransfected lines. No changes in HGPRT expression were observed (Figure 4.7E-F). These data highlight DPR expression as at least one of the causes of purine metabolism dysfunction in C9orf72 ALS. Interestingly, our hypothesis prior to this investigation was that we may not see any significant changes in purine metabolism enzyme expression via western blot from whole populations of DPR transfected HeLa cells, because transfection efficiency would not be high enough to induce such a change. The fact that we do still see a change is striking as it suggests that ADA loss through the action of these DPRs is so profound that it can lead to a statistically significant loss of both ADA and CD73, in a population without 100% transfection efficiency. As our data suggest that direct binding is not the cause of ADA downregulation (Figure 4.6) it could in fact be the case that poly-PR instead induces ADA downregulation through interference with ADA transcription. This explanation is plausible, given that in C9orf72 iAstrocytes, CD73 and ADA, along with being downregulated at a protein level, were also found to be downregulated at an RNA level (Allen et al 2019; Figure 3.4A). Conversely, RNA expression of HGPRT was unaffected in C9orf72 iAstrocytes (Figure 3.4B). We could use RT-qPCR to examine the RNA expression of HGPRT, CD73 and ADA in our DPR transfected HeLa cells. If downregulation of CD73 and ADA is confirmed on an RNA level this would provide a further link between these models and C9orf72 iAstrocytes.

Alternatively, DPR expression in one cell may trigger a signalling cascade that leads to the downregulation of purine metabolism enzymes in surrounding cells. From a qualitative perspective, our immunofluorescence suggests no distinct reduction in the expression of ADA in cells expressing V5-tagged DPRs compared to untransfected cells within the same population (Figure 4.6C-E), a signalling cascade inducing global ADA downregulation may therefore be the most likely explanation. Giving credence to this theory is the fact that several studies have demonstrated that conditioned media from ALS astrocytes are toxic to MNs (Birger et al., 2019; Haidet-Phillips et al., 2011; Re et al., 2014), including from C9orf72 iAstrocytes (Marchi et al., 2022; Varcianna et al., 2019). Secreted factors, released from DPR expressing HeLa cells could therefore be signalling untransfected HeLa cells to induce the purine metabolism dysfunction that we observe. Investigating how conditioned media from DPR transfected populations effects purine metabolism in untransfected HeLa cells is therefore a key experiment in determining why we see significant downregulation of ADA and CD73, despite observing less than 100% transfection efficiency. Determining transfection efficiency is also key as it would allow us to correlate the level of transfection with the level of purine metabolism enzyme loss. Due to time constraints, an analysis pipeline for the determination of transfection efficiency was not established.

4.8.3.3 Inflammation as a regulator of purine metabolism

As stated, CD73 and ADA are important regulators of inflammation in the cell. Gain-of-function mechanisms of the C9orf72 HRE have been linked to inflammation in models of ALS previously, and inflammation has been observed in transgenic mouse models expressing poly-PR, poly-GR and poly-GA (Hao et al., 2019; LaClair et al., 2020; Schludi et al., 2017; Y. J. Zhang et al., 2018). An investigation into inflammatory markers might therefore shed light on the altered expression of CD73 and ADA in these models. However, as previously stated, knockout and knockdown of the C9orf72 protein has been linked with dysregulation in the immune response and activation of inflammation. Amick et al. (2016) demonstrated that HeLa cells with a C9orf72 knockout exhibit excessive inflammation. Despite this we observed no alterations in purine metabolism in our C9orf72$^{-/-}$, which could either indicate that inflammation is not present in our C9orf72$^{-/-}$ HeLa, or that inflammation is present but not the inciting event for purine metabolism dysfunction. Thus, we should investigate the level of inflammatory markers in DPR expressing models as well, to ascertain whether inflammation is present and whether it is therefore the causative factor in purine metabolism dysfunction.

4.8.3.5 HGPRT expression is significantly downregulated in C9orf72 HRE expressing N2a cells but unaffected in DPR expressing HeLa cells

HGPRT was unaffected in HeLa models (Figure 4.6E-F) but in HRE expressing N2a cells, HGPRT was significantly downregulated in the C_4G_2 model (Figure 4.3.1C-D). This is the opposite of the effect observed in C9orf72 iAstrocytes. The reason that we observe this downregulation is likely to be related to upregulation in loading controls, leading to an artificial downregulation of HGPRT. However, another possible cause of the significant downregulation of HGPRT arises from the differing cell models. N2a are mouse neuronal cells, whereas iAstrocytes and HeLa are from a human origin, which could induce differing responses to HRE expression. Further, we have previously shown that ADA is significantly downregulated in iNeurons (Allen et al., 2019a), which matches what we observe here in mouse neuronal cells but we have not investigated CD73 or HGPRT expression in iNeurons. We should therefore investigate the purinergic profile of C9orf72 iNeurons, which might yet mirror our observations in N2a cells. In our HeLa cells, DPR expression had no effect on HGPRT expression, suggesting that the elevation in expression observed in C9orf72 iAstrocytes is unrelated to C9orf72 mechanisms of toxicity. We hypothesised previously that DNA damage and repair as a trigger for the upregulation of HGPRT. Poly-GR and poly-PR expression has been shown to induce DNA damage (Maor-Nof et al., 2021), therefore it would be interesting to investigate DNA damage markers in our gain-of-function N2a and HeLa models.

4.8.3.6 Conclusions

These data point towards DPR expression as a potential the cause for the loss of ADA and CD73 we observe in C9orf72 iAstrocytes but not as a driver of HGPRT upregulation. However, these are overexpression models and physiologically DPRs alone may not be sufficient to instigate these changes. Instead, there is likely a cocktail of triggers leading to purine metabolism aberration, meaning further work (as outlined above) is therefore required to understand them. The sources are likely multi-factorial and could be induced by either direct or indirect interaction with DPRs, transcriptional interference, or through the activation of some intermediate stimulus.

4.8.4 Future work

These data open multiple avenues for further investigation, some of which have been raised earlier in this chapter. Potential investigations not yet covered will be discussed here.

4.8.4.1 Potential alternative transcriptional and signalling regulation of ADA expression

In this chapter we have determined that p73 is unlikely to be a factor in ADA downregulation in C9orf72 ALS. However, there are other mechanisms, outside of those we have investigated in this study that could be responsible for altered ADA expression. Another possible transcriptional pathway for dysregulation of ADA in ALS would be via the transcription factor Sp1. There is little information available on Sp1 in relation to ALS pathology, however a recent paper using combined transcriptomic analysis identified Sp1 as a possible driver of MN degeneration in ALS and a link between differentially expressed genes in the blood and brain tissue of ALS patients (Rahman et al., 2019). Sp1 expression could therefore be analysed in C9orf72 iAstrocytes.

We have also not yet investigated extracellular signalling as a mechanism for ADA dysregulation. Tyrosine kinase signalling, leading to the activation of ERK, JNK and SAPK has been shown to induce an increase in ADA and CD73 expression and activity in rat spinal cord astrocytes. Conversely, inhibition of both the FGF2 receptor and MAPKs downregulate expression (Eguchi, 2020). Therefore, investigating the expression of MAPK proteins could also shine a light on how purine metabolism becomes dysfunctional in C9orf72 ALS.

4.8.4.2 Further investigation into C9orf72 in vitro *models*

Measuring ADA activity and the levels of downstream purine and metabolic targets is key. Inosine output and urate output were found to be downregulated in our C9orf72 iAstrocytes

and therefore might also be expected to be downregulated in C9orf72 HRE transduced N2a and DPR transfected HeLa. As we see loss of ADA (which would be expected to engender a concomitant loss of inosine output) in these models we could also explore whether the bioenergetic profile of these models is altered. Moreover, would restoring ADA expression using gene therapy to these models have any effect on the above parameters and other markers of C9orf72 pathology, such as p62 expression. These experiments would allow us to further phenotypically align our C9orf72 HRE transduced N2a and DPR transfected HeLa models with C9orf72 iAstrocytes, understand mechanistically why purine metabolism dysfunction is present in these cells and provide further areas to target for therapeutic intervention.

5. The effect of ADA gene therapy on control and C9orf72 iAstrocyte function

Our published (Allen et al., 2019a) and unpublished (Sections 3 and 4) data, suggest that restoring ADA levels in ALS iAstrocytes may be beneficial not only to astrocytic function but also to MN survival. The basis for this hypothesis stems from metabolic screening of C9orf72 iAstrocytes demonstrating that they were unable to effectively metabolise adenosine (Allen et al., 2019a). This dysfunction in adenosine metabolism was hypothesised to be caused by reduction in ADA expression, which was shown in the original publication and confirmed in this study, in which we have demonstrated that loss of ADA leads to concomitant reductions in ADA activity and inosine output (Figure 3.1). As a downstream consequence of ADA loss, C9orf72 (and sALS) iAstrocytes were more susceptible to adenosine-mediated toxicity. ADA inhibition in control iAstrocytes recapitulated this sensitivity, indicating that the toxicity was induced by a loss of ADA. As adenosine is converted to inosine by ADA, subsequent investigation revealed that, by bypassing the defect in adenosine metabolism and supplementing cells directly with inosine, iAstrocyte bioenergetic output could be improved and toxicity towards MNs in co-culture could be reduced (Allen et al., 2019a). Inosine supplementation to increase urate output has been investigated as a treatment for ALS previously but this does not tackle the potential effect of adenosine (or deoxyadenosine)-mediated toxicity. We therefore hypothesise that, by correcting this dysfunctional step in adenosine metabolism, utilising gene therapy, we can recapitulate the benefits of supplementing cells with inosine and remedy the inability of C9orf72 iAstrocytes to ineffectively metabolise adenosine and subsequent susceptibility to adenosine-mediated toxicity.

5.1 Plasmid Design

To study the effect of upregulating ADA expression on C9orf72 iAstrocytes, we generated an ADA expressing LV (ADA-LV). This was performed by initially cloning an ADA construct (pOTB7/ADA inAGE 3629376) into a SIN-PGK-cPPT-GDNF-WHV vector (Figure 5.1A-B). Following ligation, the plasmid was transformed into *E.coli*. Transformed colonies were propagated in LB Broth and purified using a midi-prep kit (QIAGEN). Successful insertion was tested by co-digestion with BamHI and XhoI to give expected fragments of 8,811bp and 1,089bp (Figure 5.1C). Successful cloning was confirmed using gel electrophoresis which showed fragments that aligned with the expected fragment size (Figure 5.1D). The plasmid was subsequently sent for sequencing with LV reverse primer and PGK forward primers to Source BioScience. We also constructed an empty vector lentivirus (EV-LV) consisting of the SIN-PGK-cPPT-GDNF-WHV vector without the ADA insertion to be used as a positive control

to measure any effect of LV transduction independent of ADA upregulation (Figure 5.1A). Digestion of this plasmid with a BamHI enzyme showed linearisation, as expected.

A

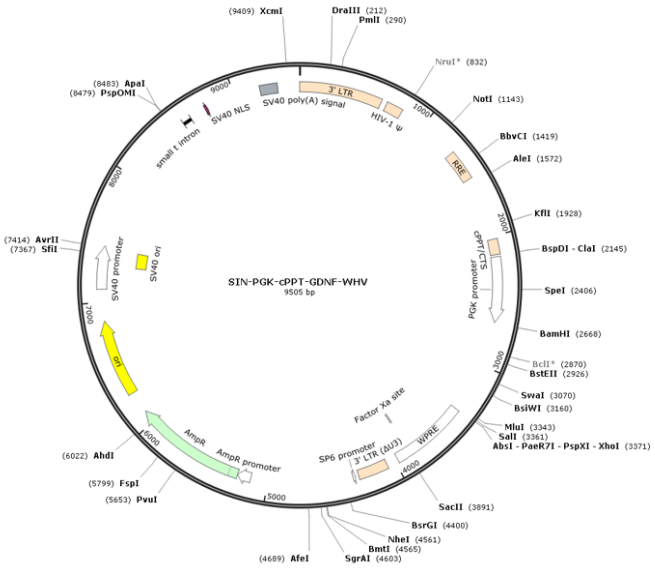

B

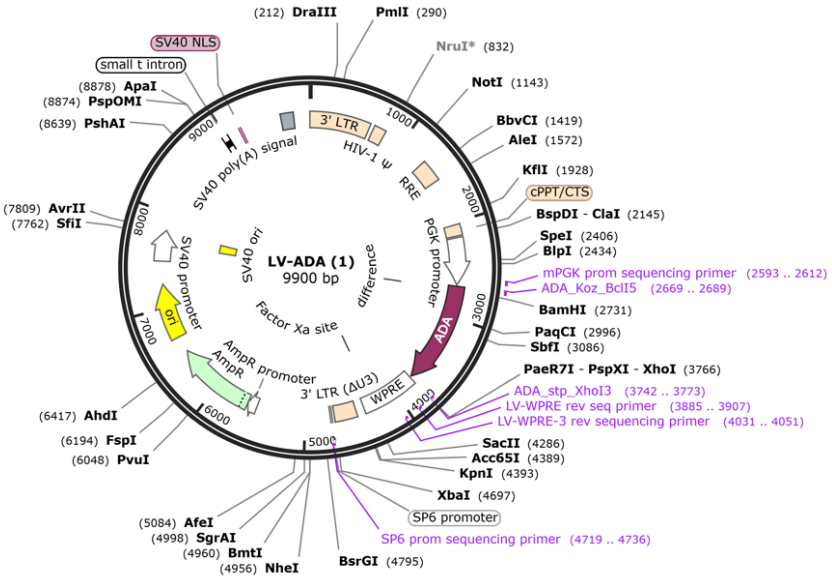

C

Enzyme	Expected fragment size (bp)
BamHI/XhoI	8811 1089

D

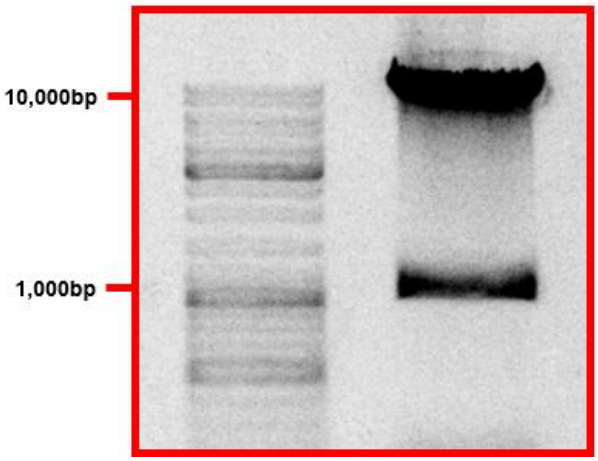

Figure 5.1. ADA cDNA was successfully cloned into a SIN-PGK-cPPT-GDNF-WHV vector. (A) Plasmid map of SIN-PGK-cPPT-GDNF-WHV vector (B) Plasmid map of the finalised ADA-LV plasmid. (C) Table showing restriction enzymes used for digestion and the expected fragment sizes. (D) Representative digest. Ladder shown is 1kb NEB ladder.

5.2 Lentiviral generation and titration

After confirming ligation of our ADA sequence into our plasmid and proliferating and purifying it as described in section 2.2.4, we transfected this, along with the genetic machinery required to form the construct into a functioning LV (pCMVDR8.92, pRSV-Rev and M2G plasmids) into HEK293T/17 cells as described in section 2.2.5. The complete LV was then isolated from the media and relative gene expression was calculated with WPRE primers using RT-qPCR against the titre of a known virus with the $2^{-\Delta\Delta Ct}$ method (Livak & Schmittgen, 2001).

5.3 ADA gene therapy increased ADA expression in iAstrocytes

After establishing a titre, we validated the virus by transducing our iAstrocytes with the EV-LV and ADA-LV. The virus was tested at several MOIs to measure levels of expression, with the aim of, at minimum, restoring ADA levels in C9orf72 iAstrocytes to endogenous control expression levels. We therefore transduced our iAstrocytes at MOI 0.25, MOI 0.5 and MOI 1 for both ADA-LV and EV-LV. We subsequently used western blot analysis to measure protein expression of ADA. We observed that ADA expression was increased at all three MOI compared to the EV-LV and untreated, reaching significance from MOI 0.25 onwards in control iAstrocytes (Figure 5.3A-B) and from MOI 0.5 onwards in C9orf72 iAstrocytes (Figure 5.3C-D). Going forward, we initially used MOI 1 but eventually used MOI 0.25 in some experiments. Motivations for these decisions will be explained throughout this chapter.

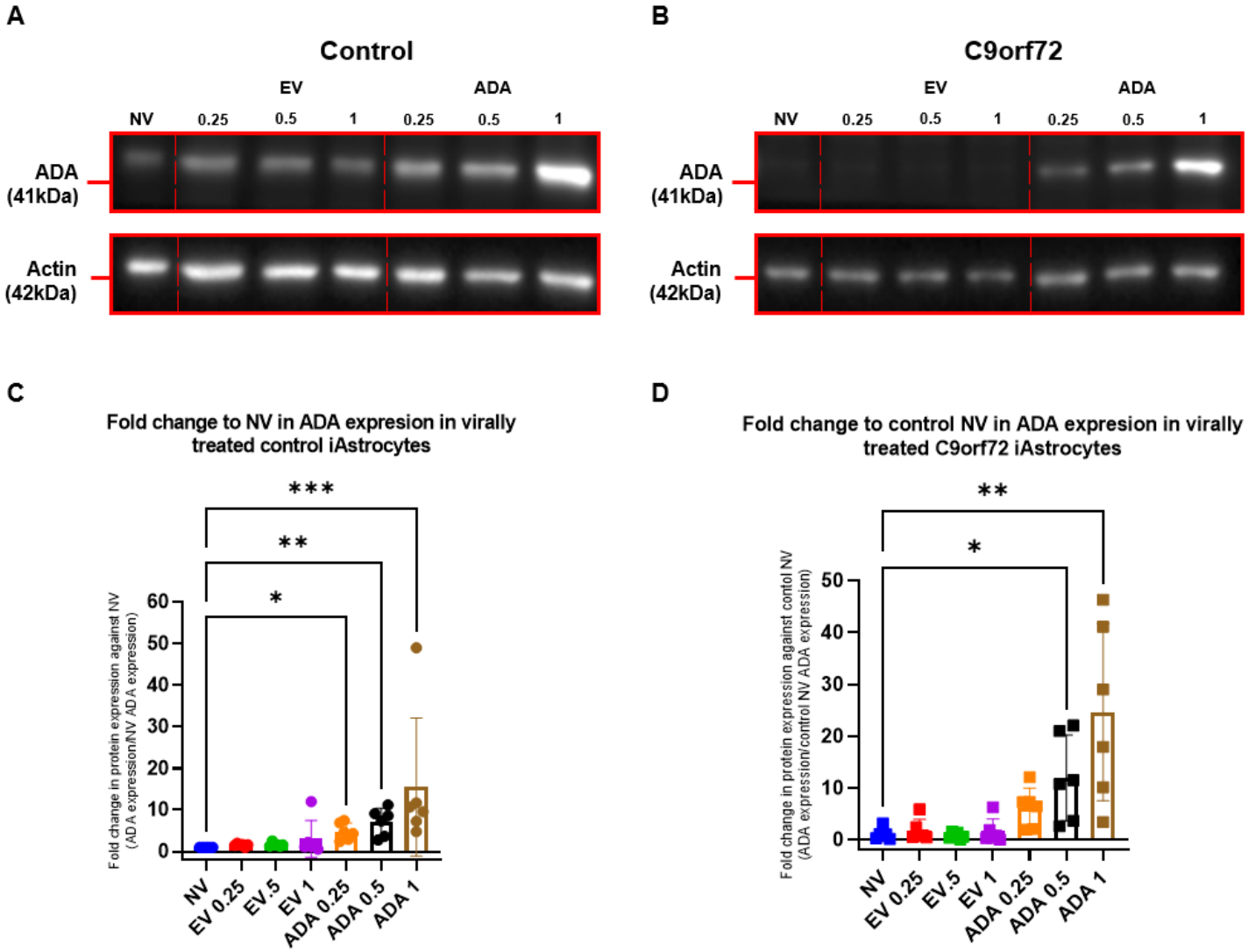

Figure 5.3. ADA gene therapy increased ADA expression in iAstrocytes. (A) Representative images of ADA expression in control iAstrocytes virally treated at MOI 0.25, 0.5 and 1. (B) Representative images of ADA expression in C9orf72 iAstrocytes virally treated at MOI 0.25, 0.5 and 1. (C) Densitometry analysis of ADA expression in control iAstrocytes virally treated at MOI 0.25, 0.5 and 1. (D) Densitometry analysis of ADA expression in C9orf72 iAstrocytes virally treated at MOI 0.25, 0.5 and 1. Data presented as mean and standard deviation of two biological replicates from three control and three C9orf72 iAstrocytes. Densitometry analysis performed by normalizing the specified protein level to actin loading control and then setting NV control values to 1, before statistical analysis by Friedman test (B and D) comparing each treatment to the corresponding NV value. *$P \leq 0.05$, **$P \leq 0.01$, ***$P \leq 0.001$. Where P value is not indicated results were non-significant.

5.4 ADA gene therapy increased ADA activity and inosine output in iAstrocytes.

5.4.1 ADA-LV at MOI 1 significantly increased ADA activity and inosine output

The data that we presented in section 3 demonstrated that reduction in ADA expression induced significant downregulation in ADA activity and inosine output in C9orf72 iAstrocytes (Figure 3.1). Moreover, we show here that LV gene therapy was able to restore ADA expression levels in the same cell model (Figure 5.3). Therefore, to assess whether this increase in expression levels led to increased enzymatic activity, we measured ADA activity and inosine output in iAstrocytes after gene therapy. Initially we assessed an MOI of 1 which produced a significant upregulation in ADA activity in control and C9orf72 iAstrocytes compared to NV and EV-LV treatment (Figure 5.4.1A-B). Control iAstrocytes also exhibited a significant increase in inosine output against NV and EV-LV treatment (Figure 5.4.1C), whereas C9orf72 iAstrocytes only showed a significant upregulation in inosine output when compared to the EV control (Figure 5.4.1D).

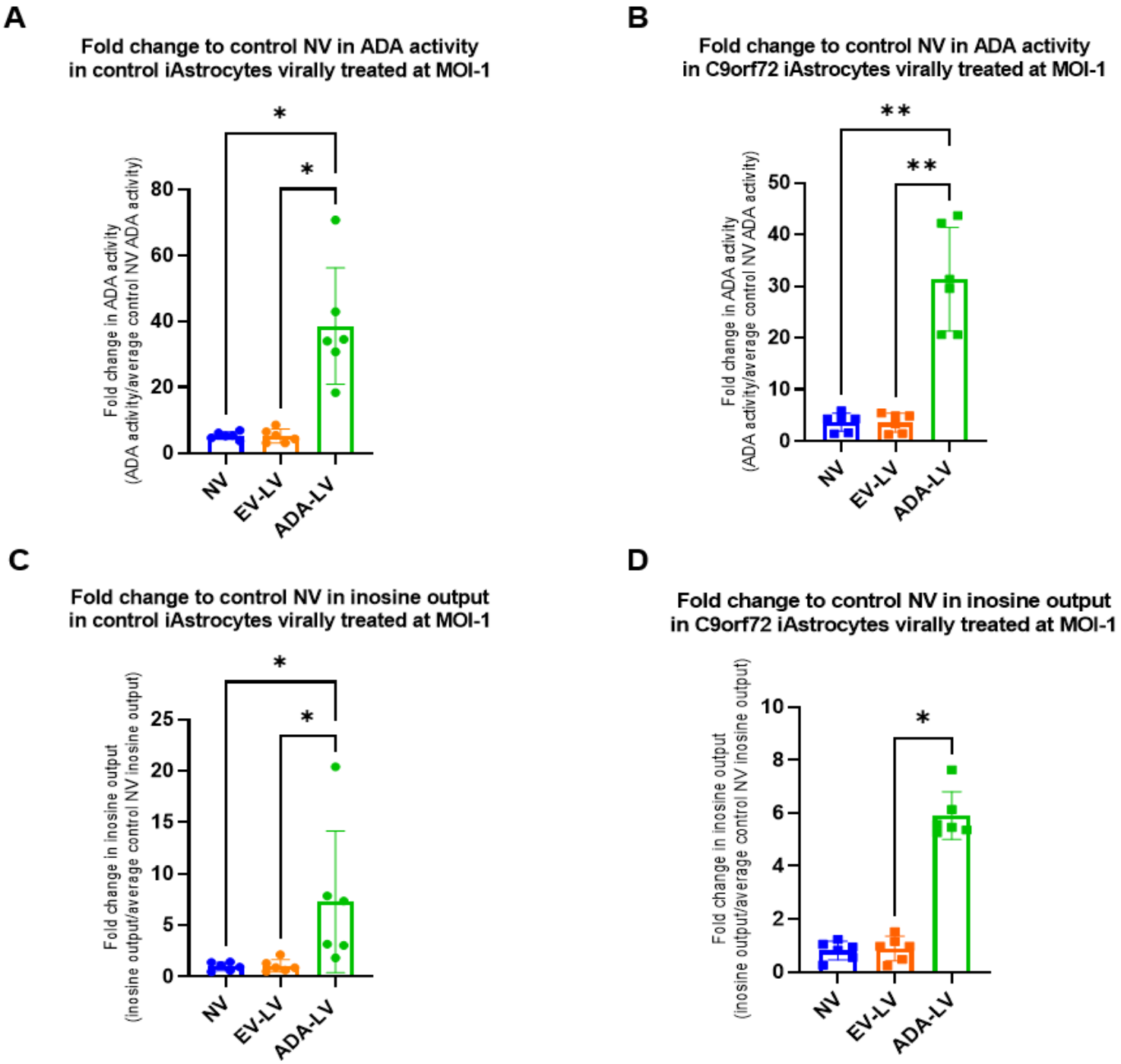

Figure 5.4.1. ADA gene therapy increased ADA activity and inosine output at MOI 1. (A) Fold change in ADA activity in control iAstrocytes virally treated at MOI 1. (B) Fold change in ADA activity in C9orf72 iAstrocytes virally treated at MOI 1. (C) Fold change in inosine output in control iAstrocytes virally treated at MOI 1. (D) Fold change in inosine output in C9orf72 iAstrocytes virally treated at MOI 1. Data presented as mean and standard deviation of two biological replicates from three control and three C9orf72 iAstrocytes. Statistical analysis by RM one-way ANOVA (A and B) or Friedman test (C and D). *$P \leq 0.05$, **$P \leq 0.01$. Where P value is not indicated results were non-significant.

5.4.2 ADA-LV treatment at MOI 0.25 increases ADA activity and inosine output

We then assessed a lower MOI which was closer to a restoration as opposed to an overexpression of ADA (Figure 5.4.2A-D). For control iAstrocytes treated at MOI 0.25, there was a clear increase in both inosine output and ADA activity, however neither reached significance likely due to the inherent variance in the data and low *n* numbers (Figure 5.4.2A and C). C9orf72 iAstrocytes treated at MOI 0.25 displayed a significant upregulation in ADA activity compared to NV and EV-LV (Figure 5.4.2B), but, as with controls, the evident increase in inosine output did not reach statistical significance (Figure 5.4.2D).

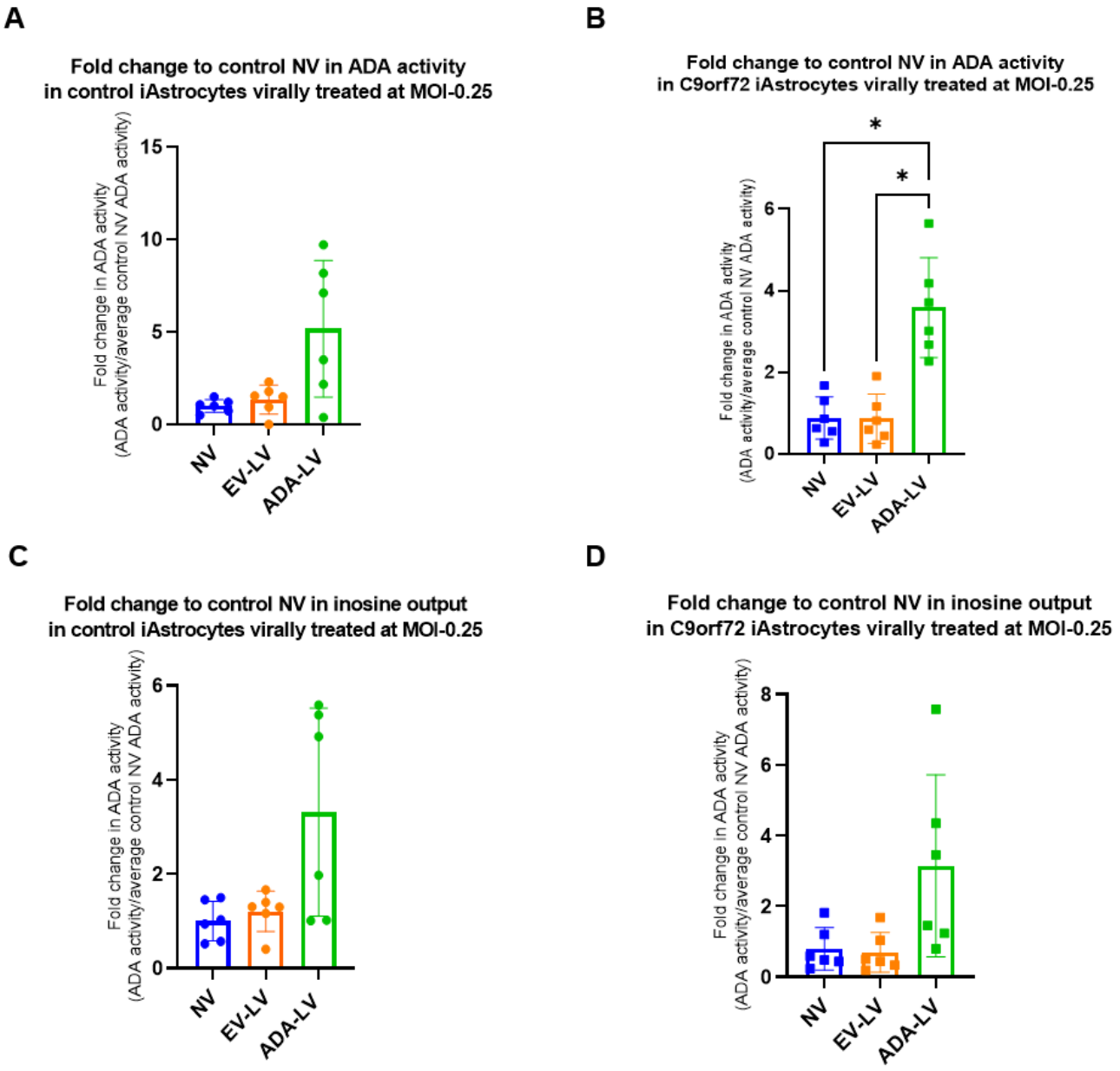

Figure 5.4.2. ADA gene therapy increased ADA activity and inosine output at MOI 0.25. (A) Fold change in ADA activity in control iAstrocytes virally treated at MOI 0.25. (B) Fold change in ADA activity in C9orf72 iAstrocytes virally treated at MOI 0.25. (C) Fold change in inosine output in control iAstrocytes virally treated at MOI 0.25. (D) Fold change in inosine output in C9orf72 iAstrocytes virally treated at MOI 0.25. Data presented as mean and standard deviation of two biological replicates from three control and three C9orf72 iAstrocytes. Statistical analysis by RM one-way ANOVA. *$P \leq 0.05$. Where P value is not indicated results were non-significant.

5.5 ADA gene therapy does not alter urate output in iAstrocytes.

We have also generated data demonstrating that urate output is significantly downregulated in a cell-line specific manner (Figure 3.1) and have previously demonstrated that inosine can significantly upregulate urate output (Allen et al., 2019a). Moreover, we have shown in this chapter that restoring ADA expression in ALS iAstrocytes increases both ADA activity and inosine output at MOI 1 (Figure 5.4), which we hypothesised would induce a concomitant increase in urate output. We therefore utilised a urate output assay to assess urate output in cells that had been treated with ADA gene therapy. We tested cells that had been virally treated at MOI 0.25 and 1 with ADA-LV and EV-LV alongside NV iAstrocytes. Here we observed that, despite witnessing an elevation in inosine output, this did not translate to a subsequent increase in urate in either control or C9orf72 iAstrocytes (Figure 5.5A-B). However, it should be noted that these investigations only include data from two biological replicates from two control and two C9orf72 cell lines.

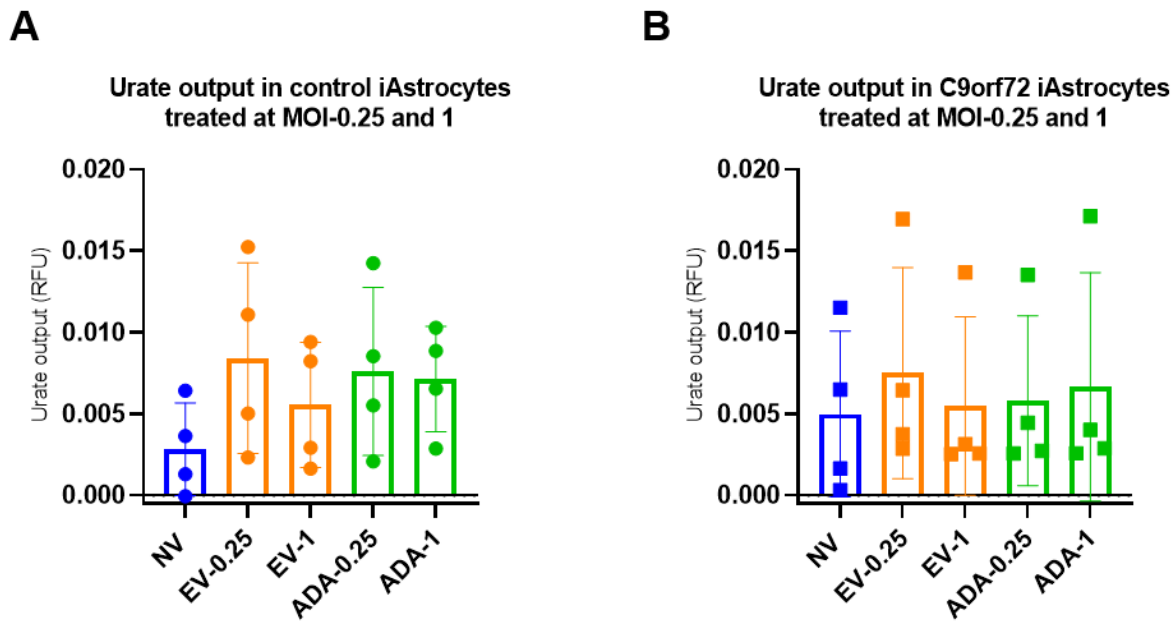

Figure 5.5. Urate output is not affected by gene therapy. (A) Effect on urate output in virally treated control iAstrocytes. (B) Effect on urate output in virally treated C9orf72 iAstrocytes. Data presented as mean and standard deviation of two biological replicates from two control and two C9orf72 iAstrocytes. Statistical analysis performed using RM one-way ANOVA.

5.6 ADA gene therapy does not alter markers of C9orf72 expression

We have previously demonstrated that p62 expression is significantly upregulated and NQO1 expression significantly downregulated in C9orf72 iAstrocytes (Allen et al., 2019a). In this study we were able to recapitulate elevated p62 and observed cell-line specific reductions in NQO1 in C9orf72 iAstrocytes (Figure 3.2). We next wanted to investigate whether ADA gene therapy had any effect on these markers in control and C9orf72 iAstrocytes. We therefore used western blots to assess expression of these markers in NV, EV-LV, and ADA-LV treated iAstrocytes at MOI 1. Here, we observed that neither ADA-LV or EV-LV gene therapy had any effect on p62 or NQO1 expression in either control or C9orf72 iAstrocytes (Figure 5.6). Though gene therapy had no effect on these key markers of C9orf72 ALS, importantly we observed no exacerbation of either phenotype.

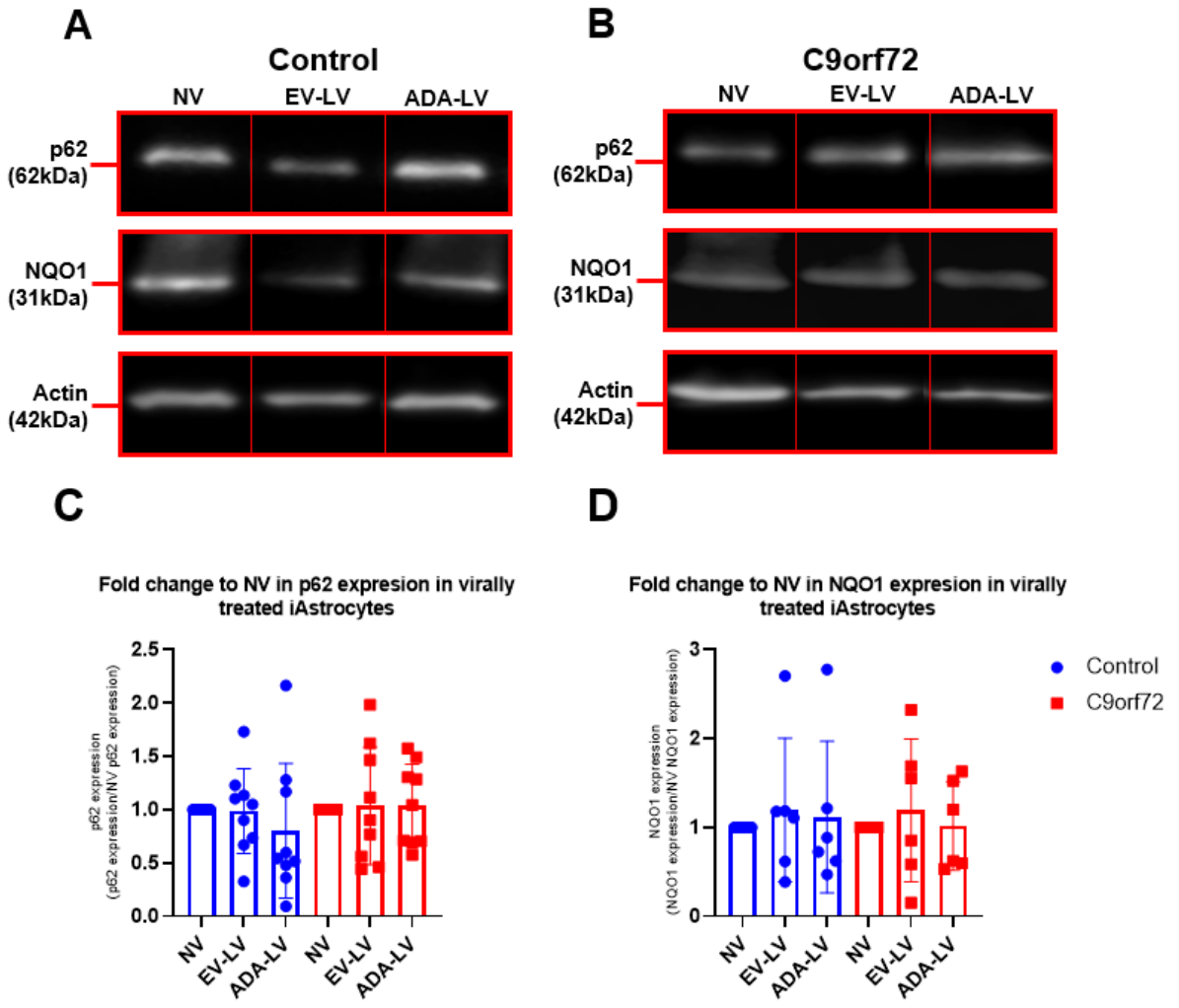

Figure 5.6. ADA gene therapy does not exacerbate markers of autophagy and oxidative stress in iAstrocytes. (A) Representative images of p62 and NQO1 expression in virally treated control iAstrocytes. (B) Representative images of p62 and NQO1 expression in virally treated C9orf72 iAstrocytes. (C) Densitometry analysis of p62 expression in virally treated control and C9orf72 iAstrocytes. (D) Densitometry analysis of NQO1 expression in virally treated control and C9orf72 iAstrocytes. Data presented as mean and standard deviation of three biological replicates from three (C) or two (D) control and C9orf72 cell lines. Densitometry analysis performed by normalizing target protein level to actin loading control and then setting NV values to 1, before statistical analysis by Friedman test (C and D) comparing each treatment to the corresponding NV value.

5.7 ADA-LV treatment had no effect on CD73 or HGPRT expression, but gene therapy reduced HGPRT expression in C9orf72 iAstrocytes

Dysfunction in adenosine metabolism suggested a precedent for wholescale purine metabolism dysfunction in C9orf72 iAstrocytes. We demonstrated that this was in fact the case as we observed that levels of CD73 were significantly downregulated and HGPRT significantly upregulated in C9orf72 iAstrocytes (Figure 3.3-3.4). We subsequently showed in C9orf72 *in vitro* models that both ADA and CD73 loss may be induced by expression of poly-PR (likely in combination with poly-GA and poly-GR that also induce downregulation, albeit to a non-significant level) (Figure 4.7). The exact cause of HGPRT upregulation is as yet unidentified, but may be regulated by DNA damage, as expression was unaffected by C9orf72 knockout (Figure 4.2) and the presence of poly-GA, poly-GR and poly-PR DPRs (Figure 4.7) (findings in HRE expressing N2a are less clear (Figure 4.3)). We hypothesised that ADA downregulation could induce HGPRT upregulation or CD73 loss. We therefore investigated how gene therapy would affect levels of these key purine metabolism enzymes using western blots. Here we demonstrated that gene therapy did not alter expression levels of CD73 (Figure 5.7C-D), likely discounting the theory that loss of ADA expression causes loss of CD73. We also observed no effect of ADA-LV compared to EV-LV gene therapy on HGPRT in C9orf72 iAstrocytes (Figure 5.7E-F), suggesting that the upregulation of HGPRT observed in C9orf72 iAstrocytes was also unrelated to ADA expression. However, the data was inconclusive due to a clear LV effect on HGPRT expression levels, which seemed to be exacerbated in the C9orf72 iAstrocytes (Figure 5.7). Unfortunately, due to time constraints we were only able to perform this in two control and two C9orf72 iAstrocytes lines. Therefore, a full data set is required before any firm conclusions can be made.

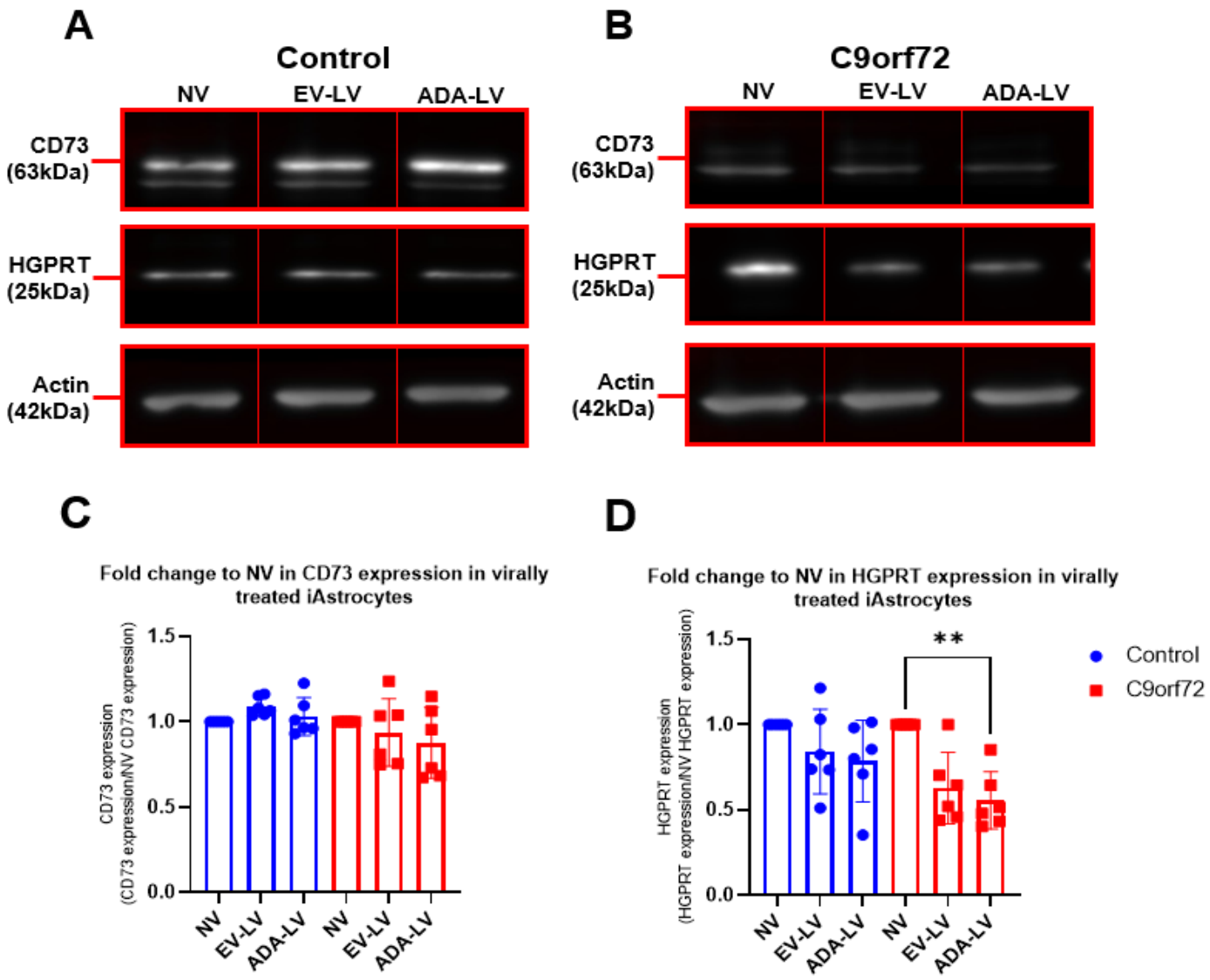

Figure 5.7. ADA-LV treatment has no effect on CD73 or HGPRT expression, but gene therapy reduces HGPRT expression in C9orf72 iAstrocytes. (A) Representative images of CD73 and HGPRT expression in control iAstrocytes virally treated at MOI 0.25. (B) Representative images of CD73 and HGPRT expression in C9orf72 iAstrocytes virally treated at MOI 0.25. (C) Densitometry analysis of CD73 expression in control and C9orf72 iAstrocytes virally treated at MOI 0.25. (D) Densitometry analysis of HGPRT expression in control and C9orf72 iAstrocytes virally treated at MOI 0.25. Data presented as mean and standard deviation of three biological replicates from two control and two C9orf72 cell lines. Densitometry analysis performed by normalizing the specified protein level to actin loading control and then setting NV values to 1, before statistical analysis by Friedman test (C and D) comparing each treatment to the corresponding NV value. $^{**}P \leq 0.01$. Where *P* value is not indicated results were non-significant.

5.8 Gene therapy may ameliorate adenosine-mediated toxicity in a cell-line specific manner in C9orf72 iAstrocytes.

C9orf72 iAstrocytes are more susceptible to adenosine-mediated toxicity than controls, ostensibly caused by loss of ADA expression and activity. We therefore hypothesised that restoring ADA expression in C9orf72 iAstrocytes would ameliorate this enhanced sensitivity to adenosine. We evaluated whether upregulation of ADA was able to prevent adenosine toxicity using CyQuant assays to measure cell number. Initially, the level of adenosine-mediated toxicity was measured in NV control and C9orf72 iAstrocytes, with cells cultured in adenosine-containing media, incrementally increasing in concentration from 0.1-10mM. Both C9orf72 and control iAstrocytes showed a progressive increase in toxicity up to 10mM adenosine (Figure 5.8A). As observed by Allen et al. (2019a), C9orf72 iAstrocytes exhibited a significant increase in adenosine-mediated toxicity compared to the controls, with 45% cell death in C9orf72 compared to 23% cell death in control at 10mM (Figure 5.8B). Based on these data we chose 10mM adenosine to assess the effect of ADA gene therapy on iAstrocyte adenosine-mediated toxicity (Figure 5.8C-D). As shown, restoring ADA levels had no effect on adenosine-mediated toxicity in control or C9orf72 iAstrocytes. However, when examining toxicity on an individual basis it was revealed that C9-183, that consistently exhibited the lowest ADA expression, does show some recovery in levels of cell survival. In NV C9-183 iAstrocytes at 10mM adenosine, toxicity levels were 55%, whilst in ADA-LV treated C9-183 at 10mM, toxicity was reduced to 28%, resulting in a statistically significant increase in cell survival. This suggests that ADA upregulation may be beneficial in a patient-dependent manner. It should be noted that GFP-LV treatment also appeared to somewhat alleviate adenosine-mediated toxicity, down to 34%. Unfortunately, we did not have EV-LV treatment available to us at the time these experiments were conducted and were therefore unable to use this more appropriate control, hence the separation of EV-LV and GFP-LV treated lines.

A

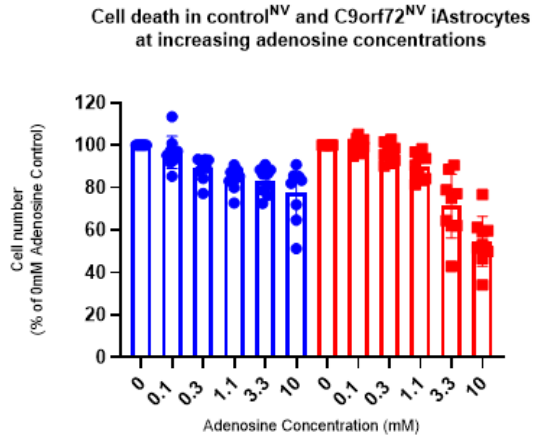
Cell death in control^NV and C9orf72^NV iAstrocytes at increasing adenosine concentrations
Cell number (% of 0mM Adenosine Control)
120
100
80
60
40
20
0
0
0.1
0.3
1.1
3.3
10
0
0.1
0.3
1.1
3.3
10
Adenosine Concentration (mM)

B

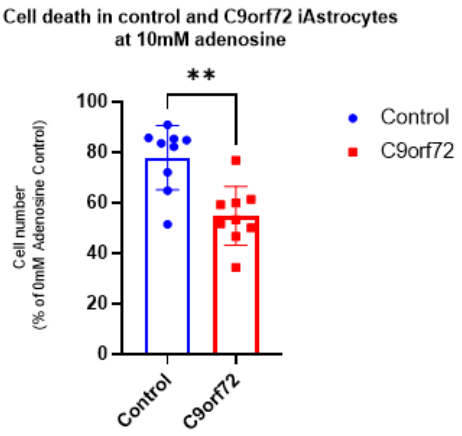
Cell death in control and C9orf72 iAstrocytes at 10mM adenosine
**
Cell number (% of 0mM Adenosine Control)
100
80
60
40
20
0
Control
C9orf72
Control
C9orf72

C

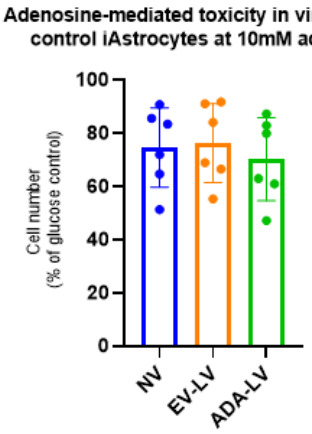
Adenosine-mediated toxicity in virally treated control iAstrocytes at 10mM adenosine
Cell number (% of glucose control)
100
80
60
40
20
0
NV
EV-LV
ADA-LV

D

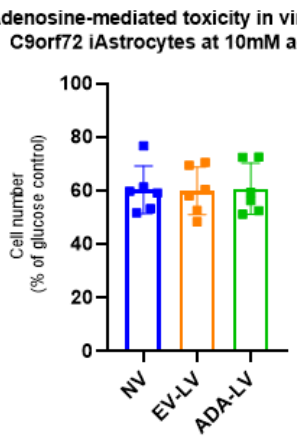
Adenosine-mediated toxicity in virally treated C9orf72 iAstrocytes at 10mM adenosine
Cell number (% of glucose control)
100
80
60
40
20
0
NV
EV-LV
ADA-LV

E

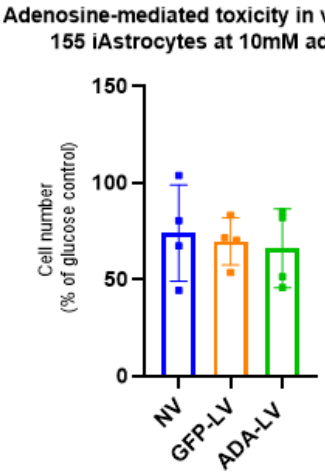
Adenosine-mediated toxicity in virally treated 155 iAstrocytes at 10mM adenosine
Cell number (% of glucose control)
150
100
50
0
NV
GFP-LV
ADA-LV

F

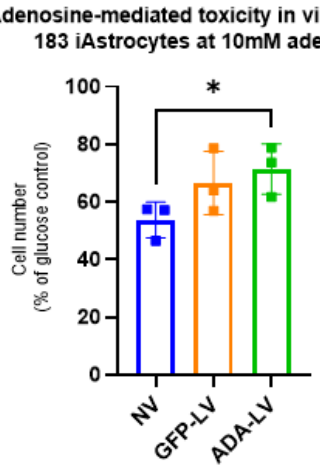
Adenosine-mediated toxicity in virally treated 183 iAstrocytes at 10mM adenosine
*
Cell number (% of glucose control)
100
80
60
40
20
0
NV
GFP-LV
ADA-LV

Figure 5.8. Gene therapy may ameliorate adenosine-mediated toxicity in a cell-line specific manner in C9orf72 iAstrocytes. (A) The effect of increasing concentrations of adenosine on cell number in control and C9orf72 iAstrocytes. (B) Comparison of control and C9orf72 iAstrocytes cultured in 10mM adenosine. (C) The effect of 10mM adenosine on NV, EV-LV, and ADA-LV control iAstrocyte cell number, virally treated at MOI 1. (D) The effect of 10mM adenosine on NV, EV-LV, and ADA-LV C9orf72 iAstrocyte cell number, virally treated at MOI 1. (E) The effect of 10mM adenosine on NV, GFP-LV, and ADA-LV Con-155 iAstrocyte cell number, virally treated at MOI 1. (F) The effect of 10mM adenosine on NV, GFP-LV, and ADA-LV C9-183 iAstrocyte cell number, virally treated at MOI 1. Data presented as mean and standard deviation of three biological replicates from one (E and F), two (C and D) or three (A and B) control and C9orf72 cell lines. Analysis performed by normalising to 0mM adenosine control at 100%, before transforming data using Y = 1/Y and Y = Logit(Y) prior to Mann-Whitney (B) or Freidman test (C, D, E and F). **P* ≤ 0.05, ***P* ≤ 0.01. Where *P* value is not indicated results were non-significant.

5.9 ADA gene therapy does not increase bioenergetic output

Breakdown of inosine into hypoxanthine generates energy (Balestri et al., 2007; Jurkowitz et al., 1998; Litsky et al., 1999; Módis et al., 2013), and is a particularly important pathway during times of cells stress and impaired energy generation (Balestri et al., 2007; Jurkowitz et al., 1998; Litsky et al., 1999). Allen et al. (2019a) observed that supplementing iAstrocytes with exogenous inosine significantly increased ATP levels. It was therefore hypothesised that restoring ADA in C9orf72 iAstrocytes would increase endogenous ATP output. Adding further credence to this theory was the fact that virally treating cells at MOI 1 was able to significantly increase inosine output (Figure 5.3C-D). This hypothesis was tested using ATP assays (Figure 5.9). ATP levels in control and C9orf72 EV-LV and ADA-LV treated iAstrocytes at MOI 1 were measured and compared directly to the ATP output in NV iAstrocytes. NV iAstrocytes cultured in 7.5mM inosine were used as a positive control. Both control and C9orf72 iAstrocytes, supplemented with inosine showed a significant increase in ATP output (Figure 5.9A-B), as previously observed (Allen et al., 2019a). Neither ADA-LV nor EV-LV treatment, however, had any effect on total ATP output (Figure 5.9A-B). We hypothesised that even with ADA gene therapy, the endogenous level of adenosine might not be sufficient to produce an adequate amount of inosine to noticeably increase energy generation. iAstrocytes were therefore also supplemented with a non-toxic concentration (1mM) of adenosine to investigate whether this would stimulate an increase in ATP output (Figure 5.9C-D). No significant difference in ATP output in adenosine supplemented C9orf72 virally treated iAstrocytes was observed, though ATP output was increased by ~10% on average with supplementation (Figure 5.9D). Interestingly, controls saw comparatively higher increases in ATP output as we observed

increases of ~32% on average in control iAstrocytes supplemented with adenosine, though this only reached significance in EV-LV virally treated cells (Figure 5.9C). The inability of C9orf72 iAstrocytes to utilise adenosine for ATP output compared to controls adds further evidence that adenosine to inosine deamination is defective in these cell models. Overall, these data suggested that ADA upregulation and concomitant increase in endogenous inosine output was not sufficient to increase ATP output.

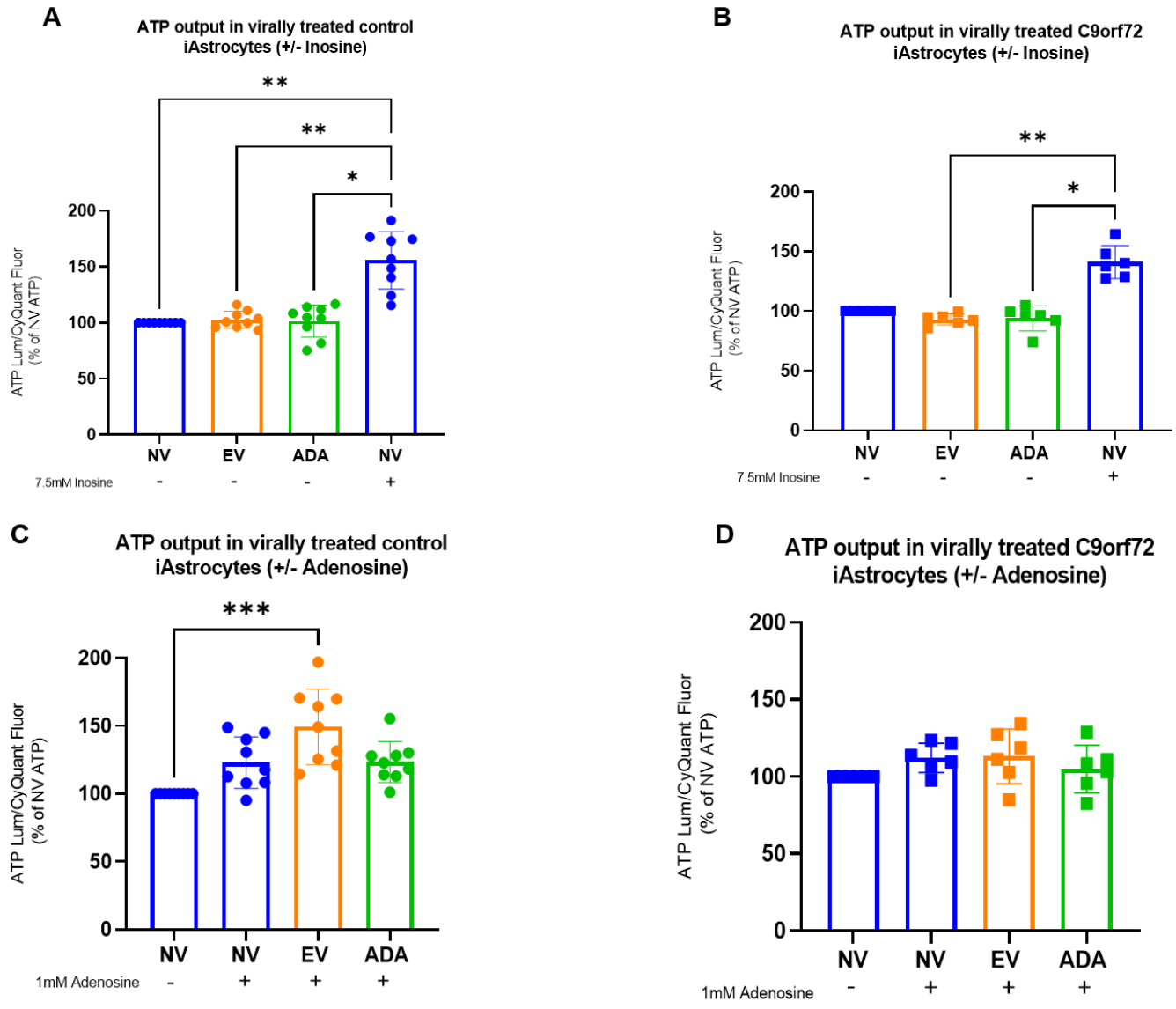

Figure 5.9. ADA gene therapy does not increase bioenergetic output. (A) ATP output in NV (+/- 7.5mM inosine), EV-LV and ADA-LV treated control iAstrocytes. (B) ATP output in NV (+/- 7.5mM inosine), EV-LV and ADA-LV treated C9orf72 iAstrocytes. (C) ATP output in NV, EV-LV and ADA-LV treated control iAstrocytes cultured in 1mM adenosine. (D) ATP output in NV, EV-LV and ADA-LV treated C9orf72 iAstrocytes cultured in 1mM adenosine. Data presented as mean and standard deviation of three biological replicates from three control and two C9orf72 cell lines. Analysis performed by normalising to corresponding NV line at 100%, before transforming data using Y = 1/Y and Y = Logit(Y) prior to Freidman test. **P* ≤ 0.05, ***P* ≤ 0.01, ****P* ≤ 0.001. Where *P* value is not indicated results were non-significant.

5.10 The effect of gene therapy on metabolic flux in control and C9orf72 iAstrocytes

To further explore how viral treatment might alter the bioenergetics of iAstrocytes we employed the use of an XF96 bioanalyser (Agilent) which measures cellular OCR and ECAR, which are representative of mitochondrial respiratory flux and glycolytic flux respectively

Additionally, through the injection of the ATP synthase inhibitor, oligomycin, the oxidative phosphorylation uncoupler, FCCP, and the complex I/III inhibitors rotenone and antimycin-A, in depth mitochondrial and glycolytic function under both physiological and stress conditions can be assessed. This allowed us to measure mitochondrial respiration (MR), coupled respiration (CR), uncoupled respiration (proton leak), mitochondrial spare respiratory capacity (SRC), basal glycolytic flux (basal ECAR), maximal glycolytic capacity (MGC) and glycolytic reserve (GR).

Published data from our laboratory has demonstrated that C9orf72 iAstrocytes have reduced SRC and that inosine supplementation reduced this deficit and increased glycolytic flux in iAstrocytes, with similar results being observed in fibroblasts (Allen et al., 2019a; Gerou et al., 2021). Therefore, we used inosine as positive control in these assays.

5.10.1 Gene therapy did not significantly alter mitochondrial respiration, coupled respiration, proton leak or spare respiratory capacity

ADA-LV gene therapy did not lead to any significant alterations in MR, CR, proton leak and SRC in control or C9orf72 iAstrocytes (Figure 5.10.1.A-H). EV-LV treatment similarly has no effect (Figure 5.10.1A-H). We did observe an increase in CR in control iAstrocytes of 44% when supplemented with inosine, replicating results observed by Allen et al. (2019a). We also demonstrated increased MR (45%), increased proton leak (43%) and increased SRC (26%) in control iAstrocytes supplemented with inosine, though again none of these parameters reached significance. There were also increases, though less substantial, in C9orf72 iAstrocytes in MR (12%), CR (12%), and proton leak (15%). ADA-LV treatment did not alter these parameters by more than 5% in any instance. We also showed that inosine supplementation was able to increase SRC by 24% in C9orf72 iAstrocytes, again recapitulating data we observed in these models previously. Interestingly, ADA-LV treatment also increased SRC by 17%. This data suggests that the increase in inosine output in C9orf72 ADA-LV treated iAstrocytes mimics, to some extent, the effect of supplementing iAstrocytes with exogenous inosine, though neither increase reached significance.

A

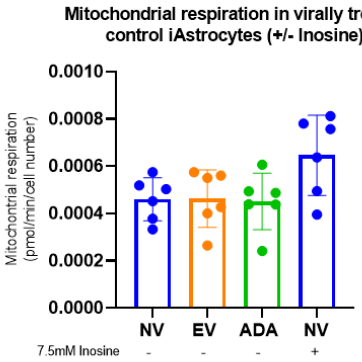
Mitochondrial respiration in virally treated control iAstrocytes (+/- Inosine)
Mitochontrial respiration (pmol/min/cell number)
0.0010
0.0008
0.0006
0.0004
0.0002
0.0000
NV
EV
ADA
NV
7.5mM Inosine
-
-
-
+

B

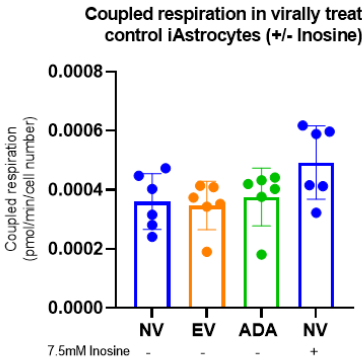
Coupled respiration in virally treated control iAstrocytes (+/- Inosine)
Coupled respiration (pmol/min/cell number)
0.0008
0.0006
0.0004
0.0002
0.0000
NV
EV
ADA
NV
7.5mM Inosine
-
-
-
+

C

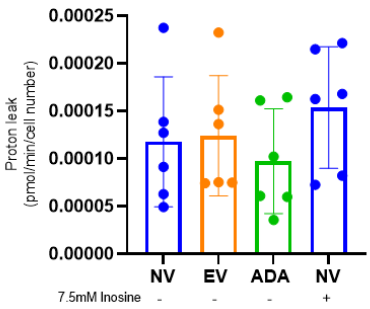
Proton leak in virally treated control iAstrocytes (+/- Inosine)
Proton leak (pmol/min/cell number)
0.00025
0.00020
0.00015
0.00010
0.00005
0.00000
NV
EV
ADA
NV
7.5mM Inosine
-
-
-
+

D

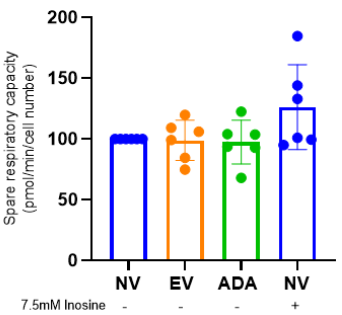
Spare respiratory capacity in virally treated control iAstrocytes (+/- Inosine)
Spare respiratory capacity (pmol/min/cell number)
200
150
100
50
0
NV
EV
ADA
NV
7.5mM Inosine
-
-
-
+

E

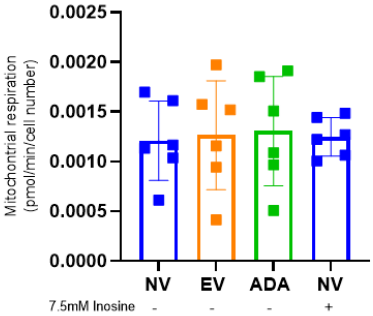
Mitochondrial respiration in virally treated C9orf72 iAstrocytes (+/- Inosine)
Mitochontrial respiration (pmol/min/cell number)
0.0025
0.0020
0.0015
0.0010
0.0005
0.0000
NV
EV
ADA
NV
7.5mM Inosine
-
-
-
+

F

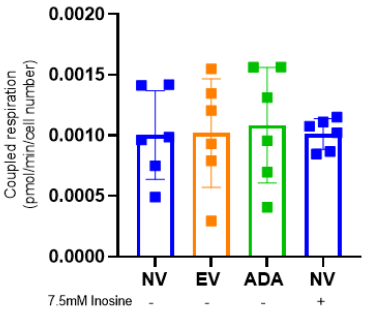
Coupled respiration in virally treated C9orf72 iAstrocytes (+/- Inosine)
Coupled respiration (pmol/min/cell number)
0.0020
0.0015
0.0010
0.0005
0.0000
NV
EV
ADA
NV
7.5mM Inosine
-
-
-
+

G

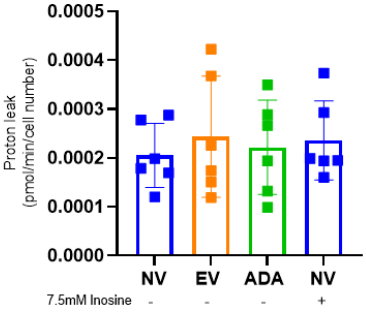
Proton leak in virally treated C9orf72 iAstrocytes (+/- Inosine)
Proton leak (pmol/min/cell number)
0.0005
0.0004
0.0003
0.0002
0.0001
0.0000
NV
EV
ADA
NV
7.5mM Inosine
-
-
-
+

H

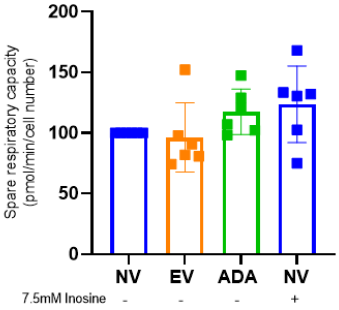
Spare respiratory capacity in virally treated C9orf72 iAstrocytes (+/- Inosine)
Spare respiratory capacity (pmol/min/cell number)
200
150
100
50
0
NV
EV
ADA
NV
7.5mM Inosine
-
-
-
+

Figure 5.10.1. Gene therapy does not significantly alter mitochondrial respiration, coupled respiration, proton leak or spare respiratory capacity in control and C9orf72 iAstrocytes. (A) MR in NV, EV-LV, and ADA-LV control iAstrocytes virally treated at MOI 0.25. (B) CR in NV, EV-LV, and ADA-LV control iAstrocytes virally treated at MOI 0.25. (C) Proton leak in NV, EV-LV, and ADA-LV control iAstrocytes virally treated at MOI 0.25. (D) Spare respiratory capacity in NV, EV-LV, and ADA-LV control iAstrocytes virally treated at MOI 0.25. (E) MR in NV, EV-LV, and ADA-LV C9orf72 iAstrocytes virally treated at MOI 0.25. (F) CR in NV, EV-LV, and ADA-LV C9orf72 iAstrocytes virally treated at MOI 0.25. (G) Proton leak in NV, EV-LV, and ADA-LV C9orf72 iAstrocytes virally treated at MOI 0.25. (H) Spare respiratory capacity in NV, EV-LV, and ADA-LV C9orf72 iAstrocytes virally treated at MOI 0.25. Data presented as mean and standard deviation of three biological replicates from two control and two C9orf72 iAstrocyte lines. Analysis performed using raw data (A, B, C, E, F, and G) or by calculating data as a percentage of the corresponding NV condition (D and H) and performing a RM one-way ANOVA (A, B, C, E, F, and G) or Friedman test (D and H). Where *P* value is not indicated results were non-significant.

5.10.2 Gene therapy did not significantly alter basal ECAR, glycolytic capacity or glycolytic reserve in control or C9orf72 iAstrocytes.

ADA-LV gene therapy, despite increasing inosine output, did not lead to any significant alterations in basal ECAR, MGC, or GR in control or C9orf72 iAstrocytes (Figure 5.10.2A-F). Interestingly, inosine supplementation did not induce any changes in basal ECAR or MGC in control or C9orf72 iAstrocytes, possibly due to using a lower concentration than we have previously (Allen et al., 2019a). Though, there was an increase in control GR that was not observed in C9orf72 iAstrocytes.

A

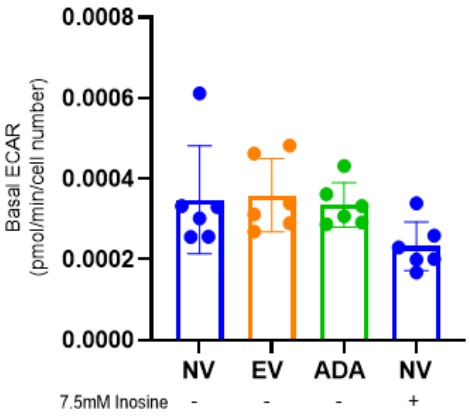
Basal ECAR in virally treated control iAstrocytes (+/- Inosine)
Basal ECAR (pmol/min/cell number)
0.0008
0.0006
0.0004
0.0002
0.0000
NV
EV
ADA
NV
7.5mM Inosine - - - +

B

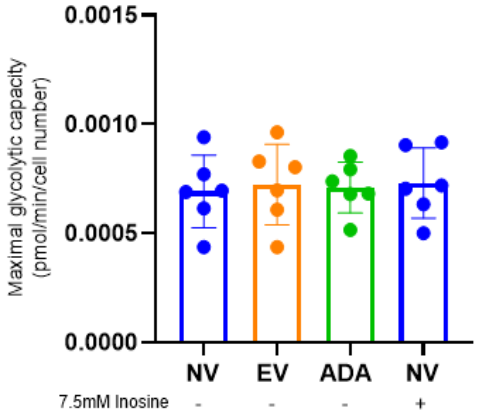
Maximal glycolytic capacity in virally treated control iAstrocytes (+/- Inosine)
Maximal glycolytic capacity (pmol/min/cell number)
0.0015
0.0010
0.0005
0.0000
NV
EV
ADA
NV
7.5mM Inosine - - - +

C

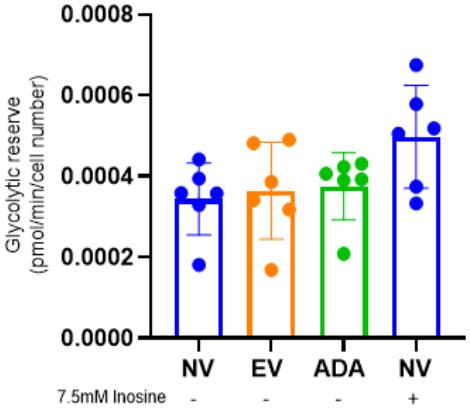
Glycolytic reserve in virally treated control iAstrocytes (+/- Inosine)
Glycolytic reserve (pmol/min/cell number)
0.0008
0.0006
0.0004
0.0002
0.0000
NV
EV
ADA
NV
7.5mM Inosine - - - +

D

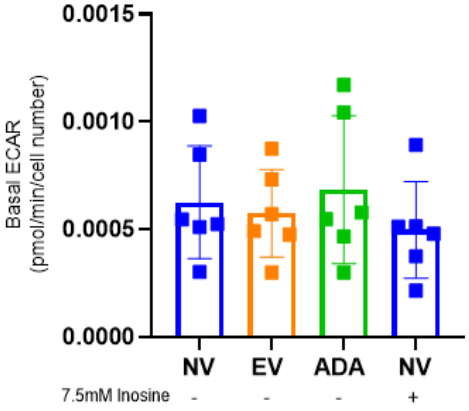
Basal ECAR in virally treated C9orf72 iAstrocytes (+/- Inosine)
Basal ECAR (pmol/min/cell number)
0.0015
0.0010
0.0005
0.0000
NV
EV
ADA
NV
7.5mM Inosine - - - +

E

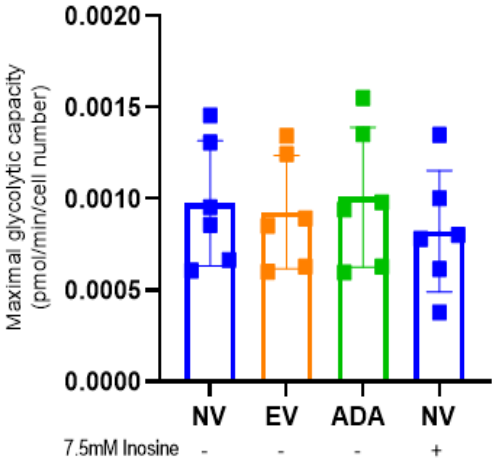
Maximal glycolytic capacity in virally treated C9orf72 iAstrocytes (+/- Inosine)
Maximal glycolytic capacity (pmol/min/cell number)
0.0020
0.0015
0.0010
0.0005
0.0000
NV
EV
ADA
NV
7.5mM Inosine - - - +

F

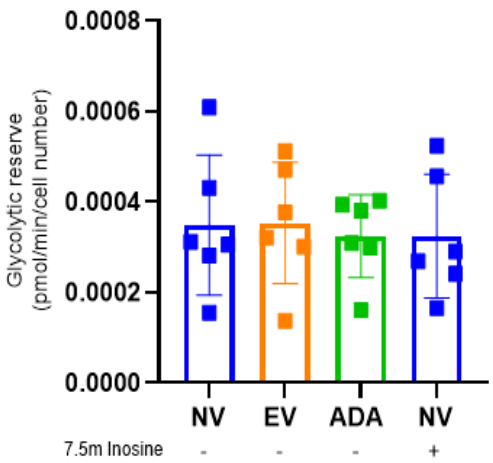
Glycolytic reserve in virally treated C9orf72 iAstrocytes (+/- Inosine)
Glycolytic reserve (pmol/min/cell number)
0.0008
0.0006
0.0004
0.0002
0.0000
NV
EV
ADA
NV
7.5m Inosine - - - +

Figure 5.10.2. Gene therapy did not significantly alter basal ECAR, glycolytic capacity or glycolytic reserve in control or C9orf72 iAstrocytes. (A) Basal ECAR in NV, EV-LV, and ADA-LV control iAstrocytes virally treated at MOI 0.25. (B) Glycolytic capacity in NV, EV-LV, and ADA-LV control iAstrocytes virally treated at MOI 0.25. (C) Glycolytic reserve in NV, EV-LV, and ADA-LV control iAstrocytes virally treated at MOI 0.25. (D) Basal ECAR in NV, EV-LV, and ADA-LV C9orf72 iAstrocytes virally treated at MOI 0.25. (E) Glycolytic capacity in NV, EV-LV, and ADA-LV C9orf72 iAstrocytes virally treated at MOI 0.25. (F) Glycolytic reserve in NV, EV-LV, and ADA-LV C9orf72 iAstrocytes virally treated at MOI 0.25. Data presented as mean and standard deviation of three biological replicates from two control and two C9orf72 iAstrocyte lines. Statistical analysis performed using RM one-way ANOVA. Where *P* value is not indicated results were non-significant.

5.11 Discussion

In this chapter we demonstrated the first use of ADA-LV gene therapy for the treatment of C9orf72 ALS. We presented data demonstrating that gene therapy significantly increased ADA expression in C9orf72 and control iAstrocytes, leading to a subsequent increase in both ADA activity and inosine output. However, we also demonstrated that this restoration of ADA to C9orf72 iAstrocytes was not sufficient to ameliorate adenosine-mediated toxicity or improve energetic output. We also showed that ADA-LV gene therapy had no effect on markers of C9orf72 or purine metabolism enzymes.

5.11.1 Generating a lentiviral vector

To induce upregulation of ADA in iAstrocytes, we chose to use a LV vector. LV vectors, originally derived from the human immunodeficiency virus, can be volatile and the unpredictability of where these viruses integrate into the genome, the potential long-term effect of this, and the immune response of the host are all factors that need to be considered, meaning that many studies have favoured alternative delivery methods (Annoni et al., 2019; Ciuffi, 2008; Sinn et al., 2005). However, LVs have been widely used as an investigative tool *in vivo* and *in vitro* without inducing an immune response or cytotoxicity (Enquist & Card, 2003; Maes et al., 2019; Naldini et al., 1996; Vannucci et al., 2013). They have also been utilised as delivery systems in C9orf72 models published from our institute, including in iAstrocytes (Bauer et al., 2022; Hautbergue et al., 2017; Webster et al., 2016). Lentiviral vectors have also been proven to be an efficacious clinical treatment (Levine et al., 2006). Notably, lentiviral-based therapies have been used to restore ADA expression in the treatment of ADA-deficient SCID (Aiuti et al., 2009; Kohn et al., 2019) and have been trialled for the treatment of neurodegenerative disorders such as PD, and were safe and well-tolerated (Palfi et al., 2014,

2018). For our study, we therefore felt a lentiviral approach was suitable to achieve effective upregulation of ADA in iAstrocytes.

In this chapter, we demonstrated production of the ADA-LV, confirming the successful cloning of our ADA construct into the vector via digestion and then utilised electrophoresis to confirm insertion of the ADA transgene (Figure 5.1). We also generated an EV-LV, using the same lentiviral plasmid without the ADA insert and validated the presence of the plasmid using a restriction enzyme digest. The EV-LV acted as a positive control for the majority of our study, allowing for the identification of effects caused by lentiviral transduction as opposed to the action of the upregulation of ADA. Both viruses were titred against a known virus using RT-qPCR which also demonstrated that they were both able to transduce cells.

One limitation of the EV-LV is the inability to consistently assess expression level, unlike with the ADA-LV for which we employed the use of western blots to measure transduction. We had initially utilised a GFP-expressing virus as a positive control, through which we could have measured transduction directly. However, because of the tendency of GFP to trigger immunogenicity, cytotoxicity, and effect specific markers in cell models (Ansari et al., 2016), we chose to develop the EV-LV as it was more closely comparable to our ADA-LV. Testing expression of the EV-LV in iAstrocytes, using RT-qPCR with WPRE primers would have been a viable method for consistently assessing the level of EV-LV compared to ADA-LV transduction in iAstrocytes. This would have allowed for a more comprehensive study of the effect of lentiviral gene therapy against the effect of the ADA transgene. Alternatively, we could have cloned a GFP-tagged ADA construct into our LV, for more efficient testing of transduction, though this would come again with the limitation of the potential off-target effects of the GFP protein.

For initial experimentation we virally treated iAstrocytes at MOI 1, however, after generating data demonstrating that viral treatment at this MOI did not alter adenosine-mediated toxicity or bioenergetic output, we used MOI 0.25 for several experiments. The rationale behind this was that it is recommended that the minimum level of LV transduction is used to achieve gene expression (Shearer & Saunders, 2015), whereas viral treatment at MOI 1 induced a significant overexpression of ADA, which might have off-target, detrimental effects on the cell. We hypothesised that these off-target effects could cause upregulation of ADA to be ineffectual at alleviating adenosine-mediated toxicity and improving ATP output. Lower MOIs offered a level of transduction in C9orf72 iAstrocytes that restored ADA to similar levels observed in control iAstrocytes, which we surmised would be more physiologically relevant. The major limitation of this approach was the expected loss of transduction efficiency. We did

begin the process of directly measuring transduction efficiency to compare the efficacy of each MOI, but were unable to generate robust, reliable data prior to the conclusion of the study. Despite this, MOI 0.25 ADA-LV therapy still restored ADA activity in C9orf72 iAstrocytes and led to an increase in inosine output. All data presented in this study was therefore performed using iAstrocytes that had been treated at either an MOI 0.25 or MOI 1, as stated previously.

5.11.2 ADA upregulation increases ADA activity and inosine output

We initially performed western blots on control and C9orf72 iAstrocytes that had been transduced with EV-LV and ADA-LV at MOI 0.25, MOI 0.5 and MOI 1. We demonstrated that transduction of ADA-LV at all three MOI was sufficient to increase ADA expression, which reached significance at MOI 0.25 to MOI 1 in control iAstrocytes and MOI 0.5 to MOI 1 in C9orf72 iAstrocytes (Figure 5.3). We subsequently utilised an ADA activity assay to test the functionality of our ADA transgene. This allowed us to establish that increasing ADA expression using this targeted gene therapy approach recovered both ADA activity and inosine output in C9orf72 iAstrocytes (Figure 5.4). These data demonstrate that lentiviral ADA gene therapy has the potential to restore adenosine metabolism function in C9orf72 ALS.

5.11.3 Urate output is not increased by ADA gene therapy

We initially employed the use of urate assays to investigate the effect of increasing inosine output downstream in purine metabolism. Unfortunately, due to time constraints, we were only able to acquire preliminary data. This data suggested that the increase in inosine output was not sufficient to induce a downstream increase in urate output (Figure 5.5). The main possible explanation for this comes from the division between purine salvage and degradation, as we have shown that urate output is likely to be more dependent on HGPRT expression and therefore hypoxanthine-IMP conversion. This means that very little urate might be generated, despite higher substrate production upstream of purine degradation. A more accurate measure of the downstream effect of ADA gene therapy might be to directly investigate hypoxanthine production, or even IMP output in virally treated iAstrocytes

The other explanation is the level of endogenous inosine produced under typical physiological conditions. When we supplemented iAstrocytes with inosine, we used millimolar levels of inosine to induce an increase in urate output. Physiologically, the average extracellular concentration of adenosine ranges between 25 to 250nm (Dunwiddie & Masino, 2001). The

level of inosine produced by cells is limited by the level of adenosine, which is unlikely to go beyond low millimolar levels and therefore, even without purine salvage diverting hypoxanthine away from degradation into urate, we were unlikely to replicate the increase we observed in urate production by supplementing iAstrocytes with inosine.

5.11.4 ADA gene therapy does not alter levels of pathogenic hallmarks of ALS

After generating our LV and confirming upregulation in ADA expression, ADA activity and inosine output, we assessed the effect on a key C9orf72 pathogenic marker, p62. p62 functions as an autophagy substrate, targeting proteins for degradation. Elevated p62 expression is a widely reported phenomenon in C9orf72 ALS, both clinically and in cell models (Al-Sarraj et al., 2011; Allen et al., 2019a; Webster et al., 2016). Links between ADA expression and autophagy are scarce, but adenosine has been shown to regulate autophagy in rat hepatocytes (Kovács et al., 1998; Samari & Seglen, 1998), and rat corticostriatal brain slices exposed to ischemic conditions, but treated with exogenous ADA, had reduced expression of autophagic signalling markers (Tamura et al., 2015). Thus, it was hypothesised that ADA upregulation might be able to reduce p62 expression in C9orf72 iAstrocytes. However, we observed here that ADA-LV did not affect p62 expression suggesting that p62 aggregation and inosine output are not linked.

We also examined expression of NQO-1, a marker of oxidative stress defence. We previously observed a significant downregulation in NQO-1 expression in C9orf72 iAstrocytes (Allen et al., 2019a) likely linked to a downregulation in Nrf2 expression or a muted Nrf-2 response (Petri et al., 2012). Allen et al. (2019a) demonstrated that inosine supplementation in iAstrocytes was able to upregulate urate output. Urate can directly scavenge oxidising agents but its indirect effects, which are mediated by astrocytes, are hypothesised to actually be the driver of the antioxidant properties of urate in the brain (Bakshi et al., 2015; Cipriani et al., 2012; N. Zhang et al., 2014). This is because urate treatment induces activation of the Nrf2 pathway, leading to a concomitant elevation in NQO1 (Bakshi et al., 2015; C. Zhang et al., 2019; N. Zhang et al., 2014). We therefore hypothesised that ADA upregulation, leading to increased urate output, could alter the expression of antioxidant markers such as NQO-1. However, this hypothesis was drawn prior to our finding that urate output was unaffected by ADA-LV treatment, thus making it improbable that ADA-LV treatment would alter NQO-1, which we confirmed by western blot analysis.

Importantly, these data demonstrated, from an ALS point of view, that ADA upregulation did not exacerbate these pathogenic mechanisms. Inducing ischemic conditions in iAstrocytes

and then measuring the expression of p62 and NQO1 with and without viral treatment could instead be used to reveal a protective role for ADA-LV treatment.

5.11.5 ADA gene therapy did not alter levels of purine metabolism enzymes

We next investigated the potential effects of gene therapy on purine metabolism enzyme expression. The hypothesis was that ADA loss leads to downregulation in CD73, possibly as a mechanism for reducing adenosine accumulation. Similarly, we hypothesised that restoring inosine output in the cells would mean a lower requirement for purine salvage and therefore HGPRT expression might be recovered back to endogenous control expression levels. We therefore used western blots on cells virally treated at MOI 0.25 and assessed protein expression of these two purine metabolism enzymes. Here we demonstrated that ADA gene therapy had no effect on either CD73 or HGPRT expression. Based on data that we derived from C9orf72 cell models, this information was not unexpected. We showed that transducing 38x G_4C_2 or 39x C_4G_2 HRE LV in N2a cells led to a significant downregulation in ADA but not in CD73, whilst in HeLa transfected with DPRs, significant downregulation of CD73 and ADA is unaccompanied by alterations in HGPRT expression. This data suggested that alterations in adenosine metabolism do not have upstream or downstream effects on purine metabolism. A more plausible theory might in fact be that CD73 loss precedes loss of ADA, which causes the loss of ADA in the first instance. This could be tested in $CD73^{-/-}$ models and investigation into markers of C9orf72 and signs of neurodegeneration in these models might also give an idea of how important CD73 downregulation is in the pathology of C9orf72.

Despite not observing any direct effect of ADA upregulation, we did observe that HGPRT is consistently reduced by the lentiviral transduction of both EV-LV and ADA-LV in C9orf72 and, to a lesser extent, control iAstrocytes (Figure 5.7). This reduction reached significance for ADA-LV transduction. As stated, lentiviral vectors are unpredictable in where they integrate into the genome (Annoni et al., 2019; Ciuffi, 2008; Shearer & Saunders, 2015; Sinn et al., 2005) as they function by reverse transcribing viral RNA into dsDNA. The DNA cassette is then inserted into the host genome via non-homologous recombination, which is a random process. This can result in the insertion of lentiviral DNA into the open reading frame or regulatory regions of a gene, altering expression of that gene (and can also induce mutation or truncation) (Shearer & Saunders, 2015). HGPRT is coded for by the *HGPRT* gene on chromosome Xq26.2 (Ricciuti & Ruddle, 1973). Viral integration on chromosome Xq26.2 has been reported previously (Sherrill-Mix et al., 2013; Tang et al., 2020; Wagner et al., 2014), but not in regions that would alter HGPRT expression and, regardless, as the process is random the likelihood of the same gene being affected over several replicates and different cell lines is unlikely. However, we could sequence transduced iAstrocytes to definitively rule out the

viral integration site as the cause of LV-induced HGPRT downregulation. Another explanation could be that the lentiviral transduction interferes with cellular processes that HGPRT is involved with. Aberrations in DNA synthesis, for example, could affect the expression of HGPRT. Alternatively, we have shown here that higher HGPRT expression may correlate with lower urate output. Thus, if lentiviral transduction induces oxidative stress, HGPRT expression might reduce as a protective mechanism to increase urate output and therefore antioxidant defence in the cell. Although we have shown that lentiviral transduction does not significantly increase urate output (Figure 5.5). We observe a similar downregulation in HGPRT in C_4G_2 transduced N2a cells. Although we initially attributed this to aberration in loading control expression, it is possible that the downregulation in HGPRT we observe here is linked somehow to the downregulation we observe in those cell lines. At this stage it is hard to definitively hypothesise the cause behind loss of HGPRT arising from lentiviral transduction, and further investigations are required into urate output, and possibly markers of oxidative stress and DNA damage in virally treated iAstrocytes.

5.11.6 ADA upregulation may protect from adenosine-mediated toxicity in a patient-specific manner

We next examined levels of adenosine-mediated toxicity, initially recapitulating the increased sensitivity of C9orf72 iAstrocytes to adenosine that we observed previously (Figure 5.8). Overall, there were no significant changes in the level of cell death in virally treated versus NV iAstrocytes (Figure 5.8). This suggested that ADA-LV was not able to alleviate the toxicity. Adenosine exists in a cycle, being formed by the dephosphorylation of AMP and then is rephosphorylated by ADK. ADA should in theory remove adenosine from this cycle via breakdown into inosine. However, once inosine is converted into hypoxanthine, it can be salvaged to form IMP and this can be converted back into AMP through the action of ADSS and ADSL (Figure 1.5B). Thus, breakdown of adenosine by ADA could merely be propagating this cycle, particularly as we see enhanced HGPRT expression in C9orf72 iAstrocytes which would indicate increased IMP output. This could therefore be the reason that we don't observe an alleviation of adenosine-mediated toxicity. It could be hypothesised that HGPRT inhibition would be beneficial, as this would shuttle hypoxanthine towards urate production, permanently removing adenosine from this cycle. However, as was pointed out in Section 3, this could have the added detriment of impairing purine cycling in the cell.

When performing patient-specific analysis, we observed significantly improved survival in C9-183, the cell line that consistently presents with the most significant reduction in endogenous ADA expression. This suggests that ADA gene therapy, in the context of reducing adenosine toxicity, may only be effective in a patient-dependent manner. This could be tested by

repeating the assay with a larger cohort. Alternatively, upregulation of ADA expression may have a limit to the level of protection it confers. Cell line 183 exhibited the highest level of adenosine mediated toxicity at 55%, whilst ADA-LV reduced toxicity to below 40%, similar to levels observed in control NV iAstrocytes. In our previous work, using a marginally higher adenosine concentration in cell culture was enough to increase adenosine-mediated toxicity to up to 80% in C9orf72 cell lines. This therefore raises the question that if higher adenosine concentrations were used, would this increase toxicity in the NV lines and enhance the level of protection conferred by ADA-LV treatment.

5.11.7 ADA upregulation does not have significant effects on metabolic output in iAstrocytes

Finally, the level of ATP output in iAstrocytes was investigated. The hypothesis was that iAstrocytes with increased ADA expression would produce more ATP due to elevated inosine production. However, no improvement in ATP generation was observed in ADA-LV treated iAstrocytes versus NV and EV-LV treated lines. The lack of response suggests that conversion of endogenous adenosine to inosine, via ADA upregulation was not sufficient to show an overall increase in ATP (Figure 5.9). To test this, iAstrocytes were supplemented with a non-toxic concentration of adenosine which was sufficient to increase ATP levels in controls but not C9orf72 iAstrocytes, a finding that adds to the evidence pointing towards adenosine metabolism dysfunction in ALS astrocytes. However, increased adenosine levels again had no effect on ATP output in ADA-LV treated cells compared to NV and EV-LV treatments. We have previously only observed a significant increase in ATP output by supplementing iAstrocytes with millimolar levels of inosine (Allen et al., 2019a). This only reached significance in iAstrocytes that were supplemented with 4mM of inosine and above. As we only cultured cells in adenosine at 1mM, and adenosine can also be converted into AMP via ADK (as opposed to solely being deaminated to form inosine), it is perhaps not unexpected that we did not observe a significant change in ATP output. Adenosine levels spike rapidly in times of cell stress. Therefore, it may be more physiologically relevant to induce cell stress by, for example, using a higher concentration of adenosine in cells that have been gene therapy treated and measuring ATP output. Inducing glucose/oxygen deprivation could also be relevant, due to the role that inosine-stimulated energy production plays during hypoxia (Balestri et al., 2007; Jurkowitz et al., 1998; Litsky et al., 1999) and ADA-LV treatment might enhance energy generated in this fashion.

As a further investigation into the metabolic changes that could be induced by viral treatment, we employed the use of an XFbioanalyser. This allowed us to investigate, simultaneously, mitochondrial and glycolytic flux under physiological and stress conditions. Here we

demonstrated that ADA-LV was insufficient to induce any significant alterations in MR, basal ECAR, CR, GR, PL and MGC. Promisingly, we did see an upregulation in SRC in C9orf72 iAstrocytes, that was close to the upregulation we observed with inosine supplementation. SRC is classified as the difference in basal mitochondrial ATP output and maximal activity and is a vitally important aspect of mitochondrial function. Cells with higher SRC are better equipped to deal with cell stress as energy demand increases (Hill et al., 2009; Yamamoto et al., 2016). This could therefore suggest a positive impact of ADA-LV on C9orf72 iAstrocyte metabolism. However, the result did not reach significance, possibly because only two cell lines were investigated for this assay. Therefore, further work should utilise a larger cohort to investigate whether this effect is universal in C9orf72 iAstrocytes.

Despite this promising result, at time of writing we have been unable to record any significant effect on energy metabolism in iAstrocytes by ADA-LV treatment. Culturing ADA-LV treated iAstrocytes in a non-toxic concentration of adenosine to provide more 'fuel' had no effect. Further, expression of PNP was found to be unchanged in C9orf72 iAstrocytes, so the lack of metabolic response we observe cannot be blamed on a lack of ribose-1-phosphate output. However, ADA-targeted gene therapy could still have some potential benefit for C9orf72 ALS cells, as outlined in this chapter.

5.11.8 Conclusion

Here we demonstrate that lentiviral gene therapy is able to upregulate expression of ADA and increase ADA activity and inosine output. We were unfortunately unable to translate this into a tangible benefit in the parameters we measured. The two potentially promising findings we made were that the amelioration of adenosine-mediated toxicity by ADA-LV may be patient-specific, and that SRC is increased to a level comparable to inosine supplementation in C9orf72 cells. One key experiment that we were unable to carry out was whether ADA-LV was beneficial to the survival of MNs in MN/iAstrocyte co-cultures and will be of utmost importance in assessing the efficacy of targeted gene therapy for the treatment of ALS.

6. General Discussion

The consequences of a loss of ADA function have been discussed several times throughout this review but will be further elaborated upon here.

6.1 Loss of ADA and it's possible contribution to ALS pathology

As previously stated, ADA downregulation in C9orf72 iAstrocytes led to an increased susceptibility to adenosine-mediated toxicity, which was shown to correlate with ADA expression (Allen et al., 2019a). Notably, when control lines were treated with the irreversible ADA inhibitor pentostatin, a level of toxicity equivocal to the C9orf72 lines was observed, indicating that C9orf72 iAstrocytes' increased sensitivity to adenosine was, at least partially, ADA dependent. Reduced ADA activity in astrocytes could mean accumulation of adenosine, both intracellularly and extracellularly in the CNS during disease progression as astrocytes and especially neurones become stressed and lose integrity. This is potentially physiologically relevant as elevated adenosine has previously been observed in the CSF of ALS patients (Yoshida et al., 1999). In terms of astrocyte function, as described previously, efficient carbon flow through ADA influences several cellular mechanisms known to be disrupted in ALS. With neuronal protection in mind, loss of ADA in astrocytes, as well as affecting purine metabolism, salvage and synthesis, could lead to reduced DNA repair mechanisms, hypomethylation, metabolic dysfunction and reduce defence against oxidative stress. The result of which could impair astrocyte function, potentially promote an activated phenotype and ultimately lead to reduced neuronal support. The ramifications of this, along with the potential links these pathogenic mechanisms share with ALS pathology will be discussed here in full.

One of the major pathogenic mechanisms of ADA-deficient SCID is dATP accumulation, disrupting DNA synthesis and repair. Loss of ADA has been shown to lead to an accumulation of dATP in several *in vivo* models (Aldrich et al., 2003; Carson et al., 1979; Cohen et al., 1978; Smith & Frank Henderson, 1982). Importantly, dATP accumulation has also been associated with the reported neurological impairment observed in patients with ADA-deficient SCID (Rogers et al., 2001). This is key for ALS because of the potential effect on DNA synthesis and repair, and impairment of these functions could easily contribute to the pathology of the disease. DNA damage and its effects are well characterised in ALS (for a recent review see Kok et al., 2021). Elevated DNA damage has long been associated with sALS patients (Blasco et al., 2017; Bogdanov et al., 2000; Ferrante et al., 1997; Fitzmaurice et al., 1996; Ihara et al., 2005; B. W. Kim et al., 2020; Mitsumoto et al., 2008; Murata et al., 2008). Several ALS causing mutations have also been associated with DNA damage, inefficient DNA repair and a

dysfunctional DDR (Fitzmaurice et al., 1996). Increased protein expression and staining for phosphorylated H2AX (γH2AX), a marker of DNA double strand breaks (Rogakou et al., 1999), has been observed in C9orf72 post-mortem spinal cord tissue, and C9orf72 neuronal and DPR cell models, possibly caused by oxidative stress or R-loop formation (Andrade et al., 2020; Choi et al., 2019b; Farg et al., 2017; Lopez-Gonzalez et al., 2016; Nihei et al., 2020; C. Walker et al., 2017). Whilst DPRs have also been shown to inhibit DNA repair by inducing chromatin compaction or interfering with non-homologous end-joining, single-strand annealing, DNA repair via NPM1 and p53 function, that can mediate the DNA repair response (Andrade et al., 2020; Farg et al., 2017; Maor-Nof et al., 2021; C. Walker et al., 2017). The above data indicate a clear association between DNA damage, insufficient DDR/DNA repair and ALS pathology. Loss of ADA, inducing dATP accumulation in ALS could represent a further link between insufficient DNA repair and ALS and could exacerbate the effect of DNA damage on ALS cells.

The second major pathogenic mechanism of ADA-deficient SCID is an accumulation of SAH, leading to reduced DNA methylation (Benveniste et al., 1995). Aberrant DNA methylation has been observed in ALS although, unlike DNA damage, the evidence is less comprehensive and somewhat conflicting. Several studies link ALS with hypermethylation (Xi et al., 2013; Tremolizzo et al., 2014; Coppedè et al., 2017; Hamzeiy et al., 2018) whilst other studies suggest no difference in methylation signatures in individuals with ALS (Garton et al., 2017; Oates and Pamphlett, 2006), and several demonstrate that there is both hyper- and hypomethylation in ALS patients (Morahan et al., 2009; Figueroa-Romero et al., 2012; Appleby-Mallinder et al., 2021). Other studies have also linked ALS with hypomethylation (Wong et al., 2013; Stoccoro et al., 2018; 2020). Wong et al. (2013) demonstrated that mitochondrial Dnmt3a, a DNA methyltransferase enzyme responsible for *de novo* methylation, had significantly lower expression levels in the skeletal muscle and spinal cord of SOD1 mouse models in presymptomatic and early disease stages (Wong et al., 2013). Significantly lower levels of D-loop methylation have also been observed in SOD1 and sALS patients (but not C9orf72 patients) which inversely correlate with mitochondrial DNA copy number (Stoccoro et al., 2018, 2020). Mice that lack Dnmt3a in the nervous system also go on to develop an ALS-like phenotype (Nguyen et al., 2007). These data suggest a role for hypomethylation in ALS, but there are clearly wide aberrations in global DNA methylation signatures that occur in ALS that include both hyper- and hypomethylation. It is therefore possible that there is a link between ADA-loss induced inhibition of SAM-mediated DNA methylation and ALS, though this may only be the case in certain cohorts, as hypomethylation is only observed in SOD1 models and SOD1 and sALS patients.

Bypassing the ADA defect with inosine supplementation was found to be bioenergetically beneficial in iAstrocytes, increasing ATP output, predominantly via glycolysis, which was confirmed by measuring metabolic flux. Moreover, inosine increased both respiratory and glycolytic capacity in these cells. Inosine supplementation also alleviated iAstrocyte-mediated toxicity to MNs in co-culture. ADA levels negatively correlated with adenosine mediated toxicity in ALS iAstrocytes and positively correlated with MN survival in the presence of inosine. Inhibition of ADA in control iAstrocytes also increased their toxicity to MNs. With these data in mind, we recently showed that inosine metabolism positively correlates with disease duration in ALS fibroblasts (Gerou et al., 2021). This suggests that higher ADA activity, in addition to reducing theoretically toxic adenosine and deoxyadenosine accumulation, would produce more inosine and may therefore be protective in ALS.

Elevated inosine production could be beneficial in two major ways. Firstly, lactate produced by astrocytes is used by MNs as a source of energy (Pellerin and Magistretti, 1994) and dysfunctions in lactate metabolism have been linked to ALS previously (Ferraiuolo et al., 2011; 2016). This is important as inosine can be converted to ribose-1-phosphate that contributes to glycolysis via the pentose phosphate pathway, producing ATP, NADH and eventually lactate (Balestri et al., 2007; Jurkowitz et al., 1998; Litsky et al., 1999; Módis et al., 2013), which was shown to be protective to astrocytes in ischemic conditions (Balestri et al., 2007; Jurkowitz et al., 1998; Litsky et al., 1999). This could therefore form part of the mechanism by which MN survival is enhanced when iAstrocytes are supplemented with inosine in MN/astrocyte co-cultures. This could also explain why enhanced inosine production is protective in ALS (Allen et al., 2019a; Gerou et al., 2021) and aligns with data demonstrating that an upregulation of glycolytic flux is neuroprotective in TDP-43 ALS iPSC-derived MNs and *Drosophila* (Manzo et al., 2019), and mouse embryonic stem cell-derived MNs, zebrafish and mice (Chaytow et al., 2022). Secondly, inosine can be converted to urate via conversion to hypoxanthine and subsequently xanthine (Figure 1.5B), and the production of urate is associated with a better prognosis in ALS (Ikeda et al., 2012; Keizman et al., 2009; Nicholson et al., 2015; Oh et al., 2015; Paganoni et al., 2018; F. Zhang et al., 2018). However, increased urate is unlikely to be the mechanism by which inosine supplementation can reduce ALS iAstrocyte-mediated toxicity to MNs, as it was shown that increased urate does not lead to a concomitant improvement in MN survival (Allen et al., 2019a). Despite this, these data suggest that both urate and inosine have an important role in ALS pathology.

The combination of disrupted DNA repair, aberrant methylation signatures, reduced energy output and reduced oxidative stress defence which could be induced by dysfunctional purine metabolism would be likely to disrupt normal astrocytic function and, as toxic insult can induce

reactivity, this may propagate astrogliosis and would be detrimental to neuronal health. We have demonstrated here that increasing ADA expression by lentiviral gene therapy is able to increase inosine output (Figure 5.4.1) and therefore could be beneficial to many of the ALS related pathogenic pathways described above. Taken together, these data indicate that the therapeutic benefits of ADA level restoration would be multifactorial for ALS patients, either from increased toxic metabolite breakdown or through increasing inosine levels and therefore urate and lactate output, or both.

6.2 Further links between purine metabolism and ALS

Alongside the consequences of dysfunctional purine metabolism outlined above, multiple instances of phenotypes that may have a link to dysfunctional purine metabolism exist in the literature. These are detailed below.

6.2.1 Immune cell regulation in ALS

Dysfunctional immune cell regulation is a common observance in ALS. Circulating monocytes from both sALS and fALS patients demonstrate aberrant subtype regulation, incorrect adhesion, and dysregulated phagocytic activity (Zondler et al., 2016). Moreover, levels of monocytes with a proinflammatory phenotype have been shown to correlate with faster disease progression (W. Zhao et al., 2017). A reduced number of circulating dendritic cells were observed in sALS patients but were also predicted to be proinflammatory (Rusconi et al., 2017), whilst dendritic cell levels were significantly increased in spinal cord tissue taken from both fALS and sALS patients, which also positively correlated with disease progression (Henkel et al., 2004). Reduced expression of T-lymphocytes has been observed in sALS patients (Mantovani et al., 2009), regulatory T-cells taken from patients were shown to be dysfunctional (Beers et al., 2017) and T-lymphocyte levels may negatively correlate with accelerated disease progression (Henkel et al., 2013). The importance of ADA in immune cell differentiation and function has been discussed in section 1.8 and, in general, the role that ADA plays in immune cell regulation is well established (for a review see Antonioli et al., 2012), as evidenced by severe disruption of immune cell function in ADA-deficient SCID (Hershfield, 2017). Immunodeficiency has recently been linked to ALS (Béland et al., 2020) and the immune cell dysfunction outlined here could therefore be linked to ADA dysregulation. However, it may be that the level of ADA loss in ALS is cell dependent. Data from our laboratory suggested that ADA loss was more severe in iAstrocytes compared to iNeurons and more severe in iNeurons compared to fibroblasts

(Allen et al., 2019a). Therefore, it remains to be seen whether loss of ADA is observed both in immune cells and, for example, in microglia and whether this negatively influences ALS disease pathology.

6.2.2 Changes in purine metabolic profiles in ALS

Multiple studies have identified purine metabolism as a pathway that undergoes significant changes over the course of ALS. A systematic review of all literature published investigating metabolite-disease associations from 2006-2016 identified purine metabolism as a pathway that becomes altered during ALS and also a unifying feature of ALS, AD and PD (Kori et al., 2016). A metabolomic study investigating alterations in metabolic signatures in whole cell and the mitochondrial endoplasmic reticulum (mito-ER) of fibroblasts from sALS patients identified purine metabolism, alongside pyrimidine metabolism as having a distinct metabolomic profile compared to controls (Veyrat-Durebex et al., 2019). Interestingly, in both whole cells and mito-ER fractions, inosine was at a higher level than controls, whilst its downstream product xanthine was expressed at lower levels, suggesting a potential dysfunction in the enzyme than catalyses inosine-xanthine conversion, PNP, though this was not observed in C9orf72 iAstrocytes (Figure 3.4). Deoxyadenosine was also reported as higher in sALS patient fibroblast mito-ER fractions, which would align with the hypothesis that loss of ADA leads to accumulation of its substrates, though no differences were reported in adenosine levels (Veyrat-Durebex et al., 2019). The same group performing similar metabolomic analysis in mutant SOD1 new-born mice spinal cord astrocytes also demonstrated distinct purine metabolic profiles compared to wildtype in astrocyte MN co-cultures (Hounoum et al., 2017) which was likely associated with an inflammatory state. Purine metabolism was also identified as a pathway of interest in a multi-omics study of $SOD1^{G93A}$ transgenic mice against wild-type littermates (Xu et al., 2023). Metabolomic analysis of plasma, lumbar spinal cord and motor cortex demonstrated global downregulation in purines and purine derivatives in transgenic mice, with purine metabolism being one of the only pathways disturbed to a significant level in the spinal cord. Plasma and spinal cord analysis showed that purine metabolism in this model was also the only pathway to exhibit evidence of disruption at the pre-symptomatic stage, which interestingly demonstrated that inosine output was significantly downregulated with no alteration in adenosine output. Proteomic analysis also identified differential expression of multiple proteins involved in the regulation of purine metabolism, including downregulation of cytosolic 5'-nucleotidase, the intracellular counterpart to CD73. Joint pathway analysis, as would be expected, confirmed that purine metabolism was a pathway of interest in ALS and

may be associated with progression of the disease (Xu et al., 2023). These data demonstrate a precedent for aberrant purine metabolism in ALS making the pathway an even more compelling target for therapeutics.

6.2.3 Oestradiol in ALS

In possible confirmation of the therapeutic benefit of elevated ADA levels in ALS patients, recent evidence suggests a protective role for oestradiol in ALS (Boddy et al., 2022; Klemann et al., 2018). Moreover, women with higher lifetime endogenous oestrogen exposure were associated with a longer survival in ALS (de Jong et al., 2012). Treatment with E2 was shown to be protective in a SOD1 mouse model (Heitzer et al., 2017) and oestradiol was also protective in a C9orf72 Zebrafish model (Boddy et al., 2022). E2 has also been shown to protect against demyelination and axonal injury in MS mouse models (Aryanpour et al., 2021) and may be generally protective in neurodegenerative diseases (Garcia-Segura et al., 2001). As discussed in section 1.7, oestradiol has been shown to increase ADA levels (Xie et al., 2001) insinuating a purine metabolism related mechanism for oestrogen's neuroprotection in ALS. Evaluating the neuroprotective effect of oestradiol *in vivo* and *in vitro* and correlating this effect with ADA expression would offer insight into what extent of oestradiol's neuroprotection is mediated by ADA.

6.2.4 Type two diabetes is neuroprotective in ALS

Type two diabetes (T2DM), which is caused by insulin resistance (Roglic, 2016) has been linked to higher serum ADA activity (Hoshino et al., 1994; Kurtul et al., 2004; J. Lee et al., 2011; Niraula et al., 2018) as ADA expression negatively correlates with insulin levels (Rutkiewicz & Górski, 1990). Several studies have also associated T2DM with neuroprotection in ALS, demonstrating that people who have T2DM have a significantly lower chance of developing ALS and a delayed disease onset (Kioumourtzoglou et al. 2015; Mariosa et al. 2015; D'Ovidio et al. 2018; Tsai et al., 2019; Zeng et al., 2019). It has been hypothesised the protective role of diabetes is related to electrolyte regulation (Ahn et al., 2017). Patients suffering from diabetes often develop electrolyte disorders that cause depletion in key electrolytes including calcium. Lower calcium levels would reduce the speed of Ca^{2+} build up in neurons reducing Ca^{2+} influx into mitochondrial cells thus preserving mitochondrial function for longer (Ahn et al., 2017) one of the major pathologies observed in ALS. However, as T2DM has been shown to lead to an increase in serum ADA levels (Hoshino et al., 1994; Kurtul et al., 2004; J. Lee et al., 2011; Niraula et al., 2018), it is

possible that the neuroprotection provided by T2DM in ALS is partially related to alterations in purine metabolism via increased ADA activity.

As evidenced here, ADA might still provide an area for therapeutic intervention. Enzyme replacement therapy is already a safe and efficacious treatment for ADA-deficient SCID which could be translated into the treatment of ALS. Regardless of the data showing lack of any true effect of ADA-LV therapy, ADA is clearly an important regulator of neuronal function, and sits at the crux of multiple pathways that have been implicated in ALS pathogenicity, which has been summarised in Figure 6.1. It therefore remains as an undeniable target for therapeutic intervention in ALS.

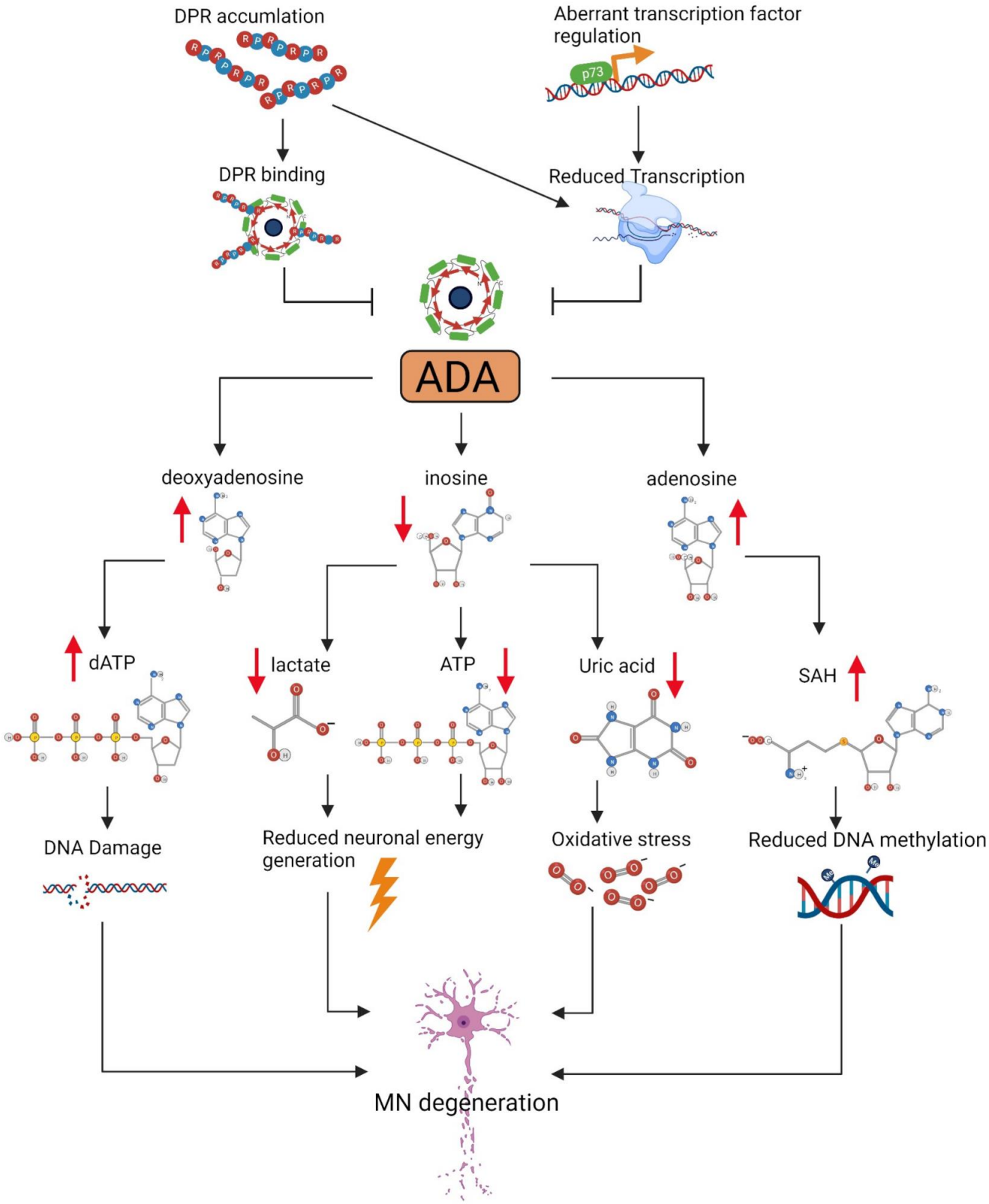

Figure 6.1. Possible mechanisms of ADA-mediated MN degeneration. Loss of ADA in ALS may lead to MN degeneration via several mechanisms. First DPR accumulation, can lead to

incorrect RNA transcription of the ADA protein, and direct binding to ADA in the cytoplasm may reduce protein function. Alternatively, transcriptional regulation could interfere with ADA expression. This would lead to a decrease in inosine output and an accumulation of adenosine and deoxyadenosine. Loss of inosine would result in a reduction in both inosine-mediated lactate and ATP output, and therefore energy generation in MNs which has been linked to ALS pathogenesis previously. It would also result in a reduction in urate levels, a potent antioxidant, which would contribute to the oxidative stress that has also been linked to ALS pathogenesis. Accumulations of deoxyadenosine and adenosine may also induce inflammation, cause immune cell dysfunction, affect DNA synthesis and repair, and methylation in ALS astrocytes, another potential pathogenic mechanism behind MN degeneration. Figure taken, with permission, from Hall et al., (2022).

6.3 Future Directions

As described previously, the purine salvage and DNPB pathways are strongly linked (Camici et a., 2018; Zhou et al., 1994). Further experimentation investigating DNPB regulation has been discussed briefly but may play a more extensive role in aberration we observe in the wider pathway. We observe that endogenous inosine output is reduced in C9orf72 iAstrocytes (Figure 3.1) which could point to reduced purine salvage due to insufficient upstream substrate production, despite observing a significant increase in HGPRT (Figure 3.4) iAstrocytes. If this was the case, then DNPB would be required to counteract reduced purine output from purine salvage. PPAT has been shown to be elevated in FUS and TDP-43 mutant mouse models (Mateeva et al., 2023), suggesting elevated DNPB in these models, though purinosome formation would be a more robust measure of DNPB activity. Therefore, dynamic characterisation of purine salvage and DNPB would be required to answer these questions. Interestingly, the purinosome is thought to be a biomolecular condensate forming through LLPS, as it shares several characteristics with other liquid-like condensates (Pedley et al., 2022). As discussed, arginine containing DPRs are known to disrupt biomolecular condensate formation by interacting with low complexity domains (Boeynaems et al., 2017; K. H. Lee et al., 2016; Lin et al., 2016; Molliex et al., 2015; White et al., 2019; Y. J. Zhang et al., 2018). It would therefore be interesting to observe purinosome formation in DPR expressing cells. If they disrupt formation of the purinosome then this could have significant implications for purine salvage and may be an instigator of downstream purine metabolism dysfunction.

Increasing ADA activity, as we demonstrate here (Figure 5.4.1) and therefore increasing adenosine or deoxyadenosine breakdown, could prevent the toxic build-up of adenosine

dATP and SAH, which we hypothesise disrupts astrocyte homeostasis, leading to MN degeneration. Further investigation of the cytotoxic mechanisms arising from a loss of ADA is also required. It would be interesting to investigate, firstly whether C9orf72 iAstrocytes are more susceptible to toxicity mediated by deoxyadenosine accumulation, as we observed with adenosine. And, secondly, to investigate whether ADA-LV gene therapy can alleviate any toxicity we hypothesise would be observed by culturing iAstrocytes in the presence of abnormal levels of deoxyadenosine. ADA-LV might also prove more protective when iAstrocytes are cultured in toxic levels of both adenosine and deoxyadenosine in tandem. Additionally, it would be interesting to observe whether higher concentrations of adenosine, that we know induce toxicity in C9orf72 iAstrocytes, have any effect on the methylation profiles of these models. It is possible that ADA-LV treatment could protect against alterations in methylation that do not lead to tangible changes in cell survival, but provide a benefit to iAstrocytes nonetheless. Assays examining methylation in virally and non-virally treated iAstrocytes, cultured in adenosine, would potentially provide a more subtle measure of the effect of gene therapy. We could also investigate inflammation and DNA damage markers which would reveal whether ADA-LV protects against toxic insult arising from adenosine and dATP accumulation respectively.

7. References

Abbott, N. J., Rönnbäck, L., & Hansson, E. (2006). Astrocyte-endothelial interactions at the blood-brain barrier. In *Nature Reviews Neuroscience* (Vol. 7, Issue 1, pp. 41–53). Nat Rev Neurosci. https://doi.org/10.1038/nrn1824

Abe, K., Aoki, M., Tsuji, S., Itoyama, Y., Sobue, G., Togo, M., Hamada, C., Tanaka, M., Akimoto, M., Nakamura, K., Takahashi, F., Kondo, K., Yoshino, H., Abe, K., Aoki, M., Tsuji, S., Itoyama, Y., Sobue, G., Togo, M., … Yoshino, H. (2017). Safety and efficacy of edaravone in well defined patients with amyotrophic lateral sclerosis: a randomised, double-blind, placebo-controlled trial. *The Lancet Neurology*, *16*(7). https://doi.org/10.1016/S1474-4422(17)30115-1

Abe, Y., Hashimoto, Y., Tomita, Y., Terashita, K., Aiso, S., Tajima, H., Niikura, T., Matsuoka, M., & Nishimoto, I. (2004). Cytotoxic mechanisms by M239V presenilin 2, a little-analyzed Alzheimer's disease-causative mutant. *Journal of Neuroscience Research*, *77*(4), 583–595. https://doi.org/10.1002/JNR.20163

Abramov, A. Y., Scorziello, A., & Duchen, M. R. (2007). Three Distinct Mechanisms Generate Oxygen Free Radicals in Neurons and Contribute to Cell Death during Anoxia and Reoxygenation. *Journal of Neuroscience*, *27*(5), 1129–1138. https://doi.org/10.1523/JNEUROSCI.4468-06.2007

Abu Shmais, G., Al-Ayadhi, L., Al-Dbass, A., & El-Ansary, A. (2012). Mechanism of nitrogen metabolism-related parameters and enzyme activities in the pathophysiology of autism. *Journal of Neurodevelopmental Disorders*, *4*(1), 1–11. https://doi.org/10.1186/1866-1955-4-4

Ahn, C., Kang, J., & Jeung, E. (2017). Calcium homeostasis in diabetes mellitus. *Journal of Veterinary Science*, *18*(3), 261–266. https://doi.org/10.4142/JVS.2017.18.3.261

Aiuti, A., Cattaneo, F., Galimberti, S., Benninghoff, U., Cassani, B., Callegaro, L., Scaramuzza, S., Andolfi, G., Mirolo, M., Brigida, I., Tabucchi, A., Carlucci, F., Eibl, M., Aker, M., Slavin, S., Al-Mousa, H., Al Ghonaium, A., Ferster, A., Duppenthaler, A., … Roncarolo, M.-G. (2009). Gene Therapy for Immunodeficiency Due to Adenosine Deaminase Deficiency. *New England Journal of Medicine*, *360*(5), 447–458. https://doi.org/10.1056/NEJMOA0805817

Aizawa, H., Sawada, J., Hideyama, T., Yamashita, T., Katayama, T., Hasebe, N., Kimura, T., Yahara, O., & Kwak, S. (2010). TDP-43 pathology in sporadic ALS occurs in motor neurons lacking the RNA editing enzyme ADAR2. *Acta Neuropathologica 2010 120:1*,

120(1), 75–84. https://doi.org/10.1007/S00401-010-0678-X

Al-Sarraj, S., King, A., Troakes, C., Smith, B., Maekawa, S., Bodi, I., Rogelj, B., Al-Chalabi, A., Hortobágyi, T., & Shaw, C. E. (2011). P62 positive, TDP-43 negative, neuronal cytoplasmic and intranuclear inclusions in the cerebellum and hippocampus define the pathology of C9orf72-linked FTLD and MND/ALS. *Acta Neuropathologica*, *122*(6), 691–702. https://doi.org/10.1007/S00401-011-0911-2/FIGURES/5

Aladesuyi Arogundade, O., Stauffer, J. E., Saberi, S., Diaz-Garcia, S., Malik, S., Basilim, H., Rodriguez, M. J., Ohkubo, T., & Ravits, J. (2019). Antisense RNA foci are associated with nucleoli and TDP-43 mislocalization in C9orf72-ALS/FTD: a quantitative study. *Acta Neuropathologica*, *137*(3), 527–530. https://doi.org/10.1007/S00401-018-01955-0/TABLES/1

Aldrich, M. B., Chen, W., Blackburn, M. R., Martinez-Valdez, H., Datta, S. K., & Kellems, R. E. (2003). Impaired Germinal Center Maturation in Adenosine Deaminase Deficiency. *The Journal of Immunology*, *171*(10), 5562–5570. https://doi.org/10.4049/JIMMUNOL.171.10.5562

Allen, S. P., Duffy, L. M., Shaw, P. J., & Grierson, A. J. (2015). Altered age-related changes in bioenergetic properties and mitochondrial morphology in fibroblasts from sporadic amyotrophic lateral sclerosis patients. *Neurobiology of Aging*, *36*(10), 2893–2903. https://doi.org/10.1016/J.NEUROBIOLAGING.2015.07.013

Allen, S. P., Hall, B., Castelli, L. M., Francis, L., Woof, R., Siskos, A. P., Kouloura, E., Gray, E., Thompson, A. G., Talbot, K., Higginbottom, A., Myszczynska, M., Allen, C. F., Stopford, M. J., Hemingway, J., Bauer, C. S., Webster, C. P., De Vos, K. J., Turner, M. R., … Shaw, P. J. (2019). Astrocyte adenosine deaminase loss increases motor neuron toxicity in amyotrophic lateral sclerosis. *Brain : A Journal of Neurology*, *142*(3), 586–605. https://doi.org/10.1093/brain/awy353

Allen, S. P., Hall, B., Woof, R., Francis, L., Gatto, N., Shaw, A. C., Myszczynska, M., Hemingway, J., Coldicott, I., Willcock, A., Job, L., Hughes, R. M., Boschian, C., Bayatti, N., Heath, P. R., Bandmann, O., Mortiboys, H., Ferraiuolo, L., & Shaw, P. J. (2019). C9orf72 expansion within astrocytes reduces metabolic flexibility in amyotrophic lateral sclerosis. *Brain*, *142*(12), 3771–3790. https://doi.org/10.1093/BRAIN/AWZ302

Allen, S. P., Rajan, S., Duffy, L., Mortiboys, H., Higginbottom, A., Grierson, A. J., & Shaw, P. J. (2014). Superoxide dismutase 1 mutation in a cellular model of amyotrophic lateral sclerosis shifts energy generation from oxidative phosphorylation to glycolysis. *Neurobiology of Aging*, *35*(6), 1499–1509.

https://doi.org/10.1016/j.neurobiolaging.2013.11.025

Alvarez-Mora, M. I., Garrabou, G., Barcos, T., Garcia-Garcia, F., Grillo-Risco, R., Peruga, E., Gort, L., Borrego-écija, S., Sanchez-Valle, R., Canto-Santos, J., Navarro-Navarro, P., & Rodriguez-Revenga, L. (2022). Bioenergetic and Autophagic Characterization of Skin Fibroblasts from C9orf72 Patients. *Antioxidants 2022, Vol. 11, Page 1129*, *11*(6), 1129. https://doi.org/10.3390/ANTIOX11061129

Ames, B. N., Cathcart, R., Schwiers, E., & Hochstein, P. (1981). Uric acid provides an antioxidant defense in humans against oxidant- and radical-caused aging and cancer: A hypothesis. *Proceedings of the National Academy of Sciences of the United States of America*, *78*(11 II), 6858–6862. https://doi.org/10.1073/pnas.78.11.6858

Amick, J., Roczniak-Ferguson, A., & Ferguson, S. M. (2016). C9orf72 binds SMCR8, localizes to lysosomes, and regulates mTORC1 signaling. *Molecular Biology of the Cell*, *27*(20), 3040–3051. https://doi.org/10.1091/MBC.E16-01-0003/ASSET/IMAGES/LARGE/3040FIG7.JPEG

An, S., Kumar, R., Sheets, E. D., & Benkovic, S. J. (2008). Reversible compartmentalization of de novo purine biosynthetic complexes in living cells. *Science*, *320*(5872), 103–106. https://doi.org/10.1126/SCIENCE.1152241/SUPPL_FILE/AN.SOM.PDF

Andrade, N. S., Ramic, M., Esanov, R., Liu, W., Rybin, M. J., Gaidosh, G., Abdallah, A., Del'Olio, S., Huff, T. C., Chee, N. T., Anatha, S., Gendron, T. F., Wahlestedt, C., Zhang, Y., Benatar, M., Mueller, C., & Zeier, Z. (2020). Dipeptide repeat proteins inhibit homology-directed DNA double strand break repair in C9ORF72 ALS/FTD. *Molecular Neurodegeneration*, *15*(1). https://doi.org/10.1186/S13024-020-00365-9

Annoni, A., Gregori, S., Naldini, L., & Cantore, A. (2019). Modulation of immune responses in lentiviral vector-mediated gene transfer. *Cellular Immunology*, *342*, 103802. https://doi.org/10.1016/J.CELLIMM.2018.04.012

Ansoleaga, B., Jové, M., Schlüter, A., Garcia-Esparcia, P., Moreno, J., Pujol, A., Pamplona, R., Portero-Otín, M., & Ferrer, I. (2015). Deregulation of purine metabolism in Alzheimer's disease. *Neurobiology of Aging*, *36*(1), 68–80. https://doi.org/10.1016/J.NEUROBIOLAGING.2014.08.004

Antonioli, L., Colucci, R., La Motta, C., Tuccori, M., Awwad, O., Da Settimo, F., Blandizzi, C., & Fornai, M. (2012). Adenosine Deaminase in the Modulation of Immune System and its Potential as a Novel Target for Treatment of Inflammatory Disorders. *Current Drug Targets*, *13*(6), 842–862. https://doi.org/10.2174/138945012800564095

Appleby-Mallinder, C., Schaber, E., Kirby, J., Shaw, P. J., Cooper-Knock, J., Heath, P. R., & Highley, J. R. (2021). TDP43 proteinopathy is associated with aberrant DNA methylation in human amyotrophic lateral sclerosis. *Neuropathology and Applied Neurobiology*, *47*(1), 61–72. https://doi.org/10.1111/NAN.12625

Araque, A., Parpura, V., Sanzgiri, R. P., & Haydon, P. G. (1998). Glutamate-dependent astrocyte modulation of synaptic transmission between cultured hippocampal neurons. *European Journal of Neuroscience*, *10*(6), 2129–2142. https://doi.org/10.1046/j.1460-9568.1998.00221.x

Archer, S., Juranka, P. F., Ho, J. H., & Chan, V.-L. (1985). An analysis of multiple mechanisms of adenosine toxicity in baby hamster kidney cells. *Journal of Cellular Physiology*, *124*(2), 226–232. https://doi.org/10.1002/jcp.1041240209

Arredondo-Vega, F. X., Santisteban, I., Kelly, S., Schlossman, C. M., Umetsu, D. T., & Hershfield, M. S. (1994). Correct splicing despite mutation of the invariant first nucleotide of a 5' splice site: a possible basis for disparate clinical phenotypes in siblings with adenosine deaminase deficiency. *American Journal of Human Genetics*, *54*(5), 820. /pmc/articles/PMC1918276/?report=abstract

Arredondo-Vega, F. X., Santisteban, I., Richard, E., Bali, P., Koleilat, M., Loubser, M., Al-Ghonaium, A., Al-Helali, M., & Hershfield, M. S. (2002). Adenosine deaminase deficiency with mosaicism for a "second-site suppressor" of a splicing mutation: decline in revertant T lymphocytes during enzyme replacement therapy. *Blood*, *99*(3), 1005–1013. https://doi.org/10.1182/BLOOD.V99.3.1005

Arthur, K. C., Calvo, A., Price, T. R., Geiger, J. T., Chiò, A., & Traynor, B. J. (2016). Projected increase in amyotrophic lateral sclerosis from 2015 to 2040. *Nature Communications*, *7*. https://doi.org/10.1038/ncomms12408

Aryanpour, R., Zibara, K., Pasbakhsh, P., Jame'ei, S. B., Namjoo, Z., Ghanbari, A., Mahmoudi, R., Amani, S., & Kashani, I. R. (2021). 17β-Estradiol Reduces Demyelination in Cuprizone-fed Mice by Promoting M2 Microglia Polarity and Regulating NLRP3 Inflammasome. *Neuroscience*, *463*, 116–127. https://doi.org/10.1016/J.NEUROSCIENCE.2021.03.025

Atanasio, A., Decman, V., White, D., Ramos, M., Ikiz, B., Lee, H. C., Siao, C. J., Brydges, S., Larosa, E., Bai, Y., Fury, W., Burfeind, P., Zamfirova, R., Warshaw, G., Orengo, J., Oyejide, A., Fralish, M., Auerbach, W., Poueymirou, W., … Lai, K. M. V. (2016). C9orf72 ablation causes immune dysregulation characterized by leukocyte expansion, autoantibody production, and glomerulonephropathy in mice. *Scientific Reports*, *6*.

https://doi.org/10.1038/SREP23204

Atasoy, U., Norby-Slycord, C., & Markert, M. (1993). A missense mutation in exon 4 of the human adenosine deaminase gene causes severe combined immunodeficiency. *Human Molecular Genetics*, *2*(8), 1307–1308. https://doi.org/10.1093/HMG/2.8.1307

Baborie, A., Griffiths, T. D., Jaros, E., Perry, R., McKeith, I. G., Burn, D. J., Masuda-Suzukake, M., Hasegawa, M., Rollinson, S., Pickering-Brown, S., Robinson, A. C., Davidson, Y. S., & Mann, D. M. A. (2015). Accumulation of dipeptide repeat proteins predates that of TDP-43 in frontotemporal lobar degeneration associated with hexanucleotide repeat expansions in C9ORF72 gene. *Neuropathology and Applied Neurobiology*, *41*(5), 601–612. https://doi.org/10.1111/NAN.12178/SUPPINFO

Bakshi, R., Zhang, H., Logan, R., Joshi, I., Xu, Y., Chen, X., & Schwarzschild, M. A. (2015). Neuroprotective effects of urate are mediated by augmenting astrocytic glutathione synthesis and release. *Neurobiology of Disease*, *82*, 574–579. https://doi.org/10.1016/J.NBD.2015.08.022

Balestri, F., Giannecchini, M., Sgarrella, F., Carta, M. C., Tozzi, M. G., & Camici, M. (2007). Purine and pyrimidine nucleosides preserve human astrocytoma cell adenylate energy charge under ischemic conditions. *Neurochemistry International*, *50*(3), 517–523. https://doi.org/10.1016/J.NEUINT.2006.10.005

Bauer, C. S., Cohen, R. N., Sironi, F., Livesey, M. R., Gillingwater, T. H., Highley, J. R., Fillingham, D. J., Coldicott, I., Smith, E. F., Gibson, Y. B., Webster, C. P., Grierson, A. J., Bendotti, C., & De Vos, K. J. (2022). An interaction between synapsin and C9orf72 regulates excitatory synapses and is impaired in ALS/FTD. *Acta Neuropathologica*, *144*(3), 437–464. https://doi.org/10.1007/S00401-022-02470-Z/FIGURES/8

Beers, D., Zhao, W., Wang, J., Zhang, X., Wen, S., Neal, D., Thonhoff, J., Alsuliman, A., Shpall, E., Rezvani, K., & Appel, S. (2017). ALS patients' regulatory T lymphocytes are dysfunctional, and correlate with disease progression rate and severity. *JCI Insight*, *2*(5). https://doi.org/10.1172/JCI.INSIGHT.89530

Beghi, E., Mennini, T., Bendotti, C., Bigini, P., Logroscino, G., Chio, A., Hardiman, O., Mitchell, D., Swingler, R., Traynor, B., & Al-Chalabi, A. (2007). The Heterogeneity of Amyotrophic Lateral Sclerosis: A Possible Explanation of Treatment Failure. *Current Medicinal Chemistry*, *14*(30), 3185–3200. https://doi.org/10.2174/092986707782793862

Béland, L.-C., Markovinovic, A., Jakovac, H., De Marchi, F., Bilic, E., Mazzini, L., Kriz, J., & Munitic, I. (2020). Immunity in amyotrophic lateral sclerosis: blurred lines between

excessive inflammation and inefficient immune responses. *Brain Communications*, *2*(2). https://doi.org/10.1093/BRAINCOMMS/FCAA124

Bélanger, M., Allaman, I., & Magistretti, P. J. (2011). Brain energy metabolism: Focus on Astrocyte-neuron metabolic cooperation. In *Cell Metabolism* (Vol. 14, Issue 6, pp. 724–738). Cell Metab. https://doi.org/10.1016/j.cmet.2011.08.016

Bensimon, G., Lacomblez, L., & Meininger, V. (1994). A Controlled Trial of Riluzole in Amyotrophic Lateral Sclerosis. *New England Journal of Medicine*, *330*(9), 585–591. https://doi.org/10.1056/NEJM199403033300901

Benveniste, P., Zhu, W., & Cohen, A. (1995). Interference with thymocyte differentiation by an inhibitor of S-adenosylhomocysteine hydrolase. *Journal of Immunology (Baltimore, Md. : 1950)*, *155*(2), 536–544. http://www.ncbi.nlm.nih.gov/pubmed/7608534

Birger, A., Ben-Dor, I., Ottolenghi, M., Turetsky, T., Gil, Y., Sweetat, S., Perez, L., Belzer, V., Casden, N., Steiner, D., Izrael, M., Galun, E., Feldman, E., Behar, O., & Reubinoff, B. (2019). Human iPSC-derived astrocytes from ALS patients with mutated C9ORF72 show increased oxidative stress and neurotoxicity. *EBioMedicine*, *50*, 274–289. https://doi.org/10.1016/J.EBIOM.2019.11.026

Bjornevik, K., Zhang, Z., O'Reilly, É. J., Berry, J. D., Clish, C. B., Deik, A., Jeanfavre, S., Kato, I., Kelly, R. S., Kolonel, L. N., Liang, L., Marchand, L. Le, McCullough, M. L., Paganoni, S., Pierce, K. A., Schwarzschild, M. A., Shadyab, A. H., Wactawski-Wende, J., Wang, D. D., … Ascherio, A. (2019). Prediagnostic plasma metabolomics and the risk of amyotrophic lateral sclerosis. *Neurology*, *92*(18). https://doi.org/10.1212/WNL.0000000000007401

Blasco, H., Garcon, G., Patin, F., Veyrat-Durebex, C., Boyer, J., Devos, D., Vourc'h, P., Andres, C. R., & Corcia, P. (2017). Panel of Oxidative Stress and Inflammatory Biomarkers in ALS: A Pilot Study. *Canadian Journal of Neurological Sciences*, *44*(1), 90–95. https://doi.org/10.1017/CJN.2016.284

Blum, D., Galas, M. C., Pintor, A., Brouillet, E., Ledent, C., Muller, C. E., Bantubungi, K., Galluzzo, M., Gall, D., Cuvelier, L., Rolland, A. S., Popoli, P., & Schiffmann, S. N. (2003). A Dual Role of Adenosine A2A Receptors in 3-Nitropropionic Acid-Induced Striatal Lesions: Implications for the Neuroprotective Potential of A2A Antagonists. *Journal of Neuroscience*, *23*(12), 5361–5369. https://doi.org/10.1523/JNEUROSCI.23-12-05361.2003

Bochner, B. R., Siri, M., Huang, R. H., Noble, S., Lei, X. H., Clemons, P. A., & Wagner, B. K.

(2011). Assay of the multiple energy-producing pathways of mammalian cells. *PLoS ONE*, *6*(3). https://doi.org/10.1371/journal.pone.0018147

Boddy, S., Islam, M., Moll, T., Kurz, J., Burrows, D., Mcgown, A., Bhargava, A., Julian, T. H., Harvey, C., Marshall, J. N. G., Hall, B. P. C., Allen, S. P., Kenna, K. P., Sanderson, E., Zhang, S., Ramesh, T., Snyder, M. P., Shaw, P. J., Mcdermott, C., & Cooper-Knock, J. (2022). Unbiased metabolome screen leads to personalized medicine strategy for amyotrophic lateral sclerosis. *Brain Communications*, *4*(2). https://doi.org/10.1093/BRAINCOMMS/FCAC069

Boer, P., & Sperling, O. (1995). Role of cellular ribose-5-phosphate content in the regulation of 5-phosphoribosyl-1-pyrophosphate and de novo purine synthesis in a human hepatoma cell line. *Metabolism*, *44*(11), 1469–1474. https://doi.org/10.1016/0026-0495(95)90148-5

Boeynaems, S., Bogaert, E., Kovacs, D., Konijnenberg, A., Timmerman, E., Volkov, A., Guharoy, M., De Decker, M., Jaspers, T., Ryan, V. H., Janke, A. M., Baatsen, P., Vercruysse, T., Kolaitis, R. M., Daelemans, D., Taylor, J. P., Kedersha, N., Anderson, P., Impens, F., … Van Den Bosch, L. (2017). Phase Separation of C9orf72 Dipeptide Repeats Perturbs Stress Granule Dynamics. *Molecular Cell*, *65*(6), 1044-1055.e5. https://doi.org/10.1016/J.MOLCEL.2017.02.013

Bogdanov, M., Brown, R. H., Matson, W., Smart, R., Hayden, D., O'Donnell, H., Flint Beal, M., & Cudkowicz, M. (2000). Increased oxidative damage to DNA in ALS patients. *Free Radical Biology and Medicine*, *29*(7), 652–658. https://doi.org/10.1016/S0891-5849(00)00349-X

Boison, D. (2011). Modulators of Nucleoside Metabolism in the Therapy of Brain Diseases. *Current Topics in Medicinal Chemistry*, *11*(8), 1068. https://doi.org/10.2174/156802611795347609

Boison, D., & Aronica, E. (2015). Comorbidities in Neurology: Is adenosine the common link? *Neuropharmacology*, *97*, 18–34. https://doi.org/10.1016/J.NEUROPHARM.2015.04.031

Bottini, N., De Luca, D., Saccucci, P., Fiumara, A., Elia, M., Porfirio, M., Lucarelli, P., & Curatolo, P. (2001). Autism: evidence of association with adenosine deaminase genetic polymorphism. *Neurogenetics*, *3*(2), 111–113. https://doi.org/10.1007/S100480000104

Boulton, T., Yancopoulos, G., Gregory, J., Slaughter, C., Moomaw, C., Hsu, J., & Cobb, M. (1990). An insulin-stimulated protein kinase similar to yeast kinases involved in cell

cycle control. *Science (New York, N.Y.)*, *249*(4964), 64–67. https://doi.org/10.1126/SCIENCE.2164259

Bouteloup, C., Desport, J. C., Clavelou, P., Guy, N., Derumeaux-Burel, H., Ferrier, A., & Couratier, P. (2009). Hypermetabolism in ALS patients: An early and persistent phenomenon. *Journal of Neurology*, *256*(8), 1236–1242. https://doi.org/10.1007/s00415-009-5100-z

Bowling, A. C., Schulz, J. B., Brown, R. H., & Beal, M. F. (1993). Superoxide Dismutase Activity, Oxidative Damage, and Mitochondrial Energy Metabolism in Familial and Sporadic Amyotrophic Lateral Sclerosis. *Journal of Neurochemistry*, *61*(6), 2322–2325. https://doi.org/10.1111/j.1471-4159.1993.tb07478.x

Bozič, J., Motaln, H., Janez, A. P., Markič, L., Tripathi, P., Yamoah, A., Aronica, E., Lee, Y. B., Heilig, R., Fischer, R., Thompson, A. J., Goswami, A., & Rogelj, B. (2022). Interactome screening of C9orf72 dipeptide repeats reveals VCP sequestration and functional impairment by polyGA. *Brain*, *145*(2), 684–699. https://doi.org/10.1093/BRAIN/AWAB300

Brambilla, R., Cottini, L., Fumagalli, M., Ceruti, S., & Abbracchio, M. P. (2003). Blockade of A2A adenosine receptors prevents basic fibroblast growth factor-induced reactive astrogliosis in rat striatal primary astrocytes. *Glia*, *43*(2), 190–194. https://doi.org/10.1002/GLIA.10243

Brandebura, A. N., Paumier, A., Onur, T. S., & Allen, N. J. (2022). Astrocyte contribution to dysfunction, risk and progression in neurodegenerative disorders. *Nature Reviews Neuroscience*, *24*(1), 23–39. https://doi.org/10.1038/s41583-022-00641-1

Brangwynne, C. P., Tompa, P., & Pappu, R. V. (2015). Polymer physics of intracellular phase transitions. *Nature Physics* , *11*(11), 899–904. https://doi.org/10.1038/nphys3532

Brasseur, L., Coens, A., Waeytens, J., Melki, R., & Bousset, L. (2020). Dipeptide repeat derived from C9orf72 hexanucleotide expansions forms amyloids or natively unfolded structures in vitro. *Biochemical and Biophysical Research Communications*, *526*(2), 410–416. https://doi.org/10.1016/J.BBRC.2020.03.108

Brown, C. A., Lally, C., Kupelian, V., & Dana Flanders, W. (2021). Estimated Prevalence and Incidence of Amyotrophic Lateral Sclerosis and SOD1 and C9orf72 Genetic Variants. *Neuroepidemiology*, *55*(5), 342–353. https://doi.org/10.1159/000516752

Brown, R. H., & Al-Chalabi, A. (2017). Amyotrophic Lateral Sclerosis. *The New England Journal of Medicine*, *377*(2), 162–172. https://doi.org/10.1056/NEJMRA1603471

Buchanan, J., & Hartman, S. (1959). Synthesis of the Purines. *Advances in Enzymology and Related Areas*, 199. https://books.google.com/books?hl=en&lr=&id=i_P1W_Cvi1QC&oi=fnd&pg=PA199&ots=AB_ScWLAIj&sig=wFtTEFsLkrEzipJCHNjyO4FXrNs

Burberry, A., Suzuki, N., Wang, J. Y., Moccia, R., Mordes, D. A., Stewart, M. H., Suzuki-Uematsu, S., Ghosh, S., Singh, A., Merkle, F. T., Koszka, K., Li, Q. Z., Zon, L., Rossi, D. J., Trowbridge, J. J., Notarangelo, L. D., & Eggan, K. (2016). Loss-of-function mutations in the C9ORF72 mouse ortholog cause fatal autoimmune disease. *Science Translational Medicine*, *8*(347). https://doi.org/10.1126/SCITRANSLMED.AAF6038/SUPPL_FILE/8-347RA93_VIDEOS_1_TO_3.ZIP

Camici, M., Allegrini, S., & Tozzi, M. G. (2018). Interplay between adenylate metabolizing enzymes and AMP-activated protein kinase. *The FEBS Journal*, *285*(18), 3337–3352. https://doi.org/10.1111/FEBS.14508

Cancino, G. I., Miller, F. D., & Kaplan, D. R. (2013). p73 haploinsufficiency causes tau hyperphosphorylation and tau kinase dysregulation in mouse models of aging and Alzheimer's disease. *Neurobiology of Aging*, *34*(2), 387–399. https://doi.org/10.1016/J.NEUROBIOLAGING.2012.04.010

Cantoni, G. (1953). S-Adenosylmethionine; a new intermediate formed enzymatically from L-methionine and adenosinetriphosphate. *The Journal of Biological Chemistry*, *204*(1), 403–416. https://pubmed.ncbi.nlm.nih.gov/13084611/

Carrì, M. T., Valle, C., Bozzo, F., & Cozzolino, M. (2015). Oxidative stress and mitochondrial damage: Importance in non-SOD1 ALS. In *Frontiers in Cellular Neuroscience* (Vol. 9, Issue FEB). Frontiers Research Foundation. https://doi.org/10.3389/fncel.2015.00041

Carson, D. A., Kaye, J., Matsumoto, S., Seegmiller, J. E., & Thompson, L. (1979). Biochemical basis for the enhanced toxicity of deoxyribonucleosides toward malignant human T cell lines. *Proceedings of the National Academy of Sciences of the United States of America*, *76*(5), 2430. https://doi.org/10.1073/PNAS.76.5.2430

Castillo, C. A., Albasanz, J. L., León, D., Jordán, J., Pallàs, M., Camins, A., & Martín, M. (2009). Age-related expression of adenosine receptors in brain from the senescence-accelerated mouse. *Experimental Gerontology*, *44*(6–7), 453–461. https://doi.org/10.1016/J.EXGER.2009.04.006

Chang, Y. J., Jeng, U. S., Chiang, Y. L., Hwang, I. S., & Chen, Y. R. (2016). The glycine-

alanine dipeptide repeat from C9 or f72 hexanucleotide expansions forms toxic amyloids possessing cell-to-cell transmission properties. *Journal of Biological Chemistry*, *291*(10), 4903–4911. https://doi.org/10.1074/jbc.M115.694273

Chaytow, H., Carroll, E., Gordon, D., Huang, Y. T., Van Der Hoorn, D., Smith, H. L., Becker, T., Becker, C. G., Faller, K. M. E., Talbot, K., & Gillingwater, T. H. (2022). Targeting phosphoglycerate kinase 1 with terazosin improves motor neuron phenotypes in multiple models of amyotrophic lateral sclerosis. *EBioMedicine*, *83*.

Chen, X., Burdett, T., Desjardins, C., Logan, R., Cipriani, S., Xu, Y., & Schwarzschild, M. (2013). Disrupted and transgenic urate oxidase alter urate and dopaminergic neurodegeneration. *Proceedings of the National Academy of Sciences of the United States of America*, *110*(1), 300–305. https://doi.org/10.1073/PNAS.1217296110

Chen, X., Wu, G., & Schwarzschild, M. (2012). Urate in Parkinson's disease: more than a biomarker? *Current Neurology and Neuroscience Reports*, *12*(4), 367–375. https://doi.org/10.1007/S11910-012-0282-7

Chew, J., Cook, C., Gendron, T. F., Jansen-West, K., Del Rosso, G., Daughrity, L. M., Castanedes-Casey, M., Kurti, A., Stankowski, J. N., Disney, M. D., Rothstein, J. D., Dickson, D. W., Fryer, J. D., Zhang, Y. J., & Petrucelli, L. (2019). Aberrant deposition of stress granule-resident proteins linked to C9orf72-associated TDP-43 proteinopathy. *Molecular Neurodegeneration*, *14*(1), 1–15. https://doi.org/10.1186/S13024-019-0310-Z/FIGURES/7

Chew, J., Gendron, T. F., Prudencio, M., Sasaguri, H., Zhang, Y. J., Castanedes-Casey, M., Lee, C. W., Jansen-West, K., Kurti, A., Murray, M. E., Bieniek, K. F., Bauer, P. O., Whitelaw, E. C., Rousseau, L., Stankowski, J. N., Stetler, C., Daughrity, L. M., Perkerson, E. A., Desaro, P., … Petrucelli, L. (2015). C9ORF72 repeat expansions in mice cause TDP-43 pathology, neuronal loss, and behavioral deficits. *Science*, *348*(6239), 1151–1154. https://doi.org/10.1126/SCIENCE.AAA9344/SUPPL_FILE/PAPV3.PDF

Chiba, S., Matsumoto, H., Saitoh, M., Kasahara, M., Matsuya, M., & Kashiwagi, M. (1995). A correlation study between serum adenosine deaminase activities and peripheral lymphocyte subsets in Parkinson's disease. *Journal of the Neurological Sciences*, *132*(2), 170–173. https://doi.org/10.1016/0022-510X(95)00136-P

Chitiprolu, M., Jagow, C., Tremblay, V., Bondy-Chorney, E., Paris, G., Savard, A., Palidwor, G., Barry, F. A., Zinman, L., Keith, J., Rogaeva, E., Robertson, J., Lavallée-Adam, M., Woulfe, J., Couture, J. F., Côté, J., & Gibbings, D. (2018). A complex of C9ORF72 and

p62 uses arginine methylation to eliminate stress granules by autophagy. *Nature Communications*, *9*(1), 1–18. https://doi.org/10.1038/s41467-018-05273-7

Choi, S. Y., Lopez-Gonzalez, R., Krishnan, G., Phillips, H. L., Li, A. N., Seeley, W. W., Yao, W. D., Almeida, S., & Gao, F. B. (2019a). C9ORF72-ALS/FTD-associated poly(GR) binds Atp5a1 and compromises mitochondrial function in vivo. *Nature Neuroscience*, *22*(6), 851–862. https://doi.org/10.1038/s41593-019-0397-0

Choi, S. Y., Lopez-Gonzalez, R., Krishnan, G., Phillips, H. L., Li, A. N., Seeley, W. W., Yao, W. D., Almeida, S., & Gao, F. B. (2019b). C9ORF72-ALS/FTD-associated poly(GR) binds Atp5a1 and compromises mitochondrial function in vivo. *Nature Neuroscience 2019 22:6*, *22*(6), 851–862. https://doi.org/10.1038/s41593-019-0397-0

Cipriani, S., Desjardins, C. A., Burdett, T. C., Xu, Y., Xu, K., & Schwarzschild, M. A. (2012). Protection of dopaminergic cells by urate requires its accumulation in astrocytes. *Journal of Neurochemistry*, *123*(1), 172–181. https://doi.org/10.1111/J.1471-4159.2012.07820.X

Ciuffi, A. (2008). Mechanisms Governing Lentivirus Integration Site Selection. *Current Gene Therapy*, *8*(6), 419–429. https://doi.org/10.2174/156652308786848021

Ciura, S., Lattante, S., Le Ber, I., Latouche, M., Tostivint, H., Brice, A., & Kabashi, E. (2013). Loss of function of C9orf72 causes motor deficits in a zebrafish model of amyotrophic lateral sclerosis. *Annals of Neurology*, *74*(2), 180–187. https://doi.org/10.1002/ANA.23946

Cohen, A., Hirschhorn, R., Horowitz, S. D., Rubinstein, A., Polmar, S. H., Hong, R., & Martin, D. W. (1978). Deoxyadenosine triphosphate as a potentially toxic metabolite in adenosine deaminase deficiency. *Proceedings of the National Academy of Sciences*, *75*(1), 472–476. https://doi.org/10.1073/PNAS.75.1.472

Conlon, E. G., Lu, L., Sharma, A., Yamazaki, T., Tang, T., Shneider, N. A., & Manley, J. L. (2016). The C9ORF72 GGGGCC expansion forms RNA G-quadruplex inclusions and sequesters hnRNP H to disrupt splicing in ALS brains. *ELife*, *5*. https://doi.org/10.7554/ELIFE.17820

Conway, E. J., & Cooke, R. (1938). Blood ammonia and the deaminases of adenosine and adenylic acid [9]. In *Nature* (Vol. 142, Issue 3598, p. 720). Nature Publishing Group. https://doi.org/10.1038/142720a0

Cooper-Knock, J., Hewitt, C., Highley, J. R., Brockington, A., Milano, A., Man, S., Martindale, J., Hartley, J., Walsh, T., Gelsthorpe, C., Baxter, L., Forster, G., Fox, M., Bury, J., Mok,

K., McDermott, C. J., Traynor, B. J., Kirby, J., Wharton, S. B., … Shaw, P. J. (2012). Clinico-pathological features in amyotrophic lateral sclerosis with expansions in C9ORF72. *Brain*, *135*(3), 751–764. https://doi.org/10.1093/BRAIN/AWR365

Cooper-Knock, J., Higginbottom, A., Stopford, M. J., Highley, J. R., Ince, P. G., Wharton, S. B., Pickering-Brown, S., Kirby, J., Hautbergue, G. M., & Shaw, P. J. (2015). Antisense RNA foci in the motor neurons of C9ORF72-ALS patients are associated with TDP-43 proteinopathy. *Acta Neuropathologica*, *130*(1), 63–75. https://doi.org/10.1007/S00401-015-1429-9/FIGURES/5

Cooper-Knock, J., Walsh, M. J., Higginbottom, A., Highley, J. R., Dickman, M. J., Edbauer, D., Ince, P. G., Wharton, S. B., Wilson, S. A., Kirby, J., Hautbergue, G. M., & Shaw, P. J. (2014). Sequestration of multiple RNA recognition motif-containing proteins by C9orf72 repeat expansions. *Brain*, *137*(7), 2040–2051. https://doi.org/10.1093/BRAIN/AWU120

Coppedè, F., Stoccoro, A., Mosca, L., Gallo, R., Tarlarini, C., Lunetta, C., Marocchi, A., Migliore, L., & Penco, S. (2017). Increase in DNA methylation in patients with amyotrophic lateral sclerosis carriers of not fully penetrant SOD1 mutations. *Amyotrophic Lateral Sclerosis and Frontotemporal Dementia*, *19*(1–2), 93–101. https://doi.org/10.1080/21678421.2017.1367401

Corrionero, A., & Horvitz, H. R. (2018). A C9orf72 ALS/FTD Ortholog Acts in Endolysosomal Degradation and Lysosomal Homeostasis. *Current Biology*, *28*(10), 1522-1535.e5. https://doi.org/10.1016/J.CUB.2018.03.063

Corte, E. D., & Stirpe, F. (1972). The regulation of rat liver xanthine oxidase. Involvement of thiol groups in the conversion of the enzyme activity from dehydrogenase (type D) into oxidase (type O) and purification of the enzyme. *Biochemical Journal*, *126*(3), 739–745. https://doi.org/10.1042/BJ1260739

Costenla, A. R., Diógenes, M. J., Canas, P. M., Rodrigues, R. J., Nogueira, C., Maroco, J., Agostinho, P. M., Ribeiro, J. A., Cunha, R. A., & Mendonça, A. de. (2011). Enhanced role of adenosine A2A receptors in the modulation of LTP in the rat hippocampus upon ageing. *European Journal of Neuroscience*, *34*(1), 12–21. https://doi.org/10.1111/J.1460-9568.2011.07719.X

D'Ovidio, F., d'Errico, A., Carnà, P., Calvo, A., Costa, G., & Chiò, A. (2018). The role of pre-morbid diabetes on developing amyotrophic lateral sclerosis. *European Journal of Neurology*, *25*(1), 164–170. https://doi.org/10.1111/ENE.13465

Daddona, P., & Kelley, W. (1977). Human adenosine deaminase. Purification and subunit structure. *The Journal of Biological Chemistry*, *252*(1), 110–115. https://pubmed.ncbi.nlm.nih.gov/13062/

Dafinca, R., Barbagallo, P., Farrimond, L., Candalija, A., Scaber, J., Ababneh, N. A., Sathyaprakash, C., Vowles, J., Cowley, S. A., & Talbot, K. (2020). Impairment of Mitochondrial Calcium Buffering Links Mutations in C9ORF72 and TARDBP in iPS-Derived Motor Neurons from Patients with ALS/FTD. *Stem Cell Reports*, *14*(5), 892–908. https://doi.org/10.1016/J.STEMCR.2020.03.023

Dafinca, R., Scaber, J., Ababneh, N., Lalic, T., Weir, G., Christian, H., Vowles, J., Douglas, A. G. L., Fletcher-Jones, A., Browne, C., Nakanishi, M., Turner, M. R., Wade-Martins, R., Cowley, S. A., & Talbot, K. (2016). C9orf72 Hexanucleotide Expansions Are Associated with Altered Endoplasmic Reticulum Calcium Homeostasis and Stress Granule Formation in Induced Pluripotent Stem Cell-Derived Neurons from Patients with Amyotrophic Lateral Sclerosis and Frontotemporal Dementia. *Stem Cells*, *34*(8), 2063–2078. https://doi.org/10.1002/STEM.2388

Dai, S. S., Zhou, Y. G., Li, W., An, J. H., Li, P., Yang, N., Chen, X. Y., Xiong, R. P., Liu, P., Zhao, Y., Shen, H. Y., Zhu, P. F., & Chen, J. F. (2010). Local Glutamate Level Dictates Adenosine A2A Receptor Regulation of Neuroinflammation and Traumatic Brain Injury. *Journal of Neuroscience*, *30*(16), 5802–5810. https://doi.org/10.1523/JNEUROSCI.0268-10.2010

Dalakas, M. C., Hatazawa, J., Brooks, R. A., & Di Chiro, G. (1987). Lowered cerebral glucose utilization in amyotrophic lateral sclerosis. *Annals of Neurology*, *22*(5), 580–586. https://doi.org/10.1002/ana.410220504

de Jong, S., Huisman, M., Sutedja, N., van der Kooi, A., de Visser, M., Schelhaas, J., van der Schouw, Y., Veldink, J., & van den Berg, L. (2012). Endogenous female reproductive hormones and the risk of amyotrophic lateral sclerosis. *Journal of Neurology 2012 260:2*, *260*(2), 507–512. https://doi.org/10.1007/S00415-012-6665-5

DeJesus-Hernandez, M., Finch, N. C. A., Wang, X., Gendron, T. F., Bieniek, K. F., Heckman, M. G., Vasilevich, A., Murray, M. E., Rousseau, L., Weesner, R., Lucido, A., Parsons, M., Chew, J., Josephs, K. A., Parisi, J. E., Knopman, D. S., Petersen, R. C., Boeve, B. F., Graff-Radford, N. R., … Rademakers, R. (2017). In-depth clinico-pathological examination of RNA foci in a large cohort of C9ORF72 expansion carriers. *Acta Neuropathologica*, *134*(2), 255–269. https://doi.org/10.1007/S00401-017-1725-7/FIGURES/7

DeJesus-Hernandez, M., Mackenzie, I. R., Boeve, B. F., Boxer, A. L., Baker, M., Rutherford, N. J., Nicholson, A. M., Finch, N. C. A., Flynn, H., Adamson, J., Kouri, N., Wojtas, A., Sengdy, P., Hsiung, G. Y. R., Karydas, A., Seeley, W. W., Josephs, K. A., Coppola, G., Geschwind, D. H., … Rademakers, R. (2011). Expanded GGGGCC Hexanucleotide Repeat in Noncoding Region of C9ORF72 Causes Chromosome 9p-Linked FTD and ALS. *Neuron*, *72*(2), 245–256. https://doi.org/10.1016/j.neuron.2011.09.011

Dérijard, B., Hibi, M., Wu, I. H., Barrett, T., Su, B., Deng, T., Karin, M., & Davis, R. J. (1994). JNK1: A protein kinase stimulated by UV light and Ha-Ras that binds and phosphorylates the c-Jun activation domain. *Cell*, *76*(6), 1025–1037. https://doi.org/10.1016/0092-8674(94)90380-8

Desport, J. C., Preux, P. M., Truong, T. C., Vallat, J. M., Sautereau, D., & Couratier, P. (1999). Nutritional status is a prognostic factor for survival in ALS patients. *Neurology*, *53*(5), 1059–1059. https://doi.org/10.1212/WNL.53.5.1059

Desport, J. C., Torny, F., Lacoste, M., Preux, P. M., & Couratier, P. (2005). Hypermetabolism in ALS: correlations with clinical and paraclinical parameters. *Neuro-Degenerative Diseases*, *2*(3–4), 202–207. https://doi.org/10.1159/000089626

Dettori, I., Gaviano, L., Ugolini, F., Lana, D., Bulli, I., Magni, G., Rossi, F., Giovannini, M. G., & Pedata, F. (2021). Protective Effect of Adenosine A2B Receptor Agonist, BAY60-6583, Against Transient Focal Brain Ischemia in Rat. *Frontiers in Pharmacology*, *0*, 1639. https://doi.org/10.3389/FPHAR.2020.588757

Dixon, A. K., Gubitz, A. K., Sirinathsinghji, D. J. S., Richardson, P. J., & Freeman, T. C. (1996). Tissue distribution of adenosine receptor mRNAs in the rat. *British Journal of Pharmacology*, *118*(6), 1461–1468. https://doi.org/10.1111/J.1476-5381.1996.TB15561.X

Dodge, J. C., Treleaven, C. M., Fidler, J. A., Tamsett, T. J., Bao, C., Searles, M., Taksir, T. V., Misra, K., Sidman, R. L., Cheng, S. H., & Shihabuddin, L. S. (2013). Metabolic signatures of amyotrophic lateral sclerosis reveal insights into disease pathogenesis. *Proceedings of the National Academy of Sciences of the United States of America*, *110*(26), 10812–10817. https://doi.org/10.1073/PNAS.1308421110/SUPPL_FILE/PNAS.201308421SI.PDF

Dolezal, T., Dolezelova, E., Zurovec, M., & Bryant, P. J. (2005). A Role for Adenosine Deaminase in Drosophila Larval Development. *PLoS Biology*, *3*(7), e201. https://doi.org/10.1371/journal.pbio.0030201

Dolphin, A. C., Forda, S. R., & Scott, R. H. (1986). Calcium-dependent currents in cultured rat dorsal root ganglion neurones are inhibited by an adenosine analogue. *The Journal of Physiology*, *373*(1), 47. https://doi.org/10.1113/JPHYSIOL.1986.SP016034

Dong, R. P., Kameoka, J., Hegen, M., Tanaka, T., Xu, Y., Schlossman, S. F., & Morimoto, C. (1996). Characterization of adenosine deaminase binding to human CD26 on T cells and its biologic role in immune response. *The Journal of Immunology*, *156*(4).

Donnelly, C. J., Zhang, P. W., Pham, J. T., Heusler, A. R., Mistry, N. A., Vidensky, S., Daley, E. L., Poth, E. M., Hoover, B., Fines, D. M., Maragakis, N., Tienari, P. J., Petrucelli, L., Traynor, B. J., Wang, J., Rigo, F., Bennett, C. F., Blackshaw, S., Sattler, R., & Rothstein, J. D. (2013). RNA Toxicity from the ALS/FTD C9ORF72 Expansion Is Mitigated by Antisense Intervention. *Neuron*, *80*(2), 415–428. https://doi.org/10.1016/J.NEURON.2013.10.015

Dunwiddie, T. V., & Masino, S. A. (2001). The Role and Regulation of Adenosine in the Central Nervous System. *Annual Review of Neuroscience*, *24*(1), 31–55. https://doi.org/10.1146/annurev.neuro.24.1.31

Dupuis, L., Corcia, P., Fergani, A., Gonzalez De Aguilar, J. L., Bonnefont-Rousselot, D., Bittar, R., Seilhean, D., Hauw, J. J., Lacomblez, L., Loeffler, J. P., & Meininger, V. (2008). Dyslipidemia is a protective factor in amyotrophic lateral sclerosis symbol. *Neurology*, *70*(13), 1004–1009. https://doi.org/10.1212/01.wnl.0000285080.70324.27

Dupuis, L., Pradat, P. F., Ludolph, A. C., & Loeffler, J. P. (2011). Energy metabolism in amyotrophic lateral sclerosis. In *The Lancet Neurology* (Vol. 10, Issue 1, pp. 75–82). Lancet Publishing Group. https://doi.org/10.1016/S1474-4422(10)70224-6

Dusing, M., & Wiginton, D. (1994). Sp1 is essential for both enhancer-mediated and basal activation of the TATA-less human adenosine deaminase promoter. *Nucleic Acids Research*, *22*(4), 669–677. https://doi.org/10.1093/NAR/22.4.669

Edbauer, D., & Haass, C. (2016). An amyloid-like cascade hypothesis for C9orf72 ALS/FTD. *Current Opinion in Neurobiology*, *36*, 99–106. https://doi.org/10.1016/J.CONB.2015.10.009

Eguchi, R., Kitano, T., & Otsuguro, K. (2020). Fibroblast growth factor 2 upregulates ecto-5′-nucleotidase and adenosine deaminase via MAPK pathways in cultured rat spinal cord astrocytes. *Purinergic Signalling*, *16*(4), 519–527. https://doi.org/10.1007/s11302-020-09731-0

Enquist, L. W., & Card, J. P. (2003). Recent advances in the use of neurotropic viruses for

circuit analysis. *Current Opinion in Neurobiology*, *13*(5), 603–606. https://doi.org/10.1016/J.CONB.2003.08.001

Epstein, F. H., Lipton, S. A., & Rosenberg, P. A. (1994). Excitatory amino acids as a final common pathway for neurologic disorders. In *New England Journal of Medicine* (Vol. 330, Issue 9, pp. 613–622). N Engl J Med. https://doi.org/10.1056/NEJM199403033300907

Eroglu, C., & Barres, B. A. (2010). Regulation of synaptic connectivity by glia. In *Nature* (Vol. 468, Issue 7321, pp. 223–231). Nature Publishing Group. https://doi.org/10.1038/nature09612

Esanov, R., Cabrera, G. T., Andrade, N. S., Gendron, T. F., Brown, R. H., Benatar, M., Wahlestedt, C., Mueller, C., & Zeier, Z. (2017). A C9ORF72 BAC mouse model recapitulates key epigenetic perturbations of ALS/FTD. *Molecular Neurodegeneration*, *12*(1), 1–11. https://doi.org/10.1186/S13024-017-0185-9/FIGURES/5

Fardaei, M., Larkin, K., Brook, J. D., & Hamshere, M. G. (2001). In vivo co-localisation of MBNL protein with DMPK expanded-repeat transcripts. *Nucleic Acids Research*, *29*(13), 2766–2771. https://doi.org/10.1093/NAR/29.13.2766

Farg, M. A., Konopka, A., Soo, K. Y., Ito, D., & Atkin, J. D. (2017). The DNA damage response (DDR) is induced by the C9orf72 repeat expansion in amyotrophic lateral sclerosis. *Human Molecular Genetics*, *26*(15), 2882–2896. https://doi.org/10.1093/HMG/DDX170

Ferraiuolo, L., Higginbottom, A., Heath, P. R., Barber, S., Greenald, D., Kirby, J., & Shaw, P. J. (2011). Dysregulation of astrocyte–motoneuron cross-talk in mutant superoxide dismutase 1-related amyotrophic lateral sclerosis. *Brain*, *134*(9), 2627–2641. https://doi.org/10.1093/BRAIN/AWR193

Ferraiuolo, L., Meyer, K., Sherwood, T. W., Vick, J., Likhite, S., Frakes, A., Miranda, C. J., Braun, L., Heath, P. R., Pineda, R., Beattie, C. E., Shaw, P. J., Askwith, C. C., McTigue, D., & Kaspar, B. K. (2016). Oligodendrocytes contribute to motor neuron death in ALS via SOD1-dependent mechanism. *Proceedings of the National Academy of Sciences*, *113*(42), E6496–E6505. https://doi.org/10.1073/PNAS.1607496113

Ferrante, R. J., Browne, S. E., Shinobu, L. A., Bowling, A. C., Baik, M. J., MacGarvey, U., Kowall, N. W., Brown, R. H., & Beal, M. F. (1997). Evidence of Increased Oxidative Damage in Both Sporadic and Familial Amyotrophic Lateral Sclerosis. *Journal of Neurochemistry*, *69*(5), 2064–2074. https://doi.org/10.1046/J.1471-

4159.1997.69052064.X

Figueroa-Romero, C., Hur, J., Bender, D. E., Delaney, C. E., Cataldo, M. D., Smith, A. L., Yung, R., Ruden, D. M., Callaghan, B. C., & Feldman, E. L. (2012). Identification of Epigenetically Altered Genes in Sporadic Amyotrophic Lateral Sclerosis. *PLoS ONE*, *7*(12), 52672. https://doi.org/10.1371/JOURNAL.PONE.0052672

Fischer, D., Weyden, M. B. Van der, Snyderman, R., & Kelley, W. N. (1976). A role for adenosine deaminase in human monocyte maturation. *Journal of Clinical Investigation*, *58*(2), 399. https://doi.org/10.1172/JCI108484

Fitzmaurice, P., Shaw, I., Kleiner, H., Miller, R., Monks, T., Lau, S., Mitchell, J., & Lynch, P. (1996). Evidence for DNA damage in amyotrophic lateral sclerosis. *Muscle & Nerve*, *19*(6), 797–798. https://europepmc.org/article/med/8609941

Florian, C., Vecsey, C. G., Halassa, M. M., Haydon, P. G., & Abel, T. (2011). Astrocyte-Derived Adenosine and A1 Receptor Activity Contribute to Sleep Loss-Induced Deficits in Hippocampal Synaptic Plasticity and Memory in Mice. *The Journal of Neuroscience*, *31*(19), 6956. https://doi.org/10.1523/JNEUROSCI.5761-10.2011

Fomin, V., Richard, P., Hoque, M., Li, C., Gu, Z., Fissore-O'Leary, M., Tian, B., Prives, C., & Manley, J. L. (2018). The C9ORF72 Gene, Implicated in Amyotrophic Lateral Sclerosis and Frontotemporal Dementia, Encodes a Protein That Functions in Control of Endothelin and Glutamate Signaling . *Molecular and Cellular Biology*, *38*(22). https://doi.org/10.1128/MCB.00155-18/SUPPL_FILE/ZMB999101858SM3.AVI

Fox, I., & Kelley, W. (1978). The role of adenosine and 2'-deoxyadenosine in mammalian cells. *Annual Review of Biochemistry*, *47*, 655–686. https://doi.org/10.1146/ANNUREV.BI.47.070178.003255

Franco, R., Casadó, V., Ciruela, F., Saura, C., Mallol, J., Canela, E., & Lluis, C. (1997). Cell surface adenosine deaminase: much more than an ectoenzyme. *Progress in Neurobiology*, *52*(4), 283–294. https://doi.org/10.1016/S0301-0082(97)00013-0

Fratta, P., Mizielinska, S., Nicoll, A. J., Zloh, M., Fisher, E. M. C., Parkinson, G., & Isaacs, A. M. (2012). C9orf72 hexanucleotide repeat associated with amyotrophic lateral sclerosis and frontotemporal dementia forms RNA G-quadruplexes. *Scientific Reports* , *2*(1), 1–6. https://doi.org/10.1038/srep01016

Fredholm, B. (2007). Adenosine, an endogenous distress signal, modulates tissue damage and repair. *Cell Death and Differentiation*, *14*(7), 1315–1323. https://doi.org/10.1038/SJ.CDD.4402132

Freibaum, B. D., Lu, Y., Lopez-Gonzalez, R., Kim, N. C., Almeida, S., Lee, K. H., Badders, N., Valentine, M., Miller, B. L., Wong, P. C., Petrucelli, L., Kim, H. J., Gao, F. B., & Taylor, J. P. (2015). GGGGCC repeat expansion in C9orf72 compromises nucleocytoplasmic transport. *Nature*, *525*(7567), 129–133. https://doi.org/10.1038/nature14974

Freibaum, B. D., & Taylor, J. P. (2017). The role of dipeptide repeats in C9ORF72-related ALS-FTD. *Frontiers in Molecular Neuroscience*, *10*, 35. https://doi.org/10.3389/FNMOL.2017.00035/XML/NLM

Garcia-Segura, L. M., Azcoitia, I., & DonCarlos, L. L. (2001). Neuroprotection by estradiol. *Progress in Neurobiology*, *63*(1), 29–60. https://doi.org/10.1016/S0301-0082(00)00025-3

Garton, F. C., Benyamin, B., Zhao, Q., Liu, Z., Gratten, J., Henders, A. K., Zhang, Z., Edson, J., Furlong, S., Morgan, S., Heggie, S., Thorpe, K., Pfluger, C., Mather, K. A., Sachdev, P. S., McRae, A. F., Robinson, M. R., Shah, S., Visscher, P. M., … McCombe, P. A. (2017). Whole exome sequencing and DNA methylation analysis in a clinical amyotrophic lateral sclerosis cohort. *Molecular Genetics & Genomic Medicine*, *5*(4), 418. https://doi.org/10.1002/MGG3.302

Gaudet, A. D., & Fonken, L. K. (2018). Glial Cells Shape Pathology and Repair After Spinal Cord Injury. In *Neurotherapeutics* (Vol. 15, Issue 3, pp. 554–577). Springer New York LLC. https://doi.org/10.1007/s13311-018-0630-7

Gendron, T. F., Bieniek, K. F., Zhang, Y. J., Jansen-West, K., Ash, P. E. A., Caulfield, T., Daughrity, L., Dunmore, J. H., Castanedes-Casey, M., Chew, J., Cosio, D. M., Van Blitterswijk, M., Lee, W. C., Rademakers, R., Boylan, K. B., Dickson, D. W., & Petrucelli, L. (2013). Antisense transcripts of the expanded C9ORF72 hexanucleotide repeat form nuclear RNA foci and undergo repeat-associated non-ATG translation in c9FTD/ALS. *Acta Neuropathologica*, *126*(6), 829–844. https://doi.org/10.1007/S00401-013-1192-8/FIGURES/7

Gendron, T. F., Chew, J., Stankowski, J. N., Hayes, L. R., Zhang, Y. J., Prudencio, M., Carlomagno, Y., Daughrity, L. M., Jansen-West, K., Perkerson, E. A., O'Raw, A., Cook, C., Pregent, L., Belzil, V., Van Blitterswijk, M., Tabassian, L. J., Lee, C. W., Yue, M., Tong, J., … Petrucelli, L. (2017). Poly(GP) proteins are a useful pharmacodynamic marker for C9ORF72-associated amyotrophic lateral sclerosis. *Science Translational Medicine*, *9*(383). https://doi.org/10.1126/SCITRANSLMED.AAI7866/SUPPL_FILE/AAI7866_SM.PDF

Gerou, M., Hall, B., Woof, R., Allsop, J., Kolb, S. J., Meyer, K., Shaw, P. J., & Allen, S. P. (2021). Amyotrophic lateral sclerosis alters the metabolic aging profile in patient derived fibroblasts. *Neurobiology of Aging*, *105*, 64–77. https://doi.org/10.1016/J.NEUROBIOLAGING.2021.04.013

Giblett, E. R., Anderson, J. E., Cohen, F., Pollara, B., & Meuwissen, H. J. (1972). Adenosine-Deaminase deficiency in two patients with severely impaired cellular immunity. *The Lancet*, *300*(7786), 1067–1069. https://doi.org/10.1016/S0140-6736(72)92345-8

Gijselinck, I., Van Langenhove, T., van der Zee, J., Sleegers, K., Philtjens, S., Kleinberger, G., Janssens, J., Bettens, K., Van Cauwenberghe, C., Pereson, S., Engelborghs, S., Sieben, A., De Jonghe, P., Vandenberghe, R., Santens, P., De Bleecker, J., Maes, G., Bäumer, V., Dillen, L., … Van Broeckhoven, C. (2012). A C9orf72 promoter repeat expansion in a Flanders-Belgian cohort with disorders of the frontotemporal lobar degeneration-amyotrophic lateral sclerosis spectrum: a gene identification study. *The Lancet Neurology*, *11*(1), 54–65. https://doi.org/10.1016/S1474-4422(11)70261-7

Gijselinck, I., Van Mossevelde, S., Van Der Zee, J., Sieben, A., Engelborghs, S., De Bleecker, J., Ivanoiu, A., Deryck, O., Edbauer, D., Zhang, M., Heeman, B., Bäumer, V., Van Den Broeck, M., Mattheijssens, M., Peeters, K., Rogaeva, E., De Jonghe, P., Cras, P., Martin, J. J., … Van Broeckhoven, C. (2015). The C9orf72 repeat size correlates with onset age of disease, DNA methylation and transcriptional downregulation of the promoter. *Molecular Psychiatry 2016 21:8*, *21*(8), 1112–1124. https://doi.org/10.1038/mp.2015.159

Gomez-Deza, J., Lee, Y. B., Troakes, C., Nolan, M., Al-Sarraj, S., Gallo, J. M., & Shaw, C. E. (2015). Dipeptide repeat protein inclusions are rare in the spinal cord and almost absent from motor neurons in C9ORF72 mutant amyotrophic lateral sclerosis and are unlikely to cause their degeneration. *Acta Neuropathologica Communications*, *3*(1), 38. https://doi.org/10.1186/S40478-015-0218-Y/FIGURES/2

Gomez-Suaga, P., Mórotz, G. M., Markovinovic, A., Martín-Guerrero, S. M., Preza, E., Arias, N., Mayl, K., Aabdien, A., Gesheva, V., Nishimura, A., Annibali, A., Lee, Y., Mitchell, J. C., Wray, S., Shaw, C., Noble, W., & Miller, C. C. J. (2022). Disruption of ER-mitochondria tethering and signalling in C9orf72-associated amyotrophic lateral sclerosis and frontotemporal dementia. *Aging Cell*, *21*(2), e13549. https://doi.org/10.1111/ACEL.13549

Goyal, N. A., Berry, J. D., Windebank, A., Staff, N. P., Maragakis, N. J., van den Berg, L. H.,

Genge, A., Miller, R., Baloh, R. H., Kern, R., Gothelf, Y., Lebovits, C., & Cudkowicz, M. (2020). Addressing heterogeneity in amyotrophic lateral sclerosis CLINICAL TRIALS. *Muscle & Nerve*, *62*(2), 156. https://doi.org/10.1002/MUS.26801

Granger, D. N. ., Hollwarth, M. E. ., & Parks, D. A. (1986). Ischemia-reperfusion injury: role of oxygen-derived free radicals - PubMed. *Acta Physiologica Scandinavica*, *548*, 47–63. https://pubmed.ncbi.nlm.nih.gov/3529822/

Greenberg, R., & Jaenicke, L. (1957). On the activation of the one-carbon unit for the biosynthesis of purine nucleotides. *The Chemistry and Biology of Purines*, 204. https://books.google.com/books?hl=en&lr=&id=FqL8dK25V-0C&oi=fnd&pg=PA204&ots=TnQ_Bxz6RO&sig=Pu9xlpfyAPWOpb43VkWh2SJAYF8

Grosskreutz, J., Van Den Bosch, L., & Keller, B. U. (2010). Calcium dysregulation in amyotrophic lateral sclerosis. In *Cell Calcium* (Vol. 47, Issue 2, pp. 165–174). Elsevier Ltd. https://doi.org/10.1016/j.ceca.2009.12.002

Haeusler, A. R., Donnelly, C. J., Periz, G., Simko, E. A. J., Shaw, P. G., Kim, M. S., Maragakis, N. J., Troncoso, J. C., Pandey, A., Sattler, R., Rothstein, J. D., & Wang, J. (2014). C9orf72 nucleotide repeat structures initiate molecular cascades of disease. *Nature*, *507*(7491), 195–200. https://doi.org/10.1038/nature13124

Haidet-Phillips, A. M., Hester, M. E., Miranda, C. J., Meyer, K., Braun, L., Frakes, A., Song, S., Likhite, S., Murtha, M. J., Foust, K. D., Rao, M., Eagle, A., Kammesheidt, A., Christensen, A., Mendell, J. R., Burghes, A. H. M., & Kaspar, B. K. (2011). Astrocytes from familial and sporadic ALS patients are toxic to motor neurons. *Nature Biotechnology* , *29*(9), 824–828. https://doi.org/10.1038/nbt.1957

Hall, B., George, J. G., & Allen, S. P. (2022). Adenosine deaminase, not immune to a mechanistic rethink in central nervous system disorders? *Histology and Histopathology*, *37*(3), 189–212. https://doi.org/10.14670/HH-18-404

Hamada, Y., Araki, N., Koh, N., Nakamura, J., Horiuchi, S., & Hotta, N. (1996). Rapid Formation of Advanced Glycation End Products by Intermediate Metabolites of Glycolytic Pathway and Polyol Pathway. *Biochemical and Biophysical Research Communications*, *228*(2), 539–543. https://doi.org/10.1006/BBRC.1996.1695

Hamzeiy, H., Savaş, D., Tunca, C., Şen, N. E., Gündoğdu Eken, A., Şahbaz, I., Calini, D., Tiloca, C., Ticozzi, N., Ratti, A., Silani, V., & Başak, A. N. (2018). Elevated Global DNA Methylation Is Not Exclusive to Amyotrophic Lateral Sclerosis and Is Also Observed in Spinocerebellar Ataxia Types 1 and 2. *Neurodegenerative Diseases*, *18*(1), 38–48.

https://doi.org/10.1159/000486201

Han, J., Lee, J.-D., Bibbs, L., & Ulevitch, R. J. (1994). A MAP Kinase Targeted by Endotoxin and Hyperosmolarity in Mammalian Cells. *Sci*, *265*(5173), 808–811. https://doi.org/10.1126/SCIENCE.7914033

Hao, Z., Liu, L., Tao, Z., Wang, R., Ren, H., Sun, H., Lin, Z., Zhang, Z., Mu, C., Zhou, J., & Wang, G. (2019). Motor dysfunction and neurodegeneration in a C9orf72 mouse line expressing poly-PR. *Nature Communications* , *10*(1), 1–11. https://doi.org/10.1038/s41467-019-10956-w

Hartman, S. C., & Buchanan, J. M. (1959). Nucleic acids, purines, pyrimidines (nucleotide synthesis). *Annual Review of Biochemistry*, *28*, 365–410. https://doi.org/10.1146/ANNUREV.BI.28.070159.002053

Hautbergue, G. M., Castelli, L. M., Ferraiuolo, L., Sanchez-Martinez, A., Cooper-Knock, J., Higginbottom, A., Lin, Y. H., Bauer, C. S., Dodd, J. E., Myszczynska, M. A., Alam, S. M., Garneret, P., Chandran, J. S., Karyka, E., Stopford, M. J., Smith, E. F., Kirby, J., Meyer, K., Kaspar, B. K., … Shaw, P. J. (2017). SRSF1-dependent nuclear export inhibition of C9ORF72 repeat transcripts prevents neurodegeneration and associated motor deficits. *Nature Communications*, *8*. https://doi.org/10.1038/ncomms16063

Heitzer, M., Kaiser, S., Kanagaratnam, M., Zendedel, A., Hartmann, P., Beyer, C., & Johann, S. (2017). Administration of 17β-Estradiol Improves Motoneuron Survival and Down-regulates Inflammasome Activation in Male SOD1(G93A) ALS Mice. *Molecular Neurobiology*, *54*(10), 1–15. https://doi.org/10.1007/S12035-016-0322-4

Henderson, J. F., & Khoo, M. K. Y. (1965). On the Mechanism of Feedback Inhibition of Purine Biosynthesis de Novo in Ehrlich Ascites Tumor Cells in Vitro. *Journal of Biological Chemistry*, *240*(7), 3104–3109. https://doi.org/10.1016/S0021-9258(18)97293-5

Henkel, J., Beers, D., Wen, S., Rivera, A., Toennis, K., Appel, J., Zhao, W., Moore, D., Powell, S., & Appel, S. (2013). Regulatory T-lymphocytes mediate amyotrophic lateral sclerosis progression and survival. *EMBO Molecular Medicine*, *5*(1), 64–79. https://doi.org/10.1002/EMMM.201201544

Henkel, J., Engelhardt, J., Siklós, L., Simpson, E., Kim, S., Pan, T., Goodman, J., Siddique, T., Beers, D., & Appel, S. (2004). Presence of dendritic cells, MCP-1, and activated microglia/macrophages in amyotrophic lateral sclerosis spinal cord tissue. *Annals of Neurology*, *55*(2), 221–235. https://doi.org/10.1002/ANA.10805

Henney, C. S., & Lichtenstein, L. M. (1971). The Role of Cyclic AMP in the Cytolytic Activity of Lymphocytes. *The Journal of Immunology*, *107*(2).

Herken, H., Gurel, A., Selek, S., Armutcu, F., Ozen, M. E., Bulut, M., Kap, O., Yumru, M., Savas, H. A., & Akyol, O. (2007). Adenosine Deaminase, Nitric Oxide, Superoxide Dismutase, and Xanthine Oxidase in Patients with Major Depression: Impact of Antidepressant Treatment. *Archives of Medical Research*, *38*(2), 247–252. https://doi.org/10.1016/J.ARCMED.2006.10.005

Hershfield, M. S. (2003). Genotype is an important determinant of phenotype in adenosine deaminase deficiency. *Current Opinion in Immunology*, *15*(5), 571–577. https://doi.org/10.1016/S0952-7915(03)00104-3

Hershfield, M. S. (2017). Adenosine Deaminase Deficiency. *GeneReviews®*. https://www.ncbi.nlm.nih.gov/books/NBK1483/

Hettinger, J., Liu, X., & Holden, J. (2008). The G22A polymorphism of the ADA gene and susceptibility to autism spectrum disorders. *Journal of Autism and Developmental Disorders*, *38*(1), 14–19. https://doi.org/10.1007/S10803-006-0354-0

Hideyama, T., Yamashita, T., Aizawa, H., Tsuji, S., Kakita, A., Takahashi, H., & Kwak, S. (2012). Profound downregulation of the RNA editing enzyme ADAR2 in ALS spinal motor neurons. *Neurobiology of Disease*, *45*(3), 1121–1128. https://doi.org/10.1016/J.NBD.2011.12.033

Hill, B. G., Dranka, B. P., Zou, L., Chatham, J. C., & Darley-Usmar, V. M. (2009). Importance of the bioenergetic reserve capacity in response to cardiomyocyte stress induced by 4-hydroxynonenal. *Biochemical Journal*, *424*(1), 99–107. https://doi.org/10.1042/BJ20090934

Hindley, S., Herman, M. A. R., & Rathbone, M. P. (1994). Stimulation of reactive astrogliosis in vivo by extracellular adenosine diphosphate or an adenosine A2 receptor agonist. *Journal of Neuroscience Research*, *38*(4), 399–406. https://doi.org/10.1002/JNR.490380405

Hink, H. U., Santanam, N., Dikalov, S., McCann, L., Nguyen, A. D., Parthasarathy, S., Harrison, D. G., & Fukai, T. (2002). Peroxidase Properties of Extracellular Superoxide Dismutase. *Arteriosclerosis, Thrombosis, and Vascular Biology*, *22*(9), 1402–1408. https://doi.org/10.1161/01.ATV.0000027524.86752.02

Hirschhorn, R., Paageorgiou, P., Kesarwala, H., & Taft, L. (1980). Amerioration of neurologic abnormalities after “enzyme replacement” in adenosine deaminase deficiency. *The*

New England Journal of Medicine, *303*(7), 377–380. https://doi.org/10.1056/NEJM198008143030706

Hirschhorn, R., Yang, D. R., & Israni, A. (1994). An Asp8Asn substitution results in the adenosine deaminase (ADA) genetic polymorphism (ADA 2 allozyme): occurrence on different chromosomal backgrounds and apparent intragenic crossover. *Annals of Human Genetics*, *58*(1), 1–9. https://doi.org/10.1111/J.1469-1809.1994.TB00720.X

Holm, T., Maier, A., Wicks, P., Lang, D., Linke, P., Münch, C., Steinfurth, L., Meyer, R., & Meyer, T. (2013). Severe loss of appetite in amyotrophic lateral sclerosis patients: Online self-assessment study. *Journal of Medical Internet Research*, *15*(4). https://doi.org/10.2196/ijmr.2463

Hönig, M., Albert, M., Schulz, A., Sparber-Sauer, M., Schütz, C., Belohradsky, B., Güngör, T., Rojewski, M., Bode, H., Pannicke, U., Lippold, D., Schwarz, K., Debatin, K., Hershfield, M., & Friedrich, W. (2007). Patients with adenosine deaminase deficiency surviving after hematopoietic stem cell transplantation are at high risk of CNS complications. *Blood*, *109*(8), 3595–3602. https://doi.org/10.1182/BLOOD-2006-07-034678

Hooten, K. G., Beers, D. R., Zhao, W., & Appel, S. H. (2015). Protective and Toxic Neuroinflammation in Amyotrophic Lateral Sclerosis. *Neurotherapeutics*, *12*(2), 364–375. https://doi.org/10.1007/S13311-014-0329-3/FIGURES/3

Hoshino, T., Yamada, K., Masuoka, K., Tsuboi, I., Itoh, K., Nonaka, K., & Oizumi, K. (1994). Elevated adenosine deaminase activity in the serum of patients with diabetes mellitus. *Diabetes Research and Clinical Practice*, *25*(2), 97–102. https://doi.org/10.1016/0168-8227(94)90034-5

Hounoum, B. M., Mavel, S., Coque, E., Patin, F., Vourc'h, P., Marouillat, S., ... & Blasco, H. (2017). Wildtype motoneurons, ALS-Linked SOD1 mutation and glutamate profoundly modify astrocyte metabolism and lactate shuttling. *Glia*, *65*(4), 592-605.

Howarth, C., Gleeson, P., & Attwell, D. (2012). Updated energy budgets for neural computation in the neocortex and cerebellum. In *Journal of Cerebral Blood Flow and Metabolism* (Vol. 32, Issue 7, pp. 1222–1232). https://doi.org/10.1038/jcbfm.2012.35

Hsiung, G. Y. R., Dejesus-Hernandez, M., Feldman, H. H., Sengdy, P., Bouchard-Kerr, P., Dwosh, E., Butler, R., Leung, B., Fok, A., Rutherford, N. J., Baker, M., Rademakers, R., & Mackenzie, I. R. A. (2012). Clinical and pathological features of familial frontotemporal dementia caused by C9ORF72 mutation on chromosome 9p. *Brain*,

135(3), 709–722. https://doi.org/10.1093/BRAIN/AWR354

Huang, W., Xu, Y., Zhang, Y., Zhang, P., Zhang, Q., Zhang, Z., & Xu, F. (2019). Metabolomics-driven identification of adenosine deaminase as therapeutic target in a mouse model of Parkinson's disease. *Journal of Neurochemistry*, *150*(3), 282–295. https://doi.org/10.1111/JNC.14774

Huang, Z., Zhang, Z., & Qu, W. (2014). Roles of adenosine and its receptors in sleep-wake regulation. *International Review of Neurobiology*, *119*, 349–371. https://doi.org/10.1016/B978-0-12-801022-8.00014-3

Ihara, Y., Nobukuni, K., Takata, H., & Hayabara, T. (2005). Oxidative stress and metal content in blood and cerebrospinal fluid of amyotrophic lateral sclerosis patients with and without a Cu, Zn-superoxide dismutase mutation. *Neurological Research*, *27*(1), 105–108. https://doi.org/10.1179/016164105X18430

Ikeda, K., Hirayama, T., Takazawa, T., Kawabe, K., & Iwasaki, Y. (2012). Relationships between Disease Progression and Serum Levels of Lipid, Urate, Creatinine and Ferritin in Japanese Patients with Amyotrophic Lateral Sclerosis: A Cross-Sectional Study. *Internal Medicine*, *51*(12), 1501–1508. https://doi.org/10.2169/INTERNALMEDICINE.51.7465

Ingwersen, J., Wingerath, B., Graf, J., Lepka, K., Hofrichter, M., Schröter, F., Wedekind, F., Bauer, A., Schrader, J., Hartung, H. P., Prozorovski, T., & Aktas, O. (2016). Dual roles of the adenosine A2a receptor in autoimmune neuroinflammation. *Journal of Neuroinflammation*, *13*(1), 1–11. https://doi.org/10.1186/S12974-016-0512-Z/FIGURES/4

Ishioh, M., Nozu, T., Igarashi, S., Tanabe, H., Kumei, S., Ohhira, M., Takakusaki, K., & Okumura, T. (2021). Activation of central adenosine A2B receptors mediate brain ghrelin-induced improvement of intestinal barrier function through the vagus nerve in rats. *Experimental Neurology*, *341*. https://doi.org/10.1016/J.EXPNEUROL.2021.113708

Iwaki, H., Ando, R., Miyaue, N., Tada, S., Tsujii, T., Yabe, H., Nishikawa, N., Nagai, M., & Nomoto, M. (2017). One year safety and efficacy of inosine to increase the serum urate level for patients with Parkinson's disease in Japan. *Journal of the Neurological Sciences*, *383*, 75–78. https://doi.org/10.1016/j.jns.2017.10.030

Jiang, H., Mankodi, A., Swanson, M. S., Moxley, R. T., & Thornton, C. A. (2004). Myotonic dystrophy type 1 is associated with nuclear foci of mutant RNA, sequestration of

muscleblind proteins and deregulated alternative splicing in neurons. *Human Molecular Genetics*, *13*(24), 3079–3088. https://doi.org/10.1093/HMG/DDH327

Johnston, R. B., Jr, Keele, B. B., Jr, Misra, H. P., Lehmeyer, J. E., Webb, L. S., Baehner, R. L., & RaJagopalan, K. V. (1975). The role of superoxide anion generation in phagocytic bactericidal activity. Studies with normal and chronic granulomatous disease leukocytes. *Journal of Clinical Investigation*, *55*(6), 1357. https://doi.org/10.1172/JCI108055

Jones, P. A., Smith, R. A., & Stone, T. W. (1998). Protection against kainate-induced excitotoxicity by adenosine A2A receptor agonists and antagonists. *Neuroscience*, *85*(1), 229–237. https://doi.org/10.1016/S0306-4522(97)00613-1

Jost, C. A., Marin, M. C., & Kaelin, W. G. (1997). p73 is a human p53-related protein that can induce apoptosis. *Nature*, *389*(6647), 191–194. https://doi.org/10.1038/38298

Juranek, J. K., Daffu, G. K., Wojtkiewicz, J., Lacomis, D., Kofler, J., & Schmidt, A. M. (2015). Receptor for advanced glycation end products and its inflammatory ligands are upregulated in amyotrophic lateral sclerosis. *Frontiers in Cellular Neuroscience*, *9*(DEC). https://doi.org/10.3389/FNCEL.2015.00485

Jurkowitz, M. S., Litsky, M. L., Browning, M. J., & Hohl, C. M. (1998). Adenosine, Inosine, and Guanosine Protect Glial Cells During Glucose Deprivation and Mitochondrial Inhibition: Correlation Between Protection and ATP Preservation. *Journal of Neurochemistry*, *71*(2), 535–548. https://doi.org/10.1046/J.1471-4159.1998.71020535.X

Kaghad, M., Bonnet, H., Yang, A., Creancier, L., Biscan, J.-C., Valent, A., Minty, A., Chalon, P., Lelias, J.-M., Dumont, X., Ferrara, P., McKeon, F., & Caput, D. (1997). Monoallelically Expressed Gene Related to p53 at 1p36, a Region Frequently Deleted in Neuroblastoma and Other Human Cancers. *Cell*, *90*(4), 809–819. https://doi.org/10.1016/S0092-8674(00)80540-1

Kalman, L., Lindegren, M. Lou, Kobrynski, L., Vogt, R., Hannon, H., Howard, J. T., & Buckley, R. (2004). Mutations in genes required for T-cell development:IL7R, CD45, IL2RG, JAK3, RAG1, RAG2, ARTEMIS, and ADA and severe combined immunodeficiency: HuGE review. *Genetics in Medicine 2004 6:1*, *6*(1), 16–26. https://doi.org/10.1097/01.gim.0000105752.80592.a3

Kameoka, J., Tanaka, T., Nojima, Y., Schlossman, S., & Morimoto, C. (1993). Direct association of adenosine deaminase with a T cell activation antigen, CD26. *Science*

(New York, N.Y.), *261*(5120), 466–469. https://doi.org/10.1126/SCIENCE.8101391

Kanekura, K., Yagi, T., Cammack, A. J., Mahadevan, J., Kuroda, M., Harms, M. B., Miller, T. M., & Urano, F. (2016). Poly-dipeptides encoded by the C9ORF72 repeats block global protein translation. *Human Molecular Genetics*, *25*(9), 1803–1813. https://doi.org/10.1093/HMG/DDW052

Kathiresan, K., Saravanakumar, K., Sahu, S. K., & Sivasankaran, M. (2013). Adenosine deaminase production by an endophytic bacterium (Lysinibacillus sp.) from Avicennia marina. *3 Biotech 2013 4:3*, *4*(3), 235–239. https://doi.org/10.1007/S13205-013-0144-2

Kaufmann, E., Boehm, B. O., Süssmuth, S. D., Kientsch-Engel, R., Sperfeld, A., Ludolph, A. C., & Tumani, H. (2004). The advanced glycation end-product Nε-(carboxymethyl)lysine level is elevated in cerebrospinal fluid of patients with amyotrophic lateral sclerosis. *Neuroscience Letters*, *371*(2–3), 226–229. https://doi.org/10.1016/J.NEULET.2004.08.071

Keizman, D., Ish-Shalom, M., Berliner, S., Maimon, N., Vered, Y., Artamonov, I., Tsehori, J., Nefussy, B., & Drory, V. E. (2009). Low uric acid levels in serum of patients with ALS: Further evidence for oxidative stress? *Journal of the Neurological Sciences*, *285*(1–2), 95–99. https://doi.org/10.1016/J.JNS.2009.06.002

Khosravi, B., LaClair, K. D., Riemenschneider, H., Zhou, Q., Frottin, F., Mareljic, N., Czuppa, M., Farny, D., Hartmann, H., Michaelsen, M., Arzberger, T., Hartl, F. U., Hipp, M. S., & Edbauer, D. (2020). Cell-to-cell transmission of C9orf72 poly-(Gly-Ala) triggers key features of ALS/FTD. *The EMBO Journal*, *39*(8), e102811. https://doi.org/10.15252/EMBJ.2019102811

Kim, B. W., Jeong, Y. E., Wong, M., & Martin, L. J. (2020). DNA damage accumulates and responses are engaged in human ALS brain and spinal motor neurons and DNA repair is activatable in iPSC-derived motor neurons with SOD1 mutations. *Acta Neuropathologica Communications*, *8*(1), 7. https://doi.org/10.1186/S40478-019-0874-4

Kim, M. J., Vargas, M. R., Harlan, B. A., Killoy, K. M., Ball, L. E., Comte-Walters, S., Gooz, M., Yamamoto, Y., Beckman, J. S., Barbeito, L., & Pehar, M. (2018). Nitration and Glycation Turn Mature NGF into a Toxic Factor for Motor Neurons: A Role for p75NTR and RAGE Signaling in ALS. *Antioxidants & Redox Signaling*, *28*(18), 1587. https://doi.org/10.1089/ARS.2016.6966

Kioumourtzoglou, M. A., Rotem, R. S., Seals, R. M., Gredal, O., Hansen, J., & Weisskopf, M. G. (2015). Diabetes mellitus, obesity, and diagnosis of amyotrophic lateral sclerosis a

population-based study. *JAMA Neurology*, *72*(8). https://doi.org/10.1001/jamaneurol.2015.0910

Kirby, J., Ning, K., Ferraiuolo, L., Heath, P. R., Ismail, A., Kuo, S. W., Valori, C. F., Cox, L., Sharrack, B., Wharton, S. B., Ince, P. G., Shaw, P. J., & Azzouz, M. (2011). Phosphatase and tensin homologue/protein kinase B pathway linked to motor neuron survival in human superoxide dismutase 1-related amyotrophic lateral sclerosis. *Brain*, *134*(2), 506–517. https://doi.org/10.1093/BRAIN/AWQ345

Klemann, C. J. H. M., Visser, J. E., Van Den Bosch, L., Martens, G. J. M., & Poelmans, G. (2018). Integrated molecular landscape of amyotrophic lateral sclerosis provides insights into disease etiology. *Brain Pathology*, *28*(2), 203–211. https://doi.org/10.1111/bpa.12485

Klyuch, B. P., Dale, N., & Wall, M. J. (2012). Deletion of Ecto-5′-Nucleotidase (CD73) Reveals Direct Action Potential-Dependent Adenosine Release. *Journal of Neuroscience*, *32*(11), 3842–3847. https://doi.org/10.1523/JNEUROSCI.6052-11.2012

Kohn, D. B., Hershfield, M. S., Puck, J. M., Aiuti, A., Blincoe, A., Gaspar, H. B., Notarangelo, L. D., & Grunebaum, E. (2019). Consensus approach for the management of severe combined immune deficiency caused by adenosine deaminase deficiency. *Journal of Allergy and Clinical Immunology*, *143*(3). https://doi.org/10.1016/j.jaci.2018.08.024

Kok, J. R., Palminha, N. M., Souza, C. D. S., El-Khamisy, S. F., & Ferraiuolo, L. (2021). DNA damage as a mechanism of neurodegeneration in ALS and a contributor to astrocyte toxicity. *Cellular and Molecular Life Sciences*, *78*(15), 5707. https://doi.org/10.1007/S00018-021-03872-0

Komaki, S., Ishikawa, K., & Arakawa, Y. (2012). Trk and cAMP-dependent survival activity of adenosine A 2A agonist CGS21680 on rat motoneurons in culture. *Neuroscience Letters*, *522*(1), 21–24. https://doi.org/10.1016/j.neulet.2012.06.003

Kori, M., Aydın, B., Unal, S., Arga, K. Y., & Kazan, D. (2016). Metabolic biomarkers and neurodegeneration: a pathway enrichment analysis of Alzheimer's disease, Parkinson's disease, and amyotrophic lateral sclerosis. *Omics: a journal of integrative biology*, *20*(11), 645-661.

Kostic Dedic, S. I., Stevic, Z., Dedic, V., Stojanovic, V. R., Milicev, M., & Lavrnic, D. (2012). Is hyperlipidemia correlated with longer survival in patients with amyotrophic lateral sclerosis? *Neurological Research*, *34*(6), 576–580. https://doi.org/10.1179/1743132812Y.0000000049

Kovács, A. L., Gordon, P. B., Grotterød, E. M., & Seglen, P. O. (1998). Inhibition of hepatocytic autophagy by adenosine, adenosine analogs and AMP. *Biological Chemistry*, *379*(11), 1341–1347. https://doi.org/10.1515/BCHM.1998.379.11.1341/MACHINEREADABLECITATION/RIS

Kovanda, A., Zalar, M., Šket, P., Plavec, J., & Rogelj, B. (2015). Anti-sense DNA d(GGCCCC)n expansions in C9ORF72 form i-motifs and protonated hairpins. *Scientific Reports* , *5*(1), 1–7. https://doi.org/10.1038/srep17944

Kredich, N. M., & Martin, D. W. (1977). Role of S-adenosylhomocysteine in adenosine-mediated toxicity in cultured mouse T lymphoma cells. *Cell*, *12*(4), 931–938. https://doi.org/10.1016/0092-8674(77)90157-X

Krenitsky, T. A., Miller, R. L., & Fyfe, J. A. (1974). Levels of nucleoside and nucleotide kinases in Rhesus monkey tissues. *Biochemical Pharmacology*, *23*(1), 170–172. https://doi.org/10.1016/0006-2952(74)90325-6

Kurtul, N., Pence, S., Akarsu, E., Kocoglu, H., Aksoy, Y., & Aksoy, H. (2004). Adenosine deaminase activity in the serum of type 2 diabetic patients. *Acta Medica (Hradec Kralove)*, *47*(1), 33–35. https://europepmc.org/article/med/15168879

Kushner, P. D., Stephenson, D. T., & Wright, S. (1991). Reactive Astrogliosis is Widespread in the Subcortical White Matter of Amyotrophic Lateral Sclerosis Brain. *Journal of Neuropathology & Experimental Neurology*, *50*(3), 263–277. https://doi.org/10.1097/00005072-199105000-00008

Kwon, I., Xiang, S., Kato, M., Wu, L., Theodoropoulos, P., Wang, T., Kim, J., Yun, J., Xie, Y., & McKnight, S. L. (2014). Poly-dipeptides encoded by the C9orf72 repeats bind nucleoli, impede RNA biogenesis, and kill cells. *Science*, *345*(6201), 1139–1145. https://doi.org/10.1126/SCIENCE.1254917/SUPPL_FILE/1254917S_TABLE_S1.XLSX

LaClair, K. D., Zhou, Q., Michaelsen, M., Wefers, B., Brill, M. S., Janjic, A., Rathkolb, B., Farny, D., Cygan, M., de Angelis, M. H., Wurst, W., Neumann, M., Enard, W., Misgeld, T., Arzberger, T., & Edbauer, D. (2020). Congenic expression of poly-GA but not poly-PR in mice triggers selective neuron loss and interferon responses found in C9orf72 ALS. *Acta Neuropathologica*, *140*(2), 121–142. https://doi.org/10.1007/S00401-020-02176-0/FIGURES/6

Lai, J. D., & Ichida, J. K. (2019). C9ORF72 protein function and immune dysregulation in amyotrophic lateral sclerosis. *Neuroscience Letters*, *713*, 134523. https://doi.org/10.1016/J.NEULET.2019.134523

Lan, Y. Y., Londoño, D., Bouley, R., Rooney, M. S., & Hacohen, N. (2014). Dnase2a Deficiency Uncovers Lysosomal Clearance of Damaged Nuclear DNA via Autophagy. *Cell Reports*, *9*(1), 180–192. https://doi.org/10.1016/J.CELREP.2014.08.074

Lavigueur, A., Branche, H. La, Kornblihtt, A. R., & Chabot, B. (1993). A splicing enhancer in the human fibronectin alternate ED1 exon interacts with SR proteins and stimulates U2 snRNP binding. *Genes & Development*, *7*(12a), 2405–2417. https://doi.org/10.1101/GAD.7.12A.2405

Lee, J., Kang, D., Yu, J., Kim, Y., Kim, J., Koh, G., & Lee, D. (2011). Changes in Adenosine Deaminase Activity in Patients with Type 2 Diabetes Mellitus and Effect of DPP-4 Inhibitor Treatment on ADA Activity. *Diabetes & Metabolism Journal*, *35*(2), 149–158. https://doi.org/10.4093/DMJ.2011.35.2.149

Lee, K. H., Zhang, P., Kim, H. J., Mitrea, D. M., Sarkar, M., Freibaum, B. D., Cika, J., Coughlin, M., Messing, J., Molliex, A., Maxwell, B. A., Kim, N. C., Temirov, J., Moore, J., Kolaitis, R. M., Shaw, T. I., Bai, B., Peng, J., Kriwacki, R. W., & Taylor, J. P. (2016). C9orf72 Dipeptide Repeats Impair the Assembly, Dynamics, and Function of Membrane-Less Organelles. *Cell*, *167*(3), 774-788.e17. https://doi.org/10.1016/J.CELL.2016.10.002

Lee, K., Li, B., Xi, X., Suh, Y., & Martin, R. (2005). Role of neuronal energy status in the regulation of adenosine 5'-monophosphate-activated protein kinase, orexigenic neuropeptides expression, and feeding behavior. *Endocrinology*, *146*(1), 3–10. https://doi.org/10.1210/EN.2004-0968

Lee, Y. B., Chen, H. J., Peres, J. N., Gomez-Deza, J., Attig, J., Štalekar, M., Troakes, C., Nishimura, A. L., Scotter, E. L., Vance, C., Adachi, Y., Sardone, V., Miller, J. W., Smith, B. N., Gallo, J. M., Ule, J., Hirth, F., Rogelj, B., Houart, C., & Shaw, C. E. (2013). Hexanucleotide Repeats in ALS/FTD Form Length-Dependent RNA Foci, Sequester RNA Binding Proteins, and Are Neurotoxic. *Cell Reports*, *5*(5), 1178–1186. https://doi.org/10.1016/J.CELREP.2013.10.049

Lehmer, C., Oeckl, P., Weishaupt, J. H., Volk, A. E., Diehl-Schmid, J., Schroeter, M. L., Lauer, M., Kornhuber, J., Levin, J., Fassbender, K., Landwehrmeyer, B., Schludi, M. H., Arzberger, T., Kremmer, E., Flatley, A., Feederle, R., Steinacker, P., Weydt, P., Ludolph, A. C., … Ziegler, G. (2017). Poly-GP in cerebrospinal fluid links C9orf72-associated dipeptide repeat expression to the asymptomatic phase of ALS/FTD. *EMBO Molecular Medicine*, *9*(7), 859–868. https://doi.org/10.15252/EMMM.201607486

Lehmkuhl, E. M., Loganathan, S., Alsop, E., Blythe, A. D., Kovalik, T., Mortimore, N. P.,

Barrameda, D., Kueth, C., Eck, R. J., Siddegowda, B. B., Joardar, A., Ball, H., Macias, M. E., Bowser, R., Van Keuren-Jensen, K., & Zarnescu, D. C. (2021). TDP-43 proteinopathy alters the ribosome association of multiple mRNAs including the glypican Dally-like protein (Dlp)/GPC6. *Acta Neuropathologica Communications* , *9*(1), 1–21. https://doi.org/10.1186/S40478-021-01148-Z

Levine, B. L., Humeau, L. M., Boyer, J., MacGregor, R. R., Rebello, T., Lu, X., Binder, G. K., Slepushkin, V., Lemiale, F., Mascola, J. R., Bushman, F. D., Dropulic, B., & June, C. H. (2006). Gene transfer in humans using a conditionally replicating lentiviral vector. *Proceedings of the National Academy of Sciences of the United States of America*, *103*(46), 17372–17377. https://doi.org/10.1073/PNAS.0608138103/SUPPL_FILE/08138SUPPAPPENDIX.PDF

Li, Y., Oskouian, R. J., Day, Y. J., Rieger, J. M., Liu, L., Kern, J. A., & Linden, J. (2006). Mouse spinal cord compression injury is reduced by either activation of the adenosine A2A receptor on bone marrow–derived cells or deletion of the A2A receptor on non-bone marrow–derived cells. *Neuroscience*, *141*(4), 2029–2039. https://doi.org/10.1016/J.NEUROSCIENCE.2006.05.014

Lin, Y., Mori, E., Kato, M., Xiang, S., Wu, L., Kwon, I., & McKnight, S. L. (2016). Toxic PR Poly-Dipeptides Encoded by the C9orf72 Repeat Expansion Target LC Domain Polymers. *Cell*, *167*(3), 789-802.e12. https://doi.org/10.1016/J.CELL.2016.10.003

Litsky, M. L., Hohl, C. M., Lucas, J. H., & Jurkowitz, M. S. (1999). Inosine and guanosine preserve neuronal and glial cell viability in mouse spinal cord cultures during chemical hypoxia. *Brain Research*, *821*(2), 426–432. https://doi.org/10.1016/S0006-8993(99)01086-0

Liu, F., Morderer, D., Wren, M. C., Vettleson-Trutza, S. A., Wang, Y., Rabichow, B. E., Salemi, M. R., Phinney, B. S., Oskarsson, B., Dickson, D. W., & Rossoll, W. (2022). Proximity proteomics of C9orf72 dipeptide repeat proteins identifies molecular chaperones as modifiers of poly-GA aggregation. *Acta Neuropathologica Communications 2022 10:1*, *10*(1), 1–18. https://doi.org/10.1186/S40478-022-01322-X

Liu, J., & Wang, F. (2017). Role of neuroinflammation in amyotrophic lateral sclerosis: Cellular mechanisms and therapeutic implications. *Frontiers in Immunology*, *8*, 1005. https://doi.org/10.3389/FIMMU.2017.01005/BIBTEX

Liu, Y., Pattamatta, A., Zu, T., Reid, T., Bardhi, O., Borchelt, D. R., Yachnis, A. T., & Ranum, L. P. W. (2016). C9orf72 BAC Mouse Model with Motor Deficits and Neurodegenerative Features of ALS/FTD. *Neuron*, *90*(3), 521–534.

https://doi.org/10.1016/J.NEURON.2016.04.005

Livak, K. J., & Schmittgen, T. D. (2001). Analysis of Relative Gene Expression Data Using Real-Time Quantitative PCR and the 2−ΔΔCT Method. *Methods*, *25*(4), 402–408. https://doi.org/10.1006/METH.2001.1262

Loganathan, S., Wilson, B. A., Carey, S. B., Manzo, E., Joardar, A., Ugur, B., & Zarnescu, D. C. (2022). TDP-43 Proteinopathy Causes Broad Metabolic Alterations including TCA Cycle Intermediates and Dopamine Levels in Drosophila Models of ALS. *Metabolites*, *12*(2), 101. https://doi.org/10.3390/METABO12020101/S1

Lopez-Gonzalez, R., Lu, Y., Gendron, T. F., Karydas, A., Tran, H., Yang, D., Petrucelli, L., Miller, B. L., Almeida, S., & Gao, F. B. (2016). Poly(GR) in C9ORF72-Related ALS/FTD Compromises Mitochondrial Function and Increases Oxidative Stress and DNA Damage in iPSC-Derived Motor Neurons. *Neuron*, *92*(2), 383–391. https://doi.org/10.1016/J.NEURON.2016.09.015

Macek, T., Schaffhauser, H., & Conn, P. (1998). Protein kinase C and A3 adenosine receptor activation inhibit presynaptic metabotropic glutamate receptor (mGluR) function and uncouple mGluRs from GTP-binding proteins. *The Journal of Neuroscience : The Official Journal of the Society for Neuroscience*, *18*(16), 6138–6146. https://doi.org/10.1523/JNEUROSCI.18-16-06138.1998

Maes, M. E., Colombo, G., Schulz, R., & Siegert, S. (2019). Targeting microglia with lentivirus and AAV: Recent advances and remaining challenges. *Neuroscience Letters*, *707*, 134310. https://doi.org/10.1016/J.NEULET.2019.134310

Mahoney, C. J., Beck, J., Rohrer, J. D., Lashley, T., Mok, K., Shakespeare, T., Yeatman, T., Warrington, E. K., Schott, J. M., Fox, N. C., Rossor, M. N., Hardy, J., Collinge, J., Revesz, T., Mead, S., & Warren, J. D. (2012). Frontotemporal dementia with the C9ORF72 hexanucleotide repeat expansion: clinical, neuroanatomical and neuropathological features. *Brain*, *135*(3), 736–750. https://doi.org/10.1093/BRAIN/AWR361

Majounie, E., Renton, A. E., Mok, K., Dopper, E. G. P., Waite, A., Rollinson, S., Chiò, A., Restagno, G., Nicolaou, N., Simon-Sanchez, J., van Swieten, J. C., Abramzon, Y., Johnson, J. O., Sendtner, M., Pamphlett, R., Orrell, R. W., Mead, S., Sidle, K. C., Houlden, H., … Logroscino, G. (2012). Frequency of the C9orf72 hexanucleotide repeat expansion in patients with amyotrophic lateral sclerosis and frontotemporal dementia: A cross-sectional study. *The Lancet Neurology*, *11*(4), 323–330. https://doi.org/10.1016/S1474-4422(12)70043-1

Malik, B. R., Maddison, D. C., Smith, G. A., & Peters, O. M. (2019). Autophagic and endo-lysosomal dysfunction in neurodegenerative disease. *Molecular Brain*, *12*(1), 1–21. https://doi.org/10.1186/S13041-019-0504-X

Mankodi, A., Urbinati, C. R., Yuan, Q. P., Moxley, R. T., Sansone, V., Krym, M., Henderson, D., Schalling, M., Swanson, M. S., & Thornton, C. A. (2001). Muscleblind localizes to nuclear foci of aberrant RNA in myotonic dystrophy types 1 and 2. *Human Molecular Genetics*, *10*(19), 2165–2170. https://doi.org/10.1093/HMG/10.19.2165

Mantovani, S., Garbelli, S., Pasini, A., Alimonti, D., Perotti, C., Melazzini, M., Bendotti, C., & Mora, G. (2009). Immune system alterations in sporadic amyotrophic lateral sclerosis patients suggest an ongoing neuroinflammatory process. *Journal of Neuroimmunology*, *210*(1), 73–79. https://doi.org/10.1016/J.JNEUROIM.2009.02.012

Manzo, E., Lorenzini, I., Barrameda, D., O'Conner, A. G., Barrows, J. M., Starr, A., Kovalik, T., Rabichow, B. E., Lehmkuhl, E. M., Shreiner, D. D., Joardar, A., Liévens, J. C., Bowser, R., Sattler, R., & Zarnescu, D. C. (2019). Glycolysis upregulation is neuroprotective as a compensatory mechanism in ALS. *ELife*, *8*. https://doi.org/10.7554/eLife.45114

Maor-Nof, M., Shipony, Z., Lopez-Gonzalez, R., Nakayama, L., Zhang, Y.-J., Couthouis, J., Blum, J. A., Castruita, P. A., Linares, G. R., Ruan, K., Ramaswami, G., Simon, D. J., Nof, A., Santana, M., Han, K., Sinnott-Armstrong, N., Bassik, M. C., Geschwind, D. H., Tessier-Lavigne, M., … Gitler, A. D. (2021). p53 is a central regulator driving neurodegeneration caused by C9orf72 poly(PR). *Cell*, *184*(3), 689-708.e20. https://doi.org/10.1016/J.CELL.2020.12.025

Marchi, P. M., Marrone, L., Brasseur, L., Coens, A., Webster, C. P., Bousset, L., Destro, M., Smith, E. F., Walther, C. G., Alfred, V., Marroccella, R., Graves, E. J., Robinson, D., Shaw, A. C., Wan, L. M., Grierson, A. J., Ebbens, S. J., De Vos, K. J., Hautbergue, G. M., … Azzouz, M. (2022). C9ORF72-derived poly-GA DPRs undergo endocytic uptake in iAstrocytes and spread to motor neurons. *Life Science Alliance*, *5*(9). https://doi.org/10.26508/LSA.202101276

Mariosa, D., Kamel, F., Bellocco, R., Ye, W., & Fang, F. (2015). Association between diabetes and amyotrophic lateral sclerosis in Sweden. *European Journal of Neurology*, *22*(11), 1436–1442. https://doi.org/10.1111/ENE.12632

Markert, M. L. (1991). Purine nucleoside phosphorylase deficiency. *Immunodeficiency Reviews*, *3*(1), 45–81. https://pubmed.ncbi.nlm.nih.gov/1931007/

Marshall, C. B., Beeler, J. S., Lehmann, B. D., Gonzalez-Ericsson, P., Sanchez, V., Sanders, M. E., Boyd, K. L., & Pietenpol, J. A. (2021). Tissue-specific expression of p73 and p63 isoforms in human tissues. *Cell Death & Disease 2021 12:8*, *12*(8), 1–10. https://doi.org/10.1038/s41419-021-04017-8

Martin, L. J., & Wong, M. (2013). Aberrant Regulation of DNA Methylation in Amyotrophic Lateral Sclerosis: A New Target of Disease Mechanisms. *Neurotherapeutics*, *10*(4), 722–733. https://doi.org/10.1007/S13311-013-0205-6/TABLES/1

Martín, M., Huguet, J., Centelles, J. J., & Franco, R. (1995). Expression of ecto-adenosine deaminase and CD26 in human T cells triggered by the TCR-CD3 complex. Possible role of adenosine deaminase as costimulatory molecule. *The Journal of Immunology*, *155*(10).

Martínez-Fábregas, J., Prescott, A., van Kasteren, S., Pedrioli, D. L., McLean, I., Moles, A., Reinheckel, T., Poli, V., & Watts, C. (2018). Lysosomal protease deficiency or substrate overload induces an oxidative-stress mediated STAT3-dependent pathway of lysosomal homeostasis. *Nature Communications* , *9*(1), 1–16. https://doi.org/10.1038/s41467-018-07741-6

Martinez-Navio, J. M., Casanova, V., Pacheco, R., Naval-Macabuhay, I., Climent, N., Garcia, F., Gatell, J. M., Mallol, J., Gallart, T., Lluis, C., & Franco, R. (2011). Adenosine deaminase potentiates the generation of effector, memory, and regulatory CD4+ T cells. *Journal of Leukocyte Biology*, *89*(1), 127–136. https://doi.org/10.1189/JLB.1009696

Matveeva, A., Watters, O., Rukhadze, A., Khemka, N., Gentile, D., Perez, I. F., Llorente-Folch I., Farrell, C., Lo Cacciato, E., Jackson, J., Piazzesi, A., Wischhof, L., Woods, I., Halang, L., Hogg, M., Muñoz, A. G., Dillon, E. T., Matallanas, D., Arijs, I., Lambrechts, D., Bano, D., Connolly, N. M. C., & Prehn, J. H. (2023). Integrated analysis of transcriptomic and proteomic alterations in mouse models of ALS/FTD identify early metabolic adaptions with similarities to mitochondrial dysfunction disorders. *Amyotrophic Lateral Sclerosis and Frontotemporal Degeneration*, 1-15.

May, S., Hornburg, D., Schludi, M. H., Arzberger, T., Rentzsch, K., Schwenk, B. M., Grässer, F. A., Mori, K., Kremmer, E., Banzhaf-Strathmann, J., Mann, M., Meissner, F., & Edbauer, D. (2014). C9orf72 FTLD/ALS-associated Gly-Ala dipeptide repeat proteins cause neuronal toxicity and Unc119 sequestration. *Acta Neuropathologica*, *128*(4), 485–503. https://doi.org/10.1007/S00401-014-1329-4/FIGURES/7

Mayeda, A., Helfman, D., & Krainer, A. (1993). Modulation of exon skipping and inclusion by

heterogeneous nuclear ribonucleoprotein A1 and pre-mRNA splicing factor SF2/ASF. *Molecular and Cellular Biology*, *13*(5), 2993–3001. https://doi.org/10.1128/MCB.13.5.2993-3001.1993

McAlpine, W., Sun, L., Wang, K. wen, Liu, A., Jain, R., Miguel, M. S., Wang, J., Zhang, Z., Hayse, B., McAlpine, S. G., Choi, J. H., Zhong, X., Ludwig, S., Russell, J., Zhan, X., Choi, M., Li, X., Tang, M., Moresco, E. M. Y., … Turer, E. (2018). Excessive endosomal TLR signaling causes inflammatory disease in mice with defective SMCR8-WDR41-C9ORF72 complex function. *Proceedings of the National Academy of Sciences of the United States of America*, *115*(49), E11523–E11531. https://doi.org/10.1073/PNAS.1814753115/SUPPL_FILE/PNAS.1814753115.SAPP.PDF

McCauley, M. E., O'Rourke, J. G., Yáñez, A., Markman, J. L., Ho, R., Wang, X., Chen, S., Lall, D., Jin, M., Muhammad, A. K. M. G., Bell, S., Landeros, J., Valencia, V., Harms, M., Arditi, M., Jefferies, C., & Baloh, R. H. (2020). C9orf72 in myeloid cells suppresses STING-induced inflammation. *Nature*, *585*(7823), 96–101. https://doi.org/10.1038/s41586-020-2625-x

Mehta, A. R., Gregory, J. M., Dando, O., Carter, R. N., Burr, K., Nanda, J., Story, D., McDade, K., Smith, C., Morton, N. M., Mahad, D. J., Hardingham, G. E., Chandran, S., & Selvaraj, B. T. (2021). Mitochondrial bioenergetic deficits in C9orf72 amyotrophic lateral sclerosis motor neurons cause dysfunctional axonal homeostasis. *Acta Neuropathologica 2021 141:2*, *141*(2), 257–279. https://doi.org/10.1007/S00401-020-02252-5

Mehta, A. R., Selvaraj, B. T., Barton, S. K., Mcdade, K., Abrahams, S., Chandran, S., Smith, C., & Gregory, J. M. (2020). Improved detection of RNA foci in C9orf72 amyotrophic lateral sclerosis post-mortem tissue using BaseScope™ shows a lack of association with cognitive dysfunction. *Brain Communications*, *2*(1). https://doi.org/10.1093/BRAINCOMMS/FCAA009

Mejzini, R., Flynn, L. L., Pitout, I. L., Fletcher, S., Wilton, S. D., & Akkari, P. A. (2019). ALS Genetics, Mechanisms, and Therapeutics: Where Are We Now? In *Frontiers in Neuroscience* (Vol. 13). Frontiers Media S.A. https://doi.org/10.3389/fnins.2019.01310

Melcher, T., Maas, S., Herb, A., Sprengel, R., Seeburg, P. H., & Higuchi, M. (1996). A mammalian RNA editing enzyme. *Nature*, *379*(6564), 460–464. https://doi.org/10.1038/379460a0

Meng, F., Guo, Z., Hu, Y., Mai, W., Zhang, Z., Zhang, B., Ge, Q., Lou, H., Guo, F., Chen, J.,

Duan, S., & Gao, Z. (2019). CD73-derived adenosine controls inflammation and neurodegeneration by modulating dopamine signalling. *Brain*, *142*(3), 700–718. https://doi.org/10.1093/BRAIN/AWY351

Mergenthaler, P., Lindauer, U., Dienel, G. A., & Meisel, A. (2013). Sugar for the brain: The role of glucose in physiological and pathological brain function. In *Trends in Neurosciences* (Vol. 36, Issue 10, pp. 587–597). https://doi.org/10.1016/j.tins.2013.07.001

Meyer, K., Ferraiuolo, L., Miranda, C. J., Likhite, S., McElroy, S., Renusch, S., Ditsworth, D., Lagier-Tourenne, C., Smith, R. A., Ravits, J., Burghes, A. H., Shaw, P. J., Cleveland, D. W., Kolb, S. J., & Kaspar, B. K. (2014). Direct conversion of patient fibroblasts demonstrates non-cell autonomous toxicity of astrocytes to motor neurons in familial and sporadic ALS. *Proceedings of the National Academy of Sciences of the United States of America*, *111*(2), 829–832. https://doi.org/10.1073/PNAS.1314085111/SUPPL_FILE/BRIANKASPARPODCAST.MP3

Michel, T. M., Camara, S., Tatschner, T., Frangou, S., Sheldrick, A. J., Riederer, P., & Grünblatt, E. (2010). Increased xanthine oxidase in the thalamus and putamen in depression. *The World Journal of Biological Psychiatry*, *11*(2 PART 2), 314–320. https://doi.org/10.3109/15622970802123695

Miller, J. W., Urbinati, C. R., Teng-Umnuay, P., Stenberg, M. G., Byrne, B. J., Thornton, C. A., & Swanson, M. S. (2000). Recruitment of human muscleblind proteins to (CUG)n expansions associated with myotonic dystrophy. *The EMBO Journal*, *19*(17), 4439–4448. https://doi.org/10.1093/EMBOJ/19.17.4439

Mitsumoto, H., Santella, R. M., Liu, X., Bogdanov, M., Zipprich, J., Wu, H.-C., Mahata, J., Kilty, M., Bednarz, K., Bell, D., Gordon, P. H., Hornig, M., Mehrazin, M., Naini, A., Beal, M. F., & Factor-Litvak, P. (2008). Oxidative Stress Biomarkers in Sporadic ALS. *Amyotrophic Lateral Sclerosis : Official Publication of the World Federation of Neurology Research Group on Motor Neuron Diseases*, *9*(3), 177. https://doi.org/10.1080/17482960801933942

Mizielinska, S., Grönke, S., Niccoli, T., Ridler, C. E., Clayton, E. L., Devoy, A., Moens, T., Norona, F. E., Woollacott, I. O. C., Pietrzyk, J., Cleverley, K., Nicoll, A. J., Pickering-Brown, S., Dols, J., Cabecinha, M., Hendrich, O., Fratta, P., Fisher, E. M. C., Partridge, L., & Isaacs, A. M. (2014). C9orf72 repeat expansions cause neurodegeneration in Drosophila through arginine-rich proteins. *Science*, *6201*, 1192–1194.

https://doi.org/10.1126/SCIENCE.1256800/SUPPL_FILE/MIZIELINSKA.SM.PDF

Mizielinska, S., Lashley, T., Norona, F. E., Clayton, E. L., Ridler, C. E., Fratta, P., & Isaacs, A. M. (2013). C9orf72 frontotemporal lobar degeneration is characterised by frequent neuronal sense and antisense RNA foci. *Acta Neuropathologica*, *126*(6), 845–857. https://doi.org/10.1007/S00401-013-1200-Z/FIGURES/8

Mizielinska, S., Ridler, C. E., Balendra, R., Thoeng, A., Woodling, N. S., Grässer, F. A., Plagnol, V., Lashley, T., Partridge, L., & Isaacs, A. M. (2017). Bidirectional nucleolar dysfunction in C9orf72 frontotemporal lobar degeneration. *Acta Neuropathologica Communications*, *5*(1), 29. https://doi.org/10.1186/S40478-017-0432-X/FIGURES/4

Módis, K., Gero, D., Stangl, R., Rosero, O., Szijártó, A., Lotz, G., Mohácsik, P., Szoleczky, P., Coletta, C., & Szabó, C. (2013). Adenosine and inosine exert cytoprotective effects in an in vitro model of liver ischemia-reperfusion injury. *International Journal of Molecular Medicine*, *31*(2), 437–446. https://doi.org/10.3892/IJMM.2012.1203/HTML

Molliex, A., Temirov, J., Lee, J., Coughlin, M., Kanagaraj, A. P., Kim, H. J., Mittag, T., & Taylor, J. P. (2015). Phase Separation by Low Complexity Domains Promotes Stress Granule Assembly and Drives Pathological Fibrillization. *Cell*, *163*(1), 123–133. https://doi.org/10.1016/J.CELL.2015.09.015

Moore, S., Alsop, E., Lorenzini, I., Starr, A., Rabichow, B. E., Mendez, E., Levy, J. L., Burciu, C., Reiman, R., Chew, J., Belzil, V. V., W. Dickson, D., Robertson, J., Staats, K. A., Ichida, J. K., Petrucelli, L., Van Keuren-Jensen, K., & Sattler, R. (2019). ADAR2 mislocalization and widespread RNA editing aberrations in C9orf72-mediated ALS/FTD. *Acta Neuropathologica 2019 138:1*, *138*(1), 49–65. https://doi.org/10.1007/S00401-019-01999-W

Morahan, J. M., Yu, B., Trent, R. J., & Pamphlett, R. (2009). A genome-wide analysis of brain DNA methylation identifies new candidate genes for sporadic amyotrophic lateral sclerosis. *Amyotrophic Lateral Sclerosis*, *10*(5–6), 418–429. https://doi.org/10.3109/17482960802635397

Moreno, E., Canet, J., Gracia, E., Lluís, C., Mallol, J., Canela, E. I., Cortés, A., & Casadó, V. (2018). Molecular Evidence of Adenosine Deaminase Linking Adenosine A2A Receptor and CD26 Proteins. *Frontiers in Pharmacology*, *9*(FEB). https://doi.org/10.3389/FPHAR.2018.00106

Mori, A., Cross, B., Uchida, S., Kerrick Walker, J., & Ristuccia, R. (2021). How Are Adenosine and Adenosine A2A Receptors Involved in the Pathophysiology of

Amyotrophic Lateral Sclerosis? *Biomedicines* , *9*(8), 1027. https://doi.org/10.3390/BIOMEDICINES9081027

Mori, K., Lammich, S., Mackenzie, I. R. A., Forné, I., Zilow, S., Kretzschmar, H., Edbauer, D., Janssens, J., Kleinberger, G., Cruts, M., Herms, J., Neumann, M., Van Broeckhoven, C., Arzberger, T., & Haass, C. (2013). HnRNP A3 binds to GGGGCC repeats and is a constituent of p62-positive/TDP43-negative inclusions in the hippocampus of patients with C9orf72 mutations. *Acta Neuropathologica*, *125*(3), 413–423. https://doi.org/10.1007/S00401-013-1088-7/FIGURES/4

Morrison, D. K. (2012). MAP kinase pathways. *Cold Spring Harbor Perspectives in Biology*, *4*(11). https://doi.org/10.1101/cshperspect.a011254

Mulder, D., Kurland, L., Offord, K., & Beard, C. (1986). Familial adult motor neuron disease: amyotrophic lateral sclerosis. *Neurology*, *36*(4), 511–517. https://doi.org/10.1212/WNL.36.4.511

Mulligan, S. J., & MacVicar, B. A. (2004). Calcium transients in astrocyte endfeet cause cerebrovascular constrictions. *Nature*, *431*(7005), 195–199. https://doi.org/10.1038/nature02827

Murata, T., Ohtsuka, C., & Terayama, Y. (2008). Increased mitochondrial oxidative damage and oxidative DNA damage contributes to the neurodegenerative process in sporadic amyotrophic lateral sclerosis. *Free Radical Research*, *42*(3), 221–225. https://doi.org/10.1080/10715760701877262

Murray-Zmijewski, F., Lane, D. P., & Bourdon, J.-C. (2006). p53/p63/p73 isoforms: an orchestra of isoforms to harmonise cell differentiation and response to stress. *Cell Death & Differentiation 2006 13:6*, *13*(6), 962–972. https://doi.org/10.1038/sj.cdd.4401914

Murray, A. W. (1971). The biological significance of purine salvage. *Annual Review of Biochemistry*, *40*, 811–826. https://doi.org/10.1146/ANNUREV.BI.40.070171.004115

Nagy, J., LaBella, L., Buss, M., & Daddona, P. (1984). Immunohistochemistry of adenosine deaminase: implications for adenosine neurotransmission. *Science (New York, N.Y.)*, *224*(4645), 166–168. https://doi.org/10.1126/SCIENCE.6142530

Naldini, L., Blömer, U., Gallay, P., Ory, D., Mulligan, R., Gage, F. H., Verma, I. M., & Trono, D. (1996). In Vivo Gene Delivery and Stable Transduction of Nondividing Cells by a Lentiviral Vector. *Science*, *272*(5259), 263–267. https://doi.org/10.1126/SCIENCE.272.5259.263

Neumann, M., Sampathu, D. M., Kwong, L. K., Truax, A. C., Micsenyi, M. C., Chou, T. T., Bruce, J., Schuck, T., Grossman, M., Clark, C. M., McCluskey, L. F., Miller, B. L., Masliah, E., Mackenzie, I. R., Feldman, H., Feiden, W., Kretzschmar, H. A., Trojanowski, J. Q., & Lee, V. M. Y. (2006). Ubiquitinated TDP-43 in frontotemporal lobar degeneration and amyotrophic lateral sclerosis. *Science*, *314*(5796), 130–133. https://doi.org/10.1126/science.1134108

Ng, S. kah, Higashimori, H., Tolman, M., & Yang, Y. (2015). Suppression of adenosine 2a receptor (A2aR)-mediated adenosine signaling improves disease phenotypes in a mouse model of amyotrophic lateral sclerosis. *Experimental Neurology*, *267*, 115–122. https://doi.org/10.1016/j.expneurol.2015.03.004

Nguyen, S., Meletis, K., Fu, D., Jhaveri, S., & Jaenisch, R. (2007). Ablation of de novo DNA methyltransferase Dnmt3a in the nervous system leads to neuromuscular defects and shortened lifespan. *Developmental Dynamics*, *236*(6), 1663–1676. https://doi.org/10.1002/DVDY.21176

Nicholson, K., Chan, J., Macklin, E. A., Levine-Weinberg, M., Breen, C., Bakshi, R., Grasso, D. L., Wills, A. M., Jahandideh, S., Taylor, A. A., Beaulieu, D., Ennist, D. L., Andronesi, O., Ratai, E. M., Schwarzschild, M. A., Cudkowicz, M., & Paganoni, S. (2018). Pilot trial of inosine to elevate urate levels in amyotrophic lateral sclerosis. *Annals of Clinical and Translational Neurology*, *5*(12), 1522–1533. https://doi.org/10.1002/ACN3.671

Nicholson, K., Paganoni, S., Shui, A., Schoenfeld, D., Sherman, A., Berry, J., Cudkowicz, M., & Atassi, N. (2015). Urate Levels Predict Disease Progression and Survival in Amyotrophic Lateral Sclerosis (ALS). (P6.100). *Neurology*, *84*(14).

Nihei, Y., Mori, K., Werner, G., Arzberger, T., Zhou, Q., Khosravi, B., Japtok, J., Hermann, A., Sommacal, A., Weber, M., Degeneration, G. C. for F. L., Alliance, B. B. B., Kamp, F., Nuscher, B., Edbauer, D., & Haass, C. (2020). Poly-glycine–alanine exacerbates C9orf72 repeat expansion-mediated DNA damage via sequestration of phosphorylated ATM and loss of nuclear hnRNPA3. *Acta Neuropathologica*, *139*(1), 99. https://doi.org/10.1007/S00401-019-02082-0

Niraula, A., Thapa, S., Kunwar, S., Lamsal, M., Baral, N., & Maskey, R. (2018). Adenosine deaminase activity in type 2 diabetes mellitus: does it have any role? *BMC Endocrine Disorders*, *18*(1). https://doi.org/10.1186/S12902-018-0284-9

Nofech-Mozes, Y., Blaser, S. I., Kobayashi, J., Grunebaum, E., & Roifman, C. M. (2007). Neurologic Abnormalities in Patients with Adenosine Deaminase Deficiency. *Pediatric Neurology*, *37*(3), 218–221. https://doi.org/10.1016/J.PEDIATRNEUROL.2007.03.011

Novitskiy, S. V., Ryzhov, S., Zaynagetdinov, R., Goldstein, A. E., Huang, Y., Tikhomirov, O. Y., Blackburn, M. R., Biaggioni, I., Carbone, D. P., Feoktistov, I., & Dikov, M. M. (2008). Adenosine receptors in regulation of dendritic cell differentiation and function. *Blood*, *112*(5), 1822–1831. https://doi.org/10.1182/BLOOD-2008-02-136325

O'Reilly, É. J., Bjornevik, K., Schwarzschild, M. A., McCullough, M. L., Kolonel, L. N., Le Marchand, L., Manson, J. E., & Ascherio, A. (2017). Pre-diagnostic plasma urate and the risk of amyotrophic lateral sclerosis. *Amyotrophic Lateral Sclerosis and Frontotemporal Dementia*, *19*(3–4), 194–200. https://doi.org/10.1080/21678421.2017.1418005

O'Rourke, J. G., Bogdanik, L., Yáñez, A., Lall, D., Wolf, A. J., Muhammad, A. K. M. G., Ho, R., Carmona, S., Vit, J. P., Zarrow, J., Kim, K. J., Bell, S., Harms, M. B., Miller, T. M., Dangler, C. A., Underhill, D. M., Goodridge, H. S., Lutz, C. M., & Baloh, R. H. (2016). C9orf72 is required for proper macrophage and microglial function in mice. *Science* , *351*(6279), 1329. https://doi.org/10.1126/SCIENCE.AAF1064

Oates, N., & Pamphlett, R. (2006). An epigenetic analysis of SOD1 and VEGF in ALS. *Amyotrophic Lateral Sclerosis*, *8*(2), 83–86. https://doi.org/10.1080/17482960601149160

Obata, T., Kubota, S., & Yamanaka, Y. (2001). Allopurinol suppresses para-nonylphenol and 1-methyl-4-phenylpyridinium ion (MPP+)-induced hydroxyl radical generation in rat striatum. *Neuroscience Letters*, *306*(1–2), 9–12. https://doi.org/10.1016/S0304-3940(01)01828-6

Oh, S., Baek, S., Park, J., Piao, L., Oh, K., & Kim, S. (2015). Prognostic Role of Serum Levels of Uric Acid in Amyotrophic Lateral Sclerosis. *Journal of Clinical Neurology (Seoul, Korea)*, *11*(4), 376–382. https://doi.org/10.3988/JCN.2015.11.4.376

Ombrello, A. K., Qin, J., Hoffmann, P. M., Kumar, P., Stone, D., Jones, A., Romeo, T., Barham, B., Pinto-Patarroyo, G., Toro, C., Soldatos, A., Zhou, Q., Deuitch, N., Aksentijevich, I., Sheldon, S. L., Kelly, S., Man, A., Barron, K., Hershfield, M., … Kastner, D. L. (2019). Treatment Strategies for Deficiency of Adenosine Deaminase 2. *New England Journal of Medicine*, *380*(16), 1582–1584. https://doi.org/10.1056/nejmc1801927

Onesti, E., Schettino, I., Gori, M. C., Frasca, V., Ceccanti, M., Cambieri, C., Ruoppolo, G., & Inghilleri, M. (2017). Dysphagia in amyotrophic lateral sclerosis: Impact on patient behavior, diet adaptation, and riluzole management. *Frontiers in Neurology*, *8*(MAR). https://doi.org/10.3389/fneur.2017.00094

Onesto, E., Colombrita, C., Gumina, V., Borghi, M. O., Dusi, S., Doretti, A., Fagiolari, G., Invernizzi, F., Moggio, M., Tiranti, V., Silani, V., & Ratti, A. (2016). Gene-specific mitochondria dysfunctions in human TARDBP and C9ORF72 fibroblasts. *Acta Neuropathologica Communications*, *4*(1), 47. https://doi.org/10.1186/S40478-016-0316-5/FIGURES/5

Orr, A. G., Orr, A. L., Li, X. J., Gross, R. E., & Traynelis, S. F. (2009). Adenosine A2A receptor mediates microglial process retraction. *Nature Neuroscience*, *12*(7), 872–878. https://doi.org/10.1038/nn.2341

Pacheco, R., Martinez-Navio, J. M., Lejeune, M., Climent, N., Oliva, H., Gatell, J. M., Gallart, T., Mallol, J., Lluis, C., & Franco, R. (2005). CD26, adenosine deaminase, and adenosine receptors mediate costimulatory signals in the immunological synapse. *Proceedings of the National Academy of Sciences*, *102*(27), 9583–9588. https://doi.org/10.1073/PNAS.0501050102

Pagani, M., Chiò, A., Valentini, M. C., Öberg, J., Nobili, F., Calvo, A., Moglia, C., Bertuzzo, D., Morbelli, S., De Carli, F., Fania, P., & Cistaro, A. (2014). Functional pattern of brain FDG-PET in amyotrophic lateral sclerosis. *Neurology*, *83*(12), 1067–1074. https://doi.org/10.1212/WNL.0000000000000792

Paganoni, S., Nicholson, K., Chan, J., Shui, A., Schoenfeld, D., Sherman, A., Berry, J., Cudkowicz, M., & Atassi, N. (2018). Urate levels predict survival in amyotrophic lateral sclerosis: Analysis of the expanded Pooled Resource Open-Access ALS clinical trials database. *Muscle & Nerve*, *57*(3), 430–434. https://doi.org/10.1002/MUS.25950

Paganoni, S., Zhang, M., Zárate, A. Q., Jaffa, M., Yu, H., Cudkowicz, M. E., & Wills, A. M. (2012). Uric acid levels predict survival in men with amyotrophic lateral sclerosis. *Journal of Neurology*, *259*(9), 1923–1928. https://doi.org/10.1007/s00415-012-6440-7

Pajski, M. L., & Venton, B. J. (2010). Adenosine release evoked by short electrical stimulations in striatal brain slices is primarily activity dependent. *ACS Chemical Neuroscience*, *1*(12), 775–787. https://doi.org/10.1021/CN100037D/SUPPL_FILE/CN100037D_SI_001.PDF

Palfi, S., Gurruchaga, J. M., Lepetit, H., Howard, K., Ralph, G. S., Mason, S., Gouello, G., Domenech, P., Buttery, P. C., Hantraye, P., Tuckwell, N. J., Barker, R. A., & Mitrophanous, K. A. (2018). Long-Term Follow-Up of a Phase I/II Study of ProSavin, a Lentiviral Vector Gene Therapy for Parkinson's Disease. *Human Gene Therapy. Clinical Development*, *29*(3), 148. https://doi.org/10.1089/HUMC.2018.081

Palfi, S., Gurruchaga, J. M., Scott Ralph, G., Lepetit, H., Lavisse, S., Buttery, P. C., Watts, C., Miskin, J., Kelleher, M., Deeley, S., Iwamuro, H., Lefaucheur, J. P., Thiriez, C., Fenelon, G., Lucas, C., Brugières, P., Gabriel, I., Abhay, K., Drouot, X., … Mitrophanous, K. A. (2014). Long-term safety and tolerability of ProSavin, a lentiviral vector-based gene therapy for Parkinson's disease: A dose escalation, open-label, phase 1/2 trial. *The Lancet*, *383*(9923), 1138–1146. https://doi.org/10.1016/S0140-6736(13)61939-X

Pang, W., & Hu, F. (2021). Cellular and physiological functions of C9ORF72 and implications for ALS/FTD. *Journal of Neurochemistry*, *157*(3), 334–350. https://doi.org/10.1111/JNC.15255

Park, H. R., & Yang, E. J. (2021). Oxidative Stress as a Therapeutic Target in Amyotrophic Lateral Sclerosis: Opportunities and Limitations. *Diagnostics 2021*, *11*(9), 1546. https://doi.org/10.3390/DIAGNOSTICS11091546

Pedley, A. M., & Benkovic, S. J. (2017). A New View into the Regulation of Purine Metabolism: The Purinosome. *Trends in Biochemical Sciences*, *42*(2), 141–154. https://doi.org/10.1016/J.TIBS.2016.09.009

Pedley, A. M., Boylan, J. P., Chan, C. Y., Kennedy, E. L., Kyoung, M., & Benkovic, S. J. (2022). Purine biosynthetic enzymes assemble into liquid-like condensates dependent on the activity of chaperone protein HSP90. *Journal of Biological Chemistry*, *298*(5).

Pellerin, L., & Magistretti, P. J. (1994). Glutamate uptake into astrocytes stimulates aerobic glycolysis: A mechanism coupling neuronal activity to glucose utilization. *Proceedings of the National Academy of Sciences of the United States of America*, *91*(22), 10625–10629. https://doi.org/10.1073/pnas.91.22.10625

Petersen, M. B., Tranebjaerg, L., Tommerup, N., Nygaard, P., & Edwards, H. (1987). New assignment of the adenosine deaminase gene locus to chromosome 20q13·11 by study of a patient with interstitial deletion 20q. *Journal of Medical Genetics*, *24*(2), 93–96. https://doi.org/10.1136/jmg.24.2.93

Petri, S., Körner, S., & Kiaei, M. (2012). Nrf2/ARE signaling pathway: Key mediator in oxidative stress and potential therapeutic target in ALS. *Neurology Research International*. https://doi.org/10.1155/2012/878030

Pozniak, C. D., Radinovic, S., Yang, A., McKeon, F., Kaplan, D. R., & Miller, F. D. (2000). An Anti-Apoptotic Role for the p53 Family Member, p73, During Developmental Neuron Death. *Science*, *289*(5477), 304–306. https://doi.org/10.1126/SCIENCE.289.5477.304

Rahman, M. R., Islam, T., Huq, F., Quinn, J. M. W., & Moni, M. A. (2019). Identification of molecular signatures and pathways common to blood cells and brain tissue of amyotrophic lateral sclerosis patients. *Informatics in Medicine Unlocked*, *16*, 100193. https://doi.org/10.1016/J.IMU.2019.100193

Ratech, H., Thorbecke, G. J., Meredith, G., & Hirschhorn, R. (1981). Comparison and possible homology of isozymes of adenosine deaminase in aves and humans. *Enzyme*, *26*(2), 74–84. https://doi.org/10.1159/000459153

Re, D. B., Le Verche, V., Yu, C., Amoroso, M. W., Politi, K. A., Phani, S., Ikiz, B., Hoffmann, L., Koolen, M., Nagata, T., Papadimitriou, D., Nagy, P., Mitsumoto, H., Kariya, S., Wichterle, H., Henderson, C. E., & Przedborski, S. (2014). Necroptosis Drives Motor Neuron Death in Models of Both Sporadic and Familial ALS. *Neuron*, *81*(5), 1001–1008. https://doi.org/10.1016/J.NEURON.2014.01.011

Reddy, K., Zamiri, B., Stanley, S. Y. R., Macgregor, R. B., & Pearson, C. E. (2013). The disease-associated r(GGGGCC)n repeat from the C9orf72 gene forms tract length-dependent uni- and multimolecular RNA G-quadruplex structures. *Journal of Biological Chemistry*, *288*(14), 9860–9866. https://doi.org/10.1074/jbc.C113.452532

Ren, X., & Chen, J. (2020). Caffeine and Parkinson's Disease: Multiple Benefits and Emerging Mechanisms. *Frontiers in Neuroscience*, *14*. https://doi.org/10.3389/FNINS.2020.602697

Riazi, M. A., Brinkman-Mills, P., Nguyen, T., Pan, H., Phan, S., Ying, F., Roe, B. A., Tochigi, J., Shimizu, Y., Minoshima, S., Shimizu, N., Buchwald, M., & McDermid, H. E. (2000). The human homolog of insect-derived growth factor, CECR1, is a candidate gene for features of cat eye syndrome. *Genomics*, *64*(3), 277–285. https://doi.org/10.1006/geno.1999.6099

Ricciuti, F. C., & Ruddle, F. H. (1973). ASSIGNMENT OF THREE GENE LOCI (PGK, HGPRT, G6PD) TO THE LONG ARM OF THE HUMAN X CHROMOSOME BY SOMATIC CELL GENETICS. *Genetics*, *74*(4), 661–678. https://doi.org/10.1093/GENETICS/74.4.661

Rizzu, P., Blauwendraat, C., Heetveld, S., Lynes, E. M., Castillo-Lizardo, M., Dhingra, A., Pyz, E., Hobert, M., Synofzik, M., Simón-Sánchez, J., Francescatto, M., & Heutink, P. (2016). C9orf72 is differentially expressed in the central nervous system and myeloid cells and consistently reduced in C9orf72, MAPT and GRN mutation carriers. *Acta Neuropathologica Communications*, *4*(1), 37. https://doi.org/10.1186/S40478-016-0306-7/TABLES/3

Rogakou, E. P., Boon, C., Redon, C., & Bonner, W. M. (1999). Megabase Chromatin Domains Involved in DNA Double-Strand Breaks in Vivo. *Journal of Cell Biology*, *146*(5), 905–916. https://doi.org/10.1083/JCB.146.5.905

Rogers, M., Lwin, R., Fairbanks, L., Gerritsen, B., & Gaspar, H. (2001). Cognitive and behavioral abnormalities in adenosine deaminase deficient severe combined immunodeficiency. *The Journal of Pediatrics*, *139*(1), 44–50. https://doi.org/10.1067/MPD.2001.115023

Roglic, G. (2016). WHO Global report on diabetes: A summary. *International Journal of Noncommunicable Diseases*, *1*(1), 3. https://www.ijncd.org/article.asp?issn=2468-8827;year=2016;volume=1;issue=1;spage=3;epage=8;aulast=Roglic

Rosen, D. R., Siddique, T., Patterson, D., Figlewicz, D. A., Sapp, P., Hentati, A., Donaldson, D., Goto, J., O'Regan, J. P., Deng, H.-X., Rahmani, Z., Krizus, A., McKenna-Yasek, D., Cayabyab, A., Gaston, S. M., Berger, R., Tanzi, R. E., Halperin, J. J., Herzfeldt, B., … Brown, R. H. (1993). Mutations in Cu/Zn superoxide dismutase gene are associated with familial amyotrophic lateral sclerosis. *Nature*, *362*(6415), 59–62. https://doi.org/10.1038/362059a0

Rudolphi, K. A., Schubert, P., Parkinson, F. E., & Fredholm, B. B. (1992). Adenosine and brain ischemia. In *Cerebrovascular and brain metabolism reviews* (Vol. 4, Issue 4, pp. 346–369). https://doi.org/10.1007/978-1-4615-2011-5_43

Rusconi, M., Gerardi, F., Santus, W., Lizio, A., Sansone, V. A., Lunetta, C., Zanoni, I., & Granucci, F. (2017). Inflammatory role of dendritic cells in Amyotrophic Lateral Sclerosis revealed by an analysis of patients' peripheral blood. *Scientific Reports*, *7*(1). https://doi.org/10.1038/S41598-017-08233-1

Russell, K. L., Downie, J. M., Gibson, S. B., Tsetsou, S., Keefe, M. D., Duran, J. A., Figueroa, K. P., Bromberg, M. B., Murtaugh, L. C., Bonkowsky, J. L., Pulst, S. M., & Jorde, L. B. (2021). Pathogenic Effect of TP73 Gene Variants in People With Amyotrophic Lateral Sclerosis. *Neurology*, *97*(3), e225–e235. https://doi.org/10.1212/WNL.0000000000012285

Rutkiewicz, J., & Górski, J. (1990). On the role of insulin in regulation of adenosine deaminase activity in rat tissues. *FEBS Letters*, *271*(1–2), 79–80. https://doi.org/10.1016/0014-5793(90)80376-T

Ryan, M., Heverin, M., Pender, N., McLaughlin, R., & Hardiman, O. (2019). Heritability of ALS: A Population-based study over 24 years. (S54.001). *Neurology*, *92*(15

Supplement).

Sabatelli, M., Conte, A., & Zollino, M. (2013). Clinical and genetic heterogeneity of amyotrophic lateral sclerosis. *Clinical Genetics*, *83*(5), 408–416. https://doi.org/10.1111/CGE.12117

Samari, H. R., & Seglen, P. O. (1998). Inhibition of Hepatocytic Autophagy by Adenosine, Aminoimidazole-4-carboxamide Riboside, and N 6-Mercaptopurine Riboside: EVIDENCE FOR INVOLVEMENT OF AMP-ACTIVATED PROTEIN KINASE. *Journal of Biological Chemistry*, *273*(37), 23758–23763. https://doi.org/10.1074/JBC.273.37.23758

Santisteban, I., Arredondo-Vega, F. X., Kelly, S., Loubser, M., Meydan, N., Roifman, C., Howell, P., Bowen, T., Weinberg, K., & Schroeder, M. (1995). Three new adenosine deaminase mutations that define a splicing enhancer and cause severe and partial phenotypes: implications for evolution of a CpG hotspot and expression of a transduced ADA cDNA. *Human Molecular Genetics*, *4*(11), 2081–2087. https://doi.org/10.1093/HMG/4.11.2081

Santisteban, I., Arredondo-Vega, F. X., Kelly, S., Mary, A., Fischer, A., Hummell, D. S., Lawton, A., Sorensen, R. U., Stiehm, E. R., & Uribe, L. (1993). Novel splicing, missense, and deletion mutations in seven adenosine deaminase-deficient patients with late/delayed onset of combined immunodeficiency disease. Contribution of genotype to phenotype. *The Journal of Clinical Investigation*, *92*(5), 2291–2302. https://doi.org/10.1172/JCI116833

Sareen, D., O'Rourke, J. G., Meera, P., Muhammad, A. K. M. G., Grant, S., Simpkinson, M., Bell, S., Carmona, S., Ornelas, L., Sahabian, A., Gendron, T., Petrucelli, L., Baughn, M., Ravits, J., Harms, M. B., Rigo, F., Frank Bennett, C., Otis, T. S., Svendsen, C. N., & Baloh, R. H. (2013). Targeting RNA foci in iPSC-derived motor neurons from ALS patients with a C9ORF72 repeat expansion. *Science Translational Medicine*, *5*(208). https://doi.org/10.1126/SCITRANSLMED.3007529/SUPPL_FILE/5-208RA149_SM.PDF

Sasaki, S., & Iwata, M. (1996). Ultrastructural study of synapses in the anterior horn neurons of patients with amyotrophic lateral sclerosis. *Neuroscience Letters*, *204*(1–2), 53–56. https://doi.org/10.1016/0304-3940(96)12314-4

Sauer, A. V., Hernandez, R. J., Fumagalli, F., Bianchi, V., Poliani, P. L., Dallatomasina, C., Riboni, E., Politi, L. S., Tabucchi, A., Carlucci, F., Casiraghi, M., Carriglio, N., Cominelli, M., Forcellini, C. A., Barzaghi, F., Ferrua, F., Minicucci, F., Medaglini, S., Leocani, L., … Aiuti, A. (2017). Alterations in the brain adenosine metabolism cause behavioral and neurological impairment in ADA-deficient mice and patients. *Scientific Reports*, *7*(1), 1–

13. https://doi.org/10.1038/srep40136

Sbisà, E., Mastropasqua, G., Lefkimmiatis, K., Caratozzolo, M. F., D'Erchia, A. M., & Tullo, A. (2006). Connecting p63 to Cellular Proliferation: The Example of the Adenosine Deaminase Target Gene. *Cell Cycle*, *5*(2), 205–212. https://doi.org/10.4161/CC.5.2.2361

Schiffer, D., Cordera, S., Cavalla, P., & Migheli, A. (1996). Reactive astrogliosis of the spinal cord in amyotrophic lateral sclerosis. *Journal of the Neurological Sciences*, *139*(Supplement), 27–33. https://doi.org/10.1016/0022-510X(96)00073-1

Schipper, L. J., Raaphorst, J., Aronica, E., Baas, F., de Haan, R., de Visser, M., & Troost, D. (2016). Prevalence of brain and spinal cord inclusions, including dipeptide repeat proteins, in patients with the C9ORF72 hexanucleotide repeat expansion: a systematic neuropathological review. *Neuropathology and Applied Neurobiology*, *42*(6), 547–560. https://doi.org/10.1111/NAN.12284

Schludi, M. H., Becker, L., Garrett, L., Gendron, T. F., Zhou, Q., Schreiber, F., Popper, B., Dimou, L., Strom, T. M., Winkelmann, J., von Thaden, A., Rentzsch, K., May, S., Michaelsen, M., Schwenk, B. M., Tan, J., Schoser, B., Dieterich, M., Petrucelli, L., … Edbauer, D. (2017). Spinal poly-GA inclusions in a C9orf72 mouse model trigger motor deficits and inflammation without neuron loss. *Acta Neuropathologica*, *134*(2), 241–254. https://doi.org/10.1007/S00401-017-1711-0/FIGURES/5

Schludi, M. H., May, S., Grässer, F. A., Rentzsch, K., Kremmer, E., Küpper, C., Klopstock, T., Ceballos-Baumann, A., Danek, A., Diehl-Schmid, J., Fassbender, K., Förstl, H., Kornhuber, J., Otto, M., Dieterich, M., Feuerecker, R., Giese, A., Klünemann, H., Kurz, A., … Roeber, S. (2015). Distribution of dipeptide repeat proteins in cellular models and C9orf72 mutation cases suggests link to transcriptional silencing. *Acta Neuropathologica*, *130*(4), 537–555. https://doi.org/10.1007/S00401-015-1450-Z/FIGURES/8

Schmitz, A., Pinheiro Marques, J., Oertig, I., Maharjan, N., & Saxena, S. (2021). Emerging Perspectives on Dipeptide Repeat Proteins in C9ORF72 ALS/FTD. *Frontiers in Cellular Neuroscience*, *15*, 3. https://doi.org/10.3389/FNCEL.2021.637548/BIBTEX

Schrader, W. P., Pollara, B., & Meuwissen, H. J. (1978). Characterization of the residual adenosine deaminating activity in the spleen of a patient with combined immunodeficiency disease and adenosine deaminase deficiency. *Proceedings of the National Academy of Sciences*, *75*(1), 446–450. https://doi.org/10.1073/PNAS.75.1.446

Scott, O., Kim, V., Reid, B., Pham-Huy, A., Atkinson, A., Aiuti, A., & Grunebaum, E. (2017). Long-Term Outcome of Adenosine Deaminase-Deficient Patients-a Single-Center Experience. *Journal of Clinical Immunology*, *37*(6), 582–591. https://doi.org/10.1007/S10875-017-0421-7

Sebastião, A., de Mendonca, A., Moreira, T., & Ribeiro, J. (2001). Activation of synaptic NMDA receptors by action potential-dependent release of transmitter during hypoxia impairs recovery of synaptic transmission on reoxygenation. *The Journal of Neuroscience : The Official Journal of the Society for Neuroscience*, *21*(21), 8564–8571. https://doi.org/10.1523/JNEUROSCI.21-21-08564.2001

Sellier, C., Campanari, M.-L., Corbier, C. J., Gaucherot, A., Kolb-Cheynel, I., Oulad-Abdelghani, M., Ruffenach, F., Page, A., Ciura, S., Kabashi, E., & Charlet-Berguerand, N. (2016). Loss of C9ORF72 impairs autophagy and synergizes with polyQ Ataxin-2 to induce motor neuron dysfunction and cell death. *The EMBO Journal*, *35*(12), 1276–1297. https://doi.org/10.15252/EMBJ.201593350

Shao, Q., Liang, C., Chang, Q., Zhang, W., Yang, M., & Chen, J. F. (2019). C9orf72 deficiency promotes motor deficits of a C9ALS/FTD mouse model in a dose-dependent manner. *Acta Neuropathologica Communications*, *7*(1), 32. https://doi.org/10.1186/S40478-019-0685-7/FIGURES/1

Shao, Q., Yang, M., Liang, C., Ma, L., Zhang, W., Jiang, Z., Luo, J., Lee, J. K., Liang, C., & Chen, J. F. (2020). C9orf72 and smcr8 mutant mice reveal MTORC1 activation due to impaired lysosomal degradation and exocytosis. *Autophagy*, *16*(9), 1635–1650. https://doi.org/10.1080/15548627.2019.1703353/SUPPL_FILE/KAUP_A_1703353_SM2447.ZIP

Shearer, R. F., & Saunders, D. N. (2015). Experimental design for stable genetic manipulation in mammalian cell lines: lentivirus and alternatives. *Genes to Cells*, *20*(1), 1–10. https://doi.org/10.1111/GTC.12183

Shekhar, S., & Dey, S. (2019). Induction of p73, Δ133p53, Δ160p53, pAKT lead to neuroprotection via DNA repair by 5-LOX inhibition. *Molecular Biology Reports 2019 47:1*, *47*(1), 269–274. https://doi.org/10.1007/S11033-019-05127-5

Sherrill-Mix, S., Lewinski, M. K., Famiglietti, M., Bosque, A., Malani, N., Ocwieja, K. E., Berry, C. C., Looney, D., Shan, L., Agosto, L. M., Pace, M. J., Siliciano, R. F., O'Doherty, U., Guatelli, J., Planelles, V., & Bushman, F. D. (2013). HIV latency and integration site placement in five cell-based models. *Retrovirology*, *10*(1), 90. https://doi.org/10.1186/1742-4690-10-90

Shi, K. Y., Mori, E., Nizami, Z. F., Lin, Y., Kato, M., Xiang, S., Wu, L. C., Ding, M., Yu, Y., Gall, J. G., & McKnight, S. L. (2017). Toxic PRn poly-dipeptides encoded by the C9orf72 repeat expansion block nuclear import and export. *Proceedings of the National Academy of Sciences of the United States of America*, *114*(7), E1111–E1117. https://doi.org/10.1073/PNAS.1620293114/SUPPL_FILE/PNAS.201620293SI.PDF

Shi, Y., Lin, S., Staats, K. A., Li, Y., Chang, W. H., Hung, S. T., Hendricks, E., Linares, G. R., Wang, Y., Son, E. Y., Wen, X., Kisler, K., Wilkinson, B., Menendez, L., Sugawara, T., Woolwine, P., Huang, M., Cowan, M. J., Ge, B., … Ichida, J. K. (2018). Haploinsufficiency leads to neurodegeneration in C9ORF72 ALS/FTD human induced motor neurons. *Nature Medicine*, *24*(3), 313–325. https://doi.org/10.1038/nm.4490

Siklós, L., Engelhardt, J., Harati, Y., Smith, R. G., Joó, F., & Appel, S. H. (1996). Ultrastructural evidence for altered calcium in motor nerve terminals in amyotrophic lateral sclerosis. *Annals of Neurology*, *39*(2), 203–216. https://doi.org/10.1002/ana.410390210

Sinn, P. L., Sauter, S. L., & McCray, P. B. (2005). Gene Therapy Progress and Prospects: Development of improved lentiviral and retroviral vectors – design, biosafety, and production. *Gene Therapy* , *12*(14), 1089–1098. https://doi.org/10.1038/sj.gt.3302570

Sitkovsky, M. V., & Ohta, A. (2005). The 'danger' sensors that STOP the immune response: the A2 adenosine receptors? *Trends in Immunology*, *26*(6), 299–304. https://doi.org/10.1016/J.IT.2005.04.004

Skaldin, M., Tuittila, M., Zavialov, A. V, & Zavialov, A. V. (2018). Secreted Bacterial Adenosine Deaminase Is an Evolutionary Precursor of Adenosine Deaminase Growth Factor. *Molecular Biology and Evolution*, *35*(12), 2851–2861. https://doi.org/10.1093/MOLBEV/MSY193

Smith, C. M., & Frank Henderson, J. (1982). Deoxyadenosine triphosphate accumulation in erythrocytes of deoxycoformycin-treated mice. *Biochemical Pharmacology*, *31*(8), 1545–1551. https://doi.org/10.1016/0006-2952(82)90379-3

Sreedharan, J., Blair, I. P., Tripathi, V. B., Hu, X., Vance, C., Rogelj, B., Ackerley, S., Durnall, J. C., Williams, K. L., Buratti, E., Baralle, F., De Belleroche, J., Mitchell, J. D., Leigh, P. N., Al-Chalabi, A., Miller, C. C., Nicholson, G., & Shaw, C. E. (2008). TDP-43 mutations in familial and sporadic amyotrophic lateral sclerosis. *Science (New York, N.Y.)*, *319*(5870), 1668–1672. https://doi.org/10.1126/SCIENCE.1154584

Staknis, D., & Reed, R. (1994). SR proteins promote the first specific recognition of Pre-

mRNA and are present together with the U1 small nuclear ribonucleoprotein particle in a general splicing enhancer complex. *Molecular and Cellular Biology*, *14*(11), 7670–7682. https://doi.org/10.1128/MCB.14.11.7670-7682.1994

Steyn, F. J., Ioannides, Z. A., Van Eijk, R. P. A., Heggie, S., Thorpe, K. A., Ceslis, A., Heshmat, S., Henders, A. K., Wray, N. R., Van Den Berg, L. H., Henderson, R. D., McCombe, P. A., & Ngo, S. T. (2018). Hypermetabolism in ALS is associated with greater functional decline and shorter survival. *Journal of Neurology, Neurosurgery and Psychiatry*, *89*(10), 1016–1023. https://doi.org/10.1136/jnnp-2017-317887

Stoccoro, A., Mosca, L., Carnicelli, V., Cavallari, U., Lunetta, C., Marocchi, A., Migliore, L., & Coppedè, F. (2018). Mitochondrial DNA copy number and D-loop region methylation in carriers of amyotrophic lateral sclerosis gene mutations. *Epigenomics*, *10*(11), 1431–1443. https://doi.org/10.2217/EPI-2018-0072

Stoccoro, A., Smith, A. R., Mosca, L., Marocchi, A., Gerardi, F., Lunetta, C., Cereda, C., Gagliardi, S., Lunnon, K., Migliore, L., & Coppedè, F. (2020). Reduced mitochondrial D-loop methylation levels in sporadic amyotrophic lateral sclerosis. *Clinical Epigenetics*, *12*(1). https://doi.org/10.1186/S13148-020-00933-2

Stubbs, G., Litt, M., Lis, E., Jackson, R., Voth, W., Lindberg, A., & Litt, R. (1982). Adenosine deaminase activity decreased in autism. *Journal of the American Academy of Child Psychiatry*, *21*(1), 71–74. https://doi.org/10.1097/00004583-198201000-00012

Sullivan, P. M., Zhou, X., Robins, A. M., Paushter, D. H., Kim, D., Smolka, M. B., & Hu, F. (2016). The ALS/FTLD associated protein C9orf72 associates with SMCR8 and WDR41 to regulate the autophagy-lysosome pathway. *Acta Neuropathologica Communications*, *4*(1), 51. https://doi.org/10.1186/S40478-016-0324-5/FIGURES/10

Suzuki, H., & Matsuoka, M. (2021). Proline-arginine poly-dipeptide encoded by the C9orf72 repeat expansion inhibits adenosine deaminase acting on RNA. *Journal of Neurochemistry*, *158*(3), 753–765. https://doi.org/10.1111/JNC.15445

Suzuki, H., Shibagaki, Y., Hattori, S., & Matsuoka, M. (2019). C9-ALS/FTD-linked proline–arginine dipeptide repeat protein associates with paraspeckle components and increases paraspeckle formation. *Cell Death & Disease* , *10*(10), 1–16. https://doi.org/10.1038/s41419-019-1983-5

Takahashi, F., Kano, O., Nagano, Y., Yoneoka, T., Nelson, S., & Ushirogawa, Y. (2022). Associations between urate levels and amyotrophic lateral sclerosis functional score with edaravone treatment: Post hoc analysis of studies MCI186-16, MCI186-17, and

MCI186-19. *Muscle & Nerve*, *66*(5), 583–592. https://doi.org/10.1002/MUS.27699

Tamura, R., Ohta, H., Satoh, Y., Nonoyama, S., Nishida, Y., & Nibuya, M. (2015). Neuroprotective effects of adenosine deaminase in the striatum. *Journal of Cerebral Blood Flow and Metabolism*, *36*(4), 709–720. https://doi.org/10.1177/0271678X15625077/ASSET/IMAGES/LARGE/10.1177_0271678X15625077-FIG2.JPEG

Tanaka, C., Hara, T., Suzaki, I., Maegaki, Y., & Takeshita, K. (1996). Sensorineural deafness in siblings with adenosine deaminase deficiency. *Brain and Development*, *18*(4), 304–306. https://doi.org/10.1016/0387-7604(96)00014-9

Tanaka, K., Watakabe, A., & Shimura, Y. (1994). Polypurine sequences within a downstream exon function as a splicing enhancer. *Molecular and Cellular Biology*, *14*(2), 1347–1354. https://doi.org/10.1128/MCB.14.2.1347-1354.1994

Tang, D., Li, B., Xu, T., Hu, R., Tan, D., Song, X., Jia, P., & Zhao, Z. (2020). VISDB: a manually curated database of viral integration sites in the human genome. *Nucleic Acids Research*, *48*(D1), D633. https://doi.org/10.1093/NAR/GKZ867

Tao, Z., Wang, H., Xia, Q., Li, K., Li, K., Jiang, X., Xu, G., Wang, G., & Ying, Z. (2015). Nucleolar stress and impaired stress granule formation contribute to C9orf72 RAN translation-induced cytotoxicity. *Human Molecular Genetics*, *24*(9), 2426–2441. https://doi.org/10.1093/HMG/DDV005

Therrien, M., Rouleau, G. A., Dion, P. A., & Parker, J. A. (2013). Deletion of C9ORF72 Results in Motor Neuron Degeneration and Stress Sensitivity in C. elegans. *PLOS ONE*, *8*(12), e83450. https://doi.org/10.1371/JOURNAL.PONE.0083450

Tian, M., & Maniatis, T. (1993). A splicing enhancer complex controls alternative splicing of doublesex pre-mRNA. *Cell*, *74*(1), 105–114. https://doi.org/10.1016/0092-8674(93)90298-5

Tian, M., & Maniatis, T. (1994). A splicing enhancer exhibits both constitutive and regulated activities. *Genes & Development*, *8*(14), 1703–1712. https://doi.org/10.1101/GAD.8.14.1703

Tissir, F., Ravni, A., Achouri, Y., Riethmacher, D., Meyer, G., & Goffinet, A. M. (2009). DeltaNp73 regulates neuronal survival in vivo. *Proceedings of the National Academy of Sciences*, *106*(39), 16871–16876. https://doi.org/10.1073/PNAS.0903191106

Titman, P., Pink, E., Skucek, E., O'Hanlon, K., Cole, T. J., Gaspar, J., Xu-Bayford, J., Jones,

A., Thrasher, A. J., Davies, E. G., Veys, P. A., & Gaspar, H. B. (2008). Cognitive and behavioral abnormalities in children after hematopoietic stem cell transplantation for severe congenital immunodeficiencies. *Blood*, *112*(9), 3907–3913. https://doi.org/10.1182/BLOOD-2008-04-151332

Tremolizzo, L., Messina, P., Conti, E., Sala, G., Cecchi, M., Airoldi, L., Pastorelli, R., Pupillo, E., Poggio, M. B. Di, Filosto, M., Lunetta, C., Agliardi, C., Guerini, F., Mandrioli, J., Calvo, A., Beghi, E., Ferrarese, C., Consortium, E., Cotelli, M. S., … Pisa, F. (2014). Whole-blood global DNA methylation is increased in amyotrophic lateral sclerosis independently of age of onset. *Amyotrophic Lateral Sclerosis and Frontotemporal Dementia*, *15*(1–2), 98–105. https://doi.org/10.3109/21678421.2013.851247

Tritsch, G., & Niswander, P. (1981). Adenosine deaminase activity and superoxide formation during phagocytosis and membrane perturbation of macrophages. *Immunological Communications*, *10*(1), 1–7. https://doi.org/10.3109/08820138109050681

Troakes, C., Maekawa, S., Wijesekera, L., Rogelj, B., Siklós, L., Bell, C., Smith, B., Newhouse, S., Vance, C., Johnson, L., Hortobágyi, T., Shatunov, A., Al-Chalabi, A., Leigh, N., Shaw, C. E., King, A., & Al-Sarraj, S. (2012). An MND/ALS phenotype associated with C9orf72 repeat expansion: Abundant p62-positive, TDP-43-negative inclusions in cerebral cortex, hippocampus and cerebellum but without associated cognitive decline. *Neuropathology*, *32*(5), 505–514. https://doi.org/10.1111/J.1440-1789.2011.01286.X

Trussell, L. O., & Jackson, M. B. (1985). Adenosine-activated potassium conductance in cultured striatal neurons. *Proceedings of the National Academy of Sciences of the United States of America*, *82*(14), 4857. https://doi.org/10.1073/PNAS.82.14.4857

Tsai, C., Lee, J., & Lee, C. (2019). Type II diabetes mellitus and the incidence of amyotrophic lateral sclerosis. *Journal of Neurology*, *266*(9), 2233–2243. https://doi.org/10.1007/S00415-019-09405-X

Tullo, A., Mastropasqua, G., Bourdon, J. C., Centonze, P., Gostissa, M., Costanzo, A., Levrero, M., Del Sal, G., Saccone, C., & Sbisà, E. (2003). Adenosine deaminase, a key enzyme in DNA precursors control, is a new p73 target. *Oncogene*, *22*(54), 8738–8748. https://doi.org/10.1038/sj.onc.1206967

Tumini, E., Porcellini, E., Chiappelli, M., Conti, C. M., Beraudi, A., Poli, A., Caciagli, F., Doyle, R., Conti, P., & Licastro, F. (2007). The G51S purine nucleoside phosphorylase polymorphism is associated with cognitive decline in Alzheimer's disease patients. *Human Psychopharmacology: Clinical and Experimental*, *22*(2), 75–80.

https://doi.org/10.1002/HUP.823

Ugolino, J., Ji, Y. J., Conchina, K., Chu, J., Nirujogi, R. S., Pandey, A., Brady, N. R., Hamacher-Brady, A., & Wang, J. (2016). Loss of C9orf72 Enhances Autophagic Activity via Deregulated mTOR and TFEB Signaling. *PLOS Genetics*, *12*(11), e1006443. https://doi.org/10.1371/JOURNAL.PGEN.1006443

Ungerer, J. P., Oosthuizen, H. M., Bissbort, S. H., & Vermaak, W. J. (1992). Serum Adenosine Deaminase: Isoenzymes and Diagnostic Application. *Clinical Chemistry*, *38*(7), 1322–1326. https://doi.org/10.1093/CLINCHEM/38.7.1322

Valbuena, G. N., Rizzardini, M., Cimini, S., Siskos, A. P., Bendotti, C., Cantoni, L., & Keun, H. C. (2016). Metabolomic Analysis Reveals Increased Aerobic Glycolysis and Amino Acid Deficit in a Cellular Model of Amyotrophic Lateral Sclerosis. *Molecular Neurobiology*, *53*(4), 2222–2240. https://doi.org/10.1007/S12035-015-9165-7/FIGURES/12

Valbuena, G. N., Tortarolo, M., Bendotti, C., Cantoni, L., & Keun, H. C. (2017). Altered Metabolic Profiles Associate with Toxicity in SOD1G93A Astrocyte-Neuron Co-Cultures. *Scientific Reports*, *7*(1), 1–14. https://doi.org/10.1038/s41598-017-00072-4

van Blitterswijk, M., Gendron, T. F., Baker, M. C., DeJesus-Hernandez, M., Finch, N. C. A., Brown, P. H., Daughrity, L. M., Murray, M. E., Heckman, M. G., Jiang, J., Lagier-Tourenne, C., Edbauer, D., Cleveland, D. W., Josephs, K. A., Parisi, J. E., Knopman, D. S., Petersen, R. C., Petrucelli, L., Boeve, B. F., … Rademakers, R. (2015). Novel clinical associations with specific C9ORF72 transcripts in patients with repeat expansions in C9ORF72. *Acta Neuropathologica*, *130*(6), 863–876. https://doi.org/10.1007/S00401-015-1480-6/TABLES/6

Van Der Weyden, M. B., & Kelley, W. N. (1976). Human adenosine deaminase. Distribution and properties. *Journal of Biological Chemistry*, *251*(18), 5448–5456. https://doi.org/10.1016/s0021-9258(17)33080-6

Van Linden, A., & Eltzschig, H. (2007). Role of pulmonary adenosine during hypoxia: extracellular generation, signaling and metabolism by surface adenosine deaminase/CD26. *Expert Opinion on Biological Therapy*, *7*(9), 1437–1447. https://doi.org/10.1517/14712598.7.9.1437

Vance, C., Rogelj, B., Hortobágyi, T., De Vos, K. J., Nishimura, A. L., Sreedharan, J., Hu, X., Smith, B., Ruddy, D., Wright, P., Ganesalingam, J., Williams, K. L., Tripathi, V., Al-Saraj, S., Al-Chalabi, A., Leigh, P. N., Blair, I. P., Nicholson, G., De Belleroche, J., …

Shaw, C. E. (2009). Mutations in FUS, an RNA processing protein, cause familial amyotrophic lateral sclerosis type 6. *Science*, *323*(5918), 1208–1211. https://doi.org/10.1126/SCIENCE.1165942/SUPPL_FILE/VANCE_SOM.PDF

Vandoorne, T., De Bock, K., & Van Den Bosch, L. (2018). Energy metabolism in ALS: an underappreciated opportunity? In *Acta Neuropathologica* (Vol. 135, Issue 4). https://doi.org/10.1007/s00401-018-1835-x

Vannucci, L., Lai, M., Chiuppesi, F., Ceccherini-Nelli, L., & Pistello, M. (2013). Viral vectors: a look back and ahead on gene transfer technology. *New Microbiologica*, *36*, 1–22. www.wiley.co.uk/genmed/clinical

Varcianna, A., Myszczynska, M. A., Castelli, L. M., O'Neill, B., Kim, Y., Talbot, J., Nyberg, S., Nyamali, I., Heath, P. R., Stopford, M. J., Hautbergue, G. M., & Ferraiuolo, L. (2019). Micro-RNAs secreted through astrocyte-derived extracellular vesicles cause neuronal network degeneration in C9orf72 ALS. *EBioMedicine*, *40*, 626–635. https://doi.org/10.1016/J.EBIOM.2018.11.067

Vargas, M. R., & Johnson, J. A. (2010). Astrogliosis in Amyotrophic Lateral Sclerosis: Role and Therapeutic Potential of Astrocytes. *Neurotherapeutics*, *7*(4), 471–481. https://doi.org/10.1016/j.nurt.2010.05.012

Vatsavayai, S. C., Nana, A. L., Yokoyama, J. S., & Seeley, W. W. (2018). C9orf72-FTD/ALS pathogenesis: evidence from human neuropathological studies. *Acta Neuropathologica* , *137*(1), 1–26. https://doi.org/10.1007/S00401-018-1921-0

Vatsavayai, S. C., Yoon, S. J., Gardner, R. C., Gendron, T. F., Vargas, J. N. S., Trujillo, A., Pribadi, M., Phillips, J. J., Gaus, S. E., Hixson, J. D., Garcia, P. A., Rabinovici, G. D., Coppola, G., Geschwind, D. H., Petrucelli, L., Miller, B. L., & Seeley, W. W. (2016). Timing and significance of pathological features in C9orf72 expansion-associated frontotemporal dementia. *Brain*, *139*(12), 3202–3216. https://doi.org/10.1093/BRAIN/AWW250

Venkatesh, J., & Oommen, A. (1998). A molecular weight study of adenosine deaminase. *Indian Journal of Biochemistry & Biophysics*, *35*(1), 16–20. https://europepmc.org/article/med/9699414

Veyrat-Durebex, C., Bris, C., Codron, P., Bocca, C., Chupin, S., Corcia, P., Vourc'h, P., Hergesheimer, R., Cassereau, J., Funalot, B., Andres, C. R., Lenaers, G., Couratier, P., Reynier, P., & Blasco, H. (2019). Metabo-lipidomics of Fibroblasts and Mitochondrial-Endoplasmic Reticulum Extracts from ALS Patients Shows Alterations in Purine,

Pyrimidine, Energetic, and Phospholipid Metabolisms. *Molecular Neurobiology*, *56*(8), 5780–5791. https://doi.org/10.1007/S12035-019-1484-7/FIGURES/4

Veyrat-Durebex, C., Corcia, P., Piver, E., Devos, D., Dangoumau, A., Gouel, F., Vourc'h, P., Emond, P., Laumonnier, F., Nadal-Desbarats, L., Gordon, P. H., Andres, C. R., & Blasco, H. (2016). Disruption of TCA Cycle and Glutamate Metabolism Identified by Metabolomics in an In Vitro Model of Amyotrophic Lateral Sclerosis. *Molecular Neurobiology*, *53*(10), 6910–6924. https://doi.org/10.1007/S12035-015-9567-6/FIGURES/7

Vincenzi, F., Corciulo, C., Targa, M., Casetta, I., Gentile, M., Granieri, E., Borea, P. A., Popoli, P., & Varani, K. (2013). A2A adenosine receptors are up-regulated in lymphocytes from amyotrophic lateral sclerosis patients. *Amyotrophic Lateral Sclerosis and Frontotemporal Degeneration*, *14*(5–6), 406–413. https://doi.org/10.3109/21678421.2013.793358

Vos, T., Abajobir, A. A., Abbafati, C., Abbas, K. M., Abate, K. H., Abd-Allah, F., Abdulle, A. M., Abebo, T. A., Abera, S. F., Aboyans, V., Abu-Raddad, L. J., Ackerman, I. N., Adamu, A. A., Adetokunboh, O., Afarideh, M., Afshin, A., Agarwal, S. K., Aggarwal, R., Agrawal, A., … Murray, C. J. L. (2017). Global, regional, and national incidence, prevalence, and years lived with disability for 328 diseases and injuries for 195 countries, 1990-2016: A systematic analysis for the Global Burden of Disease Study 2016. *The Lancet*, *390*(10100), 1211–1259. https://doi.org/10.1016/S0140-6736(17)32154-2

Wagner, T. A., McLaughlin, S., Garg, K., Cheung, C. Y. K., Larsen, B. B., Styrchak, S., Huang, H. C., Edlefsen, P. T., Mullins, J. I., & Frenkel, L. M. (2014). Proliferation of cells with HIV integrated into cancer genes contributes to persistent infection. *Science* , *345*(6196), 573. https://doi.org/10.1126/SCIENCE.1256304

Walker, C., Herranz-Martin, S., Karyka, E., Liao, C., Lewis, K., Elsayed, W., Lukashchuk, V., Chiang, S.-C., Ray, S., Mulcahy, P. J., Jurga, M., Tsagakis, I., Iannitti, T., Chandran, J., Coldicott, I., Vos, K. J. De, Hassan, M. K., Higginbottom, A., Shaw, P. J., … El-Khamisy, S. F. (2017). C9orf72 Expansion Disrupts ATM-mediated Chromosomal Break Repair. *Nature Neuroscience*, *20*(9), 1225. https://doi.org/10.1038/NN.4604

Walker, P. L. C., Corrigan, A., Arenas, M., Escuredo, E., Fairbanks, L., & Marinaki, A. (2011). Purine Nucleoside Phosphorylase Deficiency: A Mutation Update. *Nucleosides, Nucleotides & Nucleic Acids*, *30*(12), 1243–1247. https://doi.org/10.1080/15257770.2011.630852

Wang, M., Wang, H., Tao, Z., Xia, Q., Hao, Z., Prehn, J. H. M., Zhen, X., Wang, G., & Ying, Z. (2020). C9orf72 associates with inactive Rag GTPases and regulates mTORC1-mediated autophagosomal and lysosomal biogenesis. *Aging Cell*, *19*(4), e13126. https://doi.org/10.1111/ACEL.13126

Wang, T., Liu, H., Itoh, K., Oh, S., Zhao, L., Murata, D., Sesaki, H., Hartung, T., Na, C. H., & Wang, J. (2021). C9orf72 regulates energy homeostasis by stabilizing mitochondrial complex I assembly. *Cell Metabolism*, *33*(3), 531-546.e9. https://doi.org/10.1016/J.CMET.2021.01.005

Watakabe, A., Tanaka, K., & Shimura, Y. (1993). The role of exon sequences in splice site selection. *Genes & Development*, *7*(3), 407–418. https://doi.org/10.1101/GAD.7.3.407

Webster, C. P., Smith, E. F., Bauer, C. S., Moller, A., Hautbergue, G. M., Ferraiuolo, L., Myszczynska, M. A., Higginbottom, A., Walsh, M. J., Whitworth, A. J., Kaspar, B. K., Meyer, K., Shaw, P. J., Grierson, A. J., & Vos, K. J. De. (2016). The C9orf72 protein interacts with Rab1a and the ULK1 complex to regulate initiation of autophagy. *The EMBO Journal*, *35*(15), 1656–1676. https://doi.org/10.15252/EMBJ.201694401

Weihofen, W. A., Liu, J., Reutter, W., Saenger, W., & Fan, H. (2004). Crystal structure of CD26/dipeptidyl-peptidase IV in complex with adenosine deaminase reveals a highly amphiphilic interface. *Journal of Biological Chemistry*, *279*(41), 43330–43335. https://doi.org/10.1074/jbc.M405001200

Wen, X., Tan, W., Westergard, T., Krishnamurthy, K., Markandaiah, S. S., Shi, Y., Lin, S., Shneider, N. A., Monaghan, J., Pandey, U. B., Pasinelli, P., Ichida, J. K., & Trotti, D. (2014). Antisense Proline-Arginine RAN Dipeptides Linked to C9ORF72-ALS/FTD Form Toxic Nuclear Aggregates that Initiate In Vitro and In Vivo Neuronal Death. *Neuron*, *84*(6), 1213–1225. https://doi.org/10.1016/J.NEURON.2014.12.010

Wetzel, M. K., Naska, S., Laliberté, C. L., Rymar, V. V., Fujitani, M., Biernaskie, J. A., Cole, C. J., Lerch, J. P., Spring, S., Wang, S. H., Frankland, P. W., Henkelman, R. M., Josselyn, S. A., Sadikot, A. F., Miller, F. D., & Kaplan, D. R. (2008). p73 Regulates Neurodegeneration and Phospho-Tau Accumulation during Aging and Alzheimer's Disease. *Neuron*, *59*(5), 708–721. https://doi.org/10.1016/J.NEURON.2008.07.021

White, M. R., Mitrea, D. M., Zhang, P., Stanley, C. B., Cassidy, D. E., Nourse, A., Phillips, A. H., Tolbert, M., Taylor, J. P., & Kriwacki, R. W. (2019). C9orf72 Poly(PR) Dipeptide Repeats Disturb Biomolecular Phase Separation and Disrupt Nucleolar Function. *Molecular Cell*, *74*(4), 713-728.e6. https://doi.org/10.1016/J.MOLCEL.2019.03.019

Whiteman, M., Halliwell, B., & Darley-Usmar, V. M. (1996). Protection Against Peroxynitrite-Dependent Tyrosine Nitration and α1-Antiproteinase Inactivation by Ascorbic Acid. A Comparison with other Biological Antioxidants. *Free Radical Research*, *25*(3), 275–283. https://doi.org/10.3109/10715769609149052

Wiedemann, F. R., Manfredi, G., Mawrin, C., Flint Beal, M., & Schon, E. A. (2002). Mitochondrial DNA and respiratory chain function in spinal cords of ALS patients. *Journal of Neurochemistry*, *80*(4), 616–625. https://doi.org/10.1046/j.0022-3042.2001.00731.x

Wilhelm, M. T., Rufini, A., Wetzel, M. K., Tsuchihara, K., Inoue, S., Tomasini, R., Itie-Youten, A., Wakeham, A., Arsenian-Henriksson, M., Melino, G., Kaplan, D. R., Miller, F. D., & Mak, T. W. (2010). Isoform-specific p73 knockout mice reveal a novel role for ΔNp73 in the DNA damage response pathway. *Genes & Development*, *24*(6), 549–560. https://doi.org/10.1101/GAD.1873910

Wilson, D. K., Rudolph, F. B., & Quiocho, F. A. (1991). Atomic Structure of Adenosine Deaminase Complexed with a Transition-State Analog: Understanding Catalysis and Immunodeficiency Mutations. *New Series*, *252*(5010), 1278–1284.

Winn, H., Rubio, R., & Berne, R. (1981). Brain adenosine concentration during hypoxia in rats. *The American Journal of Physiology*, *241*(2), 235–242. https://doi.org/10.1152/AJPHEART.1981.241.2.H235

Wong, M., Gertz, B., Chestnut, B. A., & Martin, L. J. (2013). Mitochondrial DNMT3A and DNA methylation in skeletal muscle and CNS of transgenic mouse models of ALS. *Frontiers in Cellular Neuroscience*, *7*(DEC). https://doi.org/10.3389/FNCEL.2013.00279

Xi, Z., Zinman, L., Moreno, D., Schymick, J., Liang, Y., Sato, C., Zheng, Y., Ghani, M., Dib, S., Keith, J., Robertson, J., & Rogaeva, E. (2013). Hypermethylation of the CpG Island Near the G4C2 Repeat in ALS with a C9orf72 Expansion. *American Journal of Human Genetics*, *92*(6), 981. https://doi.org/10.1016/J.AJHG.2013.04.017

Xie, W., Duan, R., & Safe, S. (1999). Estrogen induces adenosine deaminase gene expression in MCF-7 human breast cancer cells: Role of estrogen receptor-Sp1 interactions. *Endocrinology*, *140*(1), 219–227. https://doi.org/10.1210/endo.140.1.6394

Xie, W., Duan, R., & Safe, S. (2001). Activation of adenosine deaminase in MCF-7 cells through IGF-estrogen receptor alpha crosstalk. *Journal of Molecular Endocrinology*, *26*(3), 217–228. https://doi.org/10.1677/JME.0.0260217

Xu, L., Liu, T., Liu, L., Yao, X., Chen, L., Fan, D., Zhan, S., & Wang, S. (2020). Global

variation in prevalence and incidence of amyotrophic lateral sclerosis: a systematic review and meta-analysis. *Journal of Neurology*, *267*(4), 944–953. https://doi.org/10.1007/S00415-019-09652-Y/TABLES/1

Xu, X., Yang, Q., Liu, Z., Zhang, R., Yu, H., Wang, M., Chen, S., Xu, G., Shao, Y., & Le, W. (2023). Integrative analysis of metabolomics and proteomics unravels purine metabolism dysregulation in the SOD1G93A mouse model of amyotrophic lateral sclerosis. *Neurobiology of Disease*, *181*, 106110.

Xu, Z., Poidevin, M., Li, X., Li, Y., Shu, L., Nelson, D. L., Li, H., Hales, C. M., Gearing, M., Wingo, T. S., & Jin, P. (2013). Expanded GGGGCC repeat RNA associated with amyotrophic lateral sclerosis and frontotemporal dementia causes neurodegeneration. *Proceedings of the National Academy of Sciences of the United States of America*, *110*(19), 7778–7783. https://doi.org/10.1073/PNAS.1219643110/SUPPL_FILE/SD01.XLSX

Yacoubi, M. El, Ledent, C., Ménard, J.-F., Parmentier, M., Costentin, J., & Vaugeois, J.-M. (2000). The stimulant effects of caffeine on locomotor behaviour in mice are mediated through its blockade of adenosine A2A receptors. *British Journal of Pharmacology*, *129*(7), 1465. https://doi.org/10.1038/SJ.BJP.0703170

Yagawa, K., & Okamura, J. (1981). Role of adenosine deaminase in activation of macrophages. *Infection and Immunity*, *32*(1), 394–397. https://doi.org/10.1128/IAI.32.1.394-397.1981

Yamakawa, M., Ito, D., Honda, T., Kubo, K. I., Noda, M., Nakajima, K., & Suzuki, N. (2015). Characterization of the dipeptide repeat protein in the molecular pathogenesis of c9FTD/ALS. *Human Molecular Genetics*, *24*(6), 1630–1645. https://doi.org/10.1093/HMG/DDU576

Yamamoto, H., Morino, K., Mengistu, L., Ishibashi, T., Kiriyama, K., Ikami, T., & Maegawa, H. (2016). Amla Enhances Mitochondrial Spare Respiratory Capacity by Increasing Mitochondrial Biogenesis and Antioxidant Systems in a Murine Skeletal Muscle Cell Line. *Oxidative Medicine and Cellular Longevity*, *2016*. https://doi.org/10.1155/2016/1735841

Yamaoka, T., Kondo, M., Honda, S., Iwahana, H., Moritani, M., Ii, S., Yoshimoto, K., & Itakura, M. (1997). Amidophosphoribosyltransferase limits the rate of cell growth-linked de novo purine biosynthesis in the presence of constant capacity of salvage purine biosynthesis. *Journal of Biological Chemistry*, *272*(28), 17719–17725. https://doi.org/10.1074/jbc.272.28.17719

Yamashita, T., Hatakeyama, T., Sato, K., Fukui, Y., Hishikawa, N., Ohta, Y., Nishiyama, Y., Kawai, N., Tamiya, T., & Abe, K. (2017). Flow-metabolism uncoupling in the cervical spinal cord of ALS patients. *Neurological Sciences*, *38*(4), 659–665. https://doi.org/10.1007/s10072-017-2823-y

Yang, A., Kaghad, M., Wang, Y., Gillett, E., Fleming, M. D., Dötsch, V., Andrews, N. C., Caput, D., & McKeon, F. (1998). p63, a p53 homolog at 3q27-29, encodes multiple products with transactivating, death-inducing, and dominant-negative activities. *Molecular Cell*, *2*(3), 305–316. https://doi.org/10.1016/S1097-2765(00)80275-0

Yang, A., Walker, N., Bronson, R., Kaghad, M., Oosterwegel, M., Bonnin, J., Vagner, C., Bonnet, H., Dikkes, P., Sharpe, A., McKeon, F., & Caput, D. (2000). p73-deficient mice have neurological, pheromonal and inflammatory defects but lack spontaneous tumours. *Nature*, *404*(6773), 99–103. https://doi.org/10.1038/35003607

Yanpallewar, S. U., Barrick, C. A., Buckley, H., Becker, J., & Tessarollo, L. (2012). Deletion of the BDNF truncated receptor TrkB.T1 delays disease onset in a mouse model of amyotrophic lateral sclerosis. *PLoS ONE*, *7*(6). https://doi.org/10.1371/journal.pone.0039946

Yoshida, Y., Une, F., Utatsu, Y., Nomoto, M., Furukawa, Y., Maruyama, Y., Machigashira, N., Matsuzaki, T., & Osame, M. (1999). Adenosine and neopterin levels in cerebrospinal fluid of patients with neurological disorders. *Internal Medicine*, *38*(2), 133–139. https://doi.org/10.2169/internalmedicine.38.133

Zamiri, B., Mirceta, M., Bomsztyk, K., Macgregor, R. B., & Pearson, C. E. (2015). Quadruplex formation by both G-rich and C-rich DNA strands of the C9orf72 (GGGGCC)8•(GGCCCC)8 repeat: effect of CpG methylation. *Nucleic Acids Research*, *43*(20), 10055–10064. https://doi.org/10.1093/NAR/GKV1008

Zavialov, Andrey V., Gracia, E., Glaichenhaus, N., Franco, R., Zavialov, A. V., & Lauvau, G. (2010). Human adenosine deaminase 2 induces differentiation of monocytes into macrophages and stimulates proliferation of T helper cells and macrophages. *Journal of Leukocyte Biology*, *88*(2), 279–290. https://doi.org/10.1189/JLB.1109764

Zavialov, Anton V., Yu, X., Spillmann, D., Lauvau, G., & Zavialo, A. V. (2010). Structural basis for the growth factor activity of human adenosine deaminase ADA2. *Journal of Biological Chemistry*, *285*(16), 12367–12377. https://doi.org/10.1074/jbc.M109.083527

Zavialov, Andrey V, & Engström, A. (2005). Human ADA2 belongs to a new family of growth factors with adenosine deaminase activity. *The Biochemical Journal*, *391*(Pt 1), 51–57.

https://doi.org/10.1042/BJ20050683

Zeng, P., Wang, T., Zheng, J., & Zhou, X. (2019). Causal association of type 2 diabetes with amyotrophic lateral sclerosis: new evidence from Mendelian randomization using GWAS summary statistics. *BMC Medicine 2019 17:1*, *17*(1), 1–13. https://doi.org/10.1186/S12916-019-1448-9

Zhang, C., Yang, Y., Liang, W., Wang, T., Wang, S., Wang, X., Wang, Y., Jiang, H., & Feng, H. (2019). Neuroprotection by urate on the mutant hSOD1-related cellular and Drosophila models of amyotrophic lateral sclerosis: Implication for GSH synthesis via activating Akt/GSK3β/Nrf2/GCLC pathways. *Brain Research Bulletin*, *146*, 287–301. https://doi.org/10.1016/j.brainresbull.2019.01.019

Zhang, F., Zhang, Q., Ke, Y., Hao, J., Lu, L., Lu, N., & Chen, X. (2018). Serum uric acid levels in patients with amyotrophic lateral sclerosis: a meta-analysis. *Scientific Reports 2018 8:1*, *8*(1), 1–6. https://doi.org/10.1038/s41598-018-19609-2

Zhang, N., Shu, H. Y., Huang, T., Zhang, Q. L., Li, D., Zhang, G. Q., Peng, X. Y., Liu, C. F., Luo, W. F., & Hu, L. F. (2014). Nrf2 Signaling Contributes to the Neuroprotective Effects of Urate against 6-OHDA Toxicity. *PLOS ONE*, *9*(6), e100286. https://doi.org/10.1371/JOURNAL.PONE.0100286

Zhang, Y., Burberry, A., Wang, J. Y., Sandoe, J., Ghosh, S., Udeshi, N. D., Svinkina, T., Mordes, D. A., Mok, J., Charlton, M., Li, Q. Z., Carr, S. A., & Eggan, K. (2018). The C9orf72-interacting protein Smcr8 is a negative regulator of autoimmunity and lysosomal exocytosis. *Genes & Development*, *32*(13–14), 929–943. https://doi.org/10.1101/GAD.313932.118

Zhang, Y. J., Gendron, T. F., Ebbert, M. T. W., O'Raw, A. D., Yue, M., Jansen-West, K., Zhang, X., Prudencio, M., Chew, J., Cook, C. N., Daughrity, L. M., Tong, J., Song, Y., Pickles, S. R., Castanedes-Casey, M., Kurti, A., Rademakers, R., Oskarsson, B., Dickson, D. W., … Petrucelli, L. (2018). Poly(GR) impairs protein translation and stress granule dynamics in C9orf72-associated frontotemporal dementia and amyotrophic lateral sclerosis. *Nature Medicine*, *24*(8), 1136–1142. https://doi.org/10.1038/s41591-018-0071-1

Zhang, Y. J., Gendron, T. F., Grima, J. C., Sasaguri, H., Jansen-West, K., Xu, Y. F., Katzman, R. B., Gass, J., Murray, M. E., Shinohara, M., Lin, W. L., Garrett, A., Stankowski, J. N., Daughrity, L., Tong, J., Perkerson, E. A., Yue, M., Chew, J., Castanedes-Casey, M., … Petrucelli, L. (2016). C9ORF72 poly(GA) aggregates sequester and impair HR23 and nucleocytoplasmic transport proteins. *Nature*

Neuroscience, *19*(5), 668–677. https://doi.org/10.1038/nn.4272

Zhang, Y. J., Jansen-West, K., Xu, Y. F., Gendron, T. F., Bieniek, K. F., Lin, W. L., Sasaguri, H., Caulfield, T., Hubbard, J., Daughrity, L., Chew, J., Belzil, V. V., Prudencio, M., Stankowski, J. N., Castanedes-Casey, M., Whitelaw, E., Ash, P. E. A., DeTure, M., Rademakers, R., … Petrucelli, L. (2014). Aggregation-prone c9FTD/ALS poly(GA) RAN-translated proteins cause neurotoxicity by inducing ER stress. *Acta Neuropathologica*, *128*(4), 505–524. https://doi.org/10.1007/S00401-014-1336-5/FIGURES/5

Zhao, C., Devlin, A. C., Chouhan, A. K., Selvaraj, B. T., Stavrou, M., Burr, K., Brivio, V., He, X., Mehta, A. R., Story, D., Shaw, C. E., Dando, O., Hardingham, G. E., Miles, G. B., & Chandran, S. (2020). Mutant C9orf72 human iPSC-derived astrocytes cause non-cell autonomous motor neuron pathophysiology. *Glia*, *68*(5), 1046–1064. https://doi.org/10.1002/GLIA.23761

Zhao, W., Beers, D. R., Hooten, K. G., Sieglaff, D. H., Zhang, A., Kalyana-Sundaram, S., Traini, C. M., Halsey, W. S., Hughes, A. M., Sathe, G. M., Livi, G. P., Fan, G.-H., & Appel, S. H. (2017). Characterization of Gene Expression Phenotype in Amyotrophic Lateral Sclerosis Monocytes. *JAMA Neurology*, *74*(6), 677–685. https://doi.org/10.1001/JAMANEUROL.2017.0357

Zhou, G., Smith, J. L., & Zalkin, H. (1994). Binding of purine nucleotides to two regulatory sites results in synergistic feedback inhibition of glutamine 5-phosphoribosylpyrophosphate amidotransferase. *Journal of Biological Chemistry*, *269*(9), 6784–6789. https://doi.org/10.1016/s0021-9258(17)37444-6

Zhu, Q., Jiang, J., Gendron, T. F., McAlonis-Downes, M., Jiang, L., Taylor, A., Diaz Garcia, S., Ghosh Dastidar, S., Rodriguez, M. J., King, P., Zhang, Y., La Spada, A. R., Xu, H., Petrucelli, L., Ravits, J., Da Cruz, S., Lagier-Tourenne, C., & Cleveland, D. W. (2020). Reduced C9ORF72 function exacerbates gain of toxicity from ALS/FTD-causing repeat expansion in C9orf72. *Nature Neuroscience*, *23*(5), 615–624. https://doi.org/10.1038/s41593-020-0619-5

Zimmermann, F. F., Gaspary, K. V., Siebel, A. M., Leite, C. E., Kist, L. W., Bogo, M. R., & Bonan, C. D. (2016). Analysis of Extracellular Nucleotide Metabolism in Adult Zebrafish After Embryological Exposure to Valproic Acid. *Molecular Neurobiology 2016 54:5*, *54*(5), 3542–3553. https://doi.org/10.1007/S12035-016-9917-Z

Zoccolella, S., Simone, I. L., Capozzo, R., Tortelli, R., Leo, A., D'Errico, E., & Logroscino, G. (2011). An exploratory study of serum urate levels in patients with amyotrophic lateral

sclerosis. *Journal of Neurology*, *258*(2), 238–243. https://doi.org/10.1007/S00415-010-5735-9/TABLES/2

Zondler, L., Müller, K., Khalaji, S., Bliederhäuser, C., Ruf, W. P., Grozdanov, V., Thiemann, M., Fundel-Clemes, K., Freischmidt, A., Holzmann, K., Strobel, B., Weydt, P., Witting, A., Thal, D. R., Helferich, A. M., Hengerer, B., Gottschalk, K.-E., Hill, O., Kluge, M., … Weishaupt, J. H. (2016). Peripheral monocytes are functionally altered and invade the CNS in ALS patients. *Acta Neuropathologica 2016 132:3*, *132*(3), 391–411. https://doi.org/10.1007/S00401-016-1548-Y

Zou, Z. Y., Zhou, Z. R., Che, C. H., Liu, C. Y., He, R. L., & Huang, H. P. (2017). Genetic epidemiology of amyotrophic lateral sclerosis: a systematic review and meta-analysis. *Journal of Neurology, Neurosurgery & Psychiatry*, *88*(7), 540–549. https://doi.org/10.1136/JNNP-2016-315018

Zu, T., Liu, Y., Bañez-Coronel, M., Reid, T., Pletnikova, O., Lewis, J., Miller, T. M., Harms, M. B., Falchook, A. E., Subramony, S. H., Ostrow, L. W., Rothstein, J. D., Troncoso, J. C., & Ranum, L. P. W. (2013). RAN proteins and RNA foci from antisense transcripts in C9ORF72 ALS and frontotemporal dementia. *Proceedings of the National Academy of Sciences of the United States of America*, *110*(51), E4968–E4977. https://doi.org/10.1073/PNAS.1315438110/SUPPL_FILE/PNAS.201315438SI.PDF